Virtual Network Provisioning over Flexible Optical Transport Infrastructure

Ph.D. dissertation by Albert Pagès Cruz

Advisor: Dr. Salvatore Spadaro
Co-advisor: Dr. Jordi Perelló Muntan

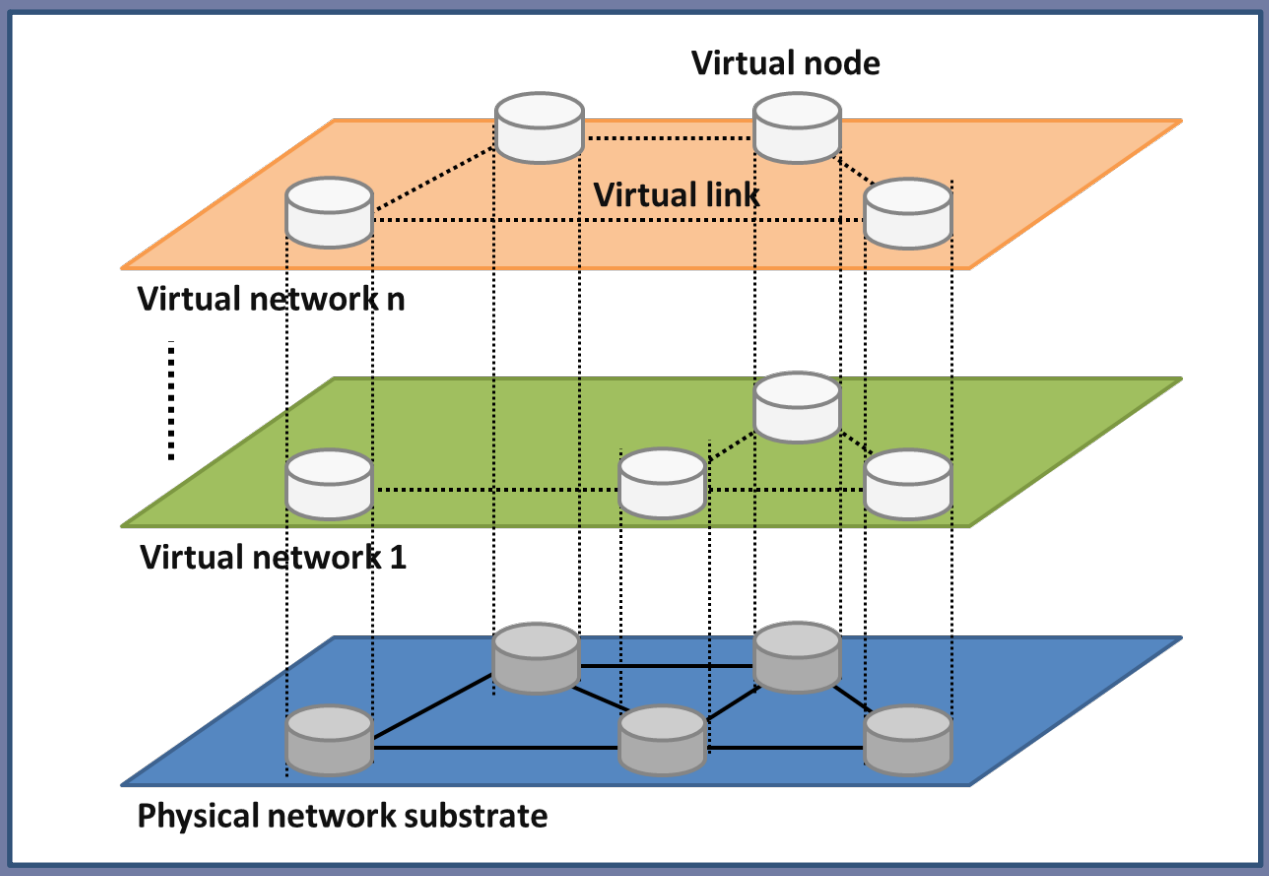

Universitat Politècnica de Catalunya (UPC)
Departament de Teoria del Senyal i Comunicacions (TSC)

Academic year 2014-2015

UNIVERSITAT POLITÈCNICA DE CATALUNYA (UPC)

Virtual Network Provisioning over Flexible Optical Transport Infrastructure

by

Albert Pagès Cruz

A thesis submitted in fulfillment for the
degree of Doctor of Philosophy

in the

Optical Communications Group (GCO)
Signal Theory and Communications Department (TSC)

Advisors: Dr. Salvatore Spadaro and Dr. Jordi Perelló Muntan

November 2014

UNIVERSITAT POLITÈCNICA DE CATALUNYA
BARCELONATECH
Escola de Doctorat

Acta de qualificació de tesi doctoral

Curs acadèmic:

Nom i cognoms

Programa de doctorat

Unitat estructural responsable del programa

Resolució del Tribunal

Reunit el Tribunal designat a l'efecte, el doctorand / la doctoranda exposa el tema de la seva tesi doctoral titulada

_____

_____.

Acabada la lectura i després de donar resposta a les qüestions formulades pels membres titulars del tribunal, aquest atorga la qualificació:

☐ NO APTE ☐ APROVAT ☐ NOTABLE ☐ EXCEL·LENT

(Nom, cognoms i signatura) President/a		(Nom, cognoms i signatura) Secretari/ària
(Nom, cognoms i signatura) Vocal	(Nom, cognoms i signatura) Vocal	(Nom, cognoms i signatura) Vocal

_____, _____ d'/de _____ de _____

El resultat de l'escrutini dels vots emesos pels membres titulars del tribunal, efectuat per l'Escola de Doctorat, a instància de la Comissió de Doctorat de la UPC, atorga la MENCIÓ CUM LAUDE:

☐ SÍ ☐ NO

(Nom, cognoms i signatura) President de la Comissió Permanent de l'Escola de Doctorat	(Nom, cognoms i signatura) Secretari de la Comissió Permanent de l'Escola de Doctorat

Barcelona, _____ d'/de _____ de _____

Contents

List of Figures

List of Tables

Abbreviations and Symbols

Abbreviations

ASON	Automatically Switched Optical Network
BBR	Bit-rate Blocking Ratio
BBw	Blocked Bandwidth
BN	Border Node
BP	Blocking Probability
BV-TSP	Bandwidth Variable Transponder
BV-WXC	Bandwidth Variable Wavelength Cross Connect
CAPEX	Capital Expenditures
CCI	Connection Controller Interface
CE	Customer Edge
DC	Data Center
DWDM	Dense Wavelength Division Multiplexing
EO	Electro-Optical
EON	Elastic Optical Network
FF	First Fit
FS	Frequency Slot
GMPLS	Generalized Multi-Protocol Label Switching
GRASP	Greedy Randomized Adaptive Search Procedures
H-PCE	Hierarchical-Path Computation Element
HT	Holding Time
IaaS	Infrastructure as a Service

IAT	Inter-arrival Time
IETF	Internet Engineering Task Force
IT	Information Technology
ITU	International Telecommunication Union
ILP	Integer Linear Programming
LL	Least Loaded
LMP	Link Management Protocol
MC	Multi-Carrier
MF-TSP	Multi-Flow Transponder
MILP	Mixed Integer Linear Programming
MLR	Mixed Line Rate
ND	Nodal Degree
NE	Network Element
NH-PCE	Non Hierarchical-Path Computation Element
NMS	Network Management System
NNI	Network-to-Network Interface
OADM	Optical Add/Drop Multiplexer
OCC	Optical Connection Controller
OCS	Optical Circuit Switching
OE	Opto-Electronic
OFDM	Orthogonal Frequency Division Multiplexing
O-E-O	Optical-Electrical-Optical
OPEX	Operational Expenditures
OPS	Optical Packet Switching
OSPF-TE	Open Shortest Path First-Traffic Engineering
OTN	Optical Transport Network
OXC	Optical Cross Connect
PE	Provider Edge
PIP	Physical Infrastructure Provider
PLI	Physical Layer Impairment
QoE	Quality of Experience

QoS	Quality of Service
REG	Regenerator
RR	Round Robin
RSA	Route and Spectrum Assignment
RSMLA	Route, Spectrum and Modulation Level Assignment
RSVP-TE	Resource Reservation Protocol-Traffic Engineering
RWA	Route and Wavelength Assignment
SC	Single-Carrier
SDI	Software Defined Infrastructure
SDN	Software Defined Network
SLR	Single Line Rate
SP	Shortest Path
SS	Split Spectrum
SSA	Split Spectrum Approach
SSRSA	Split Spectrum-enabled Route and Spectrum Assignment
TSP	Transponder
UNI	User-to-Network Interface
VDC	Virtual Data Center
VI	Virtual Infrastructure
VIO	Virtual Infrastructure Operator
VIP	Virtual Infrastructure Provider
VM	Virtual Machine
VN	Virtual Network
VNE	Virtual Network Embedding
VON	Virtual Optical Network
VONA	Virtual Optical Network Allocation
VPN	Virtual Private Network
WDM	Wavelength Division Multiplexing
WSON	Wavelength Switched Optical Network

Symbols

B	Requested bandwidth (in GHz) by a connection
B_i	Bandwidth (in GHz) of the i^{th} part of a demand in a SS-enabled EON
C_h	High priority traffic
C_l	Low priority traffic
f_{cs}	Channel spacing in the DWDM frequency grid
FL_{max}	Maximum number of flows a MF-TSP is able to produce
F_w	Spectral width (in GHz) of a FS in an EON
G	Guard band (in GHz) between connections in a optical network
G'_d	Graph of a VON or VI
G_n	Graph of a physical optical network
H	Number of parts into which a demand is divided in a SS-enabled EON
H_{max}	Maximum number of parts of a demand in a SS-enabled EON
h_p	Length in hops of a path in an optical network
L_{max}	Maximum number of paths per demand in a SS-enabled EON
l_p	Physical length (in km) of a path in a optical network
P_{idle}	Power consumption of a TSP in idle state
P_{on}	Power consumption of a TSP in on state
S	Number of FSs needed to allocate a demand in an EON
S_{max}	Maximum size in FSs of a part in a SS-enabled EON
S_{min}	Minimum size in FSs of a part in a SS-enabled EON
r_{sd}	Route between source node s and destination node d
T_w	Mean wake-up time of a sleep-enabled TSP
$\delta^+(n)$	Outgoing set of links from a physical node in an optical network
$\delta^-(n)$	Incoming set of links to a physical node in an optical network
λ_h	Mean arrival rate of high priority connections
$\lambda_{h,sd}$	Mean arrival rate of high priority connections between nodes s and d
λ_l	Mean arrival rate of low priority connections
$\lambda_{l,sd}$	Mean arrival rate of low priority connections between nodes s and d

μ	Mean duration of a connection
ω_t	Frequency of waking-up a sleep-enabled TSP

Resum

Els actuals propietaris de xarxes de transport es centren en oferir serveis mitjançant les infraestructures que posseeixen i gestionen, mentre els usuaris finals no tenen cap control sobre aquests serveis. Tradicionalment, aquest ha estat el model de negoci adoptat pels operadors de xarxa, ja que el cost de construir i mantenir les infraestructures corresponents per tal d'oferir serveis a través d'elles era, i encara és, considerablement elevat. No obstant això, el tràfic a Internet ha estat creixent de manera ràpida i sostinguda durant els últims anys i es preveu que continuarà creixent en el futur. A més, l'aparició de nous serveis i paradigmes estan portant al límit les actuals infraestructures de telecomunicacions, especialment les xarxes òptiques de transport. Per tal de superar aquesta situació, la virtualització de xarxes ha estat considerat com una solució efectiva per les futures arquitectures de xarxes òptiques. Gràcies a les Xarxes Òptiques Virtuals (VONs), és possible crear infraestructures lògiques específiques en la seva missió, les quals permeten satisfer els requisits de les aplicacions que s'executaran a través d'elles, usant i compartint un substrat físic únic. Tanmateix, l'aplicació de les tècniques de virtualització en el domini òptic encara és subjecte d'investigació, sent el mapeig entre els recursos virtuals i els recursos físics (també conegut com incrustació de la xarxa virtual) un punt clau que cal adreçar.

No obstant això, la virtualització en si mateixa no proporciona una solució prou flexible en termes d'utilització d'ample de banda. Per tal de proporcionar un entorn de virtualització suficientment flexible per tal d'acomodar qualsevol ample de banda amb suficient granularitat, és necessari que el substrat físic adopti una tecnologia de transport igualment flexible. Les Xarxes Òptiques Elàstiques (EONs) es presenten com una solució eficient per a una assignació flexible de l'ample de banda en les xarxes òptiques. A més, a causa de l'heterogeneïtat i el dinamisme dels perfils de trafic als quals s'enfrontaran les xarxes virtuals, és altament desitjable proporcionar una infraestructura física que ajudi a mantenir baixes les despeses operatives (OPEX) d'aquestes xarxes, sent un paràmetre molt important el consum d'energia associat a l'operació de les VONs. El tema del consum energètic ha estat, i encara és, subjecte de grans iniciatives de recerca centrades en desenvolupar noves arquitectures de dispositius o algoritmes d'assignació de recursos conscients del consum energètic per tal de proporcionar xarxes de transport òptiques més eficients energèticament que, al seu torn, permetran crear infraestructures virtuals menys costoses des del punt de vista del consum energètic.

Aquesta tesi està dedicada a l'estudi de la composició i l'assignació de recursos de VONs, amb l'objectiu de proporcionar un entorn flexible, eficient i optimitzat per a la incrustació de les VONs al substrat físic real. L'escenari considerat es compon d'una xarxa de transport subjacent, ja sigui una Xarxa Òptica de Commutació de Longitud d'Ona (WSON) o basada en EON, i múltiples VONs client, les quals s'han de col·locar sobre el substrat físic. En aquest escenari, un aspecte clau es refereix a com els recursos reals estan associats als virtuals, garantint l'aïllament entre VONs i satisfent els recursos demanats (per exemple, capacitat d'enllaç) per cada una d'elles.

Després d'una introducció a la tesi, el capítol 2 revisa les infraestructures de xarxa òptica en l'actualitat, concloent en la necessitat d'avançar cap a una infraestructura de xarxa òptica més dinàmica i eficient per tal de fer front al creixement del tràfic d'Internet i l'aparició de nous serveis i paradigmes. Tot seguit, es procedeix a resumir l'estat de l'art dels conceptes i paradigmes que permetran habilitar aquesta arquitectura de xarxa, bàsicament, VONs, EONs i les infraestructures òptiques de baix consum. A continuació, els capítols 3, 4 i 5 es centren en proporcionar solucions per optimitzar aspectes específics d'aquests conceptes amb la finalitat de proveir un marc optimitzat que ajudarà en la configuració de les futures infraestructures de xarxes òptiques i els seus models de negoci. Més en detall, el capítol 3 estudia els principals reptes en el problema de la incrustació de VONs i presenta solucions que permetin una assignació de recursos optimitzada a les VONs en un substrat físic en funció de les característiques de les VONs i el substrat de la xarxa. El capítol 4 proposa el concepte de l'Split Spectrum (SS) com una forma de millorar la utilització de l'espectre en les EONs. Finalment, el capítol 5 es centra en proporcionar i avaluar solucions arquitectòniques i d'enrutament amb l'objectiu de reduir el consum d'energia del substrat òptic de tal manera que VONs amb menor OPEX puguin ser desplegades a través d'ell.

Mencionar que part del treball presentat en aquesta tesi s'ha realitzat en el marc de diversos projectes europeus i nacionals: STRONGEST (INFSO-ICT-247674), GEYSERS (FP7-248657), LIGHTNESS (FP7-318606) i COSIGN (FP7-619572), finançats per la Comissió Europea, i els projectes ENGINE (TEC2008-02634) i ELASTIC (TEC2011-27310), finançats pel Ministerio Español de Ciencia e Innovación.

Resumen

Los actuales propietarios de las redes de transporte se centran en ofrecer servicios mediante las infraestructuras que poseen y gestionan, mientras que los usuarios finales no tienen ningún control sobre estos. Tradicionalmente, este ha sido el modelo de negocio adoptado por los operadores de redes, ya que el coste de construir y mantener las infraestructuras correspondientes por tal de ofrecer servicios mediante ellas era, y aun es, considerablemente elevado. No obstante, el trafico en Internet ha crecido de manera rápida y sostenida durante los últimos años y se prevé que continuara con este crecimiento en el futuro. Además, la aparición de nuevos servicios y paradigmas, están llevando al limite las actuales infraestructuras de telecomunicaciones, especialmente las redes de trasporte óptico. Por tal de superar dicha situación, la virtualización de redes ha sido considerada como una solución efectiva para las futuras arquitecturas de redes ópticas. Gracias a las Redes Ópticas Virtuales (VONs), es posible crear infraestructuras lógicas especificas en su misión, las cuales podrán satisfacer los requisitos de las aplicaciones que se ejecutaran a través de ellas, usando y compartiendo un único sustrato físico. No obstante, la aplicación de las técnicas de virtualización en el dominio óptico aun es sujeto de investigación, siendo el mapeo entre los recursos virtuales y los físicos (también conocido como incrustación de la red virtual) un punto clave a solucionar.

No obstante, la virtualización por si misma no ofrece una solución suficientemente flexible en términos de utilización del ancho de banda. Por tal de proporcionar un entorno de virtualización suficientemente flexible para acomodar cualquier ancho de banda con suficiente granularidad, es necesario que el sustrato físico adopte una tecnología de transporte igual de flexible. Las Redes Ópticas Elásticas (EONs) se presentan como una solución eficiente para una asignación flexible del ancho de banda en redes ópticas. Además, debido a la heterogeneidad y dinamismo de los perfiles de trafico a los cuales se enfrentaran las redes virtuales, es altamente deseable proporcionar una infraestructura física que ayuda a mantener bajos los gastos operativos (OPEX) de estas redes, siendo un parámetro muy importante el consumo energético asociado a la operación de las VONs. El tema del consumo energético ha sido, y aun es, sujeto de grandes iniciativas de investigación centradas en desarrollar nuevas arquitecturas de dispositivos o algoritmos de asignación de recursos conscientes del consumo energético por tal de proporcionar redes de transporte ópticas mas eficientes energeticamente que, a su vez, permitan crear infraestructuras virtuales menos costosas des del punto de vista energético.

Esta tesis se centra en el estudio de la composición y asignación de recursos a las VONs, con el objetivo de proporcionar un entorno flexible, eficiente y optimizado para la incrustación de las VONs en el sustrato físico real. El escenario considerado se compone de una red de transporte subyacente, ya sea una Red Óptica de Conmutación de Longitud de Onda (WSON) o EON, y múltiples VONs cliente, las cuales se colocaran encima del sustrato físico. En este escenario, un aspecto clave se refiere a como los recursos reales se asocian a los virtuales, garantizando el aislamiento entre VONs y satisfaciendo los recursos pedidos (por ejemplo, capacidad de enlace) por cada una de ellas.

Después de una introducción a la tesis, el capitulo 2 revisa las infraestructuras de redes ópticas actuales, concluyendo en la necesidad de avanzar hacia una infraestructura de red óptica mas dinámica y eficiente por tal de afrontar el crecimiento del trafico en Internet y la aparición de nuevos servicios y paradigmas. Seguidamente, se procede a resumir el estado del arte de los conceptos y paradigmas que permitirán habilitar esta arquitectura de red, básicamente, VONs, EONs y las infraestructuras ópticas de bajo consumo energético. A continuación, los capítulos 3, 4 y 5 se centran en proporcionar soluciones para optimizar aspectos específicos de estos conceptos con la finalidad de proporcionar un marco optimizado que ayudara en la configuración de las futuras infraestructuras de redes ópticas y sus modelos de negocio. Concretamente, el capitulo 3 estudia los principales retos en el problema de la incrustación de VONs y presenta soluciones que permiten una asignación de recursos optimizada a las VONs en un sustrato físico dependiendo de las características de las VONs y del sustrato de red. El capitulo 4 propone el concepto de Split Spectrum (SS) como una forma de mejorar la utilización del espectro en las EONs. Finalmente, el capitulo 5 se centra en proporcionar y evaluar soluciones arquitectónicas y de enrutamiento con el objetivo de reducir el consumo energético del sustrato óptico de tal manera que VONs con menor OPEX puedan ser desplegadas mediante este sustrato.

Mencionar que parte del trabajo presentado en esta tesis se ha realizado dentro del marco de varios proyectos europeos y nacionales: STRONGEST (INFSO-ICT-247674), GEYSERS (FP7-248657), LIGHTNESS (FP7-318606) y COSIGN (FP7-619572), financiados por la Comisión Europea, y los proyectos ENGINE (TEC2008-02634) y ELASTIC (TEC2011-27310), financiados por el Ministerio Español de Ciencia e Innovación.

Summary

Current transport network owners are focused on offering services on top of the infrastructures they own and manage, while end users have no control over these services. Traditionally, this has been the business model adopted by the operators, as the cost of building and maintaining the related infrastructures to provide services over them was, and still is, considerably high. However, the traffic on Internet has been rapidly and steadily increasing over the years and will continue to increase in the future. Additionally new emerging services and paradigms are pushing the limits of existing telecommunication infrastructures, particularly transport optical networks. To overcome such situation, network virtualization has been considered as an effective solution for the future optical networks architectures. Thanks to Virtual Optical Networks (VONs), it is possible to create mission-specific logic infrastructures, which fulfil the exact requirements of the applications that will run on top of them, using and sharing a unique physical substrate. However, the applicability of virtualization techniques to the optical domain is still under research, being on key point to be addressed the mapping of the virtual resources to the actual physical ones (also known as virtual network embedding).

However, virtualization per se does not provide a solution flexible enough in terms of bandwidth utilization. In order to provide a virtualization environment flexible enough to accommodate any desirable bandwidth with fine granularity, an equally flexible transport technology must be adopted by the physical substrate. Elastic Optical Networks (EONs) have been presented as an efficient solution for flexible bandwidth allocation in optical networks. Additionally, due to the heterogeneity and dinamicity of the traffic patterns that such virtual networks will face, it is highly desirable to provide a physical infrastructure that will help on keeping the associated operational expenditures (OPEX) at low levels, being a very important parameter the energy consumption associated to the operation of the VONs. The energy consumption topic has been, and still is, subject of big research efforts in developing new device architectures or energy-aware resource allocation algorithms so as to provide more energy efficient optical transport networks, which, at their turn, will help on the creation of less costly virtual infrastructures, energy consumption-wise speaking.

This thesis is devoted to the study of composition and resource allocation of VONs, aiming to provide a flexible, efficient and optimized environment for the embedding of the VONs to the actual physical substrate. The considered scenario is composed of an

underlying transport network, either Wavelength Switched Optical Network (WSON) or EON-based, and multiple client VONs that have to be allocated on top. In such scenario, a key aspect relates to how actual resources are associated to the virtual ones, guaranteeing the isolation among VONs and satisfying the resources requirements (e.g. link capacity) of every one of them.

After an introduction to the thesis, chapter 2 surveys nowadays optical network infrastructures, concluding on the need to move towards a more dynamic and efficient optical network infrastructure in order to cope with the growth of internet traffic and the advent of new services and paradigms. With such consideration, it proceeds to summarize the state of the art of the concepts and paradigms that enable for such network architecture, namely, VONs, EONs and energy efficient optical infrastructures. Next, chapters 3, 4 and 5 focus on providing solutions to optimize specific aspects of these enabling concepts so as to provide an optimized framework that will help on shaping the future optical networks' infrastructures and business models. More in details, chapter 3 studies the main challenges on the VON embedding problem and presents solutions that allow for an optimized resource assignment to VONs in a physical substrate depending on the VONs characteristics and the specific network substrate. Chapter 4 proposes the Split Spectrum (SS) approach as a way to improve the spectrum utilization of EONs. Finally, chapter 5 focuses on provide and evaluate routing and architectural solutions in aims to reduce the energy consumption of the optical substrate so as VONs with lower OPEX can be deployed on top of it.

It shall be mentioned that part of the work reported in this thesis has been done within the framework of several European and National projects, namely STRONGEST (INFSO-ICT-247674), GEYSERS (FP7-248657), LIGHTNESS (FP7-318606) and COSIGN (FP7-619572), founded by the European Commission, and the projects ENGINE (TEC2008-02634) and ELASTIC (TEC2011-27310) founded by the Spanish Science Ministry.

I would like to dedicate this thesis to my parents and sister,
they have been the driving force behind this work.
Specially thank my advisors Salvatore Spadaro and
Jordi Perelló for their invaluable guidance and support.

Chapter 1

Introduction

Current transport network owners are focused on offering services on top of the infrastructures they own and manage, while end users have no control over these services. Traditionally, this has been the business model adopted by the operators, as the cost of building and maintaining the related infrastructures to provide services over them was, and still is, considerably high. However, the traffic on Internet has been rapidly and steadily increasing over the years and will continue to increase in the future.

This growing is fostered by the evolution of existing solutions towards higher bandwidths and the increase of the number of users. Also, new emerging services, such as ultra-high definition video streaming, 3D Internet or multimedia social networks will gain great impulse. Furthermore, new paradigms such as cloud computing are gaining strength in the arena. These new requirements are difficult to accommodate with the existing rigid telecommunications architecture models. In order to support such applications and paradigms, cost-efficient, dynamic and mission-specific networks infrastructures are required. Additionally, due the unpredictable growing of the traffic, new management policies based on flexible bandwidth allocation become highly interesting in contrast to the current coarse bandwidth provisioning.

Network virtualization has been considered as an effective solution that will allow transport network owners to not only offer data transport services over their physical infrastructures, but also portions of such infrastructures as a service for exploitation by external service providers, which will manage the rented portion of infrastructure to provide to their clients the desired resources that fit with their business and applications. Thanks to Virtual Optical Networks (VONs), it is possible to create mission-specific logic infrastructures, which fulfil the exact requirements of the applications that will run on top of them, using and sharing a unique physical substrate. However, although virtualization techniques are well studied and mature enough for layer-2/3 networks, their applicability to the optical domain is still under research, being on key point to be addressed the mapping of the virtual resources to the actual physical ones (also known as virtual network embedding).

However, virtualization per se does not provide a solution flexible enough in terms of bandwidth utilization, mainly because the attributes of the virtual infrastructure are tightly related to the underlying physical substrate. Indeed, current transport network solutions are based on rigid and coarse technologies in terms of bandwidth. In order to provide a virtualization environment flexible enough to accommodate any desirable bandwidth with fine granularity, an equally flexible transport technology must be adopted by the physical substrate. Elastic Optical Networks (EONs) have been presented as an efficient solution for flexible bandwidth allocation in optical networks. The basic idea behind is to adopt a flexible spectral grid capable to provide fine granularity either for low or high data-rate demands, opposed to the fixed-size spectral grid standardized by the International Telecommunication Union (ITU), solution adopted by the vast majority of Wavelength Switched Optical Networks (WSONs).

Additionally, due to the heterogeneity and dinamicity of the traffic patterns that such virtual networks will face, it is highly desirable to provide a physical infrastructure that will help on keeping the associated operational expenditures (OPEX) at low levels, being a very important parameter the energy consumption associated to the operation of the VONs. The energy consumption topic has been, and still is, subject of big research efforts in developing new device architectures or energy-aware resource allocation algorithms so as to provide more energy efficient optical transport networks, which, at their turn, will help on the creation of less costly virtual infrastructures, energy consumption-wise speaking.

This thesis is devoted to the study of composition and resource allocation of VONs, aiming to provide a flexible, efficient and optimized environment for the embedding of the VONs to the actual physical substrate. The considered scenario is composed of an underlying transport network, either WSON or EON-based, and multiple client VONs that have to be allocated on top. In such scenario, a key aspect relates to how actual resources are associated to the virtual ones, guaranteeing the isolation among VONs and satisfying the resources requirements (e.g. link capacity) of every one of them. To this end, individual chapters deal with the embedding of the virtual resources and how to improve the spectrum utilization and the energy efficiency of the underlying physical substrate. Along this process, the problem under study is stated, followed by a review of existing work in the literature. Next, contributions addressing the identified issues are provided and validated. Finally, main achievements in each chapter are highlighted.

1.1 Overview of the thesis

This thesis is structured into a background chapter on dynamic and efficient optical infrastructures (chapter 2), one chapter concerning the embedding of virtual optical networks (chapter 3), one chapter aiming to improve the spectrum utilization in elastic optical

networks (chapter 4) and one chapter proposing and evaluating multiple solutions for energy efficient optical networks (chapter 5).

Chapter 2, entitled *Towards dynamic and efficient optical network infrastructures*, surveys nowadays optical networks infrastructures, concluding in the necessity to evolve to more flexible and dynamic architectures in order to cope with the growth of the traffic on Internet as well as emerging new services and paradigms. In this regard, the concepts of Infrastructure as a Service (IaaS) and Virtual Networks (VNs) are presented as a potential solutions for the future optical networks infrastructures. Being VONs one of the main focuses of this thesis, a dedicated section is devoted on explaining their benefits and challenges. This leads to conclude that, in order to provide an environment flexible enough for future optical network architectures, VONs are not enough since their performance is tightly related to the underlying physical substrate. Hence EONs are presented as a solution to provide a more efficient physical substrate in terms of spectrum utilization. Specific sections detailing the evolution from Wavelength Division Multiplexing (WDM)-based to EON-based optical networks are provided. Finally, some background in regards of energy efficiency in optical infrastructures is provided, since it is a key factor on the development of cost effective solutions for future optical networks.

Chapter 3, *Virtual optical network embedding*, introduces the importance of resource embedding in VONs. An optimized resource embedding arises of paramount importance in order to maximize the number of VONs that can be allocated in top of a physical network substrate, improving the usage of the available physical resources. In this context, the challenges when embedding a virtual optical network are identified. Next, multiple mechanisms to optimally embed VONs according to the underlying physical substrate technology and the characteristics of the VONs and services that will run on top of them are proposed and thoroughly evaluated.

Chapter 4, *Improving EONs efficiency: the split spectrum approach*, concentrates on enhancing the performance of EONs as a mean of providing a more efficient physical network substrate for the embedding of VONs. The particular focus is on the spectrum utilization of EONs. In order to improve the spectrum utilization of such networks, so more demands can be allocated, the Split Spectrum Approach (SSA) is proposed. To achieve the desired spectrum utilization, multiple techniques to perform the resource assignment in Split Spectrum (SS)-enabled EONs are presented. The benefits of the proposed solutions are quantified by simulations, comparing them against traditional resource assignment techniques in EONs. Furthermore, multiple implementations of the SSA are discussed and evaluated.

Chapter 5 *Energy efficiency in transport networks*, focuses on solutions for reducing the energy consumption on core optical networks. Energy efficiency has been widely recognized as an important target for the management of optical networks. As a consequence, it becomes highly desirable to provide a physical substrate more efficient in this regard

so less costly VONs can be deployed in top of it. To this end, multiple solutions are proposed. First, an end-to-end energy-aware routing mechanism for multi-domain transport optical networks is presented. Multiple simulations are done to evaluate the benefits of the proposal. Next, to further reduce the energy consumption of core optical networks, the concept of sleep-enabled transport networks is introduced. In order to asses the impact of such network architecture in terms of energy savings and connection blocking a Markov-based analytical model is developed.

Finally, chapter 6 summarizes this thesis and opens future lines of research.

Chapter 2

Towards dynamic and efficient optical network infrastructures

This chapter surveys enabling technologies and concepts to dynamic and efficient optical network infrastructures. To introduce, a glance at current optical network infrastructures is firstly taken. There, several network evolutionary steps are identified, ranging from first static optical networks to Automatically Switched Optical Networks (ASONs) defined by the ITU-T. This leads to conclude on the necessity for more dynamic and efficient optical network infrastructures to cope with emerging new services and the growth and high heterogeneity of the traffic on the networks. Aiming to provide a suitable framework for future optical network infrastructures, the concept of VON is introduced.

To this, the general paradigm of IaaS is surveyed. Although VONs appear as promising candidates to overcome the limitations of current optical infrastructures, their intrinsic dependence on the underlying physical network may result in a poor utilization of the available spectrum. In fact, the vast majority of nowadays optical transport networks is based on WDM for the purpose of bandwidth provisioning. In such networks, as the minimum granularity for serving a connection request is a wavelength, it means to dedicate the whole capacity of a wavelength for the connection, wasting the residual bandwidth of the wavelength.

Moreover, in order to accommodate very high bit-rate connections (the so called super-channels), several wavelengths have to be grouped and allocated according to the request. Since spectrum guard bands are necessary between wavelengths for de-multiplexing purposes, it results in a poor spectrum utilization. For these reasons, it is necessary to provide more spectrum efficient physical networks in order to fully realize effective VONs. In this regard, EONs emerge as a very promising candidate thanks to their finer spectrum granularity. To better understand the benefits of EONs, the evolution from fixed to elastic optical networks is surveyed, putting special emphasis on the resource allocation process to the connections.

Besides the spectrum efficiency, another key point in the development of next-generation optical network infrastructures relates to the energy consumption of the optical layer. As a matter of fact, with the increase of the traffic in core optical networks, the energy consumption on the networks is growing and may reach unsustainable levels if not taken care off. The third section of this chapter summarizes the efforts done during the last years in order to provide energy efficient optical networks along with the main challenges in the topic. Finally, last section summarizes main achievements of the chapter.

2.1 Evolution of optical network infrastructures: past and present

Over the past decade, optical network infrastructures have gone through an extensive and rapid evolution [Muk00, Alf12]. Figure 2.1 summarizes the evolution of optical networks through the years, highlighting the main traits of each evolutionary step. First optical networks were based on static point-to-point optical links connecting optical nodes mainly present in major cities. Although they provided high transmission capacities thanks to the emergence of WDM technologies [Hen90], where multiple wavelength channels were multiplexed into the same fibre link, such networks largely lacked any switching capability. Moreover, although the transmission between end points of a single fibre link was optical, the whole end-to-end path was not. In fact, all the traffic incoming to a node had to undergo an Opto-Electronic (OE) conversion in order to process the control data and switch the traffic data accordingly. Then, the outgoing traffic had to be converted again to the optical domain through an Electro-Optical (EO) conversion before the transmission. For these reasons, an optical transponder (TSP) was needed at each node for every incoming/outgoing wavelength channel, increasing substantially the cost and the power consumption of nodal equipment. Furthermore, as the bandwidth solutions were evolving to higher bit-rates, the electronic processing was starting to become an important bottleneck in terms of network scalability.

The recognition of this bottleneck imposed by electronic technologies was an important stimulus for the development of all-optical solutions, where the connection would remain in the optical domain through the whole end-to-end path connecting source and destination nodes. To better understand the value of all-optical transmission, let us put an example. For instance, it may happen that the link connecting two end-points carries much more traffic than what is just required between those two nodes, with the rest of the traffic coming from connections between other nodes for which the end-to-end paths include the end-points of the link. Since such traffic does not terminate on the remote end-point of the link, it would not be necessary to de-multiplex the associated wavelength channels but simply bypass such wavelength without any electronic processing involved. By distinguishing these two types of traffic, it would be possible to only de-multiplex the wavelengths destined for a particular node while the rest pass transparently through the

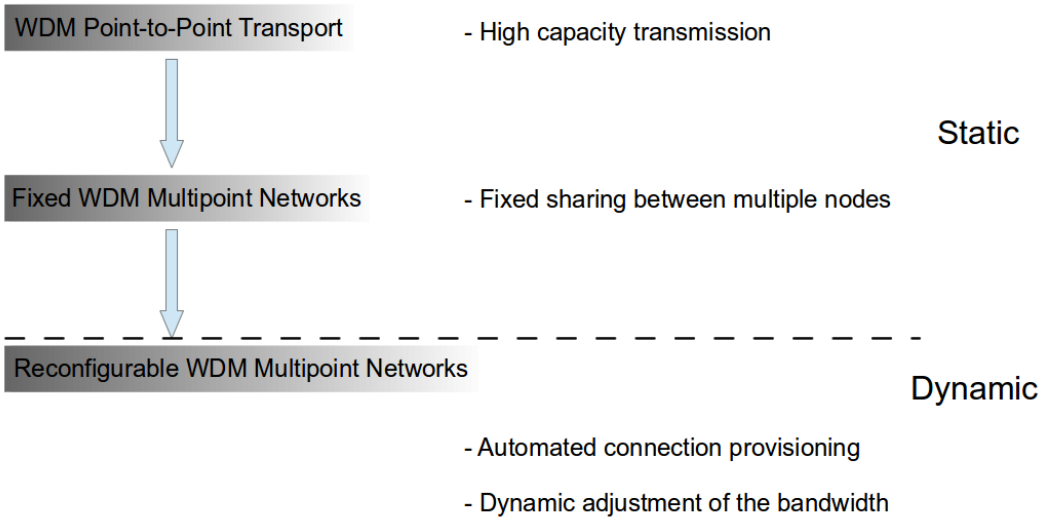

FIGURE 2.1: Evolution of optical networks.

node, thus reducing the need of electronic processing. As a consequence, the cost and power consumption of the node's equipment would be reduced as well as it would improve the overall scalability of the network.

The key element that enabled such functionality was the Optical Add/Drop Multiplexer (OADM) [TS06, ZM05]. When deployed into network nodes, OADMs allow for the local insertion/extraction of certain wavelengths to/from the network, while letting the remaining wavelengths to optically pass through the node. This removes the need to perform any electronic processing to the bypass traffic that does not end in the node, which in second generation multipoint optical networks arises as the majority of the total incoming traffic amount. An added benefit on the adoption of OADMs towards all-optical networks was that the time required to provision a new connection decreased significantly, as EO and OE conversion needed to only be done at the endpoints of the connections. Such technology advancements supposed a rapid development of multipoint optical network solutions.

As a first step in this direction, the Optical Transport Network (OTN) architecture was proposed by the ITU-T in [G.872]. The OTN architecture is intended to provide a general framework for the handling of different client signals while introducing switching, multiplexing, management and resilience functionalities directly in the optical layer. Moreover it introduced the importance of meshed topologies as a mean to provide better optical resource utilization as well the implementation of multiple resilience schemes. Since in meshed networks, any node can be connected directly to several other nodes, each node must not only capture and disseminate its own data, but also serve as hops for other nodes, that is, it collaborates in data transmission over the network. For this to happen, any node in the network should be able to capture the traffic terminating at the node while perform the switching and routing of the wavelength directly as they carry the high bit rate signals. Optical Cross Connects (OXCs) become the key devices in order to

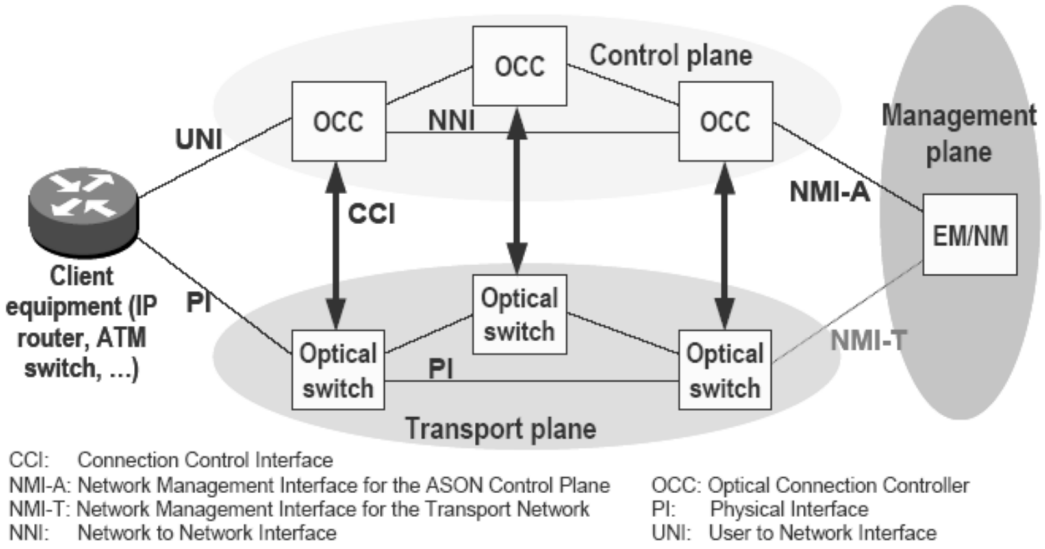

FIGURE 2.2: The ASON architecture.

enable such functionalities [OK98, TZT03]. Similar to OADMs, OXCs allow for a totally optical commutation of the signals coming from any incoming port to any outgoing port, thus eliminating costly electronic processing. For these reasons OTNs become very interesting candidates for an efficient transmission of end-to-end connections in WDM-based networks.

However, in OTNs the connection provisioning and release are still done in a manual fashion from a centralized Network Management System (NMS). Such manual operations can take very long times (hours or even days), resulting in a network architecture incapable to react to rapid traffic fluctuations or to provision bandwidth on-demand services to end-users. To overcome such limitations, a control plane is introduced in OTNs with the aim to automatically provision and release connections over the physical network, providing a more dynamic optical network architecture. In this regard, the ASON architecture, as defined by the ITU-T in [G.8080], arises as the leading architecture for the management and control of all-optical transport networks.

In order to provide intelligence to the network, the ASON architecture (Figure 2.2) defines the control plane functional modules and related interfaces, enabling functionalities such as resource discovery, routing or signalling. To this end, a routing controller module at each control plane node (called Optical Connection Controller (OCC)) maintains the current state of all resources in the network. With this information, the computation of the valid routes between source and destination is done. Next, the OCC module utilizes these computed routes to disseminate the control information in the network in order to create, maintain and release the connection. To enable the communication between OCC modules, the Network-to-Network Interface (NNI) is utilized. In turn, a resource manager module keeps the state of the local resources. Besides, it is also responsible for configuring the related optical node through the Connection Controller Interface (CCI). Finally, a

call controller module is also defined in the OCC, which accepts or rejects connection requests coming from the end-user domain through the User-to-Network Interface (UNI).

Although the ASON architecture provides many advantages, such as automatic connection provisioning, thanks to the inclusion of an intelligent control plane, as the traffic on the networks grow, paired with an increase of network devices, such architecture will unlikely meet new requirements, particularly in terms of flexibility. Moreover, with the emergence of new services and paradigms that require the provisioning of both network and Information Technology (IT) resources and very specific rules so as to guarantee a proper Quality of Service (QoS), it becomes more and more challenging for a single control plane technology to handle such heterogeneity on the services that must be controlled and provisioned through it. Since the control plane is linked to the data plane by an internal network, handling change is difficult because each change to the physical infrastructure requires a corresponding modification to the control plane, such as reconfiguring the tunable parameters in the routing protocols. New management strategies are needed because service and infrastructure providers must ensure operational simplicity in planning, engineering, deployment, and operation of services and networks in order to reduce associated OPEX while improving network performance. Addressing all of these challenges with current infrastructures and technology practices could lead to unmanageable networks for operators aiming to maximize fibre capacity and service reconfigurability.

The emergence of these new services and paradigms would require to provide to the end user some control over the applications so as to offer a proper Quality of Experience (QoE). However, with nowadays optical infrastructures it is not possible since they are completely managed by the operators that own them, with end user having no control over the infrastructures nor the services and applications that run on top of the physical infrastructures. A possible way to overcome such limitation would be to decouple the service and application layer from the physical infrastructure layer and then exposing to the end user the necessary tools to control the services by proper interaction with the physical devices. Such functionalities would require sophisticated middleware layers, enabling the abstraction of the physical substrate for control by the end user.

Furthermore, nowadays service providers base their business in renting physical infrastructures to the operators and then offer services on top of them to end users, since physical infrastructures are very expensive to build and maintain. In this sense, physical operators are the responsible for the deployment, management and maintenance of the infrastructures while service providers are relegated to exploit the connectivity and IT services leased by operators, without any control over them. Such business model makes it difficult to have adequate prices and control over the whole infrastructure used to provide services. Furthermore, it becomes impossible to perform any dynamic management of the rented infrastructures in order to adjust to the traffic patterns or optimize the use of the resources.

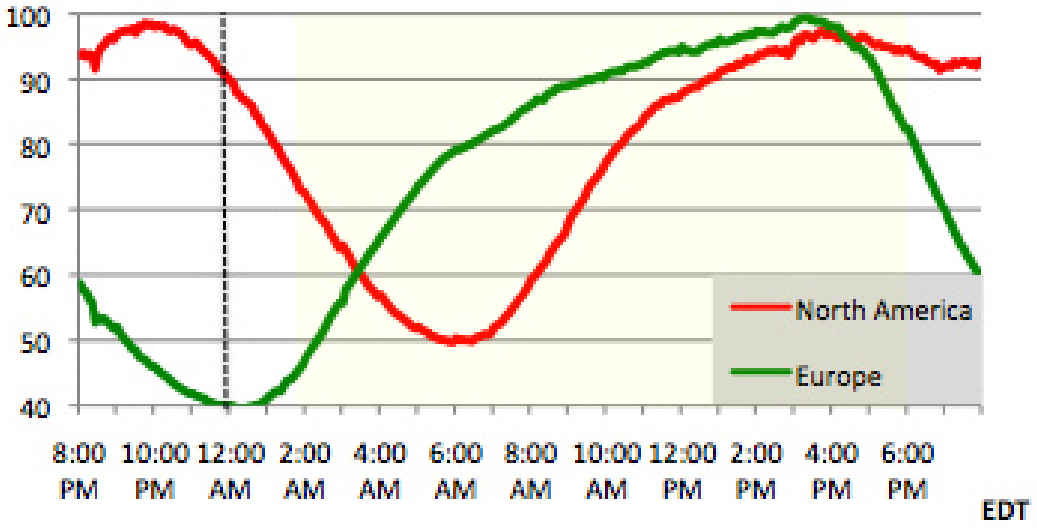

FIGURE 2.3: Daily Internet traffic pattern [ARB].

Besides the need of more dynamic management and control of the infrastructures in order to meet the requirements of new services and applications, another key point that drives this evolution towards more customizable optical infrastructures arises from the necessity to optimize the utilization of the physical resources. Nowadays physical infrastructures are build and planned to support a peak traffic during the daily utilization so as to guarantee that during high periods of traffic the blocking probability of the connections remains very low. As the traffic on the networks growth and their capacity starts to be exhausted, new resources have to be deployed on the network so as to absorb the new peak traffic [NS03, ZSiL10]. Such upgrade strategy, based on traffic growth models, is the nowadays common strategy followed by network operators in order to guarantee that all the traffic flowing through the network can be absorbed, resulting in a proper service of the connections.

Although such approach on the dimensioning of the infrastructures guarantees that all traffic through the day will be properly served, it usually results in an overdimensioned physical infrastructure. To exemplify this, Figure 2.3 depicts the daily Internet traffic pattern on both Europe and North America, representing for each time of the day the traffic volume respect to the peak. It can be seen that important differences are found between peak hours and valley periods in terms of traffic volume: around 50% and 60% for Europe and North America, respectively. Since networks are usually dimensioned to support the traffic at peak periods, it means that during the rest of the day, a substantial amount of resources is not utilized. This translates for both network operators and services providers into a poor cost efficiency of the infrastructures, since they are only used at full capacity during short periods of time. In order to improve the utilization of the infrastructures, network operators could lease their infrastructures to multiple service providers or deploy on top of them several services at once for a better filling of the underlying physical infrastructure. As for service providers, a more on-demand

bandwidth and/or infrastructure provisioning from the operator would allow for better adjustments on the rented infrastructure so as to fit dynamic traffic patterns, thus saving costs. Nevertheless, such functionalities are hard to implement with nowadays optical infrastructure architectures.

For all these reasons, in order to build the future optical network infrastructures, it is necessary to define new architectures and paradigms that will allow for the co-existence of vastly heterogeneous services on top of a physical infrastructure, with the possibility to finely control and manage the infrastructures that will support them. The following section will detail potential solutions to enable such optical infrastructures.

2.2 Dynamic optical infrastructures

The previous section summarized nowadays optical network architectures and identified their main drawbacks, being the main one the limited reconfigurability of the network in order to adapt to highly dynamic traffic patterns and to the heterogeneity of the services that run on top of the network. To overcome such limitations, more dynamic and efficient optical network infrastructures have to be designed. A key enabling concept towards dynamic optical network infrastructures is the concept of IaaS and more specifically the concept of VN or Virtual Infrastructure (VI). This section is devoted on describing such concepts, highlighting their benefits and why they are promising candidates for future dynamic optical networks and infrastructures. To this end, first the concept of IaaS is described as well as the concept of VIs in general. Next, VONs are introduced as the mean to realize the IaaS concept in the optical domain.

2.2.1 IaaS: concept and benefits

The aforementioned technical, management and operational complexities, coupled with the inability to react to very dynamic traffic patterns in an efficient way, may limit the ability of operators and service providers to support new services for their customers. Thus, it becomes crucial to be able to deploy and support new services quickly and easily, with minimum manual intervention, hardware deployment, or complex engineering processes. IaaS [NCL13, KFW+14] has been introduced to meet such new management and operational requirements. The rational behind of IaaS is to offer physical infrastructures from an operator as a service for exploitation by third party entities, giving the possibility to fully configure and manage the rented infrastructures as if they were owned by those external entities. Additionally, IaaS is envisioned as a way to compose highly customizable and very specific infrastructures by merging physical resources from diverse natures, such as network resources, storage or computational capacities. The key enabling technology in order to realize this is the virtualization of the physical infrastructures. Thanks

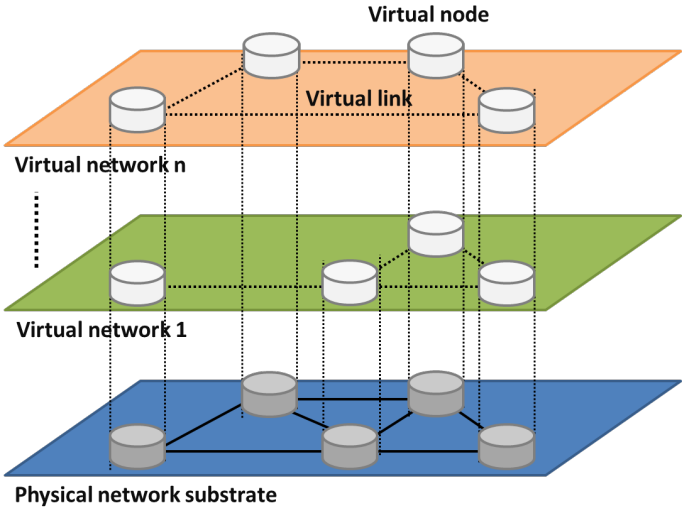

FIGURE 2.4: Example of IaaS.

to virtualization, it is possible to slice an underlying physical infrastructure into multiple virtual elements. Then, by federating and composing such virtual elements it is possible to create VIs with very specific requirements, both in terms of resource characteristics and management and control. Thus, such approach allows service providers to create their underlying service infrastructures by acquiring resources from different providers on an as-needed basis. Moreover, it allows for physical infrastructure owners for a better resource usage of their infrastructures, since multiple isolated VIs may coexists on top of the same physical infrastructure (see Figure 2.4).

As it can be seen, there are many advantages to the IaaS concept and relevant virtualization techniques. It mainly brings new business models and a potential optimization of the physical infrastructure resources transparently to users. The main benefits for operators and service providers are summarized as follows.

- **Better scaling of the management and services.** IaaS allows an infrastructure to start small and scale according the services that are provisioned on top of it in a rapid and efficient manner, since virtual resources can be requested and decommissioned on-demand. Moreover, creating smaller VIs dedicated to specific services allows a better management of the individual infrastructures when compared to the case where a big and multi-purpose infrastructure is employed to accommodate multiple services at once.

- **Lower capital and operational costs.** Service providers require some network and IT infrastructures in order to develop their activities. However, physical infrastructures are expensive to deploy and maintain. Hence, traditionally service providers rent some connectivity services to network operators. Nevertheless, this presents the drawback of not having the opportunity to do management and control operations as they would do if the infrastructure was owned by them. With IaaS, it

is possible to rent fully manageable and controllable virtual infrastructures, reducing the infrastructure costs. Moreover, since most of the infrastructure operation and control is done by service providers, it allows for a reduction of the operational costs of the shared infrastructures for the physical infrastructure operator.

- **Programmable infrastructures and ease of upgrade.** Emerging services require for a tight integration of all layers up to the application level for an optimized QoS. This requires the possibility of extending network and infrastructure devices functionalities. Thanks to IaaS and virtualization, this approach of programmable virtual infrastructures is possible. Moreover, thanks to the decoupling of the services and the infrastructure, it is possible to upgrade the services by modifying the properties of the virtual elements in a fast and efficient way, without experiencing disruption of the services.

- **Enable new business models.** With IaaS, current infrastructure owners can increase they revenues by offering unused parts of their infrastructure to service providers with no infrastructures. In this way, new business models can appear, where specialized infrastructure owners build, deploy and maintain the physical infrastructures (network and IT) and specialized service providers control and manage the virtual partitions of these physical infrastructures in order to offer services to the end users. This opens new roles on the telecommunication market. Papers in the literature as [PSV09] and some European projects investigating the subject of virtualization, such as GEYSERS [TAG+14] have identified the following main roles regarding the new business model to be adopted in this context: 1) *Physical Infrastructure Provider* (PIP), which is the owner of the physical substrate, over which virtual networks will be provided. The PIP offers parts of its infrastructure as a service to be exploited by external entities to develop its own business models; 2) *Virtual Infrastructure Provider* (VIP), which is the client of the PIP. By renting resources from multiple PIPs, it composes VIs in order to offer them as a service; 3) *Virtual Infrastructure Operator* (VIO), which is the client of the VIP and the responsible to offer services to the end-users by managing the VI rented to the VIP. Through a proper control plane, it can manage the VI depending on its needs; and 4) *Consumers*, which are the end-users of the services that are offered through the VIs. Nevertheless, these roles may overlap, such as the VIP also being the VIO.

- **Federation and integration of multiple infrastructures.** Multiple resources coming from different administrative domains can be integrated into the same VI, thus federating disparate resources under the same domain which is managed by a single service provider. These eliminates inter-domain issues, since the whole infrastructure and the resources composing it are under the same administrative domain. Moreover, it allows for a seamless composition of very heterogeneous resources into a unique and cohesive VI.

As it can bee seen, IaaS offers many interesting possibilities, arising as a strong candidate to enable the future telecommunication infrastructures. In this process, virtualization becomes the key in order to realize all the promises and enable all the functionalities of IaaS. When applying virtualization to a physical device, a logical representation of it is created, which then can be partitioned into several virtual devices offering the same behaviour as the physical device but logically separated, keeping isolation between multiple VIs sharing the same physical device. Although each one of the partitions has its administrative domain, the virtualization creator keeps the ownership and responsibility for the whole physical device, but not its services management or configuration. The following sub-section discusses about the virtualization of physical infrastructures.

2.2.1.1 Infrastructure and network virtualization

The concept of virtualization was introduced in the IT realm by IBM in the 1960s [PPTH72, Gol74]. They introduced the Virtual Machine (VM), as result of introducing a virtual layer between hardware and software layers. This allowed the abstraction of portions of an underlying physical resource, so that an end-user could directly interact with a portion of this resource, while perceiving it as a single real resource. As a result, it was possible to run multiple autonomous and isolated VMs in top of a single shared physical machine, each one having its own resources and running its own operating system and applications, which can be different from the ones of the host physical machine. Additionally, VMs can be dynamically provisioned when and where they are needed, enhancing the physical resources utilization.

Network virtualization extended this concept from individual nodes or resources to data communication networks resulting in the advent of the so called Virtual Private Networks (VPNs). VPNs [KK04] where initially thought as a way to provision logically separated private networks over a public infrastructure by tunneling data traffic between geographically distant sites. Depending on the protocols used by the data plane, VPN can be roughly classified into Level 1 VPNs, Level 2 VPNs, Level 3 VPNs or Higher-layer VPNs.

At all layers, VPNs pursue the same goal: the provisioning of connectivity services between far off sites (see Figure 2.5). The network operator owning the physical infrastructure establishes the connections composing the VPN and provides them together as a connectivity service to the client. Note that VPNs are completely limited to the delivery of connectivity services among geographically distributed sites over a data network, being all the connections established and managed by the network owner. This results in a client-server relationship, where clients of a VPN can only request more resources for the point-to-point links among the Provider Edge (PE) devices where their Costumer Edge (CE) devices are attached.

An evolution of the VPN is the VI or VN paradigm, which results in one step ahead on the evolutionary path towards the next-generation Internet. Such paradigm pleads for a

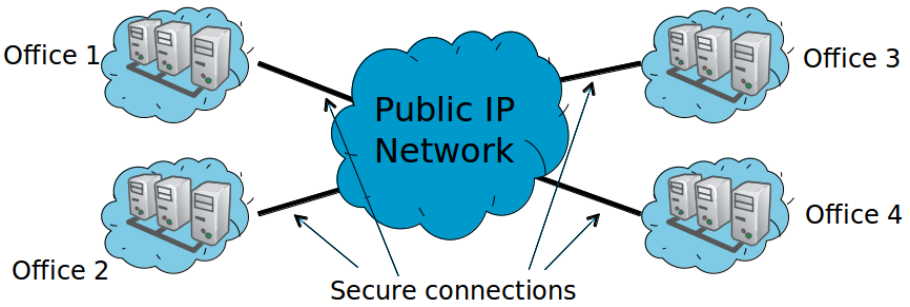

FIGURE 2.5: Example of VPN.

more disruptive approach, where network owners can offer parts of their infrastructures as services to external service providers, so that they are completely free to manage them to offer end-to-end services to final users. It aims at introducing the essentials of virtualization to not only computers (such as with the case of VMs) but to all devices of an underlying physical infrastructure. In a few words, VIs are slices (partitions) of the physical infrastructure, which are offered as a service to the client. In such a paradigm, the client is not restricted to only use the bandwidth of some connections, but can also interact with the underlying physical equipment to configure it as if it was of their property. The main idea consists of creating several co-existing logical infrastructure instances, each one with its own topology and resources, over a shared physical substrate.

Although virtualization techniques are quite mature for some type of physical devices (e.g. computers), the application of virtualization to generic devices is still a challenge. A first challenge comes from the fact that, in order to virtualize a physical device, it is needed to somehow abstract the relevant properties of the device, which then will be used to create software representations (virtual devices). Software Defined Infrastructures (SDIs) [KFW+14] and Software Defined Networks (SDNs) [ONF] offer a framework that allows for the abstraction of underlying physical infrastructures through proper information models and then the composition of the abstracted physical devices into complex virtual objects, thanks to suitable virtualization protocols (e.g. OpenFlow [LKR14]) or software platforms (e.g. OpenDaylight [Ope]). For example, OpenFlow, which is based on flow switching, allows for the capability to execute software/user-defined flow-based routing, control, and management in a controller outside the data path, effectively creating virtual objects with the desired characteristics.

Besides the abstraction and composition of virtual objects, a VI must also be composed of a virtual control plane (e.g. [LZT+13], with the purpose of providing the required independent and full control functionalities (i.e., optical connection provisioning, traffic engineering, protection/restauration, etc.). As virtual objects are software abstractions of physical devices, a virtual control plane is the software realization of a more generic control plane technology (e.g. Generalized Multi-Protocol Label Switching (GMPLS), OpenFlow), tailored to the specific needs of the VI. Coupled with management and orchestration modules, the virtual control plane allows for the dynamic management of

a VI, adjusting the characteristics of the infrastructure to the services that run on top of it.

2.2.2 Virtual optical networks

Virtualization techniques have been historically employed in Layer2/3 networks (e.g. Ethernet, IP). However, the increasing bandwidth requirements of the applications that run over the Internet, jointly with the need to offer a transport network more efficient in terms of energy utilization and resource cost, are the driving reasons for most of the transport network owners to migrate their electrical backbone infrastructures towards the optical domain [LGF+06]. For this reason, many efforts are being devoted on bringing virtualization to the optical domain [NEPS11], so as to create VIs and VNs that fully exploit the benefits of optics in terms of high capacity and energy efficiency.

As in electrical networks, the general framework of SDN is being utilized in order to compose VONs. By developing the proper extensions to virtualization protocols (e.g. OpenFlow), it will be possible to slice an optical device into multiple virtual devices (Figure 2.6.a) or agglutinate multiple physical devices so as to compose an integrated virtual device that unifies their properties (Figure 2.6.b). However, the virtualization of optical infrastructures poses several challenges.

For instance, when creating virtual optical elements, the presence of the Physical Layer Impairments (PLIs) can create several problems, such as the resulting virtual device being interfered for other virtual devices obtained through the same physical device due to non-linearities of the optical medium. This comes from the analogical nature of the optical medium, which difficults separating or composing effectively from physical devices when compared to the digital nature of electrical networks. This problem is tightly related to the resource allocation in VONs. The well known Route and Wavelength Assignment (RWA) problem of optical networks comes in the arena when assigning physical resources to virtual ones, complicating the whole resource assignment problem. Solutions to this challenge will be discussed later on during chapter 3.

Other potential challenges that appear when trying to bring virtualization in the optical domain are:

- Definition of a unified optical transport and switching granularity (i.e., optical flow) that can be generalized for different optical transport technologies (Optical Circuit Switching (OCS), Optical Packet Switching (OPS), etc.) and be compatible with electronic packet switching technology.
- Design and implementation of an abstraction mechanism that can hide the heterogeneous optical transport layer technology details and realize the aforementioned generalized switching entity definition.

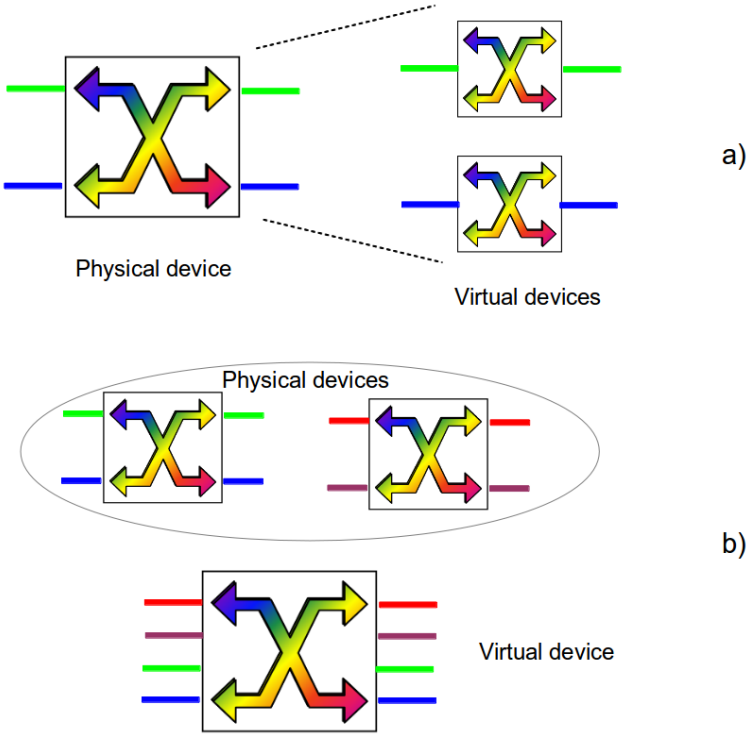

FIGURE 2.6: Creation of virtual OXC by means of a) slicing a physical device and b) composing multiple physical devices.

- Cross technology constraints for bandwidth allocation and traffic mapping in networks comprising heterogeneous technological domains. This plays an important role in provider networks where multiple operational units are consumed to maintain different technology domains.

Despite these challenges, VONs are strong candidates for the realization of future telecommunication infrastructures, combining both the flexibility and adaptability of IaaS and the high bandwidth provision of photonic technologies.

2.3 From fixed to elastic optical networks

Besides the importance of having a flexible enough optical infrastructure to fit the requirements of the services and that can be dynamically tuned to match the variability of the applications and paradigms that will run on top of them, it is necessary to also provide an equally flexible network in terms of bandwidth assignment to fully realize the promises of such flexible optical infrastructures. Nowadays optical networks are based on Dense Wavelength Division Multiplexing (DWDM) as standardized by the ITU-T, which may allow up to 100 Gb/s per wavelength channel. Thanks to the various advancements over the past years, DWDM optical networks provide many advantages, such as cost effectiveness as well as automated provisioning of end-to-end optical connections, i.e.

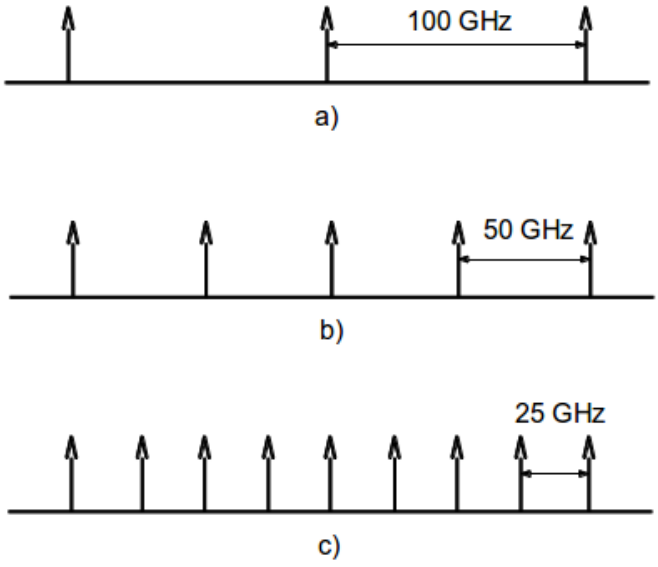

FIGURE 2.7: ITU-T DWDM frequency grid with channel spacing of a) 100 GHz, b) 50 GHz and c) 25 GHz.

lightpaths. However, the employed spectral grid standardized by the ITU-T in [G.694.1] and its rigid granularity limits to a great extent their bandwidth utilization. Specifically, current ITU-T DWDM grid is anchored to 193.1 THz and supports various channel spacings, particularly, 25, 50 and 100 GHz (see Figure 2.7). In such a grid, the central optical frequency of a channel can be determined as $193.1 + n \cdot f_{cs}$ THz, where f_{cs} represents the channel spacing and n is an integer representing the grid frequency number. This central frequency will then be employed to provision the requested bandwidth of a lightpath, allocating half of it to the right and left side of the central frequency, respectively, along with the necessary guard bands between channels to allow a correct switching of the signals.

Although decreasing the channel spacing, as depicted in Figure 2.7, allows for a better spectrum utilization thanks to the guard bands between channels being smaller, such rigid spectral grid results in a very poor spectrum utilization, specially when accommodating sub-wavelength connections or when needing to construct very high bit-rate connections (super-channels). To exemplify these limitations, Figure 2.8 depicts both situations. Current DWDM networks allocate a full wavelength channel to a lightpath. If the traffic demand is not enough to fill the entire capacity of the wavelength (sub-wavelength), it results in the rest of the capacity of the wavelength to be wasted, since it cannot be utilized by other traffic demands. On the other hand, when needing to allocate a traffic demand whose capacity is greater than the actual capacity provided by a single wavelength (super-channel), it is necessary to allocate multiple independent wavelength to the demand. Since spectral guard bands are necessary between adjacent wavelength channels for switching purposes, such operation results in significant spectrum overheads.

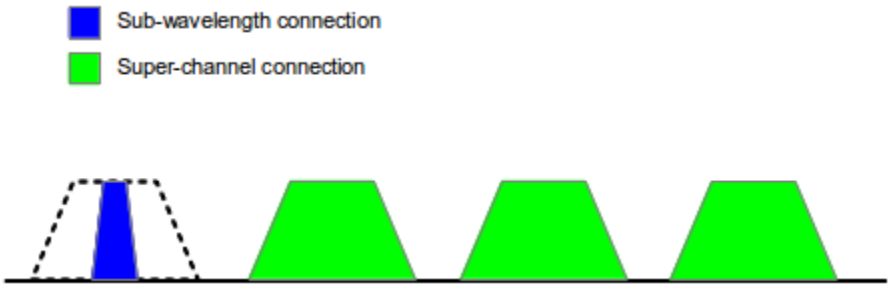

FIGURE 2.8: Spectrum assignment in a DWDM optical network.

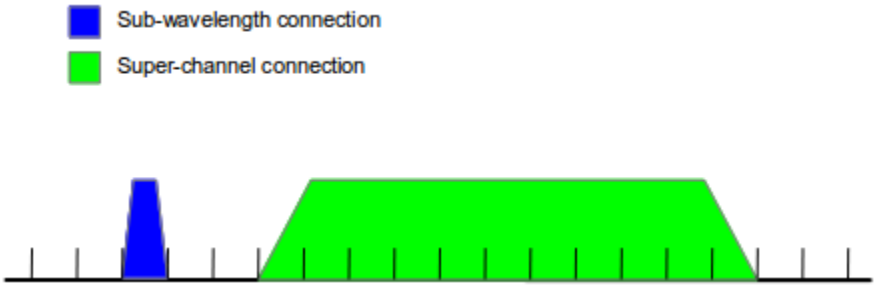

FIGURE 2.9: Spectrum assignment in an EON.

To overcome such limitations, a novel spectrum efficient and scalable optical transport network was proposed in [JTK+09]. Such architecture, known as EON, allows for the allocation of an appropriately sized portion of spectrum to fit the requirements of a connection. To do so, instead of relying to a rigid frequency grid as the one standardized by the ITU-T for WDM networks, the concept of Frequency Slot (FS) is introduced. According to this idea, the available spectrum in an optical fibre link is discretized into smaller spectrum units (e.g. 6.25 GHz) known as FSs. For example, an optical spectrum of 1, 2 and 5 THz would correspond to 160, 320 and 800 FSs available per fibre link, respectively.

In this regard, contrary to the rigid bandwidth allocation of DWDM networks, the spectrum assigned to a connection in an EON may grow or shrink according to the traffic volume and the requirements of the connection by allocating enough contiguous FSs. Such feature allows for a greater efficiency in the spectrum utilization and a better scalability of the network, either when serving sub-wavelength or super-channel connections, by tightly tailoring the allocated spectrum to the specific demand requirements (see Figure 2.9).

Such elasticity and flexibility regarding the bandwidth allocation may be achieved thanks to two important technology advancements. The first one is the optical Orthogonal Frequency Division Multiplexing (OFDM) [ZLMM13]. Thanks to optical OFDM it is possible to allocate a variable number of low symbol-rate sub-carriers in order to allow the transmission of a connection matching its exact requirements in terms of bandwidth needs. Moreover, due to their orthogonality properties, adjacent sub-carriers may overlap in the frequency domain, enabling for a better spectral efficiency. Furthermore, by adjusting the

symbol-rate of the OFDM signal, it is possible to overcome the limitation posed by the PLIs [KTJ10]. The other major technology advancement are Bandwidth Variable Wavelength Cross Connects (BV-WXCs) and Bandwidth Variable transponders (BV-TSPs) [NNR+14, KTJ10]. Thanks to BV-TSPs, it is possible to transmit an OFDM modulated signal from source to destination with the desired bit-rate in order to accommodate a demand request, while BV-WXCs allow for the cross-connections with the corresponding spectrum in every intermediate node along the end-to-end route, efficiently switching the connection. All these technologies are the ones that enable the elastic bandwidth transmission in EONs.

However, although EONs provide significant benefits when compared against traditional WDM-based optical network, they also pose significant challenges, specially when assigning resources to lightpaths. The following sub-section discusses about the assignment problem in EONs in what is known as the Route, Spectrum and Modulation Level Assignment (RSMLA) problem in the literature. To better understand the new challenges that appear in the RSMLA problem, a brief introduction of the RWA problem in WDM networks is presented.

2.3.1 Route, spectrum and modulation level assignment

In order to transmit data from one node to another on an optical network, it is necessary to establish a connection on the optical layer. In WDM networks, such connection, known as lightpath, can be realized by determining a path in the network between the two nodes and allocating a free wavelength on all fibre links than span the end-to-end path. One important point in such process is to guarantee that no two lightpaths that share a physical link use the same wavelength on that link, otherwise the two connections would collide in the frequency (wavelength) domain. Additionally, in the absence of wavelength conversion, it is necessary to provision the same wavelength on all links that span the end-to-end path, which is known as the *wavelength continuity constraint*. The problem of how to assign the path and wavelengths to properly accommodate a lightpath in a WDM network is known as the RWA problem and has been widely studied in the literature [OB03, RS95].

The RWA problem can be categorized mainly into: 1) static and 2) dynamic. In the static case (e.g. [CMV10]), the entire traffic matrix between all network nodes in known is advance. In such scenario the objective is to serve all the connections among all node pairs while minimizing the necessary number of resources (e.g. wavelengths per fibre link) to properly accommodate all lightpaths. Conversely, an alternative goal would be to set-up the maximum possible of lightapths from a known set given a network with limited resources. Typically, in order to obtain the optimal solution in the static case, Integer Linear Programming (ILP) formulations are employed [ZJ00]. However, such approaches are very time consuming. Alternatively, the RWA problem can be divide into

two sub-problems: 1) the routing sub-problem and 2) the wavelength assignment sub-problem. Then, exact methods can be applied to solve the two sub-problems separately or apply heuristics in order to find fast and near optimal solutions. On the other hand, in the dynamic scenario, the whole traffic matrix is not known in advance but connections arrive to the network one by one in a random fashion and are released after some time [CL05]. In such circumstances, the typical goal is to minimize the blocking probability of the connections. Due to the dynamic nature of this scenario, ILP-based solutions are not suitable. Therefore, in dynamic RWA algorithms, the use of heuristic mechanisms is the common choice.

As was discussed above, EONs introduce a way to discretize the spectrum into smaller units called FSs. Then, by assigning the necessary number of contiguous FSs to a connection, it is possible to stablish an end-to-end spectrum path, i.e. lightpath, to satisfy the exact requirements of the connection. At first, this whole assignment process, may seem to share some similarities with the aforementioned RWA problem in WDM networks. For instance, in transparent EONs, the same spectrum portion must be provisioned in all links along the end-to-end path (*spectrum continuity constraint*). Moreover, the whole assignment process must guarantee that two or more lightpaths that share a physical link are allocated into completely disjoint spectrum portions in that link, in what is known as the *spectrum clashing constraint*. However, the fact that lightpaths in EONs have to be provisioned into contiguous spectrum portions, due to the necessity to transmit several adjacent OFDM sub-carriers to form the optical channel, makes the whole assignment process substantially different and more difficult than in WDM networks.

The problem of assigning resources to lightpaths in an EON is known in the literature as the Route and Spectrum Assignment (RSA) problem [CTV11, KW11]. Similar to the RWA found in WDM networks, the RSA problem is devoted to find the most appropriate route and spectrum portion for every optical connection that have to be set-up in the network. The main difference with respect to the RWA problem is that in EONs connections instead of requesting a number of wavelengths, they request for a contiguous number of FSs tailored to their needs. This constraint, known as the *spectrum contiguity constraint*, makes the RSA problem more difficult to solve and treat than the RWA problem, specially in scenarios with demands requesting heterogeneous sizes of contiguous spectrum portions, i.e. number of FSs. In such circumstances, for a demand that requests S FSs, once a particular FSs has been chosen as the first indexed slot for the demand in a particular end-to-end path, the following $S-1$ FSs have to be assigned to that demand. However, due to the heterogeneity of the sizes of the demands can happen that there is not enough room to fit exactly the desired number of contiguous FSs. Such phenomena, known as spectrum fragmentation, is one of the main challenges when facing the RSA problem, specially in dynamic scenarios [MFS14]. More details about the problem and the techniques proposed in the literature to overcome its limitations will be discussed during Chapter 4.

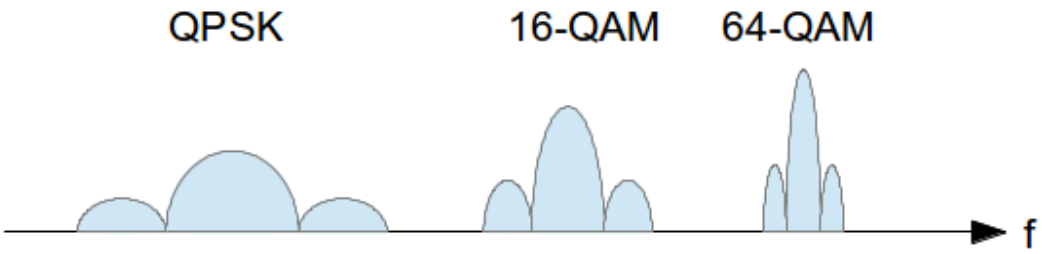

FIGURE 2.10: Example of modulation formats' spectral widths.

As in the RWA problem, the RSA problem can be solved employing exact ILP formulations, such as the ones presented in [KW11]. However, the mathematical representation of the spectrum contiguity constraint requires a series of complex constraints that complicate to a great extent the solution of the problem, increasing considerably the execution times of ILP-based techniques. For this, several heuristic approaches have been proposed in order to solve more efficiently the RSA problem in EONs. In this regard, like in the WDM case, the problem is further divided into two sub-problems: 1) routing and 2) spectrum assignment. For the routing sub-problem, the same techniques that have been applied in RWA heuristic mechanisms are usually employed. As for the spectrum assignment sub-problem, novel assignment heuristics have been proposed in the literature in order to match the particular challenges of the problem [ZLMM13]. However, such two-step approaches may lead to poor results. To this end, heuristic mechanisms aiming to attack jointly the two phases have been proposed (e.g. [WWH+11]).

As a mean to enhance the RSA problem and reflect more accurately the actual resource assignment that happens in an EON, the RSMLA problem has been presented in the literature [KWJ11, RTPG13]. Aside from the route and the spectrum portion, the RSMLA problem also seeks to find the most suitable modulation format to be assigned to the connections in order to reach the destination node. This becomes specially important since BV-TSPs in EONs are capable to transmit various modulation formats (e.g. SP-BPSK, PS-QPSK, etc.) depending on the desired bit-rate and the distance between source and destination. Because different modulation formats may occupy different spectral widths (see Figure 2.10) and, as a consequence, different number of FSs, the choice of the modulation format impacts directly in the overall spectrum occupation of the network. For this reason, in order to ensure that all lightpaths in a EON are properly allocated, the choice of the modulation format arises of paramount importance. Nevertheless, such selection adds another dimension on the whole assignment aspect, increasing even more the complexity of the problem.

2.4 Energy efficient optical infrastructures

Energy-efficiency has been widely recognized as an important target in the management of optical WDM networks. As the traffic on Internet grows, it is forecast that in three years

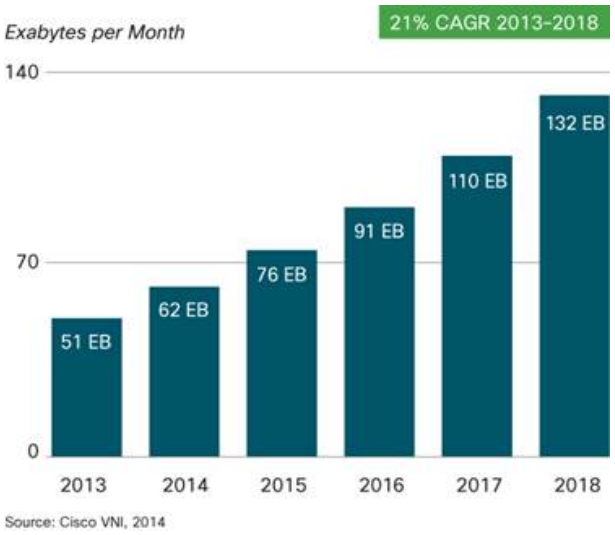

FIGURE 2.11: Overall IP traffic growth forecast [CIS]

from now, the global IP traffic will increase almost twofold (see Figure 2.11). Looking at today's optical networks, access networks represent around 70% of the overall power consumption of telecommunications networks, while core networks represent about 15% of it. However due to this traffic growth, the power consumption in telecommunications networks will increase almost threefold by 2017 [HBF+11], with access and core networks accounting for around 38% and 42% of such power consumption, respectively [LKWG11]. Although WDM-based core optical networks have helped reducing the energy consumption in telecommunications networks by allowing large amounts of traffic to bypass core routers through optical switching, due to the said forecasts it becomes crucial to reduce the energy consumption in core networks for the future optical network infrastructures.

Nevertheless, the energy-efficient optical network is a fairly new concept, which have been investigated during the recent years, becoming a hot topic among the research community in optical networks. The energy efficiency in optical networks can be addressed roughly in two levels: components and network [JZZ+14]. At the component level, highly integrated optical components as well as energy efficient transmission systems as a whole can help on reducing the energy consumption substantially. On the other hand, energy-efficient resource assignment mechanisms and green routing algorithms, among other strategies, are being investigated in order to reduce the energy consumption at the network level.

Due to the network size increase, fostered by the growth of the traffic, it becomes more and more important to fully exploit the potential of all-optical switching, specially in core networks, where the power consumption will significantly grow during the future as commented previously. In core networks, the energy is mostly consumed in transmission and switching equipment, resulting in huge amounts of energy consumed [BAH+09, DLEGE12]. However, nowadays optical network infrastructures do not take

into account the energy efficiency aspect, resulting in very power hungry optical networks. For this reason, many research efforts are focused on energy efficient core optical networks.

A first approach to energy efficient optical core networks consist on the design of green or energy-aware routing algorithms. Such routing algorithms incorporate the energy consumption of the network equipment during the routing process so the routes and wavelengths assigned to the connections will entail the minimum energy consumption [MAV13, CLVM11a]. As a consequence, energy-aware routing algorithms can save large amounts of energy when compared to traditional Shortest Path (SP)-based or non-energy-aware algorithms. A key point on energy-aware routing algorithms is traffic grooming, in which multiple low bit-rate requests are groomed into a high capacity lightpath. Energy-aware traffic grooming techniques can reduce substantially the energy consumption of connections by avoiding to power up additional equipment in the network when serving a new incoming connection [ZX14]. For a better understanding, Figure 2.12 depicts an example of energy savings in a core network thanks to traffic grooming. In sub-figure 2.12.a, two previously established lightpaths from node 1 to 2 (L_1) and 4 to 1 (L_2), respectively, are supporting each one a connection request from the source to the destination nodes of the lightpaths (R_1 and R_2). In sub-figure 2.12.b, a new connection request from node 4 to 2 has to be established (R_3). If a SP-based routing algorithm is employed to assign resources to the connection, a new lightpath L_3 will have to be established in order to support request R_3. To do so, it would be necessary to power-up new equipment at both source and destination nodes (e.g. TSPs) as well as along the end-to-end path (e.g. amplifiers), increasing the energy consumption of the network. However, R_3 could be served employing the already established lightpaths L_1 and L_2 by grooming the request sequentially in these lightpath (sub-figure 2.12.c), avoiding to power-up extra equipment, thus, reducing the energy consumption in the network.

However, although energy-aware routing algorithms may alleviate the growth of the energy consumption in core optical networks, it is not sufficient to compensate such increasing trends. In light of these, it is necessary to develop other strategies to further reduce the energy consumption in core transport networks. A second major strategy for reducing the energy consumption in core optical networks consists on selectively turning off network elements when they are not carrying traffic (specially during low load periods) while maintaining the rest of the network powered on to support residual traffic [CLVM11b, JMST13, RMT13]. In this regard, two main approaches are present in the literature: 1) power off OE devices, namely TSPs and regenerators (REGs); and 2) power off optical amplifiers in fibre links. For the first approach, as usually networks have some degree of redundancy, it is possible to completely turn-off nodes when they are not source or destination of some connection nor they are essential to perform bypass function. However, such approach would entail a significant control plane burden in order to manage the dynamic power states of the nodes according to the current traffic on the network to efficiently save energy during low traffic periods. In a similar manner, the second approach aims at switching off optical amplifiers on links in the network to save

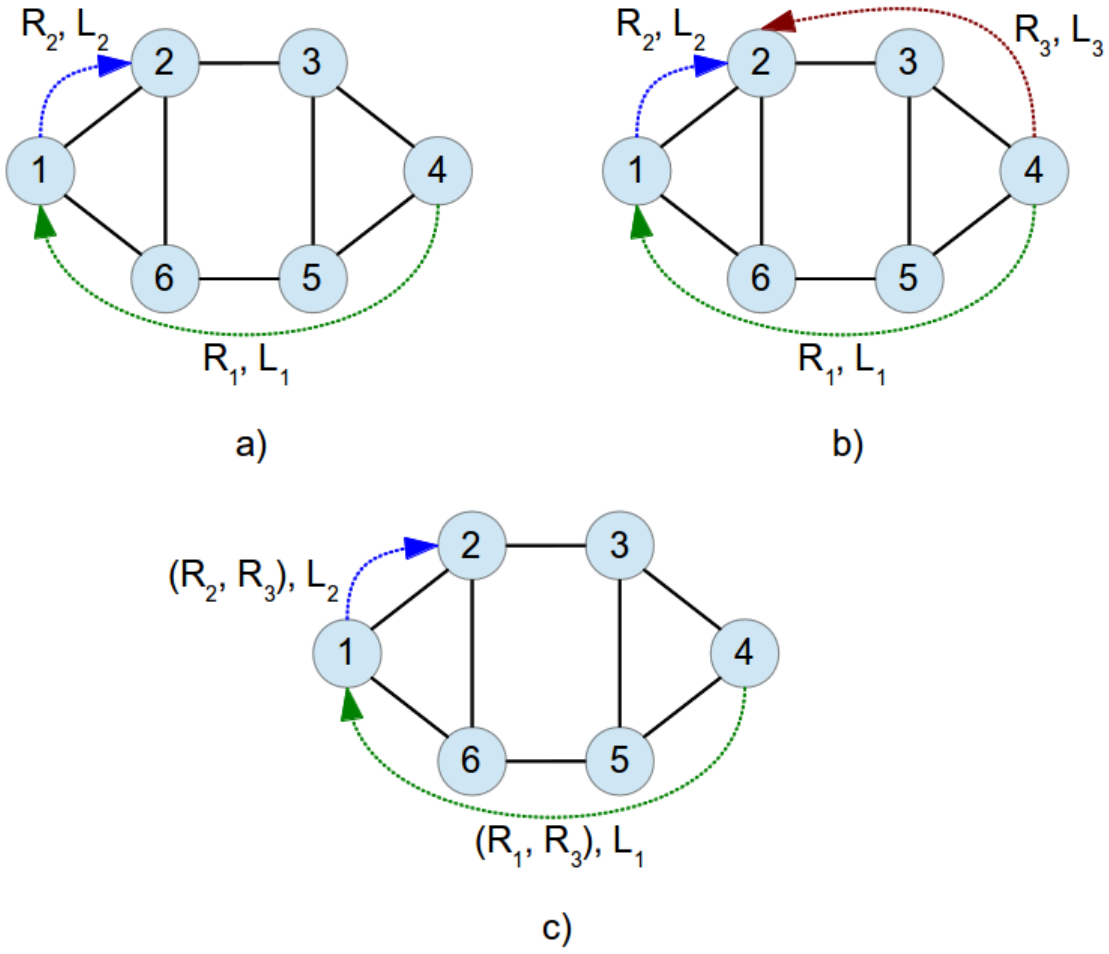

FIGURE 2.12: Example of energy savings thanks to traffic grooming.

energy when there is no traffic on them or it is possible to re-route the traffic flowing through them.

Although such approaches can save large amount of energy, shutting down elements in a core optical network may result in some side effects degrading significantly the overall network performance, e.g. if a network node is turned-off, it may be necessary to re-route connections to longer end-to-end routes, increasing the end-to-end delay of the connections, which may be intolerable for some kinds of traffic. Furthermore, it may happen that it is necessary to power on again node or link equipment in order to support an incoming connection. In such situation, the time required to boot-up the devices may affect negatively to the set-up time of the connections, specially for real time traffic. To overcome such limitation, the concept of sleep-enabled devices has been introduced in the literature for both node equipment (TSPs and REGs) [MSR+11] and link equipment [CSC11]. The basic idea behind is that optical devices can be put in a low power consumption mode called sleep or idle and be turned-on in a very short time. In this way, it is possible to compensate the long boot-up times of completely powered-off devices and still achieve significant energy consumption reductions. Nevertheless, the impact of

such sleep-enabled devices in the network performance has to be carefully evaluated and dimension the network accordingly.

Lastly, a third major approach to energy efficient core optical networks would be to incorporate energy efficiency decisions during the network planning and design phase. For example, in [ZCJ+12] the authors propose both exact and heuristic design approaches for translucent optical networks considering the problem of REG placement in order to reduce the energy consumption in such networks. Regeneration in translucent optical networks plays a very important role towards the overall network performance, as it allows to compensate the degradations in the transmission quality posed by the presence of PLIs. In such operation, the location of regeneration sites becomes crucial, as resources to the connections have to be assigned according to the position and availability of the regeneration sites in order to avoid excessive degradations of the signal that would otherwise render regeneration impossible and to avoid the saturation of the REGs due to excessive traffic handling.

For this, the problem of REG placement has been studied in the literature (e.g. [MKCV10]) with the objective to provision the necessary number of REGs in the network to efectively handle a given traffic matrix and at the same time reduce the capital expenditures (CAPEX) associated to the deployment of regeneration sites. With such concept in mind, the work presented in [ZCJ+12] aims at minimizing the energy associated in the regeneration operation by proposing a translucent network infrastructure that uses all-optical 2R (reamplification and reshaping) REGs to partially replace Optical-Electrical-Optical (O-E-O) 3R (reamplification, reshaping, and retiming) REGs. Utilizing such approach, authors reported around 60-70% energy savings when compared to traditional schemes that do not utilize all-optical 2R REGs.

Another example of energy efficient optical network design was presented in [CTN+12], where authors propose various mathematical models for the design of energy efficient and cost effective Mixed Line Rate (MLR) optical transport networks. With the increase of the amounts of traffic and their heterogeneity that core optical networks have to handle, future optical network will no more require to support a single bit-rate on their line cards, as in Single Line Rate (SLR) networks, but various bit-rates (e.g. 10/40/100 Gbps) to efficiently serve all the traffic that will flow through them. Hence, the adoption of MLR-based solutions and the associated energy-aware techniques becomes highly desirable. In this regard, authors in [CTN+12] studied the energy savings that a MLR-based network can achieve when compared to a SLR one when a green network design is considered. From their results, MLR networks performs better than the SLR networks by reducing the network wide energy consumption.

2.5 Chapter summary

This chapter has provided a comprehensive explanation of the evolution of current optical network infrastructures and its limitations as well as the key points in order to realize the future optical network infrastructures. From legacy static networks to dynamic ASON-based networks, optical networks have undergone through significant technological advances, becoming the de-facto choice for long-haul high capacity transport networks thanks to their cost and power consumption effectiveness as well as the almost unlimited bandwidth per fibre link when compared to electrical-based networks. However, despite this numerous advances, traditional WDM optical network infrastructures have reached their limits when facing the constant growth of the traffic they have to handle due to the highly dynamic patterns as well as their heterogeneous nature.

In light of this, the IaaS paradigm and more specifically the concept of VONs arise as a very promising candidate to overcome such limitations. VONs will allow to dynamically adjust the network characteristics (topology, capacity, etc.) in order to fit the specific requirements of the services that will run on top of them. Additionally, they become a very cost effective solution for external operators in order to develop their own business models without having to deploy expensive physical infrastructures.

While VONs will allow for a more customizable network environment, it is still necessary to undergo through more advances in terms of bandwidth provisioning to cope with the explosive growth of future networks. To this end, EONs have been introduced as a potential solution for short- to mid-term transport optical network in terms of more flexibility in the spectrum assignment. Nevertheless, despite the new degree of freedom introduced by EONs, they also pose several challenges, both in terms of hardware development as well as in terms of resource assignment, that will have to be carefully addressed to fully realize their promises.

A third major point for future optical network infrastructures relates to the cost associated with their energy consumption, since the growth of traffic on transport network will increase several times their associated energy consumption. In view of this, section 2.4 has reviewed the main advances for energy efficient optical network infrastructures, ranging from green routing algorithms to energy-efficient network design techniques.

The following chapters will address particular challenges on the three main topics that constitute the present thesis, namely VONs, EONs and energy efficient optical networks.

Chapter 3

Virtual optical network embedding

This chapter focuses on the VON embedding problem. The efficient embedding of VNs into the actual physical substrate is a critical phase inside the IaaS paradigm. An efficient VN embedding allows the PIP to use better its physical resources, maximizing the number of VNs that can be embedded into it and, as a consequence, the revenues. Additionally, it is a very important aspect in order to satisfy the requirements of all VNs (e.g. in terms of link capacity) and provide a correct isolation between the virtual instances so they do not interfere with each other and can be properly managed by the VIPs leasing them.

For this, the first section presents the concept of VON embedding, hereafter referred as the Virtual Optical Network Allocation (VONA) problem, and the main challenges that the optical medium poses when performing the embedding operation. This leads to conclude that new embedding techniques have to be defined according to the properties of the optical substrate and the characteristics of the VNs to be allocated. To this end, sections 2 and 3 propose various mechanisms to optimally perform the embedding of the VONs in a static scenario. Specifically, section 2 studies how to optimally tackle the VONA problem depending on the nature of the connection services (i.e. lightpaths) that will be provisioned over the VNs. In this sense, it differentiates between opaque and transparent VONs and provides ILP formulations to optimally embed them in an optical network substrate. However, as already mentioned during Chapter 2, in order to provide VONs that are efficient in the use of the available spectrum, an equally efficient network substrate has to be used. To this end, EONs have been introduced as a very promising candidate to enable the provisioning of spectrum efficient VONs. Nevertheless, the different nature of EONs when compared to traditional WSONs requires that embedding algorithms specially tailored to the new characteristics of the physical substrate have to be defined. To this end, section 3 studies of to efficiently embed VONs when an EON physical substrate is considered. After having studied how to optimally tackle the VONA problem in a static scenario, section 4 deals with the allocation of VONs in an online environment. The main trait of such online scenario is that full knowledge of the VONs to be embedded in the physical substrate is not possible, since demand requests arrive

at random. Hence, specific algorithms for this kind of scenario have to be proposed to optimally tackle the VONA problem under such traffic uncertainty conditions.

Moreover, new emerging paradigms, such as Cloud Computing, require that not only VIs composed of optical resources have to be considered but VIs encompassing both optical and IT resources (e.g. memory, storage, etc.). In such situation, the goal is not to only provide connectivity services between geographically distant nodes but also provide computational and storage capabilities so a greater range of services (e.g. online storage, video streaming, etc.) can be efficiently provided. To this end, section 5 studies the challenges that the composition of hybrid VIs, composed of both optical and IT resources, poses and provides mechanisms to optimally perform the embedding of such VIs into the physical substrate. Finally, the last section summarize the main achievements of the presented chapter.

3.1 Concept and challenges

In a virtualized network environment, the problem of how to map the virtual resources to the physical ones, that is, how to associate a virtual resource to a subset of physical devices into the network substrate is known as the Virtual Network Embedding (VNE) problem [CB09, FBB+13]. An optimal VNE plays a capital role in a virtualized network scenario, allowing to maximize the number of VNs that can be allocated in top of a physical network substrate or minimize the amount of resources that are needed to satisfy a specific VN demand set. For these reasons, multiple ILP- or heuristic-based mechanisms have been proposed in the literature so as to provide optimized ways to perform the VNE (e.g. [MSK+13, SS14, HWC13]).

Concerning the embedding process, the VNE problem can be sub-divided into two sub-problems, namely the node and link mapping sub-problems. As its name suggests, the node mapping sub-problem studies how to map the virtual nodes of a demand into a subset of physical nodes of the underlying substrate, while the link mapping problem studies the proper way of mapping the virtual links between virtual nodes into the physical network. Traditionally, both sub-problems have been addressed separately, such as in [ZA06]. Firstly, the node mapping is tackled, mapping the virtual nodes as if they where isolated entities and not considering the implications on the network resources. Once the node mapping has been done, the link mapping is performed. In this regard, it provides the necessary path between the already chosen end points (i.e. virtual nodes) so as to guarantee connectivity between them along with the desired bandwidth. Figure 3.1 depicts an example of the whole embedding process, considering that both sub-problems are tackled separately. Note, however, that separating the VNE problem into two sub-problems (node and link mapping) may result into sub-optimal solutions, since the node mapping is performed without taking into considerations the impact of the virtual node location into the network resources. Indeed, as the link mapping depends on the decision

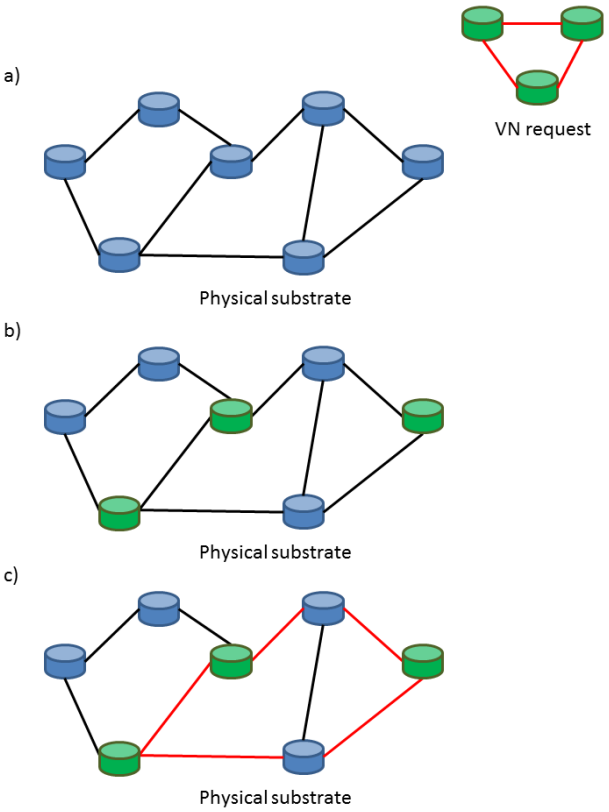

FIGURE 3.1: Example of VNE in two phases: a) a VN request has to be allocated in the physical substrate; b) the node mapping is performed; c) the link mapping is performed according to the decisions made on the previous phase.

made during the node mapping phase, it may happen that the actual link mapping gets trapped into a local optima in the solution space, hence an overall absolute optimal solution is not possible to be achieved.

To overcome such limitation, more refined studies propose that both stages should be attacked simultaneously or in a coordinated way to increase the optimality of the mapping solution [CRB09, LXMT11]. In this way, a true optimal solution can be achieved since the node mapping does not trap the link mapping phase into a local optima. Figure 3.2 depicts an example of a joint node and link VNE. Nevertheless, such joint approach complicates to a large extent the whole embedding process, becoming an NP-hard problem.

Various aspects of the VNE problem have been studied in the literature. For instance, a very important aspect relates to the resilience and survivability of the VNs. That is, in the event of a failure in the physical substrate, all the affected VNs (i.e. all VNs that had some virtual resource mapped over the physical resource that experienced the failure) must be remapped or find alternative locations for the affected virtual resources. For instance, authors in [RB13] presented a fast heuristic mechanism to do the re-routing of the virtual links in the case of a failure in a physical link, so the bandwidth of the virtual links can be guaranteed. Also related to this aspect, authors in [JYK13] presented a

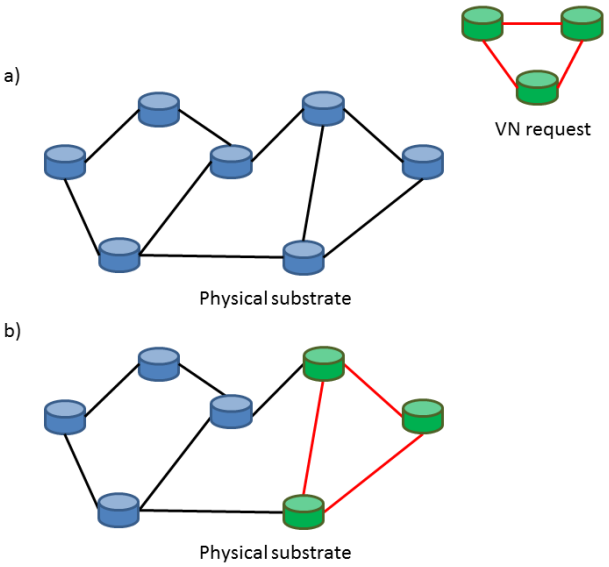

FIGURE 3.2: Example of joint VNE: a) a VN request has to be allocated in the physical substrate; b) the joint node and link mapping is performed.

VNE mechanism based on p-cycles in order to guarantee a full protection scheme against physical failures.

Another widely researched topic regarding the VNE problem relates to the energy efficiency of the VNs (e.g. [BHD+12, ZSN+12, SZX+14, FBdM13]). Since usually VNs encompass a geographically distributed area, the composed virtual links may be mapped to long physical paths. Such long physical paths can result in a high energy consumption since multiple routers (i.e. nodes) are traversed along the end-to-end path between virtual link end points. For this, in order to reduce the OPEX of the VNs, it becomes of paramount importance to incorporate energy parameters into the VNE process or design energy-aware embedding mechanisms so as to compose energy efficient VNs.

However, despite the vast research done regarding the topic of VNE, the majority of work has focused on Layer 2/3 electrical networks (e.g. IP and Ethernet networks) due to the maturity of virtualization technologies on this kind of networks. On the other hand, since virtualization techniques are still in a very early development stage for optical networks, the VNE problem in optics (the aforementioned VONA problem) is still under research and huge efforts are devoted into various aspects of the problem (e.g. [LBDM12, HNS13, VMCM13]).

When focusing on the VONA problem, one major difference respect to the VNE embedding present in electric networks comes from the fact that to provision the virtual links of the VONs, it is necessary to provision a lightpath between the end nodes, hence the well-known RWA problem appears on the arena. This makes the embedding problem much more difficult since it is not only necessary to find a path between the end points of a virtual link but also, in the absence of regeneration or wavelength conversion, the same wavelength must be provisioned along the virtual link. This is known as

the wavelength continuity constraint and must be respected when placing VONs into an all-optical network substrate. Additionally, depending on the kind of connectivity services provided over a VON (opaque, translucent or transparent), such RWA may differ notoriously on the case, complicating further the VONA problem [PPSJ12]. Another critical point when tackling the VONA process comes from the so called PLI limitations posed by the physical optical medium. Indeed, PLIs are well-known in the literature so as a limiting factor on optical networks [SK12, SS09, SSS11], challenging the composition of transparent services. For this, it is necessary to account for the PLI limitations when embedding VONs into the physical substrate so as to avoid any service degradation [PNA+11, PNS13, FDM+12].

Moreover, although algorithms for the VNE problem on electric networks are normally technology-agnostic, since the composition of the virtual links only requires to provision a physical path and some bit-rate in the said path, the VONA problem becomes strongly technology dependent, since the way a lightpath is represented in the embedding algorithm differs substantially depending on the technology employed at the physical layer. For instance, and following the trend imposed by EONs, it becomes increasingly interesting to provision VONs in network substrates more efficient in the use of the spectrum. However, in such type of networks the RWA problem present in the VONA problem becomes replaced by the RSA problem, which is known to be even more hard to solve than the RWA problem found in traditional WSONs. Indeed, any embedding algorithm that pursues to allocate VONs in such a EON-based physical substrate must account for the particularities posed by this type of technology (e.g. [GZWZ13, ZSBP13, GZ14]). Finally, following the trend imposed by new emerging paradigms such as Cloud Computing or Virtual Data Center (VDC), the composition of hybrid VIs with both optical and IT resources becomes highly desirable and much efforts are being devoted into the design of embedding algorithms so as to efficiently addres the VONA problem considering the co-existence of optical network resources and geographically distributed IT sites [SS14, ATG11].

With all these discussions, the following sections are devoted to the study of optimally allocate VONs considering various network technologies and operation scenarios.

3.2 Transparent vs opaque virtual optical networks

As mentioned during the previous section, the VONA problem includes a RWA problem that can differ depending on the VIP's needs and the actual characteristics of the VON. This section will study how the VONA problem changes depending on the nature of the connectivity services that will be offered over the VON. In this regard, two types of VONs are considered, namely, transparent VONs and opaque VONs. In a transparent VON, optically transparent end-to-end services are intended to be provisioned over the VON. That is, as in a transparent physical network, the connections that are established in the

VON must remain always in the optical domain, having the same wavelength assigned in all virtual links that crosses. This requires the allocation of exactly the same set of wavelengths for every virtual link as otherwise it would not be possible to guarantee the wavelength continuity for all end-to-end path combinations. On the other hand, in an opaque VON electronic termination capabilities are physically present at each VON node and opaque transport services are provided from the VON viewpoint. In such a case, there is no need to allocate the same set of wavelengths for each virtual link, but can differ thanks to the O-E-O conversion stages.

With such definitions, this section focuses on providing mechanisms to optimally embed a VON depending if it requires that end-to-end transparent connectivity services have to be provisioned over the VON (transparent case) or not (opaque case). The scenario under evaluation consists on a static scenario, where the demand set is known beforehand, reflecting the network planning phase. In such situation, the goal is to maximize the number of VONs that can be embedded in the limited resources available at the physical optical substrate. To this end, ILP formulations are provided for both VONA problems, so as to accommodate all or the maximum number of VONs from the demand set given the limited capacity of the underlying optical network. Note, however that VONs have to be treated as entities instead of a composition of lightpaths, which makes the VONA problem differ from the traditional RWA problem with the objective to maximize the number of lightpaths established. Indeed, a specific demand is accommodated if and only if all its virtual links and nodes can be mapped over available resources. In this section, the presented mechanisms focus on the mapping of VONs considering only the link mapping. That is, it is assumed that the embedding (i.e. location) of the virtual nodes into the physical substrate it is already done, only the embedding of the virtual links into physical resources (paths and wavelengths) is required.

Additionally, for the present work, an all-optical network substrate without wavelength conversion capabilities is assumed. That is, all virtual links must ensure the *wavelength continuity constraint*, regardless if transparent or opaques VONs are intended. Moreover, it is assumed that PLI degradations do not compromise the feasibility of the optical channels. Very large network scenarios may require the introduction of PLI information in both transparent and opaque VONA problems in order to ensure the feasibility of the provisioned VONs. However, this is not considered in this work and left for further study. Also, note that, in its current form, the presented formulations are still valid for a wide range of transparent network scenarios. For instance, studies done by authors in [RM11], where a quite restrictive scenario was considered (i.e., impact of both linear and non-linear PLIs as well as the co-existence of different bit rates and modulation formats), reveal that transparent reaches of 3000 and 1600 km are feasible for 10 and 40 Gb/s, respectively.

After all these discussions, the exact details of both solutions for the transparent and opaque VONA problems are depicted in the following subsections.

3.2.1 Transparent VON embedding

This subsection presents an ILP model of the transparent VONA problem called TVONA_ILP. For this, let the optical network substrate be characterized by a graph $G_n = (N, E)$, where N denotes the set of nodes and $E = \{(i,j),(j,i) : i,j \in N, i \neq j\}$ the set of physical links. Let W denote the set of available wavelengths per physical link. Consider D as the set of VON demands to be allocated over the optical network. Each demand $d \in D$, is characterized by a graph $G'_d = (N'_d, E'_d)$, $N'_d \subseteq N$, $E'_d = \{(i,j),(j,i) : i,j \in N'_d, i \neq j\}$. Let W_d denote the number of wavelengths per virtual link desired by demand $d \in D$. Additionally, let P define the set of paths in the physical network, $P^e_{e'}$ define the set of $p \in P$ associated with virtual link e' that traverse edge $e \in E$, and $P^d_{e'}$ define the set of $p \in P$ associated with virtual link e' in demand d. The problem variables of TVONA_ILP are:

$x^{p,w}_{d,e'}$: binary; 1 if for demand d the virtual link e' is supported through path p and wavelength w, 0 otherwise.

y^w_d: integer; minimum number of times wavelength w is used to serve demand d.

z_d: binary; 1 if demand d can be satisfied, 0 otherwise.

Objective function (3.1) aims at maximizing the number of VONs to be allocated in the underlying optical network. Constraints (3.2) are the wavelength clashing constraints, which avoid that two virtual links are supported over the same wavelength in the same physical link. Constraints (3.3) ensure that at most W_d different (p,w) will be assigned to every virtual link belonging to demand d. Constraints (3.4) discriminate if wavelength $w \in W$ is being used by all virtual links in demand d. Constraints (3.5) discriminate whether demand d is supported over the requested number of wavelengths W_d.

$$max \sum_{d \in D} z_d, s.t. \tag{3.1}$$

$$\sum_{d \in D} \sum_{e' \in E'_d} \sum_{p \in P^e_{e'}} x^{p,w}_{d,e'} \leq 1, \forall e \in E, w \in W \tag{3.2}$$

$$\sum_{p \in P^d_{e'}} \sum_{w \in W} x^{p,w}_{d,e'} \leq W_d, \forall d \in D, e' \in E'_d \tag{3.3}$$

$$y^w_d \leq \sum_{p \in P^d_{e'}} x^{p,w}_{d,e'}, \forall d \in D, e' \in E'_d, w \in W \tag{3.4}$$

$$z_d \leq \sum_{w \in W} y^w_d / W_d, \forall d \in D \tag{3.5}$$

Phase 1: Preprocessing
Eliminate $d \in D$ with nodes with degree greater than physical ones
$BestSol = \emptyset$
for $i = 0$ **to** $i = MaxIterations$ **and** $Obj(Sol) \neq |D|$ **do**
  $Sol = \emptyset$; Candidate list $C = \emptyset$
  Phase 2: Solution construction
  $C \leftarrow \cup x_{d,e'}^{p,w} \forall d \in D, e' \in E'_d, p \in P_{e'}^d, w \in W$
  Assign cost equal to physical hops $\forall c \in C$
  $U_d = \emptyset$ wavelengths already allocated to $d, \forall d \in D$
  while $C \neq \emptyset$ **do**
    $cost_{min} \leftarrow$ min cost from C
    $RCL \leftarrow \{c \in C | cost(c) = cost_{min}\}$
    Select an element c from the RCL at random
    $Sol \leftarrow Sol \cup \{c\}$
    if $|U_d| \neq W_d$ **then**
      $U_d \leftarrow U_d \cup$ {wavelength associated to c}
    Erase from C c and candidates causing wavelength clash
    if *num_wavelengths of* e' *in Sol* $= W_d$ **then**
      Erase from C all candidates of e'
    if $|U_d| = W_d$ **then**
      Erase from C candidates of d with w not in W_d
    for *all* $c \in C$ **do**
      if *some elements of* d *are in Sol* **then**
        $cost(c) =$ num_hops
      else
        $cost(c) =$ num_hops $\times$ multiplicative_factor
  if $Obj(Sol) \neq |D|$ **then**
    Phase 3: Solution improvement
    Temporally extract partially satisfied demands d_p
    for *less constructed* d_p **to** *more constructed* **do**
      Find combination of (p, w) that satisfies d_p
      if *found* **then**
        $Sol \leftarrow Sol \cup \{d_p\}$
  if $Obj(Sol) > Obj(BestSol)$ **then**
    $BestSol \leftarrow Sol$

TABLE 3.1: TVONA_GRASP heuristic pseudo-code

As will be shown in subsection 3.2.3, the execution time of the TVONA_ILP model grows substantially up as the number of VONs in D increases. In view of this, a heuristic for the transparent VONA problem based on the Greedy Randomized Adaptive Search Procedures (GRASP) meta-heuristic [RR11] is presented in the following, which ensures practical execution times even when the number of VONs in D is large. The pseudo-code of this heuristic, called TVONA_GRASP, is depicted in Table 3.1.

After some preprocessing, TVONA_GRASP builds a feasible solution in phase 2, considering the same constraints as the model. The purpose of the *multiplicative_factor* is to assign higher costs to variables associated with demands not under construction, thus

favoring those demands with elements already in the solution (i.e., the probability to build full demands increases). During the evaluation of the algorithm, this factor has been fixed to 4, which has resulted in the best accuracy in the scenarios under study. Nonetheless, its configuration is left to the transport network owner's discretion. Phase 3 tries to improve this solution by local search in the solution space around the solution from phase 2. After each iteration, if a solution with a better objective value than the overall best solution found so far is found, this solution becomes the new best solution. At the end of the process, the best solution is returned.

3.2.2 Opaque VON embedding

This subsection presents an ILP formulation of the opaque VONA problem called OVONA_ILP. In OVONA_ILP, variables y_d^w, unnecessary here, are suppressed along with constraints (3.4). The rest of the formulation is almost identical to the TVONA_ILP formulation. Objective function (3.6) aims at maximizing the number of VONs to be allocated in the underlying optical network. Constraints (3.7) are the wavelength clashing constraints, which avoid that two virtual links are supported over the same wavelength in the same physical link. Constraints (3.8) ensure that at most W_d different (p, w) will be assigned to every virtual link belonging to demand d. Constraints (3.5) are slightly modified to fit the characteristics of such an opaque scenario, now transformed into constraints (3.9), whose purpose is to discriminate whether demand d is fully served or not.

$$max \sum_{d \in D} z_d, s.t. \tag{3.6}$$

$$\sum_{d \in D} \sum_{e' \in E'_d} \sum_{p \in P^e_{e'}} x^{p,w}_{d,e'} \leq 1, \forall e \in E, w \in W \tag{3.7}$$

$$\sum_{p \in P^d_{e'}} \sum_{w \in W} x^{p,w}_{d,e'} \leq W_d, \forall d \in D, e' \in E'_d \tag{3.8}$$

$$z_d \leq \sum_{p \in P^d_{e'}} \sum_{w \in W} x^{p,w}_{d,e'} / W_d, \forall d \in D, e' \in E'_d \tag{3.9}$$

The removal of variables y_d^w and constraints (3.4), ensuring that each virtual link $e' \in E'_d$ uses the exact same subset of wavelengths in TVONA_ILP, lightens OVONA_ILP when compared to its transparent counterpart. This makes OVONA_ILP solvable to optimality within a reasonable time span, as will be illustrated in the following section. Hence, no heuristic approach has been considered as necessary to solve the opaque VONA problem.

3.2.3 Simulation results

As mentioned in subsection 3.2.1, the TVONA_ILP model becomes impracticable for large D sizes, which motivated the proposal of the TVONA_GRASP heuristic, as a way to obtain results close to optimality but in a much shorter time. In order to highlight the accuracy of TVONA_GRASP, as well as its running times compared to the exact TVONA_ILP model, a series of simulations have been executed both of them on the 16-Node EON core network topology as presented in Appendix A with 8 wavelengths per physical link. In particular, $|D|$ equal to 10, 20 and 30 has been considered, assuming that each demand requests 1 wavelength, that is, $W_d = 1, \forall d \in D$.

The generation of the demand sets for all experiments throughout this subsection follows a 2-step process. Firstly, 3 or 4 physical network nodes (with equiprobability) are randomly selected as virtual nodes for each demand. In this way, reasonable medium-sized VONs are obtained when compared to the underlying physical network size. Next, the selected virtual nodes are then randomly connected using the Erdős-Rényi algorithm [CMP+10], here slightly modified to prevent the generation of non-connected graphs. The parameter p has been set to 0.5 in the algorithm, which leads to the generation of any connectivity matrix with equiprobability.

For the TVONA_GRASP heuristic, some limitations have been imposed to restrict its execution time while still producing good results: 1) the *MaxIterations* field is set to 125; 2) the number of paths associated to the virtual links of the demands is limited to 30 paths per virtual link; 3) the number of combinations to check during phase 3 is limited to 10^6. Table 3.2 compares the performances of TVONA_ILP and TVONA_GRASP in terms of execution time and number of successfully allocated demands. The presented results have been averaged over 25 executions, randomly generating a new set of demands at the beginning of each execution. The experiments have been launched on Intel Core Duo at 3 GHz PCs with 4 GB RAM memory.

As seen, the execution times of TVONA_GRASP stay largely below the ones of TVONA_ILP. This reduction is especially important as the number of offered demands increases (e.g., a four orders of magnitude reduction is achieved for $|D| = 30$). Moreover, TVONA_GRASP still provides accurate results, showing relative errors between 0.46% and 6.98% in the worst case. Note, however, that such errors represent one more demand blocked in average barely. As stated before, the execution times of OVONA_ILP are much lower than those of TVONA_ILP. Indeed, additional experiments to the ones presented in Table 3.2 showed us average execution times of OVONA_ILP around 14.2 s, 116.1 s and 131.2 s for $|D| = 10$, $|D| = 20$ and $|D| = 30$, respectively.

Aiming to quantify the benefits of the proposed contributions for efficient VON allocation, simpler allocation approaches have been used as benchmarks. To this end, a SP strategy which serves the demands in D on a one-by-one basis, mapping their virtual links to the shortest physical path that connects both endpoints, has been considered. On these

Table 3.2: TVONA_ILP vs TVONA_GRASP

	TVONA_ILP		TVONA_GRASP		
	Time (s.)	Result	Time (s.)	Result	% Error
$\|D\| = 10$	1533.52	8.68	366.49	8.64	0.46
$\|D\| = 20$	$1.64 \cdot 10^6$	14.48	601.67	13.96	3.59
$\|D\| = 30$	$2.38 \cdot 10^6$	17.76	612.5	16.52	6.98

physical paths, a First Fit (FF) wavelength selection is performed. Note, however, that in the transparent case, the wavelength selection in the virtual link firstly allocated for a demand constrains those selections in the remainder ones.

Figure 3.3.a shows the number of allocated demands as a function of the demand set size in both transparent and opaque VON scenarios. Due to the impracticality of TVONA_ILP for large D sizes, TVONA_GRASP has been used in the transparent case. The presented results have been averaged over 100 executions with newly generated demand sets per execution, which provides us with statistically relevant results. Again, $W_d = 1, \forall d \in D$. As observed, both OVONA_ILP and TVONA_GRASP outperform their shortest-path-based counterparts, showing more pronounced improvements as the number of offered demands increases. In the transparent case, for example, while a 12.8% improvement is achieved for $|D| = 10$, this one raises up to around 30% for $|D| = 30$. Even more pronounced improvements are observed in the opaque case, ranging from 9.3% for $|D| = 10$ to 42.8% for $|D| = 30$. This is due to the fact that more flexibility is given to the VON allocation in the opaque case, as different sets of wavelengths can be used to allocate each VON virtual link.

So far, it has been shown that TVONA_ILP is strongly affected by D size. To complete the study, it has been analyzed how TVONA_ILP and OVONA_ILP execution times scale as W_d increases. To this goal, $|D| = 10$ have been set and 100 executions of both models have been launched, with newly generated demand sets per execution. Interestingly, the obtained results reveal that neither TVONA_ILP nor OVONA_ILP show noticeable scalability issues in this regard. For example, while the execution times of TVONA_ILP remain around 1530 s for $W_d = 1$, they even decrease down to 52.6 s and 43 s for W_d equal to 6 and 12, respectively. In the case of OVONA_ILP, execution times remain in the same order of magnitude for all W_d values (e.g., 14.2 s, 42.3 s and 31.7 s for W_d equal to 1, 6 and 12, respectively). Figure 3.3.b shows the number of VONs finally allocated in all experimented scenarios. As expected, both models present similar behavior in this sense, due to the resource scarcity in the optical network substrate as each VON requests more and more resources. A noteworthy point in the graph appears when W_d changes from 8 to 9. Indeed, having 8 wavelengths per physical link, virtual links must unavoidably be mapped over multiple physical paths between the virtual link endpoints, which limits to a large extent the number of VONs that can be allocated over the optical network substrate.

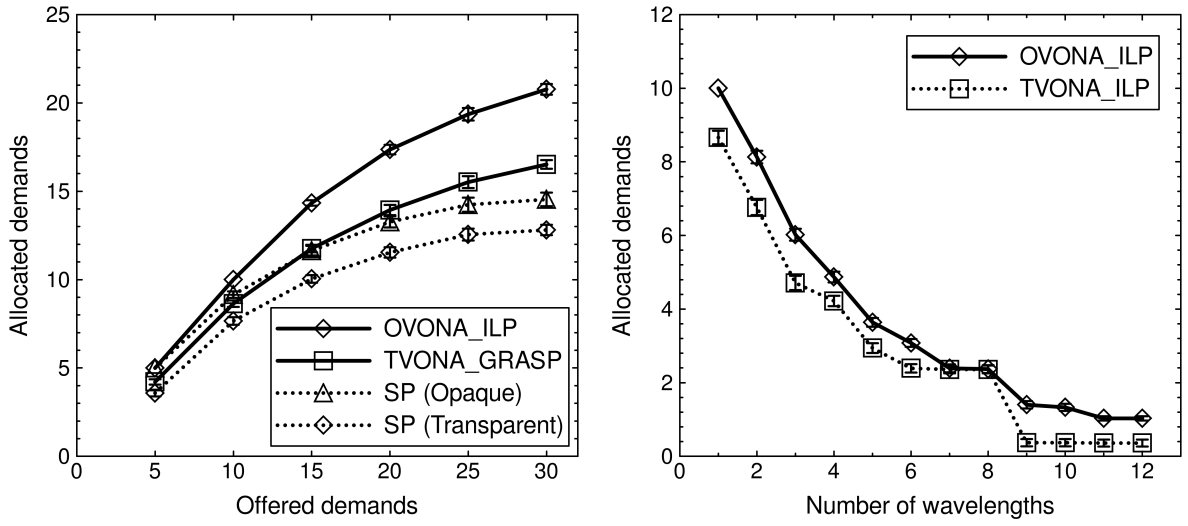

a) b)

FIGURE 3.3: Simulation results: a) Average number of allocated demands as a function of the offered demands set size; b) Average number of allocated demands as a function of the number of wavelengths/demand.

3.3 VON embedding in EONs

The previous section analyzed the implications on the VON embedding process depending on the nature of the connectivity services that are intended to be offered on top of them. To this end, the transparent and opaque VONA cases have been studied and mechanisms to optimally embed the VONs in such scenarios have been provided. On the other hand, another aspect that arises of paramount importance when tackling the VONA problem relates to the technology used by the underlying physical network substrate. Precisely, the whole embedding process depends strongly on the characteristics of the physical substrate when mapping the virtual resources to physical ones. For these, embedding mechanisms specially tailored for the current technology used in the physical network are needed.

Additionally, different physical technologies may impact on the number of VONs that can be correctly allocated on top of the physical substrate. For example, if a more efficient physical technology in terms of spectrum usage is employed, the number of VONs that can be allocated would be superior when compared to another technology where the spectrum utilization is worse. Moreover, as already mentioned during Chapter 2 an efficient physical substrate is of capital importance in order to realize VONs flexible enough to accommodate efficiently the services intended to be allocated on top of them.

To this end, two alternatives enabling optical transport technologies have been considered as cases of study for determining the impact of the underlying optical network substrate technology on the number of VONs that can be allocated on top: 1) wavelength switching following the fixed-size spectrum grid defined by the ITU, where the minimum granularity for allocating a connection is a full wavelength [G.694.1]; and 2) spectrum switching,

following a flexible spectrum grid as proposed in the EON architecture [JTK+09]. In such a case, demands request a portion of spectrum, equivalent to a number of FS. In order to optimally perform the embedding of the VONs in for both said technologies, ILP formulations are provided with the goal to maximize the number of VONs that can be allocated given a demand set and the available resources at the physical substrate.

With this, let the optical network substrate be characterized by a graph $G_n = (N, E)$, where N denotes the set of nodes and $E = \{(i,j),(j,i) : i,j \in N, i \neq j\}$ the set of physical links. Consider D as the set of VON demands to be allocated over the optical network. Each demand $d \in D$, is characterized by a graph $G'_d = (N'_d, E'_d)$, $N'_d \subseteq N$, $E'_d = \{(i,j),(j,i) : i,j \in N'_d, i \neq j\}$. Also, let P define the set of paths in the physical network, $P^e_{e'}$ define the set of $p \in P$ associated with virtual link e' that traverse edge $e \in E$, and $P^d_{e'}$ define the set of $p \in P$ associated with virtual link e' in demand d. As in section 3.2, the VONA problem under study consists in accommodating all or the maximum number of VONs from D, considering that a specific demand $d \in D$ is accommodated if and only if all its virtual links in E'_d can be mapped over available resources. Note that also in this case the node mapping is assumed to be already done (i.e. the correspondence between virtual and physical nodes is know beforehand) and only the link mapping is performed.

Additionally, opaque transport services are assumed to be provisioned over the VONs, assuming that every node in the VON has electronic termination capabilities, hence it is not necessary to provision the same spectrum (wavelength or FSs) in every virtual link. Moreover, an all-optical network substrate without wavelength/spectrum conversion capabilities is assumed, so that every virtual link of the VON must ensure the wavelength-/spectrum continuity constraint. Finally, it is assumed that in the wavelength switching case, all wavelength requested by a virtual link must be routed over the same physical path. Such assumption is to avoid delay problems when sending data through different wavelength in the same link that would require to perform some reordering at the end of the virtual link so as to compensate the differential delay among the paths.

With such assumptions, the following subsections present the proposed ILP formulations for both scenarios under study.

3.3.1 Fixed-grid VON embedding

This subsection presents an ILP model of the fixed-size grid VONA problem, hereafter referred as Fixed-VONA. For this, let W denote the set of available wavelengths per physical link and W_d denote the number of wavelengths per virtual link desired by demand $d \in D$. The presented formulation is based on the ILP formulation for the opaque VONA problem discussed during subsection 3.2.2, here slightly modified to fit the requirements of the problem under study. The problem variables of Fixed-VONA are:

$x_{d,e'}^{p,w}$: binary; 1 if for demand d the virtual link e' is supported through path p and wavelength w, 0 otherwise.

$y_{d,e'}^{p}$: binary; 1 if in demand d all the wavelengths requested by virtual link e' use the same path p, 0 otherwise.

z_d: binary; 1 if demand d can be satisfied, 0 otherwise.

The ILP formulation is stated below:

$$\max \sum_{d \in D} \alpha_d z_d, \text{s.t.} \tag{3.10}$$

$$\sum_{d \in D} \sum_{e' \in E'_d} \sum_{p \in P^e_{e'}} x_{d,e'}^{p,w} \leq 1, \forall e \in E, w \in W \tag{3.11}$$

$$\sum_{p \in P^d_{e'}} \sum_{w \in W} x_{d,e'}^{p,w} \leq W_d, \forall d \in D, e' \in E'_d \tag{3.12}$$

$$y_{d,e'}^{p} \leq \frac{1}{W_d} \sum_{w \in W} x_{d,e'}^{p,w}, \forall d \in D, e' \in E'_d, p \in P^d_{e'} \tag{3.13}$$

$$z_d \leq \frac{1}{|E'_d|} \sum_{e' \in E'_d} \sum_{p \in P^d_{e'}} y_{d,e'}^{p}, \forall d \in D \tag{3.14}$$

Objective function (3.10) aims at maximizing the number of VONs to be allocated in the underlying optical network, where factors α_d are pondering factors used to put more or less weight in specific demands according to the network operator policies. Constraints (3.11) are the wavelength clashing constraints, avoiding that two virtual links are supported over the same wavelength in the same physical link. Constraints (3.12) ensure that at most W_d different wavelengths are assigned to every virtual link belonging to demand d. Constraints (3.13) ensure that every wavelength requested by virtual link e' is routed through the same path. Such constraints are adopted to avoid packet reordering problems that might appear at destination when sending data over different paths with different physical lengths and, thus, different end-to-end delays. Constraints (3.14) discriminate whether demand d is satisfied or not.

3.3.2 Flex-grid VON embedding

As explained during Chapter 2, EONs allow to efficiently serve low data-rate sub-wavelength transmissions and ultra-high capacity super-wavelength transmissions onto the available network spectral resources, but poses new challenges compared to the classical RWA problem applicable to WSONs. Instead of wavelengths, a contiguous spectrum portion has to be allocated in flexible optical networks. Moreover, given a lack of spectrum conversion capabilities in the network, the assigned spectrum portion must show a continuity

between the remote endpoints of the incoming connection requests (i.e., VON neighbouring nodes in this work). Both constraints, namely, spectrum contiguity and continuity constraints, must be ensured by the RSA algorithm in the network. Since the VONA problem includes a RWA problem, it is necessary to adapt the formulation proposed in the previous subsection so as to fit the needs of the RSA problem present when embedding VONs in top of an EON.

In most works related to RSA, such as in [WCP11, KW11], it is assumed that the usable bandwidth of an optical fiber can be discretized into multiple FSs and so, the bandwidth requested by a demand can be converted into a number of FSs. Specifically, the authors in [KW11] proposed an ILP formulation for EONs targeting at the minimization of the number of FSs that must be provisioned per fiber link in order to serve the entire set of demands offered to the network. In contrast to this, the presented formulation in this subsection also depart, as in Fixed-VONA, from a capacitated optical network substrate, with a number of FSs per link instead of wavelengths, where it aims at maximizing the number of VONs that can be allocated. Hence, the ILP model for the flexible grid problem, called Flex-VONA, becomes a modification of the formulation presented in [KW11]. The definitions for the paths sets already presented are the same here. Besides, we define $F = \{f_1, f_2, ..., f_{|F|}\}$ as the ordered set of available FSs per physical link and F_d as the number of FSs per virtual link desired by demand $d \in D$. With this, the problem variables of Flex-VONA are:

$x^{p,f}_{d,e'}$: binary; 1 if FS f in path p is selected to be the lowest indexed slot assigned to virtual link e' in demand d, 0 otherwise.

$y^{p,f}_{d,e'}$: binary; 1 if FS f in path p is assigned to virtual link e' in demand d, 0 otherwise.

z_d: binary; 1 if demand d can be satisfied, 0 otherwise.

The ILP formulation is stated below:

$$\max \sum_{d \in D} \alpha_d z_d, \text{s.t.} \tag{3.15}$$

$$\sum_{p \in P^d_{e'}} \sum_{f \in F} x^{p,f}_{d,e'} \leq 1, \forall d \in D, e' \in E'_d \tag{3.16}$$

$$x^{p,f_i}_{d,e'} \leq y^{p,f_j}_{d,e'}, \quad \begin{array}{c} \forall d \in D, e' \in E'_d, p \in P^d_{e'}, \\ f_i, f_j \in F, i = 1, ..., |F| - F_d + 1, \\ j = i, ..., i + F_d - 1 \end{array} \tag{3.17}$$

$$x^{p,f_i}_{d,e'} = 0, \quad \begin{array}{c} \forall d \in D, e' \in E'_d, p \in P^d_{e'}, \\ f_i \in F, i = |F| - F_d + 2, ..., |F| \end{array} \tag{3.18}$$

$$\sum_{d \in D} \sum_{e' \in E'_d} \sum_{p \in P^e_{e'}} y^{p,f}_{d,e'} \leq 1, \forall e \in E, f \in F \tag{3.19}$$

$$\sum_{p \in P^d_{e'}} \sum_{f \in F} y^{p,f}_{d,e'} \leq F_d, \forall d \in D, e' \in E'_d \tag{3.20}$$

$$z_d \leq \frac{1}{|E'_d|} \sum_{e' \in E'_d} \sum_{p \in P^d_{e'}} \sum_{f \in F} x^{p,f}_{d,e'}, \forall d \in D \tag{3.21}$$

Objective function (3.15) seeks to maximize the number of VONs to be allocated in the underlying optical network. Factors α_d have the same role as before. Constraints (3.16) serve the purpose of selecting for every virtual link $e' \in E'_d$ a unique path from the candidate paths set and a FS to be the lowest indexed slot assigned to the virtual link. Constraints (3.17) are the contiguous FS assignment constraints. If slot f_i is selected as the lowest indexed slot for virtual link e', the consecutive $F_d - 1$ slots should be assigned to this virtual link. Constraints (3.18) ensure that any FS selection option will have enough space in the frequency spectrum, if chosen. Constraints (3.19) are the spectrum clashing constraints, avoiding that two virtual links are supported over the same FS in the same physical link. Constraints (3.20) ensure that at most F_d different FSs are assigned to every virtual link of demand d. Constraints (3.21) discriminate whether demand d is satisfied or not.

3.3.3 Simulation results

To analyze the impact of the underlying physical technology used by the substrate network on the number of VONs that can be allocated, a series of simulations have been executed using both Fixed-VONA and Flex-VONA formulations. The simulations have been executed on the 16-Node EON core network topology as presented in Appendix A, assuming that every physical link has a usable bandwidth of 400 GHz. In the fixed-size grid scenario, following a grid with a 50 GHz channel spacing, it results in 8 wavelengths per link; in the flexible grid scenario, considering a FS width of 6.25 GHz, it results in 64 FS per link. In particular, $|D|$ sizes from 5 to 25, in steps of 5, have been considered, assuming for both models that all factors $\alpha_d = 1$, that is, regardless of its size or the spectral resources demanded, all VONs are treated equally. Moreover, the number of candidate paths per virtual link has been fixed to the first 6 shortest paths using the distance in hops as the metric, so as to avoid excessive execution times for the models. Although the presented results may not match the optimal ones in some occasions, the presented formulations are still valid and the absolute optimal could be obtained if the whole set of candidate paths per virtual link is considered.

The generation of the demand sets for all experiments throughout this section follows a 3-step process. Firstly, 3 or 4 physical network nodes (with equiprobability) are randomly selected as virtual nodes for each demand. In this way, reasonable medium-sized VONs are obtained when compared to the underlying physical network size. Next, the selected virtual nodes are then randomly connected using the Erdős-Rényi algorithm, here slightly modified to prevent the generation of non connected graphs (any connected connectivity

TABLE 3.3: Complexity comparison of the models

	Fixed-VONA			Flex-VONA		
	Variables	Constraints	Time (s.)	Variables	Constraints	Time (s.)
$\|D\| = 5$	840	289	0.272	13440	53760	2.37
$\|D\| = 15$	2520	499	3.28	40320	161280	$1.25 \cdot 10^4$
$\|D\| = 25$	4200	709	18.03	67200	268800	$7.29 \cdot 10^4$

matrix is generated with equiprobability). Finally, the bandwidth requested by the demand in GHz is selected from the set {25, 50, 100} with probabilities of 0.4, 0.4 and 0.2, respectively. In the fixed-size grid scenario such bandwidth requests are translated to 1, 1 and 2 wavelengths. In the flexible grid scenario they are equivalent to 4, 8 and 16 FSs. It is assumed that any guard band needed by the physical equipment to perform correctly the switching between demands is included in the bandwidth requested by them.

From the assumptions above, one can conclude that the complexity of both models is closely related to the size of the set of candidate paths for the virtual links. In more detail, in the Fixed-VONA model, the number of decision variables is in the order of $\mathcal{O}(|D||\bar{E}'_d||\bar{P}^d_{e'}||W|)$ and the number of constraints is in the order of $\mathcal{O}(|E||W| + |D||\bar{E}'_d||\bar{P}^d_{e'}|)$, being $|\bar{E}'_d|$ the average number of virtual links per demand, and $|\bar{P}^d_{e'}|$ the average number of candidate paths per virtual link. It can be seen that the main contributions to the complexity of Fixed-VONA are the wavelength clashing constraints (3.11) and the unique path constraints (3.13). In the Flex-VONA model, the number of decision variables is in the order of $\mathcal{O}(2|D||\bar{E}'_d||\bar{P}^d_{e'}||F|)$ and the number of constraints is in the order of $\mathcal{O}(|D||\bar{E}'_d||\bar{P}^d_{e'}||F||\bar{F}_d|)$, being $|\bar{F}_d|$ the average number of FSs requested by the demands. Therefore, the main contribution to the complexity of Flex-VONA is the large number of FSs in some network scenarios, resulting in a huge number of contiguity constraints (3.17).

To exemplify the complexity of both formulations, Table 3.3 displays the value of these expressions for the scenario considered in the executions plus the average execution time of both models. The results shown throughout this section have been averaged over 100 executions, randomly generating a new set of demands at the beginning of each execution. The experiments have been launched on Intel Core2 Quad at 2.66 GHz PCs with 4 GB RAM memory. The optimization software used for all executions is IBM ILOG CPLEX Optimizer v.12.2.

Table 3.3 shows that the complexity of Flex-VONA, in terms of number of variables and constraints, is substantially greater than the one of Fixed-VONA. This comes from the fact that the number of FSs in the flexible grid scenario is substantially larger than the number of wavelengths in the fixed-size grid scenario. Besides this, the spectrum contiguity constraints adds a considerable complexity to the problem. Focusing on the execution times of Flex-VONA, they notoriously increase with the size of D. Hence,

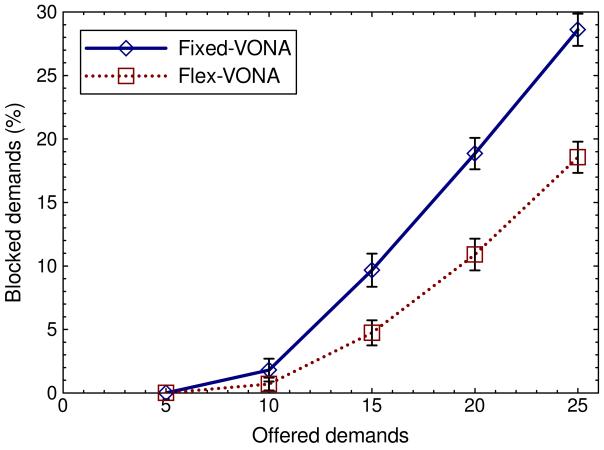

FIGURE 3.4: Blocking probability as a function of the size of the demand set.

an heuristic for the flexible grid scenario might be necessary when dealing with large scenarios as the the execution of the exact ILP formulation becomes impractical. The study and development of an heuristic for the flexible grid scenario is left for future work.

As for the results obtained through the executions of both models, Figure 3.4 shows the Blocking Probability (BP) of the demands as a function of the size of the demand set. It can be observed that the flexible grid scenario provides a lower BP figure (i.e. allocates a larger number of VONs) than the fixed-size grid scenario, being the difference more notorious as $|D|$ increases (e.g., a difference in BP of around 1.1% for $|D| = 10$ is observed while a difference of around 8% is observed for $|D| = 20$).

This capacity of being able of allocating a larger number of VONs in the flexible grid scenario is due the fact that its granularity is more finner than the fixed-grid scenario's granularity, making it possible to adjust more to the bandwidth needs of the demands. Focusing on the traffic profile considered for the experiments, for the demands requesting 25 GHz, the flexible grid scenario allocates exactly 25 GHz of spectrum to these demands, while in the fixed-size grid scenario, due its coarser granularity, it allocates 50 GHz of spectrum to these demands, adding an overhead of 100%. The capacity of the flexible grid scenario to allocate more VONs than the fixed-size grid could be potentially greater for traffic profiles where the disparity between the requested bandwidth by the demands and the channel spacing in the fixed-size grid scenario is big, either for sub-wavelength or super-wavelength traffic demands.

3.4 Online VON embedding

The previous sections studied various aspects of the VONA problem in a static, also called offline, scenario. That is, given a demand set, the objective is to optimally embed the VONs in the demand set considering that demands are permanent, with very long services

times, and the goal is to maximize the number of requests that can be allocated into the physical substrate given the limited resources of it. On the other hand, in an online (dynamic) scenario, demands are not known in advance but they arrive dynamically at the network. Such limited knowledge makes the previously presented mechanisms unsuitable for their use in a dynamic scenario, since they require full knowledge of the demand set in order to provide an optimal solution. Moreover, since VON requests arrive dynamically at the network one by one, it is not possible to provide an overall optimal solution since the available information only concerns about the request to be served and the status of the network, but any information regarding future demands is unknown. Additionally, a critical point in a dynamic scenario is the service time of the demands; it is required to serve the demands as soon as they arrive, with reasonable delays, so the techniques employed in a static scenario are not suitable due to its high execution times. For all these reasons, it is necessary to develop suitable techniques in order to efficiently allocate VON requests in a dynamic scenario.

Looking at the literature regarding the problem of VNE in dynamic scenarios, a common strategy is to try to embed the VNs in a way that will favor the embedding of future demands [GZWZ13, XYWD13, MSK+13]. Since knowledge about the demands to come is not possible, a way to realize such approach consists on balancing the use of the network resources (e.g. [MSK+13]). In this way, the chance that future VN requests find enough free resources increase and, as a consequence, the acceptance ratio of the requests. Note, however, that an excessive load balancing may spread too much the VN requests in the network, so simultaneous saturation of some parts of the network may happen. Additionally, as demands are served on the fly, sub-optimal solution when embedding a VN request are found. This leads to a very inefficient use of the physical resources. In order to obtain a better resource usage of the physical resources, bulk connection provisioning has been proposed in the literature [ACMW12, KPV+09]. In bulk connection provisioning, connections are served in batches after a desired batch size has been reached or a timeout has expired in contrast with a per-connection provisioning, where demands are served one by one when they arrive. With such approach it is possible to increase the efficiency of the use of network resources in a dynamic network scenario.

With such discussion, this section focuses on the dynamic scenario in the context of VONs. In this regard, it is assumed that VON demands arrive following a dynamic traffic profile at a physical substrate network with limited resources. The aim in such scenario, as it has been said before, is to embed the VONs in a manner that will favour the embedding of future incoming demands. To this end, an ILP formulation whose goal is to balance the load of the underlying physical resources is presented, with the addition that demands may be served in batches to increase the optimality of the mapping solution provided by the ILP formulation as commented before. In this sense, the objective of the presented formulation is dual: maximize the number of successfully embedded VONs inside the batch while at the same time balance the load of the physical resources. Opaque VONs are assumed throughout this section. Additionally, the solution presented focuses on the link mapping sub-problem. That is, it is assumed that the node mapping is already given.

Let the optical network substrate be characterized by a graph $G_n = (N, E)$, where N denotes the set of nodes and $E = \{(i,j),(j,i) : i,j \in N, i \neq j\}$ the set of physical links. Consider D as the batch of VON demands to be allocated over the optical network. Each demand $d \in D$, is characterized by a graph $G'_d = (N'_d, E'_d)$, where N'_d denotes the set of virtual nodes and $E'_d = \{(i,j),(j,i) : i,j \in N'_d, i \neq j\}$ the set of virtual links. Let W denote the set of available wavelengths per physical link and W_d denote the number of wavelengths per virtual link desired by demand $d \in D$. Moreover, let P define the set of paths in the physical network, $P^d_{e'} \subseteq P$ the set of candidate paths for virtual link e' in demand d and $P^e_{e'} \subseteq P$ the set of candidate paths for virtual link e' that traverse physical link $e \in E$. Additionally, let R_p denote the residual bandwidth of physical path p, being the residual bandwidth the number of wavelength with continuity between source and destination of the path. Such parameter will be used to balance the mapping of virtual links in the physical substrate. The strategy followed in this regard is to favor physical paths that have higher values of R_p when embedding the VONs. In this way, the saturation of the physical links is avoided, hence balancing the load in the network. Finally, let W^u_p define the set of wavelength that are already in use in path p. It is also assumed that physical nodes have no limitations in the number of TSPs that are using. With such definitions, the problem variables are:

$x^{p,w}_{d,e'}$: binary; 1 if virtual link e' in demand d is mapped over physical path p and wavelength w, 0 otherwise.

$y^p_{d,e'}$: binary; 1 if virtual link e' in demand d is exclusively mapped over physical path p, 0 otherwise.

z_d: binary; 1 if demand d is successfully mapped, 0 otherwise.

The ILP formulation is stated below:

$$\max\ \alpha\frac{1}{|D|}\sum_{d\in D} z_d + \beta\frac{1}{|D|}\frac{1}{|W|}\sum_{d\in D}\frac{1}{|E'_d|}\sum_{e'\in E'_d}\frac{1}{|P^d_{e'}|}\sum_{p\in P^d_{e'}} R_p \sum_{w\in W} x^{p,w}_{d,e'},\ \text{s.t.} \tag{3.22}$$

$$\sum_{p\in P^d_{e'}}\sum_{w\in W} x^{p,w}_{d,e'} \leq W_d, \forall d \in D, e' \in E'_d \tag{3.23}$$

$$\sum_{d\in D}\sum_{e'\in E'_d}\sum_{p\in P^e_{e'}} x^{p,w}_{d,e'} \leq 1, \forall d \in D, e \in E, w \in W \tag{3.24}$$

$$x^{p,w}_{d,e'} = 0, \forall d \in D, e' \in E'_d, p \in P^d_{e'}, w \in W^p_u \tag{3.25}$$

$$y^p_{d,e'} \leq \frac{1}{|W_d|}\sum_{w\in W} x^{p,w}_{d,e'}, \forall d \in D, e' \in E'_d, p \in P^d_{e'} \tag{3.26}$$

$$z_d \leq \frac{1}{|E'_d|} \sum_{e' \in E'_d} \sum_{p \in P^d_{e'}} y^p_{d,e'}, \forall d \in D \tag{3.27}$$

Objective function (3.22) aims at maximizing the number of successfully served demands inside the batch while balancing the load in the physical network by choosing the less congested paths. The factors α and β are pondering factors that serve to put more or less weight to the terms. Constraints (3.23) ensure that at most W_d wavelength will be provisioned for every virtual link in demand d. Constraints (3.24) are the wavelength clashing constraints. Constraints (3.25) avoid using pairs (p, w) to map the demand that are already in use by previous allocated demands. Constraints (3.26) ensure that all wavelengths requested by a virtual link are mapped over the same path; this is to avoid delay problems at destination. Finally, constraints (3.27) discriminate if demand d is successfully served.

3.4.1 Simulation results

In order to test the presented formulation, some simulations have been performed. They have been run over the 16-Node EON core network topology assuming 40 wavelengths per physical link. For the results, it is assumed that VON requests arrive at the network following a Poisson traffic profile with exponentially distributed mean Holding Times (HTs). Hence, different load scenarios are obtained modifying the demands' mean Inter-arrival Times (IATs) accordingly (load = HT/IAT). It is assumed that 10^5 random VON requests arrive at the network. Each VON request is generated following a 3 step process: firstly, 3 or 4 physical network nodes (with equiprobability) are randomly selected as virtual nodes for each demand. Next, the selected virtual nodes are then randomly connected with equiprobability and preventing the generation of non-connected graphs.

Finally, the parameter W_d is set to {1, 2} with probabilities equal to 80 and 20%, respectively. Moreover, the size of the candidate path set per virtual link is limited to 10, since in an online scenario the critical point is to obtain a good trade-off between execution time and optimality of the solution found. Also, different sizes of the batch have been considered in order to analyze the impact of this factor on the BP and execution time of the model. In this regard, a batch is constructed putting in a queue the demands until the desired size is reached. Note, however, that any timeout for which the batch would be automatically processed if it has not reach the desired size after a set period of time is not considered. The inclusion of such timeout and the implications on the performance of the proposed mechanism are left for future work.

Figure 3.5.a depicts the BP as a function of the network load for different batch sizes while Figure 3.5.b displays the execution time of the model. Simulations are run in i5 with four cores at 3.3 GHz PCs with 4 GB of ram memory and using IBM Cplex v12.2 as optimization software. For these results we have considered $\alpha = 1$ and $\beta = 0.5$, that is,

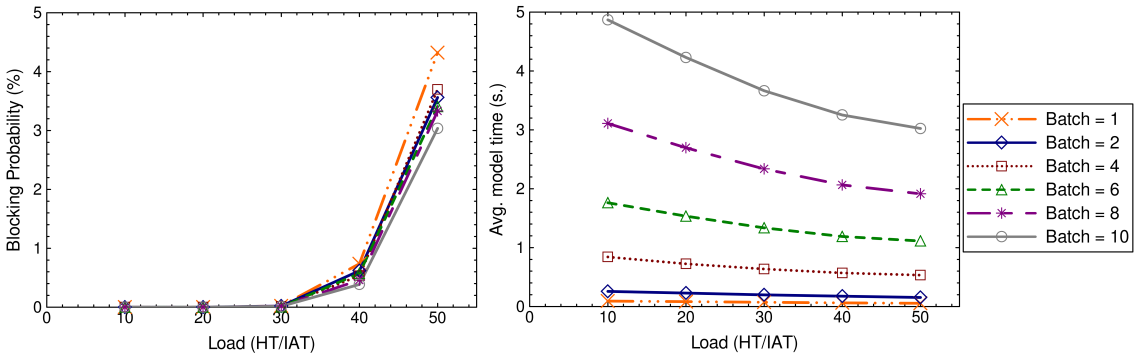

FIGURE 3.5: Simulation results: a) blocking probability and b) average model execution time as a function of the load.

the number of VONs that are successfully embedded inside the batch is prioritized over balancing the load of the physical paths in the network.

From the depicted results, it can be observed that using bigger batches does not present a clear advantage in front of smaller batches. Focusing in the BP, for a load equal to 40 the difference between a batch of size 1 and 10 is about 0.35 % while this difference rises up to 1.3 % for a load equal to 50. On the other hand, for a batch equal to 1, the model execution times remains in the order of few milliseconds while for a batch equal to 10 this time ranges from about 5 to 3 seconds. In view of this, due the little improving in BP that offers the use of bigger batches compared to smaller batches, it may not justify the extra amount of time needed to construct the batch and execute the model, so smaller batches or even serve the demands one by one would be the preferred option.

3.5 Optical and IT virtual infrastructure composition

Up to now, the previous sections in this chapter have dealt with the VONA considering that the intended VONs were meant to only provide connectivity services in a geographically distributed, so the target was to compose VONs considering only the allocation of lightpaths (pairs of path and wavelengths). However, as mentioned during section 3.1, new emerging paradigms such as Cloud Computing require not only the provisioning of VNs encompassing exclusively connectivity services (such as the VONs presented so far) but also some IT capacities (e.g., storage, computational capacity, etc.) in some selected nodes in the VN so combined services composed of connectivity services plus IT capacities can be provisioned over the VN. In this regard, it becomes of capital importance to develop techniques that efficiently account for the particularities of both realms (optics and IT) so as to optimally compose VIs that combine both optical transport services among a geographically distributed area and IT capacities in some selected nodes. To this end, the current section presents an ILP-based heuristic in order to optimally accommodate

VI demands into a physical network substrate composed by a transport transparent optical network connecting geographically distributed IT sites, such as Data Centers (DCs), where IT resources are present.

The intended scenario under study relates to the situation where a new infrastructure provider, willing to deliver both IT and network resources as a service, is interested in planning the amount of IT and optical resources that must be deployed to serve an already known set of VI demands. In other words, the VI embeddings (virtual-physical node and link mappings) that minimize the amount of IT and optical resources in the substrate are targeted. Note that, departing from the previous sections, where the node mapping was assumed to be already done and only the node mapping was performed, the current section peruses a joint node plus link mapping of the VIs, giving the freedom to select the best physical location of the virtual nodes so as to obtain a more optimized embedding of the VIs. As it will be shown later, such joint optimization becomes a very challenging task, since the freedom existent in the virtual-physical node mapping (a virtual node can, in principle, be mapped to any physical node in the substrate network) makes the problem of embedding a VI on a physical network substrate to be NP-hard [CRB09]. This has been one of the motivations behind the proposal of the heuristic depicted below.

With such scenario in mind, let the optical network substrate be represented by a graph $G_n = (N, E)$, where N denotes the set of nodes and $E = \{(i,j),(j,i) : i,j \in N, i \neq j\}$ the set of physical links. Each physical link is equipped with a set of wavelengths represented by W. In this regard, it is assumed an all-optical network, without regeneration or wavelength conversion capabilities. Hence, all virtual links of the demands must ensure the wavelength continuity constraint between their end points. Moreover, it is assumed that all wavelength requested by a particular virtual link in a specific VI request must be routed through the same physical path. This is done to avoid reordering problems associated to the differential delay that would happen if the wavelengths where routed through different paths. With this, the electronic buffers at the end points of the virtual links are kept at a minimum size, reducing the overall network cost. Additionally, it is assumed that IT sites are connected to the core transport network through a network with sufficient capacity. This is equivalent to having some nodes in the optical network substrate graph with IT resources associated to them. Thus, $N_{IT} \subseteq N$ defines the set of nodes with IT resources. The considered IT resources per node are CPU frequency (in GHz), storage capacity (in GB), memory capacity (in GB) and number of CPU cores.

Moreover, let D denote the set of demands to be accommodated on the physical substrate. Each demand $d \in D$ is characterized by a graph $G'_d = (N'_d, E'_d)$, $N'_d \subseteq N_{IT}$, $E'_d = \{(i,j),(j,i) : i,j \in N'_d, i \neq j\}$, where each of the virtual nodes $n' \in N'_d$ requests for a certain amount of IT resources. Let $F^d_{n'}$ (CPU frequency), $S^d_{n'}$ (storage), $M^d_{n'}$ (memory) and $C^d_{n'}$ (cores) define the particular IT resources requested by virtual node $n' \in N'_d$, and F^d_{max}, S^d_{max}, M^d_{max} and C^d_{max} define the maximum amount of IT resources requested by some virtual node in demand $d \in D$. It is assumed that two virtual nodes belonging to the same VI request cannot be mapped to the same physical node. This is done for

Inputs: D, G_n, W, α, β_F, β_S, β_M, β_C
Output: Sol

Phase 1: Pre-processing
$Sol \leftarrow \emptyset$ Calculate $Cost_d$ for every demand $d \in D$
Order demands in D in descending order according to $Cost_d$
for $n = 1$ **to** $|D|$ **do**
    Phase 2: ILP solving
    $Sol \leftarrow Sol \bigcup$ output from ILP for demand d_n
    Actualize substrate state according to model output
Return Sol

TABLE 3.4: DOVIP mechanism pseudo-code.

reliability issues, guaranteeing that if a physical node hosting virtual nodes from various demands fails, the whole VIs will not be affected but only the virtual nodes mapped over tha particular physical resource. Additionally, W_d denotes the number of wavelengths per virtual link requested by demand $d \in D$. The pseudo-code of the proposed heuristic, called Deterministic Ordering Virtual Infrastructure Planner (DOVIP), is displayed in Table 3.4.

Firstly, demands are ordered in descending order according to the expression depicted in (3.28), where $m(\cdot)$ denotes the maximum function among all demands $d \in D$. In this way, the heuristic initially tries to fit the biggest demands, which may be more complicated to allocate, and then the smaller demands, more easily allocable. Factors α, β_F, β_S, β_M and β_C are used to put more or less weight to the terms of the expression. Once the demands are ordered, the heuristic iteratively executes for each demand an ILP model whose goal is to jointly minimize the number of wavelengths per physical link and, at the same time, the amount of IT resources in the more congested node $n \in N_{IT}$ once the current demand is served. After each model execution, the state of the physical substrate is updated before starting with the next iteration.

$$\begin{aligned} Cost_d = \alpha \frac{|E'_d| W_d}{m(E'_d|) m(W_d)} + (1-\alpha)(\beta_F \frac{F^d_{max}}{m(F^d_{max})} + \beta_S \frac{S^d_{max}}{m(S^d_{max})} + \\ + \beta_M \frac{M^d_{max}}{m(M^d_{max})} + \beta_C \frac{C^d_{max}}{m(C^d_{max})}) \frac{|N'_d|}{m(|N'_d|)}, \forall d \in D \end{aligned} \tag{3.28}$$

The details of the ILP model executed at each iteration of the DOVIP heuristic are discussed below. To this, let F^n_u, S^n_u, M^n_u and C^n_u define the amount of IT resources that are already in use in node $n \in N_{IT}$; F^u_{max}, S^u_{max}, M^u_{max} and C^u_{max} the maximum amount of IT resources that are already in use for some node $n \in N_{IT}$; and W^e_u define the set of wavelengths that are already in use in physical link $e \in E$. Additionally, let $\delta^+(n)$ and $\delta^-(n)$ define the set of outgoing and incoming edges from/to $n \in N$ respectively. Finally, let $a(e')$ and $b(e')$ denote the source and destination of virtual edge $e' \in E'_d$. The decision variables of the model are:

$x_{n'}^{n}$: binary; 1 if virtual node n' is mapped over physical node n, 0 otherwise.

$y_{e'}^{e,w}$: binary; 1 if virtual link e' is mapped over physical link e and wavelength w, 0 otherwise.

t_w: binary; 1 if wavelength w is used in any physical link, 0 otherwise.

F_n, S_n, M_n, C_n: integers; IT capacities in node $n \in N_{IT}$.

S_{max}, M_{max}, C_{max}: integers; maximum values among S_n, M_n and C_n.

The ILP formulation is:

$$\begin{aligned}\min\ & \alpha\frac{1}{|W|}\sum_{w\in W} t_w + (1-\alpha)\Big(\frac{1}{F_{max}^{u}|N_{IT}|}\beta_F \sum_{n\in N_{IT}} F_n + \beta_S\frac{S_{max}}{S_{max}^{u}+S_{max}^{d}} + \\ & + \beta_M\frac{M_{max}}{M_{max}^{u}+M_{max}^{d}} + \beta_C\frac{C_{max}}{C_{max}^{u}+C_{max}^{d}}\Big),\ \text{s.t.}\end{aligned} \tag{3.29}$$

$$F_{n'}^{d}x_{n'}^{n} \le F_n, \forall n' \in N_d', n \in N_{IT} \tag{3.30}$$

$$F_u^n \le F_n, \forall n \in N_{IT} \tag{3.31}$$

$$S_n = S_u^n + \sum_{n'\in N_d'} S_{n'}^{d}x_{n'}^{n}, \forall n' \in N_d', n \in N_{IT} \tag{3.32}$$

$$S_n \le S_{max}, \forall n \in N_{IT} \tag{3.33}$$

$$M_n = M_u^n + \sum_{n'\in N_d'} M_{n'}^{d}x_{n'}^{n}, \forall n' \in N_d', n \in N_{IT} \tag{3.34}$$

$$M_n \le M_{max}, \forall n \in N_{IT} \tag{3.35}$$

$$C_n = C_u^n + \sum_{n'\in N_d'} C_{n'}^{d}x_{n'}^{n}, \forall n' \in N_d', n \in N_{IT} \tag{3.36}$$

$$C_n \le C_{max}, \forall n \in N_{IT} \tag{3.37}$$

$$y_{e'}^{e,w} \le t_w, \forall e' \in E_d', e \in E, w \in W \tag{3.38}$$

$$1 \leq t_w, \forall e \in E, w \in W_u^e \tag{3.39}$$

$$y_{e'}^{e,w} = 0, \forall e' \in E'_d, e \in E, w \in W_u^e \tag{3.40}$$

$$\sum_{n \in N_{IT}} x_{n'}^{n} = 1, \forall n' \in N'_d \tag{3.41}$$

$$\sum_{n' \in N'_d} x_{n'}^{n} \leq 1, \forall n \in N_{IT} \tag{3.42}$$

$$x_{n'}^{n} = 0, \forall n' \in N'_d, n \notin N_{IT} \tag{3.43}$$

$$\sum_{e' \in E'_d} (y_{e'}^{e_{i,j},w} + y_{e'}^{e_{j,i},w}) \leq 1, \forall e \in E, w \in W, i \neq j \tag{3.44}$$

$$\sum_{e \in \delta^+(n)} \sum_{w \in W} y_{e'}^{e,w} - \sum_{e \in \delta^-(n)} \sum_{w \in W} y_{e'}^{e,w} = W_d(x_{a(e')}^{n} - x_{b(e')}^{n}), \forall e' \in E'_d, n \in N \tag{3.45}$$

$$-x_{b(e')}^{n} \leq \sum_{e \in \delta^+(n)} y_{e'}^{e,w} - \sum_{e \in \delta^-(n)} y_{e'}^{e,w} \leq x_{a(e')}^{n}, \forall e' \in E'_d, n \in N, w \in W \tag{3.46}$$

$$y_{e'}^{e,w} \leq 1 - x_{b(e')}^{n}, \forall e' \in E'_d, n \in N, e \in \delta^+(n), w \in W \tag{3.47}$$

$$y_{e'}^{e,w} \leq 1 - x_{a(e')}^{n}, \forall e' \in E'_d, n \in N, e \in \delta^-(n), w \in W \tag{3.48}$$

$$W_d y_{e'}^{e,w} \leq \sum_{w \in W} y_{e'}^{e,w}, \forall e' \in E'_d, e \in E, w \in W \tag{3.49}$$

The ILP objective function is depicted in (3.29). Constraints (3.30), (3.31), (3.32), (3.34) and (3.36) serve to give value to the IT resource variables, taking into account the current state of the physical resources and those resources requested by the demand. Constraints (3.33), (3.35) and (3.37) are the constraints that enable the minimization of the IT resources in the most congested IT node. Constraints (3.38) account for the wavelengths that are being used to serve the demand, while constraints (3.39) account for the wavelengths that are already in use due to previous allocations. Constraints (3.40) avoid the use of pairs (e, w) that are already in use when allocating the demand. Constraints (3.41) ensure that all virtual nodes $n' \in N'_d$ are being mapped over a unique physical

node, while constraints (3.42) ensure that a physical node $n \in N_{IT}$ does not support more than one virtual node per demand. Constraints (3.43) avoid using physical nodes $n \notin N_{IT}$ for mapping virtual nodes. Constraints (3.44) are the wavelength clashing constraints, implicitly accounting for the true bidirectional nature of the demands through considering both directions of physical arc (i, j), (j, i), although unidirectional demands were defined; in this way, the complexity of the model is reduced and, hence, its execution time. Constraints (3.45) ensure that all virtual links $e' \in E'_d$ are provided with the required number of wavelengths. Constraints (3.46) are the flow conservation and wavelength continuity constraints. Constraints (3.47) and (3.48) serve to avoid loops at the remote endpoints of a virtual link; in the source remote endpoint, traffic can only flow outside the node, while in the destination remote endpoint, traffic can only enter at the node. Finally, constraints (3.49) ensure that for a virtual link, all requested wavelengths follow the same route; this is done to avoid delays.

It is worth to mention that, while the proposed formulation only takes a single VI demand as input, placing it optimally according to the current substrate state and the characteristics of the VI itself, the feasibility of an offline ILP planning model that takes the entire demand set D, and tries to place all demands over the underlying physical substrate in an optimal way was alternatively evaluated. Nevertheless, the experienced execution times where extremely long, even for small demand set sizes. For example, for $|D| = 5$, execution times in the order of 10^6 seconds were registered. This became a key motivation behind DOVIP heuristic as a way to solve the addressed problem in a reasonable time.

3.5.1 Simulation results

In order to illustrate the performance of the DOVIP heuristic, a series of executions for various sizes of the demand set D and values of the factor α have been carried out; factors β_F, β_S, β_M and β_C are fixed to 0.25. Results throughout this section have been averaged over 20 random generations of the demand sets, being executed in an Intel Core i5 PC with 4 cores at 3.3 GHz and 4 GB of RAM PCs, running CPLEX v.12.2.

The DT network topology (see Appendix A) is used as the physical substrate network, assuming that IT resources are present in Berlin, Munchen, Stuttgart, Dusseldorf, Hamburg and Hannover (Figure 3.6). Demands in the set are generated randomly, considering 3 or 4 nodes per demand and connecting them with probability 0.5, preventing the generation of non-connected graphs. It is assumed $W_d = 1$ for all demands. As for the IT resources requested by virtual nodes of the demands, these are chosen with equiprobability between 1.0-2.2 with steps of 0.2 for the CPU frequency, 10-30 with steps of 5 for the storage capacity, 2-8 with steps of 2 for the memory capacity and 1-4 with steps of 1 for the number of CPU cores.

Table 3.5 displays the average values for the physical substrate resources that take a role in objective function (3.29), along with the average execution time. Results for various values

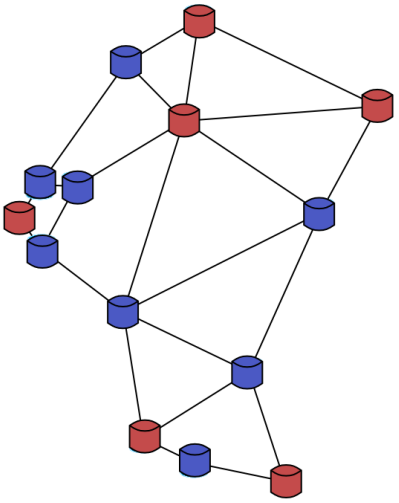

FIGURE 3.6: DT network topology scenario used for the simulations; red nodes depict IT sites.

TABLE 3.5: DOVIP performance comparison

		$\alpha = 1$	$\alpha = 0.75$	$\alpha = 0.5$	$\alpha = 0.25$	$\alpha = 0$
$\|D\| = 10$	**Sum**(t_w)	5.55	5.8	5.9	6.65	14.65
	Sum(F_n)	12.43	12.12	12.1	12.06	11.95
	S_{max}	180	137.25	132	129.75	128.75
	M_{max}	43.7	30.8	30.5	30.1	29.9
	C_{max}	21.85	15.4	15.25	15.05	14.95
	Time (s.)	11.74	66.44	79.43	61.94	48.57
$\|D\| = 15$	**Sum**(t_w)	7.9	8.5	8.95	9.95	19.8
	Sum(F_n)	12.8	12.63	12.53	12.46	12.4
	S_{max}	262.5	192.5	191.5	188	185.75
	M_{max}	68	47.1	46.5	45.2	45
	C_{max}	34	23.55	23.25	22.7	22.5
	Time (s.)	25.87	150.49	150.76	138.4	86.24
$\|D\| = 20$	**Sum**(t_w)	10.2	11.2	11.2	12.1	20
	Sum(F_n)	12.83	12.61	12.56	12.55	12.29
	S_{max}	351.5	255	250.5	248.25	245.5
	M_{max}	87.4	61.3	61.1	60.1	59.7
	C_{max}	43.7	30.65	30.55	30.05	29.85
	Time (s.)	31.31	146.65	161.8	158.5	99.35

of $|D|$ and α have been obtained. Note that $\alpha = 1$ and $\alpha = 0$ identify extreme situations, only focusing on the minimization of optical resources or IT resources, respectively. It can be appreciated that $\alpha = 0.5$ working point offers a fair trade-off between the amount of network and IT resources needed for any of the considered $|D|$ sizes. It uses much less optical resources than $\alpha = 0$ (around a 50% less) and less IT resources than $\alpha = 1$ (around a 2% less for the CPU frequency and a 30% less for the rest of IT resources), while it only uses around a 2% more IT resources than $\alpha = 0$ and a 10% more optical resources than $\alpha = 1$. In this sense, it can be appreciated that the joint optimization of optical and IT resources results in a good trade-off between the two parts.

3.6 Chapter summary

The advent of VNs has helped to shape the future Internet and new network architectures and business models so as to cope with the increasing traffic on Internet and the emerging of new services and paradigms. Such services and paradigms require mission-specific networks, tailored to its exact needs, so as to perform an optimized management and control of the services that will run on top of them. One critical aspect on the design of such VNs refers to how the virtual resources are mapped into physical resources of the substrate network. Such problem is known as the Virtual Network Embedding problem, and has been extensively studied for electrical networks (Layer 2/3) in the literature. However, although the VN paradigm has recently been adopted on the optical network field and massive research is being done on VONs, the lack of maturity of the virtualization techniques on this field requires that specific algorithms, accounting for the particularities and challenges posed by the optical medium, have to be developed to perform an optimized embedding of the VONs into the physical network substrate.

With such goal in mind, the presented chapter has studied various aspects of the VNE in optical substrate networks and proposed various mechanisms in this regard. Firstly, the VNE problem has been introduced, along with the main literature regarding the topic, so as to contextualize the sections to come. This has lead to the proposal of various mechanisms to optimally embed VONs depending on the services intended to be offered on top of them, the technology employed by the physical substrate and the dynamicity of the network scenario.

Specifically, section 2 has focused on developing mechanisms to optimally allocate VONs in top of a physical substrate focusing on the nature of the connectivity services that will run on top of them. To this end, opaque and transparent VONs have been defined, with transparent VONs offering fully transparent end-to-end connections along its topology while opaque VONs not. The proposed mechanisms for each kind of VON have been benchmarked with simpler embedding mechanism, highlighting the superior performance that can be obtained when optimally allocating a VON demand set.

However, despite the flexibility that VONs offer in regards of the management of the virtual resources and the optimized resource allocation that can be achieved with the proper embedding mechanisms, the performance of the VONs (e.g. in terms of use of the spectrum) is highly tied to the underlying physical technology. To achieve a better resource utilization and more flexibility on the VON level, equally efficient and flexible network substrates have to be considered. A promising candidate to realize this are EONs, thanks to their finner spectrum granularity that allows to efficiently serve high and low bit-rate demands, achieving the desired flexibility in terms of spectrum provisioning at the VON level. However, due to the different physical technology employed by EONs, it is necessary to develop embedding mechanisms that account for the particularities of this new network substrate. To this end, section 3 has provided ILP mechanisms to optimally embed VONs into an EON-based physical substrate. The performance study of the proposed mechanisms has reveled that, indeed, EONs provide a much more efficient network substrate when compared to traditional wavelength switched networks, allowing to allocate a higher number of VON requests into the network substrate.

After these studies, section 4 has focused on the development of embedding techniques into more dynamic network scenarios, where a full knowledge of the demand set in not possible. In such a dynamic scenario, VON requests arrive one by one at random to the physical network substrate and have to be allocated according to the actual state of the network and the characteristics of the request. In order to enhance the performance of the whole embedding process, a load distribution-based mechanism have been employed, so as to facilitate the embedding of future VON requests. Additionally, a bulk provisioning of the VONs have also been considered so as to obtain more optimum embeddings and a better resource usage of the physical substrate.

To finalize the studies regarding the VON embedding problem, section 6 has extended the scenario under study to also consider the presence of IT resources in some selected nodes in the optical network substrate, so VI requests combining both IT capacities and optical transport services can be composed. Such hybrid substrate requires that specific optimization methods accounting for the particularities of both realms have to be developed. To this end, an ILP-based heuristic has been proposed with the goal to minimize the amount of resources (IT and optical) that have to be provisioned into the physical substrate so as to correctly allocate a known VI request set. In this regard, it has been shown that a joint optimization of both IT and optical resources results in a good trade-off when compared against scenarios that only focus on the optimization of one type of resources, either IT or optical ones.

Chapter 4

Improving EONs efficiency: the split spectrum approach

This chapter focuses on improving the efficiency of EONs in terms of spectrum utilization. An efficient spectrum utilization plays an important role when serving connections in EONs, due to the fact that the random arrival and departure process of connections in this kind of networks tends to fragment the available spectrum over the time. In such situation, it becomes challenging to serve connections, specially connections requiring large bit-rates, as the chances to find a sufficient number of contiguous FSs to accommodate them decreases. Hence, it becomes highly desirable to provide mechanisms to mitigate such effect and improve the allocation of demands.

To begin, first section presents the spectrum fragmentation problem in EONs and its main consequences on the performance of such networks. Additionally, it surveys the work present in the literature that deal with such problem by means of de-fragmentation techniques. The second section presents the SSA as an alternative method to overcome the spectrum fragmentation problem in EONs and its enabling technologies. This leads to the proposal of various mechanisms to efficiently perform the resource assignment of incoming connections in a SS-enabled EON in section three and four. Specifically, section three introduces the problem of route and spectrum assignment in SS-enabled EONs and proposes various solutions to tackle the problem. Next, in section four, the problem is extended to also consider the assignment of the most suitable modulation format to the connections depending on the desired bit-rate and the network characteristics and status. To this end, a novel assignment mechanism is proposed and thoroughly evaluated. The last section summarizes the achievements of the presented chapter.

4.1 The spectrum fragmentation problem

Although EONs present large benefits when compared to traditional WDM optical networks, they also pose important challenges, being the main one the so called spectrum fragmentation effect [WM12], which can greatly affect the performance (e.g., the Bit-rate Blocking Ratio (BBR)) of such networks. This effect refers to the fact that, due to the random arrival and departure process of the demands over the network, the available spectral resources (the FSs) become highly fragmented, forming spectral gaps (i.e., bunches of free contiguous FSs) of heterogeneous sizes scattered along the spectrum, thus making more complex the allocation of future demands. This happens because in EONs, demands, instead of a full wavelength, request for a contiguous spectrum portion tailored to their own needs. Hence, their chances to find a contiguous spectrum portion decrease, potentially leading to blocking situations. Figure 4.1 illustrates this situation. In Figure 4.1.a, a certain number of connections, with different bandwidth requirements, is established over a given network link. After some time, in Figure 4.1.b, one of these connections is released, thus freeing a portion of the spectrum in that link. Finally, in Figure 4.1.c, a new high data-rate connection request arrives at the network and should be allocated on the link under study. Even though the total spectrum available on that link would be enough to allocate the new connection, such spectrum is fragmented into smaller portions than the contiguous spectrum requested by the incoming connection, which eventually causes its blocking.

To mitigate the spectrum fragmentation effects in EONs, spectrum defragmentation strategies have been proposed in the literature [WM12, ZYP+13, PJJW11, KHSI11, YWG+12], which may be performed preventively when a demand is allocated (e.g. [WM12]) or reactively when blocking occurs (e.g. [YWG+12]). Essentially, the rationale behind these strategies is to properly rearrange active connections in the network, so as to free as much contiguous spectrum as possible to be used by future connection requests. In this regard, the techniques can be classified as techniques that re-route the existing connections (disruptive techniques), or techniques that only rearrange the utilized spectrum without changing connections' routes (hitless techniques). In the latter case, the established connections are not disrupted when performing the spectrum defragmentation.

Note, however, that disruptions of active traffic caused by a reallocations is not admissible for certain classes of service, being hitless spectrum defragmentation of paramount importance in such a context. For these reason, make-before-break strategies are normally adopted in defragmentation mechanisms: before tearing down a lightpath, the new associated lightpath resulting from the defragmentation mechanisms is first created, so the traffic does not experience any disruption. However, this operation presents some drawbacks: note that to create the new ligthpath before tearing down the old one requires to allocate at a given time twice the resources needed to serve that ligthpath. This could lead to not having the sufficient resources to perform the make-before-break operation and, consequently, the traffic could experience some disruptions. Moreover, if

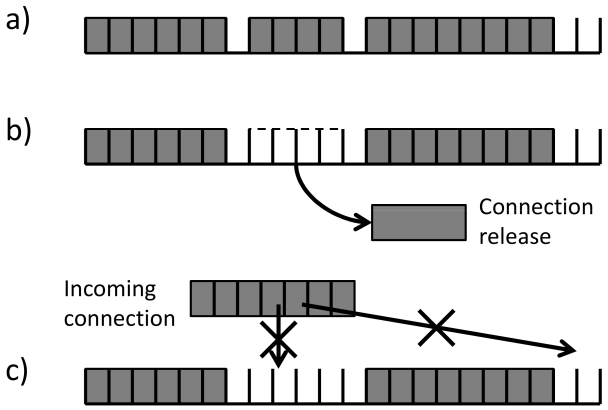

FIGURE 4.1: Example of spectrum fragmentation in a dynamic EON scenario.

there are enough spectral resources to perform this operation, during the time where both lighpaths, new and old, are present, it could happen that a possible incoming demand can not be served due the lack of spectral resources. Also, defragmentation techniques add an extra complexity to the control plane in order to perform and manage all the re-allocations properly.

On the other hand, equipping the nodes with spectrum conversion capabilities [BMS+14] would allow to reduce the blocking of some demands through using not necessarily the same spectrum in all the links in the path from source to destination node. However, spectrum conversion devices are expensive and introduce some delay in the demands (due the conversion) that may not be admissible for certain classes of service. For all these reasons, it is necessary to propose alternative approaches to overcome the limitations posed by the spectrum fragmentation effect. To this end, the SSA is introduced in the following section.

4.2 Split spectrum-enabled EONs

Running away from the spectrum defragmentation or spectrum conversion the SSA has been recently proposed and is arising as a promising way to further increase the efficiency of EONs, mitigating the effect of the spectrum fragmentation and lowering the BBR [XPDY12, JTS+12, CJG13, PPSC14]. The main rationale behind the SSA lays on dividing a high bit-rate demand into a set of lower bit-rate sub-demands if a blocking situation arises, making the resulting sub-demands more easily allocable in the available FSs. This approach can basically be triggered in two kind of situations: 1) when there are not enough contiguous FSs to serve the demand due to the spectrum fragmentation effect or 2) when the modulation format used to transmit the desired bit-rate becomes infeasible due to transmission impairments that limit the transmission reach. In both cases, the demand can be split to better take advantage of the spectral gaps. Moreover,

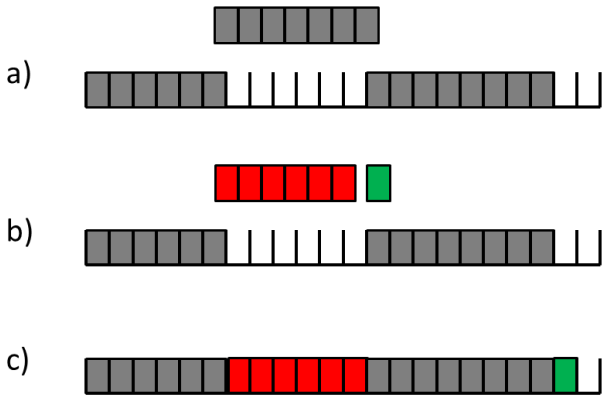

FIGURE 4.2: Example of a SS-enabled EON.

more robust modulation formats can be used, since the resulting sub-demands are transmitted at lower bit-rate. Figure 4.2 depicts a situation where the SSA is employed to overcome a potential blocking situation due to the lack of enough contiguous FSs. In Figure 4.2.a, a high bit-rate connection arrives to a network link. Due to the spectrum fragmentation effect, although there are enough spectral resources (i.e. FS) to serve the connection, they are scattered in non-contiguous spectral gaps, so the connection cannot be served in a contiguous way. To overcome this, in Figure 4.2.b the original demand is split into smaller sub-demands. Since the sub-demands require less contiguous FSs, they can be allocated in the available spectral resources, as seen in Figure 4.2.c, thus, solving a potential blocking situation.

Once the original demand is split, the resulting sub-demands, hereafter referred as parts, have to be routed and spectral resources assigned to them, signaled and managed. This operation could be driven from the network control plane (e.g., based on GMPLS [FB06]), which could trigger the split of the incoming signal in the source node of the demand into multiple parts, to be transmitted to the destination over separated lightpaths. The reconstruction of the original signal would be therefore performed on reception, by electrically multiplexing those incoming sub-signals belonging to the same demand. In this process, the role of the control plane would be of key importance to manage the signaling and maintenance of the lightpath bundle [RFC3717] supporting a particular traffic demand which, in turn, would require an adequate configuration of the signal splitting and multiplexing operations at the source and destination nodes, respectively.

Concerning the routing process, the different parts can be either routed over the same physical path (single path approach) or over multiple physical paths (multipath approach). The first one provides the advantage of simplifying the signaling and routing process, as only one route has to be signaled and established. Additionally, the differential delay among the parts is kept very low, making the hardware needed at the destination node (electronic buffers) for the reconstruction of the original demand less complex. On the contrary, in the multipath approach, the different parts can be routed over different physical paths. Although this second approach may achieve better performance in terms

of BBR, the routing process is more complex since a routing instance must be triggered for each part. Furthermore, the size of the electronic buffers at the destination node must be large enough to mitigate the propagation delay differences between the parts.

Concerning the enabling technologies that make the SSA possible, there are basically two implementations regarding TSP architecture and utilization, namely, the BV-TSP-based and the Multi-Flow TSP (MF-TSP)-based. In the BV-TSP-based implementation [PPS12], once the demand has gone through the splitting process, the resulting parts are transmitted using independent BV-TSPs. That is, as many BV-TSPs as parts into which the demand has been split are employed, as shown in Figure 4.3.a. To do so, the mechanism takes advantage of the BV-TSPs at the nodes that are not in use when splitting the demand. In this implementation the number of parts into which a demand is split takes a capital role in the overall performance of SSA, since too many parts can rapidly exhaust available TSPs at nodes and lead to blocking due to the lack of them. For this reason, any allocation mechanism employing such an implementation has to carefully take into account this issue. On the other hand, this implementation does not impose additional hardware complexity with the sole SSA purpose, as basically relies on the hardware already deployed in the network, keeping the CAPEX within reasonable limits.

As for the MF-TSP-based implementation, as its name suggests, it employs MF-TSPs to transmit the split demand [XPDY12, JTS+12]. A MF-TSP is capable of transmitting and receiving multiple elastic optical channels (flows), operating at independent bit-rates, that can be routed independently. Therefore, SSA can be realized employing a unique MF-TSPs to transmit all the parts resulting from the split procedure. A simplified practical architecture of a MF-TSP, as proposed in [XPDY12], is depicted in Figure 4.3.b. Essentially, it would consist of an array of tunable lasers and blocks of modulators to support different types of modulation formats and bit-rates, terminated with an optical combiner at the transmitter side, while an optical splitter followed by an array of detectors is placed at the receiver side. The advantage that the MF-TSP implementation presents in front of the BV-TSP one, is that it only employs a TSP per demand, being split or not, so the potential lack of TSPs is not as pronounced in this scenario. On the other hand, the complexity and hardware requirements of this type of TSPs are higher, which may lead to higher overall network CAPEX.

For all of these, the SSA has triggered the interest of standardization organisms [HPS+13, SRML12] and the research community [XPDY12, TFB11, LZG+13, ZLZA13, PPS12]. For example, the Internet Engineering Task Force (IETF) is currently working on extending control plane architectures and protocols of fixed-grid optical networks to be able to also control and manage elastic optical networks. In this framework, the SSA is also being considered to be one of the choices for establishing a connection in flex-grid networks. However, the standardization proposals in this regard are at their very early stage (e.g., [HPS+13]).

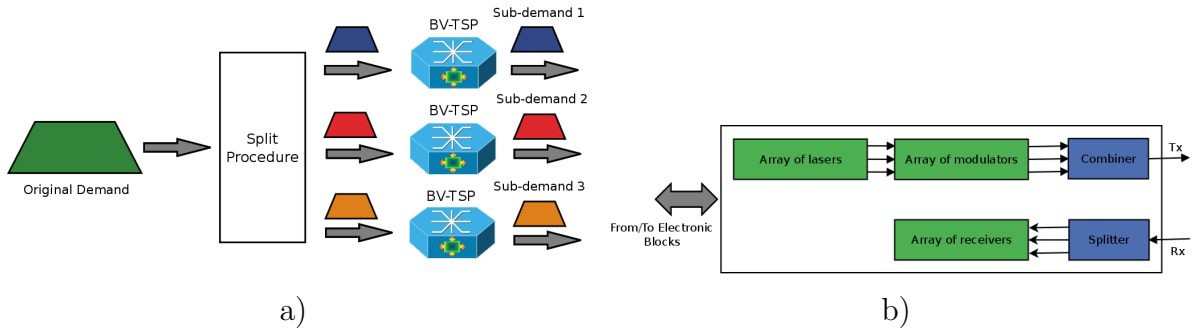

FIGURE 4.3: SSA enabling technologies: a) Example of BV-TSP-based SSA implementation; b) Architecture of a MF-TSP.

On the other hand, much effort has been already done to evaluate SSA as a solution to increase the performance of elastic optical networks. For instance, authors in [PPS12] proposed a simple algorithm for splitting in a SS-enabled elastic optical network demands that face blocking situations due to the spectrum fragmentation effect. The authors demonstrated that substantial improvements in terms of blocking can be achieved. Nonetheless, the authors only considered the single-path routing approach and did not tackle the choice of the best modulation format according to the demands needs.

Besides, authors in [LZG+13, ZLZA13] investigated the multi-path routing approach in SS-enabled optical networks, proposing multiple algorithms to intelligently split the demands, and showed that the multi-path routing approach, or even a hybrid single/multi-path approach, can lead to further gains in terms of blocking when compared to the single-path approach. Although authors in [ZLZA13] introduced the selection of the modulation format according to the specific bit-rate of the demands and the transmission reach of the modulation formats, they did not tackle the optimal selection of neither the route, spectrum portion nor the modulation format to serve a demand.

Similar work has been done by authors in [XPDY12, TFB11], where multiple algorithms are proposed to choose the route, spectrum and modulation format of demands in a SS environment. Additionally, authors in [XPDY12] introduced the concept of MF-TSP as a way to realize the SSA in elastic optical networks. However, none of these works is devoted to finding the optimal solution to the RSMLA problem in SS-enabled networks.

Authors in [CJG13] proposed an ILP-based mechanism to tackle the optimal route and spectrum assignment under multi-path SSA considering the differential delay issue. They showed that a correct dimensioning of the electronic buffers at the receiver end can compensate such delay and provide a better performance in terms of blocking than the single-path approach. Despite providing a mechanism capable of finding the optimal resources assignment, authors did not consider the selection of the modulation format, restricting the assignment to only selection of paths and FSs.

With all this said, it becomes of capital importance to provide mechanisms to optimally assign resources (paths, FSs and modulation formats) to a demand in a SS-enabled optical network for a dynamic scenario, considering both single and multi-path routing approaches as well as BV-TSPs or MF-TSPs. To this end, the rest of the chapter works progressively from the simplest case towards more complex scenarios in order to provide a mechanism that optimally assigns resources utilizing the SSA in EONs, considering both the aforementioned TSP implementations (BV-TSP and MF-TSP) and routing strategies (single and multipath).

4.3 Route and Spectrum Assignment (RSA) in SS-enabled EONs

The previous subsection introduced the SSA as a very interesting way to enhance the efficiency of EONs along with potential technologies to realize such approach. With such discussion, it is now turn to propose mechanisms to properly assign network and spectrum resources to incoming connections in a SS-enabled EON. To this end, this section begins targeting the RSA problem present in EONs as introduced during subsection 2.3.1, now adapted to the particularities and new challenges that the SSA poses. Next, it introduces a basic mechanism to tackle this problem in a dynamic scenario where connections arrive and depart at random, which later on is enhanced with additional considerations so as to provide a more optimized mechanism for the resource assignment.

Before introducing the proposed mechanisms, let us provide a more insight view about the differences between the RSA problem in traditional EONs and SS-enabled EONs. Without loss of generality, let us assume that the bit-rate of a connection can be translated to a specific bandwidth (i.e. spectrum portion) given the modulation format used to successfully reach the destination node. Ideally, and defining B as the requested bandwidth (in GHz) of a connection and F_w as the spectral width (in GHz) of a single FS, the requested bandwidth of a connection could be translated to a number of FSs equal to the ceiling of the division between B and F_w. However, BV-WXCs require guard bands between demands to properly perform the switching of the demands [AMZ+11]. Defining G as the guard band size (in GHz), the actual number of FSs needed to allocate a demand, denoted as S, can be calculated as:

$$S = \left\lceil \frac{B+G}{F_w} \right\rceil \tag{4.1}$$

Guard band requirements increase the initial value of S, fact that difficults even more the allocation of demands in a traditional EON, since the spectrum contiguity constraint must be respected. On the other hand, although in a SS-enabled EON the spectrum contiguity constraint can be relaxed due to the possibility of serving a demand in multiple parts,

such guard band requirements have to also be respected for every one of the parts. In fact, the number of necessary FSs to allocate a demand divided into H parts in a SS-enabled EON can be calculated as:

$$S = \sum_{i=1}^{H} \left\lceil \frac{B_i + G}{F_w} \right\rceil \tag{4.2}$$

where B_i is the amount of B allocated in the i^{th} part, that is, $B = \sum_{i=1}^{H} B_i$. It can be seen that the guard band requirements imposed by BV-WXCs may notoriously increase the value of S if the demand is divided into many parts. Moreover, there may be limitations on the number of parts into which a demand can be divided depending on the implementation of the SSA (BV-TSP or MF-TSP). Additionally, although the SSA tries to exploit the available spectral gaps to serve a demand and overcome blocking situations due to the lack of enough contiguous FSs, in a transparent EON, where connections remain always in the optical domain, all the individual parts into a demand is split must satisfy the spectrum contiguity constraint along the end-to-end path. All this particularities have to be carefully taken into account for any RSA mechanism that peruses to operate in a SS environment.

With all of this said, the following subsection introduces a first approach to efficiently perform the RSA in a SS-enabled EON.

4.3.1 First approach to SS-enabled RSA

The first approach to SS-enabled RSA is intended to operate in a dynamic environment, where connection requests between geographically distributed nodes arrive and depart at random in a core transport network without spectrum conversion capabilities, that is, end-to-end transparent lightpaths are established. Additionally, as a first step into the problem, it is only considered the BV-TSP implementation of the SSA, where every split part is served employing an independent BV-TSP. The proposal of mechanisms to properly operate in a MF-TSP implementation will be done later on this chapter.

The proposed mechanism tries to take advantage of the available fragmented spectral resources, when a connection blocking situation may arise due the lack of enough contiguous FSs to serve its entire bandwidth requirements. With this in mind, the foundation of the mechanism is the following. If a traffic demand can not be served because the number of requested FSs exceeds the size of any available spectral gap in the candidate paths between the source and destination nodes, it may still be possible to accommodate it by splitting the demand into multiple independent lower data-rate signals, and allocate them into multiple non adjacent spectral gaps, assuming that enough spectral resources exist in any of those candidate paths. To enable such splitting operation, the mechanism takes

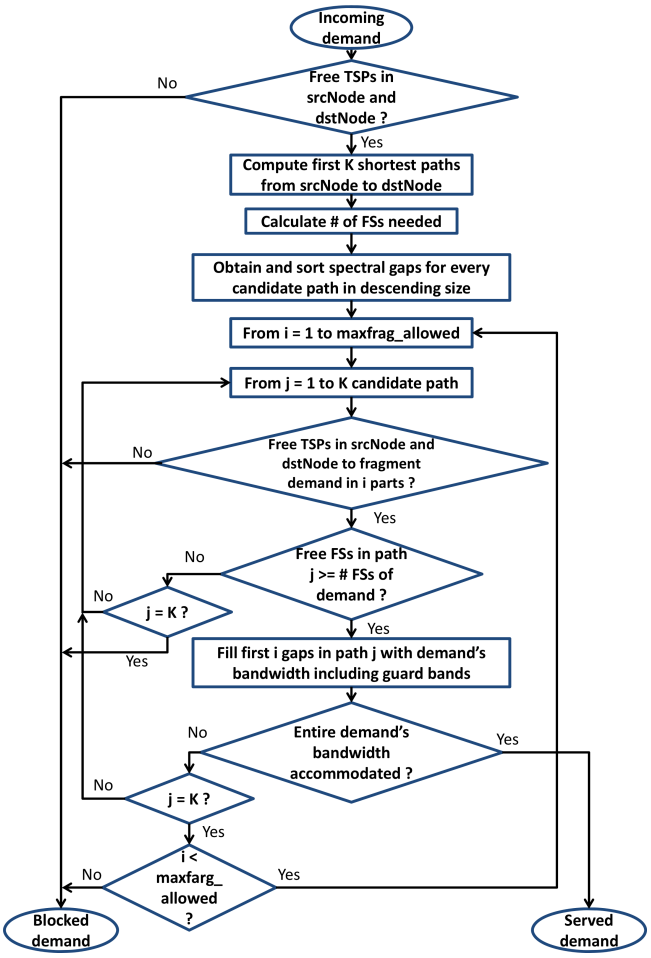

FIGURE 4.4: SS-enabled RSA algorithm.

advantage of those idle BV-TSP at the source and destination nodes of a high data-rate connection, so every split part will be served employing an independent BV-TSP. That is, the establishment of multiple lightpaths for a single demand implies that a BV-TSP at the source and destination must be allocated to each one of them. Hence, a trade-off exists between the number of parts into which a demand is split, which facilitates the allocation of a high data-rate demand over a highly fragmented network spectrum, and the cost (in terms of TSPs) required to allocate the split demand on the network: assigning multiple TSPs to a single demand could strongly impact on the blocking of subsequent requests due to the unavailability of TSPs to allocate them on the network. For this reason, it is desirable to keep the number of split parts as low as possible so as to avoid blocking of demands due to the exhaustion of BV-TSPs. An additional argument to minimize the number of split parts required to allocate an incoming demand is the spectrum overhead that the guard bands needed by BV-WXCs introduce, as guard bands must be left to each part allocated on the network. Taking this into account, the flowchart in Figure 4.4 discloses the proposed mechanism's operation.

For an incoming demand, the mechanism firstly checks if there is any BV-TSP available in both source and destination nodes as otherwise it would not be possible to establish the

demand due to the lack of BV-TSPs. Once this verification is performed, the mechanism calculates the first K shortest paths (e.g., in terms of number of hops) from source to destination. Next, it calculates the minimum number of FSs needed for accommodating the demand using the formula introduced in (4.1). That is, the value of S in the case that no splitting is performed.

The next step consists in obtaining the spectral gaps for each of the K candidate paths. Specifically, a spectral gap is a contiguous number of FSs available from the source to the destination node, that is, in absence of spectrum converters in the network, the continuity of the FSs must be ensured along the end-to-end candidate path. Right after obtaining them, the mechanism sorts the available spectral gaps for every candidate path in descending order, starting from the one with the largest number of contiguous FSs to the one with the lowest number of them. The average complexity of an appropriate sorting algorithm stays commonly in $\mathcal{O}(n\log n)$, being n the number of elements to sort. Under this assumption, the average total complexity of the aforementioned operation in the presented algorithm will be $\mathcal{O}(Kn\log n)$, being K the number of candidate paths computed previously and n the number of spectral gaps in the paths, making the mechanism perfectly scalable if the number of candidate paths or FSs per fiber increases.

Once the spectral gaps in every candidate path are found and sorted, the mechanism checks if the demand can be allocated in any of the candidate paths starting as is, like in a usual RSA mechanism without splitting. Being the algorithm unsuccessful, it splits the demand in two parts (i.e., lightpaths) and checks if it can be allocated. Note that the bandwidth of each part is initially unspecified and will depend on the width of the available spectrum gaps on any candidate path. Being still unsuccessful, the algorithm repeats this operation by increasing the number of demand fragments by one each time, until $maxfarg\_allowed$ is reached. This field allows controlling the amount of splitting done to the demands, that will impact on the BV-TSPs usage and the overhead of guard bands, by putting an upper limit of allowed parts per demand that can be adjusted depending on the bandwidth requested by the demand. This value is left to the network operator discretion.

The process of checking if a demand can be accommodated in a determined number of parts in any of the candidate paths entails multiple phases. First, the mechanism checks if both source and destination nodes have enough available BV-TSPs to serve the demand into the desired number of fragments. Although at the beginning of the mechanism a TSP availability check was performed, at this point it is necessary to check it again as, even though both source and destination nodes have some free TSPs, it could be that one or neither of them have the sufficient available TSPs to serve the demand into the determined number of parts. If this happens, the demand is directly blocked. Otherwise, the mechanism verifies if the candidate path has, at least, a number of available FSs equal to the number of FSs determined through the formula in (4.1). This is done to ensure that the candidate path has a minimum capacity to potentially serve the demand. If the path does not have this minimum capacity, the next candidate path is explored.

The following stage of the mechanism involves how the bandwidth of the demand is accommodated into the spectral gaps of the candidate path without exceeding the number of allowed parts in the current iteration. From the sorted list of spectral gaps of the candidate path, the mechanism selects the first i gaps, being i the number of allowed parts in the current iteration, and tries to fit the bandwidth of the demand in those gaps. Because spectral gaps are sorted in descending order, the chances of fitting the entire demand bandwidth into the first i gaps increases, thus reducing the demand blocking probability. The distribution of the bandwidth of the demand into the i gaps goes as follows: if the size of the first gap is greater or equal than the number of FSs needed to accommodate the demand, all the bandwidth of the demand is accommodated in this gap, filling only a number of FSs as determined from (4.1). Conversely, if the size of the first gap is smaller, only part of the useful bandwidth of the demand is accommodated into the gap. Such an amount is determined through the following formula:

$$\text{Amount of useful bandwidth accommodated} = \text{Size of the gap in FSs} \times F_w - G \tag{4.3}$$

The accommodated bandwidth is subtracted from the requested bandwidth by the demand. The remaining bandwidth is accommodated in the next $i - 1$ gaps in a similar manner: if the size of the next gap is greater or equal than the number of needed FSs determined through (4.1), where the remaining unallocated bandwidth of the demand is considered, all the FSs are accommodated into this gap. Otherwise, the bandwidth that can be fit into the gap is calculated using formula (4.3) and subtracted from the remaining bandwidth. If using these i gaps the remaining bandwidth becomes 0, it means that the demand is successfully accommodated in the path using i different parts. Contrarily, the mechanism proceeds to the next iteration. Once all the candidate paths are explored using all the allowed values of parts, if it is not possible to accommodate the demand, it is finally blocked. Note that if a demand has to be split into multiple parts, the mechanism routes every of these parts through the same physical path. This is to avoid any delay between the parts that would difficult reordering the related data at the reception node, thus adding extra complexity to the control plane and the nodes to perform correctly this operation.

4.3.1.1 Simulation results

Aiming to quantify the benefits of the proposed mechanism, simulation studies over the DT network topology, composed of 14 nodes and 23 bidirectional links have been carried out. The exact topological details are depicted in subsection A.2. Additionally, a total usable bandwidth of 1 THz divided into FSs with a spectrum width of 6.25 GHz, which results in 160 FSs per fiber link has been assumed. Moreover, in all simulations it has been considered that nodes are equipped with 13 BV-TSPs per node, a value that allows a full-meshed virtual connectivity between nodes, and a value of $G = 10$ GHz.

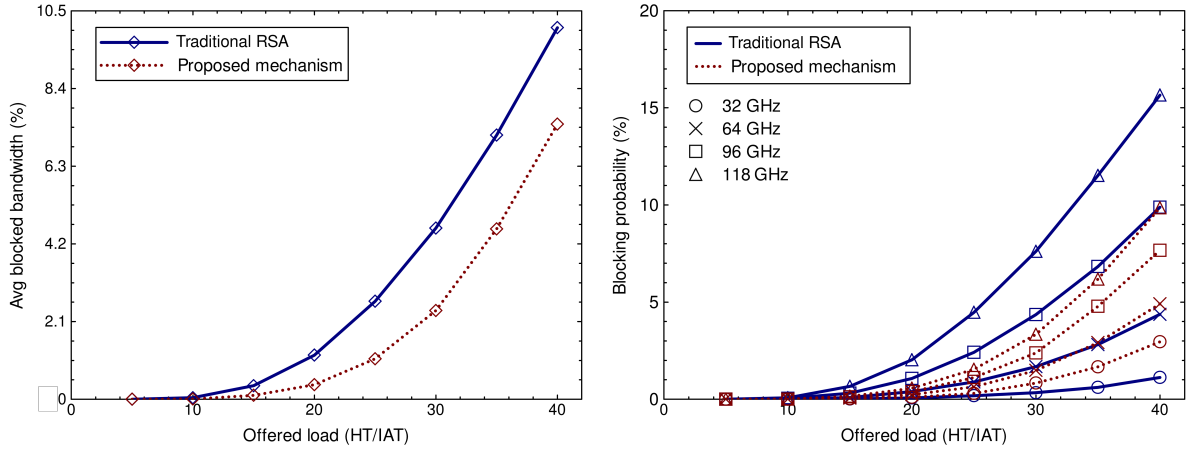

a) b)

FIGURE 4.5: Simulation results: a) average blocked bandwidth as a function of the offered load; b) blocking probability per category as a function of the offered load.

Simulation results have been extracted through the generation of $4 \cdot 10^5$ bidirectional demand requests per execution. Such requests arrive to the network following a Poisson process. Moreover, demand HTs are exponentially distributed with mean 600 s. Different loads are thus generated by modifying the demand IATs accordingly (load = HT/IAT). Bandwidth requirements of the demands in GHz are uniformly chosen among {32, 64, 96, 118}. Besides, the algorithm $maxfrag\_allowed$ field is set to {1, 2, 3, 4}, depending on the bandwidth requirements of the demands. Particularly, 1 fragment is allowed for the demands requesting a bandwidth of 32 GHz (i.e., fragmentation is not allowed for low data-rate demands), while 2, 3, and 4 fragments are allowed to the demands requesting 64, 96 and 118 GHz, respectively.

With comparison purposes, the performance of the proposed mechanism has been benchmarked against a traditional RSA mechanism, where the spectrum contiguity constraint must be ensured to all incoming demand requests. Particularly, a light-weight FF slot allocation strategy has been considered in this mechanism. In both mechanisms, $K = 3$ candidate paths for each demand are taken into consideration, using the distance in hops as the metric. Figure 4.5.a shows the average blocked bandwidth as a function of the offered load. The blocked bandwidth refers to the useful bandwidth of demands that are blocked, without the bandwidth allocated due to the guard bands. From the results, it can be observed that the proposed mechanism yields significant improvements when compared against the traditional RSA mechanism. These benefits become more remarkable as the offered load to the network increases, which arises as a consequence of the high spectrum fragmentation preventing high data-rate demand requests to be allocated contiguously over the spectral resources. For example, the average blocked bandwidth differences stay around 0.8% for an offered load equal to 20, whereas they increase up to 2.6% for an offered load equal to 40.

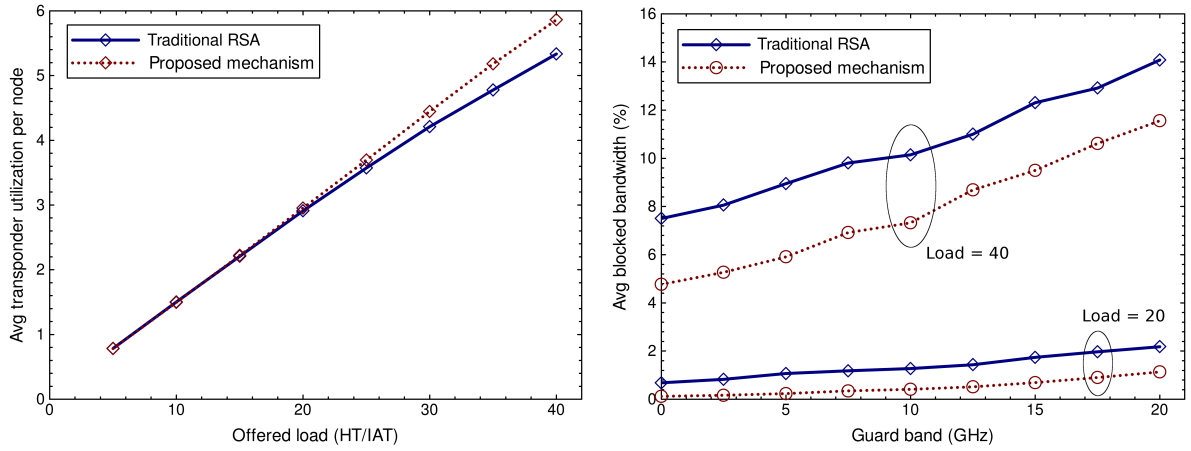

a) b)

FIGURE 4.6: Simulation results: a) average TSP utilization per node as a function of the offered load; b) average blocked bandwidth as a function of the size of the guard band.

In order to analyze the causes of such a behavior in more detail, Figure 4.5.b depicts the BP of the offered demand requests, based on their bandwidth requirements. Looking at the obtained results, a drastically reduced BP can be appreciated for the high data-rate demands when the proposed mechanism is employed. Indeed, thanks to the fragmentation of such demands into multiple lower data-rate ones, available spectral gaps can still be employed to allocate them. Focusing on the 118 GHz demands, for instance, the BP that they experience can be reduced from 2.02% to 0.56% for an offered load equal to 20. Even more pronounced differences can be identified for higher loads, such as a reduction from 7.61% to 3.33% when a load equal to 30 is offered to the network. It is interesting to note as well, that such a BP reduction for high data-rate demands does not entail a pernicious performance degradation of the low data-rate demands. From the figure, the only low data-rate demands experiencing slightly increased BP are those requesting 32 GHz. However, the performance deterioration is only remarkable in highly loaded scenarios, which would probably lay out of the network load operating range.

Heretofore, the obtained results highlight that the proposed mechanism succeeds in improving the BP figures in EONs, being high data-rate demands those experiencing the highest benefits. However, little attention has been paid to the real effects of the additional BV-TSPs used at the source and destination nodes to enable the SSA. To give insight into this effect, Figure 4.6.a depicts the average number of TSP used per node, depending on whether the traditional RSA or the proposed mechanism is applied as a function of the offered load. As can be observed, up to a load equal to 20, the average number of TSPs used per node in our mechanism is practically identical as with the traditional RSA. Moreover, even for loads beyond this value, the average TSP utilization does not increase so notoriously, so as to imply a strong TSP unavailability in any network node. These results could be explained from the fact that, in the usual network operating

range (e.g., offered loads resulting in BP around 1%), the fragmentation of the demands are only required in a small number of occasions.

To complete the study, the effect of the guard band when accommodating the demands has been also analyzed. To this goal, two different offered load scenarios have been considered, namely, 20 and 40. Then, in such scenarios, the size of the guard band has been modified from 0 (ideal situation) to 20 GHz. Figure 4.6.b shows the average blocked bandwidth as a function of the size of G. We can see that both traditional RSA and proposed mechanism show similar behaviors in this regard. As the size of G increases, so it does the blocked bandwidth. Moreover, even though the proposed mechanism requires the allocation of an extra number of guard bands for those high data-rate demands that need to be split in multiple parts, the resulting behavior does not show a clear performance degradation, since the spectrum utilization still remains higher than in the traditional RSA.

4.3.2 Optimal SS-enabled RSA

The previous subsection presented a mechanism capable of efficiently perform the resource assignment of incoming connections in a SS-enabled EON. However, its design only considered the BV-TSP implementation as the enabling technology to perform the splitting of the demands. Additionally, although the mechanism encouraged the minimization of the number of parts a demand is split, the decisions made by the mechanism are purely heuristic-based. Hence, to really obtain a solution that minimizes the number of employed parts and, as a consequence, the number of FSs used to serve a demand, a more optimized mechanism has to be designed. To this end, in what follows, a Mixed Integer Linear Programming (MILP)-based mechanism called Split Spectrum-enabled RSA (SSRSA) is proposed to efficiently allocate incoming demands in SS-based dynamic EONs, with the objective to find the optimal resource assignment that minimizes the number of parts into which a demand is split, jointly with the undesired spectrum fragmentation. The SSRSA mechanism is valid for both SSA implementation strategies using BV-TSPs or MF-TSPs. Note, however, that SSRSA only employs the SSA to solve demand blocking due to lack of enough contiguous FSs, as its use is reserved for moderately-sized networks where all candidate paths are within the maximum transmission reach of the signals. Moreover, the routing of the parts follows the single path strategy, that is, all the parts into which a demand is split are routed through the same physical path. The incorporation of the multipath routing strategy and the implications on the resource assignment will be studied in the following section.

Before proceeding with the mechanism details, let us discuss more in depth some extra considerations regarding the number of parts a demand may be split in a SS-enabled EON as well as the size of the said parts when optimally tackling the resource assignment for every one of the split parts. Although the actual number of necessary FSs to allocate a demand in a SS-enabled EON can be computed according to Equation (4.1) as stated before, its value may vary significantly depending on the amount of B allocated to each

one of the parts. Hence, it is necessary to estimate the range of possible values of S as a function of the number of parts resulting from the split procedure.

Taking as an example the case where a demand is split into two parts, that is $H = 2$, and developing the expression depicted in Equation (4.1), thanks to the mathematical properties of the ceiling function the following expression is obtained:

$$\left\lceil \frac{B + 2G}{F_w} \right\rceil + 1 \geq S \geq \left\lceil \frac{B + 2G}{F_w} \right\rceil \tag{4.4}$$

Such expression allows us to determine the valid range of employed parts when dividing a demand. If we extend the expression to the generic case where a demand may be split in H different parts, the previous expression becomes:

$$\left\lceil \frac{B + H \times G}{F_w} \right\rceil + H - 1 \geq S \geq \left\lceil \frac{B + H \times G}{F_w} \right\rceil \tag{4.5}$$

This relationship serves in determining how many FSs are needed when dividing B in a number of parts H, also giving upper and lower bounds of this value. Note, however, that some restrictions apply on the minimum and maximum part size as well. The minimum size of a part that allows allocating some amount of B is:

$$S_{min} = \left\lceil \frac{G + \epsilon}{F_w} \right\rceil \tag{4.6}$$

where ϵ denotes an infinitesimal amount of B. Otherwise, the part would not be compliant with the guard band requirements when allocating useful demand bandwidth. The maximum size of a part, referred as S_{max}, is equal to the number of FSs determined by Equation (4.1), avoiding to waste spectral resources due to allocating more FSs than needed.

With such considerations, let us now proceed with the mechanism description. Let the optical network substrate be characterized by a graph $G_n = (N, E)$, where N denotes the set of nodes and $E = \{(i, j), (j, i) : i, j \in N, i \neq j\}$ the set of physical links. Let F denote the set of available FSs per physical link and d the incoming demand to be allocated. We define P_d as the set of candidate paths over G_n for demand d, with h_p the length in hops of path p, F_u^p as the set of FSs already in use over $p \in P_d$, and TSP_s and TSP_d as the number of unused TSPs at source and destination nodes, respectively. Finally, H_{max} denotes the maximum number of parts into which a demand can be split (i.e., to avoid excessive splitting) and FL_{max} denotes the maximum number of independent flows a MF-TSP is capable to produce. Regarding the MF-TSP-base implementation, it is considered that a single MF-TSP is used to transmit at most one demand, being split or not, with the aforementioned limit of independent flows.

```
Inputs: d, G_n, F, G, F_w, K, H_max, FL_max, α;
Output: Sol

Phase 1: Pre-processing
TSP_s ← free transponders at source node
TSP_d ← free transponders at destination node
if TSP_s = 0 or TSP_d = 0 then
    Demand blocked
else
    P_d ← K shortest paths in terms of number of hops
    for i = 1 to K do
        F_u^i ← set of end-to-end busy FSs in path i

    Phase 2: MILP solving
    Sol ← output from MILP

    Phase 3: Solution evaluation
    if Sol = ∅ then
        Demand blocked
    else
        Return Sol
        Update network resources according to Sol
        Demand allocated
```

TABLE 4.1: SSRSA mechanism pseudo-code.

The proposed mechanism executes a MILP formulation, considering the demand needs, the candidate paths and the actual state of the network resources, with the objective of minimizing the number of parts required to allocate d, together with the spectrum fragmentation on the network. The aim of the first objective is to reduce the number of required TSPs to serve the demand (BV-TSP-based implementation) as well as the complexity of the whole assignment process since more parts will require a larger control plane burden in terms of setup, management and release operations. Moreover, another reason to encourage the minimization of the number of parts is that, due to the presence of the guard bands, dividing a demand into a large number of parts will usually result in more spectral resources (i.e. FSs) needed to allocate the demand as it was already stated during the previous subsection.

As for the second objective, since the problem under consideration deals with an online optimization scenario, where demands arrive and depart at random, the aforementioned spectrum fragmentation effect becomes a limiting factor when trying to establish a new connection. Under such scenario, it is desirable to keep the spectrum fragmentation at minimum in order to facilitate the establishment of future demands. The approach that the presented mechanism follows in this respect is to minimize the average end-to-end spectrum fragmentation in the candidate paths for the demand that is being established, since an overall network defragmentation would be too costly to perform. In this regard, the MILP formulation minimizes the contiguous busy portions in the spectrum, that is, it tries to fit the demands so as to avoid having idle spectrum gaps in between occupied resources. Doing so the free spectral resources will become less scattered along the total fiber spectrum, hence, reducing the spectrum fragmentation in the network.

If the model finds a non empty solution, it means that a feasible RSA for the demand has

been found. In this event, resources are reserved and the network status is updated accordingly. Otherwise, the demand is marked as blocked. A pseudo code of the mechanism is depicted in Table 4.1.

Regarding the specific MILP formulation, the model variables are as stated below:

$x_{p,f}$: binary; 1 if slot f is the first slot of a part in path p, 0 otherwise.

$y_{p,f}$: binary; 1 if slot f is used in path p to allocate d, 0 otherwise.

$z_{p,f}$: binary; 1 if slot f is occupied in path p, 0 otherwise.

u_p: binary; 1 if path p is used to allocate d, 0 otherwise.

m_p: integer; number of parts into which d is split that are routed through path p.

s_p: integer; number of FSs needed to allocate d that are routed through path p.

t_p: integer; number of busy contiguous spectrum portions in path p.

c: integer; used to calculate the ceiling function present in Eq. 4.5

$v_{p,f,f+1}$, $w_{p,f,f+1}$: real; auxiliary variables $\in$ [0,1].

Before detailing the exact MILP formulation, it is necessary to introduce the procedure that is followed to compute m_p in a candidate path. Taking the state of the spectral FSs, a potential part of d is discriminated by a free-to-allocated and another allocated-to-free FS transition, namely, a 0-1 and a 1-0 transition in variables $y_{p,f}$. Thus, subtracting $y_{p,i+1}$ from $y_{p,i}$, if the result is different than 0, a transition is detected. Therefore:

$$m_p = 0.5 \sum_{i=1}^{|F|-1} |y_{p,i} - y_{p,i+1}| \tag{4.7}$$

However, equation (4.7) does not detect correctly transitions before the initial and after the last FS of the fiber link spectrum. To this end, it is necessary to add $y_{p,1}$ and $y_{p,|F|}$ in (4.7) to properly compute m_p:

$$m_p = 0.5(y_{p,1} + y_{p,|F|} + \sum_{i=1}^{|F|-1} |y_{p,i} - y_{p,i+1}|) \tag{4.8}$$

The term within the sum in (4.8) can only take values equal to -1, 0 or 1. Hence, the absolute value function can be substituted by the square function, which results in:

$$m_p = 0.5(y_{p,1} + y_{p,|F|} + \sum_{i=1}^{|F|-1} (y_{p,i}^2 - 2y_{p,i}y_{p,i+1} + y_{p,i+1}^2)) \tag{4.9}$$

Thanks to the binary nature of the variables, quadratic terms can be simplified. Thus, rearranging expression (4.9):

$$m_p = \sum_{i=1}^{|F|} y_{p,i} - \sum_{i=1}^{|F|-1} y_{p,i} y_{p,i+1} \tag{4.10}$$

Using expression (4.10) the number of parts into which d is split and are routed through path p can be now obtained. A similar reasoning can be applied to obtain the number of busy contiguous spectral portions in a candidate path (i.e., considering variables t_p and $z_{p,f}$). However, a product of decision variables is encountered, making the expression non-linear. To linearize it, auxiliary variables $v_{p,f,f+1}$ and $w_{p,f,f+1}$ are introduced, together with some additional constraints in the proposed MILP formulation, which is detailed in what follows:

$$\begin{aligned} min\ \ & \alpha \frac{1}{H_{max}|P_d|} \sum_{p \in P_d} h_p m_p + (1-\alpha) \frac{2}{|P_d||F|} \sum_{p \in P_d} h_p t_p + \\ & \epsilon \frac{1}{|P_d||F|} \sum_{p \in P_d} \sum_{i=1}^{|F|} i h_p y_{p,i} \end{aligned} \tag{4.11}$$

subject to:

$$\frac{B + \sum\limits_{p \in P_d} m_p \times G}{F_w} + 1 \geq c \geq \frac{B + \sum\limits_{p \in P_d} m_p \times G}{F_w} \tag{4.12}$$

$$c + \sum_{p \in P_d} m_p - 1 \geq \sum_{p \in P_d} s_p \geq c \tag{4.13}$$

$$\sum_{p \in P_d} s_p \geq S_{min} \times \sum_{p \in P_d} m_p \tag{4.14}$$

$$\sum_{j=i}^{i+S_{max}} y_{p,j} \leq S_{max}, \forall\ p \in P_d, i = 1, ..., |F| - S_{max} \tag{4.15}$$

$$\begin{aligned} x_{p,i} \leq y_{p,j}, \forall\ & p \in P_d, i = 1, ..., |F| - S_{min} + 1 \\ & j = i, ..., i + S_{min} - 1 \\ x_{p,i} = 0, \forall\ & p \in P_d, i = |F| - S_{min} + 2, ..., |F| \end{aligned} \tag{4.16}$$

$$y_{p,i-1} \leq 1 - x_{p,i}, \forall\ p \in P_d, i = 2, ..., |F| \tag{4.17}$$

$$m_p = \sum_{i=1}^{|F|} y_{p,i} - \sum_{i=1}^{|F|-1} v_{p,i,i+1}, \forall\ p \in P_d \tag{4.18}$$

$$t_p = \sum_{i=1}^{|F|} z_{p,i} - \sum_{i=1}^{|F|-1} w_{p,i,i+1}, \forall\ p \in P_d \tag{4.19}$$

$$\sum_{i=1}^{|F|} x_{p,i} = m_p, \forall\ p \in P_d \tag{4.20}$$

$$\sum_{i=1}^{|F|} y_{p,i} = s_p, \forall\ p \in P_d \tag{4.21}$$

$$y_{p,f} = 0, \forall\ p \in P_d, f \in F_u^p \tag{4.22}$$

$$\begin{aligned} z_{p,f} &= 1, \forall\ p \in P_d, f \in F_u^p \\ z_{p,f} &= y_{p,f}, \forall\ p \in P_d, f \in F \backslash F_u^p \end{aligned} \tag{4.23}$$

$$\begin{aligned} v_{p,i,i+1} &\leq y_{p,i}, y_{p,i+1} \\ v_{p,i,i+1} &\geq y_{p,i} + y_{p,i+1} - 1, \forall\ p \in P_d, i = 1, ..., |F| - 1 \end{aligned} \tag{4.24}$$

$$\begin{aligned} w_{p,i,i+1} &\leq z_{p,i}, z_{p,i+1} \\ w_{p,i,i+1} &\geq z_{p,i} + z_{p,i+1} - 1, \forall\ p \in P_d, i = 1, ..., |F| - 1 \end{aligned} \tag{4.25}$$

$$\sum_{p \in P_d} m_p \leq TSP_s, TSP_d \tag{4.26a}$$

$$\sum_{p \in P_d} m_p \leq FL_{max} \tag{4.26b}$$

$$\sum_{p \in P_d} m_p \leq H_{max} \tag{4.26c}$$

$$u_p \geq y_{p,f}, \forall\ p \in P_d, f \in F \tag{4.27}$$

$$\sum_{p \in P_d} u_p = 1 \tag{4.28}$$

Objective function (4.11) has a twofold goal. First, it minimizes the number of parts into which d is split in order to be served. Moreover, it minimizes the spectrum fragmentation in the candidate paths through the minimization of the number of contiguous busy spectrum portions. Parameter $\alpha \in [0, 1]$ is used for pondering purposes, while the last term in (4.11) aims to speed up the convergence time of the model, with $\epsilon \ll 1$. The usefulness of the convergence term comes from the fact that, initially, the MILP formulation may find itself with a lot of symmetrical solutions with different RSA which evaluate the objective function to the same value. In such conditions, the MILP formulation will have troubles on deciding an initial root solution for starting the exploration of the solution space. In order to help the MILP formulation making faster decisions when it faces the situation where many different solutions lead to the same objective value, we introduce the convergence factor.

Essentially, it prioritizes the lower part of the spectrum when assigning resources to d, so in this way the model will quickly prefer lower indexed slots when there are multiple candidate slots, exploring faster the solution space. Furthermore, the convergence term also helps in providing a solution that requires less spectral resources (i.e., FSs), since the model will try to minimize the summation of the used FSs. Finally, all terms in the objective function are pondered by the length in hops of the associated candidate path (h_p). This is done since shorter candidate paths will usually entail using less network resources, hence, helping on having enough free resources for future demands.

Constraints (4.12) and (4.13) build the relationship depicted in (4.5), where variable c is used to calculate the ceiling function that appears in that expression. Constraint (4.14) adds an additional lower bound for the total number of allocated FSs due to the presence of S_{min}, ensuring that the total number of allocated FSs does not fall below the number of used parts multiplied by the minimum size of a part (S_{min}). Constraints (4.15) and (4.16) bound the minimum and maximum individual part size as presented before. Note that, despite the presence of constraint (4.14), constraints (4.16) are still necessary to guarantee that the size of each individual part does not fall below the minimal allowed size part. Constraints (4.17) set the minimum separation between parts to one FS.

Constraints (4.18) and (4.19) account for the number of parts into which d is split and the number of contiguous busy spectrum portions in the candidate paths, respectively. Constraints (4.20) and (4.21) are the traffic constraints, accounting for the number of needed FSs. Constraints (4.22) prevent the use of FSs that are already occupied. Constraints (4.23) give value to variables $z_{p,f}$ according to the current state of the FSs and

the choice made by the model, while constraints (4.24) and (4.25) give value to auxiliary variables $v_{p,f,f+1}$ and $w_{p,f,f+1}$.

Constraints (4.26) set the upper limit of parts into which d may be split. More specifically, constraint (4.26a) avoids splitting d in more parts than available TSPs at source and destination nodes, constraint (4.26b) avoids splitting d in more parts than flows a MF-TSP is able to produce, while constraint (4.26c) sets the upper limit of the allowed number of parts as commented before. Note that the first constraint (4.26a) is only applied in a BV-TSP-based implementation while the second constraint (4.26b) is only applied in a MF-TSP-based implementation. As for constraint (4.26c), its is applied for both MF-TSP and BV-TSP-based implementations.

Finally, constraints (4.27) and (4.28) restrict the routing to a unique candidate path since the presented mechanism focuses on the single-path approach, where all parts are routed through the same physical path. Note that the presented model is based on a link-path formulation, so restricting the size of P_d to K may not lead to obtaining the overall optimal solution. The reason to follow such approach is due to the fact that the mechanism is targeting an online optimization problem, so the execution times of the model have to be under a reasonable time threshold. Such time requirements would not be met if other modeling approaches where to be adopted, such as a flow-based formulation. For this reason, a link-path-based formulation that allows to find a trade-off between computational requirements of the model and optimality of the solution found by properly setting the value of K has been adopted.

Although the presented SSRSA mechanism allows top optimally find the resource assignment (both route and FSs) for every split part of a demand in a SS-enabled EON, its dependence in a MILP may challenge its scalability in large network scenarios. To this end, an heuristic mechanism called H-SSRSA that has the same objective as SSRSA is also presented. The H-SSRSA can be used in large network scenarios and is based on the assignment procedure presented during subsection 4.3.1. Indeed, the actual steps of the H-SSRSA are as follows:

1. Check if there is at least one available TSP in both source and destination nodes. Not being the case, mark the demand as blocked.
2. Compute K-shortest candidate paths from source to destination nodes.
3. For each candidate path, check if the total number of available FSs is equal or higher than the minimum number of FSs needed to allocate d (i.e., in a single part). If not, mark the candidate path as infeasible. Otherwise, sort the available spectral gaps in descending order according to the following expression:

$$\alpha \frac{g}{G_{max}} + (1-\alpha)\frac{G_{min}}{g} \tag{4.29}$$

where g denotes the size of the particular gap and G_{max} and G_{min} the sizes of the largest and smallest gaps in the path, respectively.

4. For each of the feasible candidate paths, start filling the available spectral gaps from the first to the last one, according with the previous ordering, with useful bandwidth of d plus the guard bands (each gap will allocate a part of d). If d cannot be completely allocated in the path, or the number of resulting parts exceeds H_{max}, or there are not enough TSPs at source/destination nodes to support the resulting RSA (BV-TSP case), or the number of parts exceeds FL_{max} (MF-TSP case), mark the path as infeasible.

5. If no feasible candidate path still exists, set d as blocked. Otherwise, evaluate the objective function as in the MILP model particularized for each one of the feasible candidate paths, and choose the path with the smallest value. Take its RSA as the solution of H-SSRSA, reserve the associated network resources and set d as served.

Note that by sorting the available spectral gaps according to (4.29), the H-SSRSA mechanism tries to replicate the behavior of the SSRSA mechanism. If $\alpha = 1$, the available gaps will be ordered from the biggest to the smallest, so once they are filled with useful bandwidth of d, the number of parts is being minimized. In the opposite case ($\alpha = 0$), the available gaps will be ordered from the smallest to the biggest, so when filling them, the total number of spectral gaps after the filling process is minimized. Any case in between would lead to a trade-off solution between the minimization of the number of parts and the spectral gaps in the candidate path. Indeed, it can be seen that with this ordering, jointly with the evaluation of the same objective function as in the MILP formulation, H-SSRSA pursues the same optimization goal as SSRSA.

4.3.2.1 Simulation results

To evaluate the performance of both SSRSA and H-SSRSA mechanism, some simulation studies have been performed. In order to quantify the benefits of optimally splitting demands, a scenario where no splitting is performed (hereafter referred as 1-SSRSA) as been used, forcing $H_{max} = 1$ and $\alpha = 0$ in the formulation. Two network scenarios have been considered, namely, the EON16 (16 nodes, 23 links) and DT (14 nodes, 23 links) network topologies as depicted in Appendix A. Besides, two situations with 160 and 320 FSs per fiber link have been assumed, with $F_w = 6.25$ GHz and $G = 10$ GHz. Regarding network nodes, it is assumed that every node in the network is equipped with an infinite pool of TSPs (i.e., no blocking occurs due to the lack of TSPs).

Results have been extracted by generating 10^5 bidirectional demand requests per execution. Requests arrive to the network following a Poisson process, with exponentially distributed HTs. Loads are thus generated by adjusting the ratio between the mean HT and IAT, so that load = HT/IAT. Bandwidth requirements of the demands are uniformly

TABLE 4.2: SSRSA performance comparison

Scenario			1-SSRSA		SSRSA		
Network	**|F|**	**Load**	**% BBw**	**BV-TSPs/node**	**% BBw**	**BV-TSPs/node**	**MF-TSPs/node**
EON16	160	5	0	0.69	0	0.69	0.69
		10	0.0108	1.3	0.0016	1.3	1.3
		15	0.1721	1.92	0.0319	1.93	1.93
		20	1.0435	2.53	0.2499	2.58	2.55
		25	3.3271	3.09	1.0503	3.27	3.18
	320	30	0.0016	3.77	0	3.79	3.79
		40	0.0344	5.05	0.0039	5.06	5.06
		50	0.3627	6.28	0.0402	6.38	6.36
		60	1.86	7.54	0.244	7.67	7.55
		70	4.04	8.55	1.1244	9.21	8.79
DT	160	5	0	0.78	0	0.78	0.78
		10	0.0152	1.5	0.0012	1.5	1.5
		15	0.1677	2.21	0.0256	2.21	2.21
		20	0.6769	2.9	0.1716	2.94	2.93
		25	2.2554	3.57	0.6914	3.67	3.61
	320	30	0.0016	4.33	0	4.4	4.4
		40	0.0204	5.75	0.0068	5.76	5.76
		50	0.2648	7.25	0.0392	7.26	7.18
		60	1.0758	8.64	0.2206	8.76	8.67
		70	2.7075	9.91	0.6764	10.24	9.98

chosen among 32, 64, 96 and 128 GHz. Moreover, $K = 3$, $H_{max} = FL_{max} = 4$ and $\alpha = 0.5$ are set in all cases. All simulations are run in standard PCs with i7-3770 CPUs at 3.4 GHz and 16 GB RAM using CPLEX v12.5.

Table 4.2 displays the percentage of blocked bandwidth (BBw) for 1-SSRSA and SSRSA, as well as the average number of TSPs used per node when either BV-TSPs or MF-TSPs are equipped in network nodes. As seen, SSRSA lowers BBw significantly in contrast to 1-SSRSA. Particularly, we can observe differences of one order of magnitude for low loads in both networks and scenarios, with relative gains no worse than 69% for higher loads. As in the study performed during subsection 4.3.1, demands requesting larger bandwidth are the most benefited as they can be split up and be more easily allocated.

Regarding the average number of TSPs used per node with SSRSA, they are generally reduced when MF-TSPs are employed, since all parts of a split demand can be supported over a unique MF-TSP. However, note that such differences remain very small under realistic offered loads (e.g., offered loads leading to BBw $\leq$ 1%). This is because a low percentage of incoming demands need to be split in such scenarios (around 1% of the total in average), which makes the MF-TSP capability to be considerably wasted most of the time. In light of the above,the network CAPEX investments that would be incurred to implement the SSA with either BV-TSPs or MF-TSPs in EON16 and DT networks, as a function of the relative cost of a MF-TSP against a BV-TSP has been analyzed. Parameter γ is used for these purposes, so that $Cost_{MF-TSP} = \gamma \cdot Cost_{BV-TSP}$. Specifically, the study has focused on the scenario with 320 FSs/link in both networks, as well as on two of the tested loads, namely, 60 and 70. The obtained results are shown in Figure 4.7. The average network cost is calculated as Avg. TSPs/node $\times$ Nr of nodes $\times$

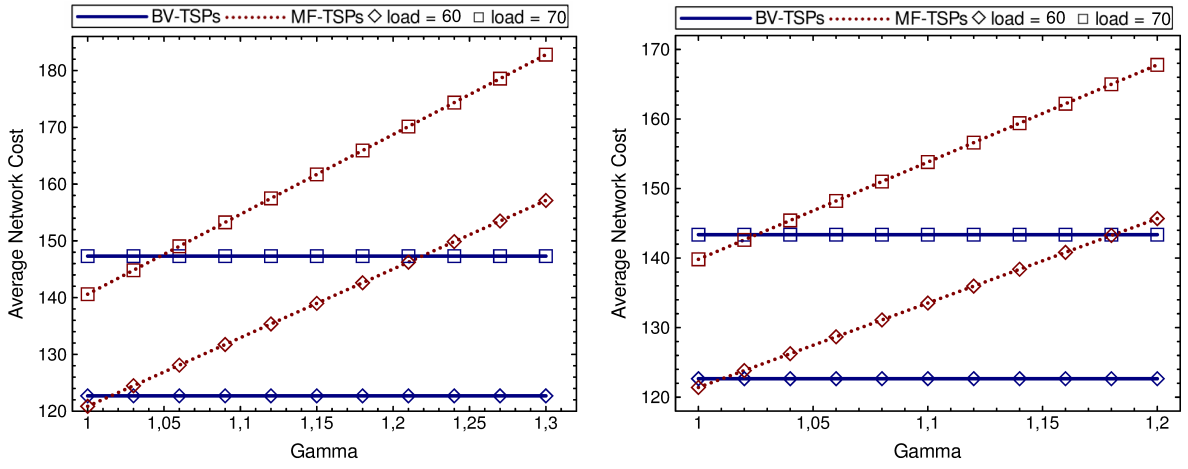

FIGURE 4.7: Simulation results: average network cost comparison in a) EON16/320 and b) DT/320 scenarios.

Cost of a TSP in both BV-TSP and MF-TSP implementations, setting $Cost_{BV-TSP} = 1$ as the base unit of cost.

As observed, MF-TSPs are only cost-effective with γ very close to 1, since demand splitting is infrequent under such a realistic offered loads leading to BBw $< 1\%$. Conversely, assuming that $\gamma > 1$ due to the inherently higher complexity of MF-TSPs compared to BV-TSPs, it is generally more appropriate to deploy a slightly overprovisioned number of BV-TSPs per node to perform SSA. For example, looking at Table 4.2 for the EON16 network and a load of 60, around 0.13 more BV-TSPs per node would be required to perform SSA, compared to a non-splitting scenario (1-SSRSA). In the same network, this value is increased to 0.66 for an offered load of 70.

Finally, as we commented during the description of H-SSRSA, SSRSA may suffer from scalability issues in larger network scenarios. Let us discuss in more depth the computational complexity of SSRSA. Looking back at its description, one can see that the number of binary variables of the MILP formulation is in the order of $\mathcal{O}(3K|F|)$ and the number of constraints is in the order of $\mathcal{O}((S_{min} + 5)K|F|)$. It can be appreciated that its complexity is tightly related to the size of F. As for the value of K, this parameter can be tuned to find a trade-off between optimality and swiftness of the mechanism. However, little can be done regarding $|F|$, as it is an intrinsic characteristic of the network scenario. For this reason, the H-SSRSA mechanism has been proposed as an alternative mechanism to find good solutions at a lower computational cost. Fig. 4.8 depicts the comparison of H-SSRSA against SSRSA in terms of BBw as a function of the offered load. For this results, $K = 3$, $\alpha = 0.5$ have been considered, as well as no blocking due to the lack of TSPs. All the results have been extracted focusing on the 160 FSs scenarios.

It can be appreciated that H-SSRSA produces BBw figures very close to the ones obtained through SSRSA. As for the execution times experienced for both mechanisms, they are in

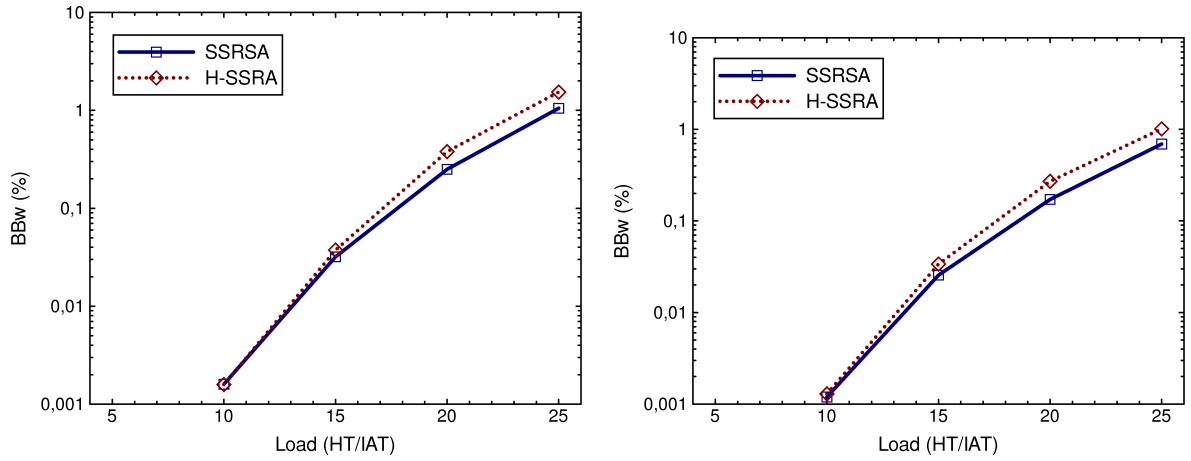

FIGURE 4.8: Simulation results: H-SSRSA vs SSRSA in a) EON16/160 and b) DT/160 scenarios.

the range 1.43-1.54 ms and 270-450 ms for H-SSRSA and SSRSA, respectively, in the 160 FSs scenarios, while they are in the range 1.33-1.74 ms and 340-730 ms for H-SSRSA and SSRSA, respectively, in the 320 FSs scenarios. It can be appreciated that, as pinpointed before, the execution times of SSRSA increase substantially as the size of F grows up, while the execution times of H-SSRSA remain steady for all tested scenarios and more than one order of magnitude below those of SSRSA. For these reasons, H-SSRSA succeeds in its goal of providing near optimal solutions in much less time.

4.4 Route, Spectrum and Modulation level Assignment (RSMLA) in SS-enabled EONs

During the previous section, the benefits of the SSA have been clearly stated through the evaluation of the proposed mechanisms to perform the RSA in SS-enabled EONs. However, it was considered that the bandwidth of a demand could be split in any way among the resulting parts from the splitting procedure. In a more realistic scenario, this is not the case, as the bandwidth of the parts is strictly related to the modulation format employed to establish the different lightpaths. In fact, when serving an incoming demand requesting for a bit-rate equal to R_d that needs to be split in multiple parts, the actual bit-rate that will be served is equal to $\sum_{i=1}^{H} R_{m_i}$, where R_{m_i} is the bit-rate of the modulation format employed to serve the i^{th} part. At its turn, the bit-rate of each of the individual parts will occupy a spectral bandwidth equal to B_{m_i} depending on the spectral efficiency of the employed modulation format i.e., how many bits per second can be squeezed per unit of spectrum. It can be clearly seen then that the total number of FSs needed to allocate a demand in a SS-enabled EON strongly depends of the available modulation

formats at the nodes and the current modulation formats assigned to each one of the split parts. For this reason, it is necessary to extend the previous studies to also consider the choice of the modulation format of the parts so as to address more accurately the resource assignment when employing the SSA.

Additionally, as commented during section 4.2, the SSA may be used to overcome blocking situations due to physical transmission reasons, since the resulting split parts are of a lower bit-rate and more robust modulation formats can be used to serve them. In this sense, it may happen that, although there are enough contiguous FSs to serve a high bit-rate demand it has to be split into lower bit-rate sub-demands due to the fact that it is not possible to establish a high-bit rate connection between the source and the destination nodes due to transmission reach limitations.

Moreover, even though that the SSA allows to solve potential blocking situations (due to the lack of contiguous FSs or transmission reach reasons) by exploiting the spectral gaps on the end-to-end path of the connection, it may still be insufficient as the employed FSs are constrained to the available spectral resources of the path. In this sense, it may happen that there are not enough FSs in a single candidate path to allow the splitting of the demand. To this end, the multipath routing strategy as introduced in section 4.2 can be employed. In such situation, the different parts can be routed through totally different physical paths, taking advantage even more of the available spectral gaps in the whole network.

With all these considerations, a MILP-based mechanism called SSRSMLA to optimally tackle the RSMLA problem in a dynamic SS-enabled EON is presented. The objective of the optimization problem at hand is to find the most suitable resources (paths, spectrum portion and modulation formats) to allocate an incoming demands (in one or multiple parts) in the network, according to the current resources state, so that the overall BBR is minimized. To encourage the minimization of BBR, two main sub-objectives are pursued: 1) Minimize the number of resources to serve the incoming demand; 2) Minimize the spectrum fragmentation in the network.

To achieve the first sub-objective, multiple action lines are defined. Firstly, the number of parts into which the demand is split should be minimized, as dividing the demands into too many parts may exhaust rapidly the available TSPs in the nodes (BV-TSP case). Moreover, as each of the resulting parts must be surrounded by guard bands, using more parts to serve the demand implies occupying more spectral resources in the network. Secondly, as a demand can be served employing multiple paths and modulation formats, it may happen that different feasible solutions employing the same number of parts may result in different number of required FSs. Therefore, the explicit minimization of the total of FSs employed by the demand should be also encouraged. And thirdly, it is clear that the sum of the bit-rates of all parts used to serve a demand has to be, at least, equal to the original bit-rate of the demand. But, depending on the demand bit-rate and the modulation formats supported by the TSPs, it may be infeasible to allocate exactly the

requested bit-rate due to the limitations imposed by the granularity of the TSPs. With this in mind, the disparity between these two values, stated as $\sum_{i=1}^{H} R_{m_i} - R_d$, should be minimized. The main reason for doing so is to minimize the amount of spectrum finally used by the demand, as higher bit-rate modulation formats usually require larger spectral widths.

As for the second sub-objective, its main goal is to facilitate the allocation of future incoming demands, as spectrum fragmentation may lead to undesired BBR due to demands not finding enough contiguous spectral resources, even if the SSA is applied. To achieve such goal, as an overall network defragmentation would be too costly in terms of time and complexity, the number of spectral gaps present in the candidate paths of the demand is minimized, as already presented for the SSRSA mechanism in 4.3.2 By minimizing the spectral gaps, spectral resources are less scattered along the candidate paths, helping future demands in finding large portions of contiguous FSs.

Before depicting the details of the SSRSMLA mechanism, additional definitions aside from the ones introduced in 4.3.2 are stated. Let d represent the incoming demand to be served which is characterized by its requested bit-rate R_d and its source and destination nodes (s_d and t_d), l_p the physical length of the candidate path $p \in P_d$ and $P_e \subseteq P_d$ the set of candidate paths for d that traverse physical link $e \in E$. Additionally, let M represent the set of modulation formats supported by TSPs at nodes and $M_p \subseteq M$ as the set of feasible modulation formats for demand d in path $p \in P_d$, that is, the modulation formats that support a transmission reach equal or greater than the physical length of the candidate path. Every modulation format m belonging to M_p is characterized by its transmission reach TR_m, bit-rate R_m, spectral bandwidth B_m and associated number of FSs S_m calculated using expression (4.1). Finally, L_{max} represents the maximum number of paths that a demand is allowed to use. This parameter will be used to avoid employing too many paths, which may result in spectrum allocation inefficiency.

Moreover, reviewing the literature related to MILP-based formulations tackling the optimal solution of the RSMLA problem [CTV11, WCP11, KW11, WHZ12] it can be appreciated how the consideration of the spectrum contiguity constraint greatly increases the complexity of the formulations. Note that in SS-enabled EONs such a constraint still has to be ensured for each one of the parts into which the demand is split. To this end, the spectrum contiguity constraint is modeled following the same approach proposed by the authors in [VKRC12]. There, authors use pre-computed sets of contiguous FSs, named channels. Each channel consists of a subset of adjacent FSs providing just enough spectrum to support the spectral needs of a particular demand. This approach makes MILP-based solutions for the RSMLA problem solvable in practical times.

With all this in mind, let C represent the set of pre-computed candidate channels for demand d, $C_p \subseteq C$ the set of channels for candidate path $p \in P_d$, $C_{p,m} \subseteq C_p$ the set of channels employing modulation format $m \in M_p$ in path p and $C_{p,f} \subseteq C_p$ the set of channels that are mapped in FS f in path p. Note that all channels belonging to $C_{p,m}$

Inputs: d,G_n,F,M,K,H_{max},L_{max},FL_{max},α,β,γ,δ; **Output:** Sol

Phase 1: Pre-processing
if $TSP_s = 0$ *or* $TSP_t = 0$ **then**
  Demand blocked
$P_d \leftarrow K$ shortest paths from s_d to t_d using l_p as the metric
for $i = 1$ **to** K **do**
  $M_i \leftarrow$ set of modulations belonging to M with $TR_m \geq l_i$
  if $M_i = \emptyset$ **then**
    Remove p_i from P_d
if $P_d = \emptyset$ **then**
  Demand blocked
$C \leftarrow \emptyset$
for $i = 1$ **to** $|P_d|$ **do**
  $C_i \leftarrow \emptyset$
  for $j = 1$ **to** $|M_i|$ **do**
    $C_{i,j} \leftarrow \emptyset$
    $c \leftarrow \emptyset$
    for $k = 1$ **to** $|F|$ **do**
      if $f_k \in F$ *in path* p_i *is free* **then**
        $c \leftarrow f_k \cup c$
      else
        $c \leftarrow \emptyset$
      if $|c| = S_j$ **then**
        $C_{i,j} \leftarrow c \cup C_{i,j}$
        $c \leftarrow \emptyset$
    $C_i \leftarrow C_{i,j} \cup C_i$
  if $C_i = \emptyset$ **then**
    Remove p_i from P_d
  else
    $C \leftarrow C_i \cup C$

Phase 2: MILP solving
if $P_d = \emptyset$ **then**
  Demand blocked
else
  $Sol \leftarrow$ output from MILP(d, P_d, C, H_{max}, L_{max}, FL_{max},α, β, γ, δ)

Phase 3: Solution evaluation
if $Sol = \emptyset$ **then**
  Demand blocked
else
  Return Sol
  Update network resources according to Sol
  Demand allocated

TABLE 4.3: SSRSMLA mechanism pseudo-code.

will have an associated number of FSs equal to S_m as they are the candidate sets of contiguous FSs that fit the spectral needs of modulation format $m \in M_p$. Specifically, every channel $c \in C$ has its own value of associated bit-rate, number of FSs and first FS of the channel, denoted as S_c, R_c and f_c, respectively.

Considering these definitions, Table 4.3 depicts the pseudo-code of the presented mechanism. Essentially, given an incoming demand, a MILP formulation is executed in order to find the optimal RSMLA depending on the network status and the demand needs. More specifically, the mechanism is structured in three phases. The first phase is devoted to obtaining the sets that will be later used in the MILP formulation, namely, the candidate path and channel sets. For the candidate path set, a K link-distinct SP strategy, where K is an input parameter. The metric of the paths is the physical distance, as it becomes

a very relevant factor in order to maximize the possibilities to successfully allocate a demand. That is, shorter paths allow more modulation formats than longer ones, hence supporting more candidate channels to serve a demand.

As for the channel calculation, firstly it determines for every of the previously calculated paths which are the modulation formats supported through that path, that is, the modulation formats so that $TR_m \geq l_p$. If no path has at least one feasible candidate modulation, the demand is automatically blocked, as it will be impossible to reach the destination in a transparent way as an all-optical scenario is being targeted. For the candidate paths that have at least one feasible candidate modulation, the mechanism proceeds to calculate the candidate channels, given the modulation characteristics and FS availability over the path. The operation to determine the candidate channels is very simple, it consist on just finding spectral gaps of equal width as the spectral width of the modulation format to be associated to the channel.

Once the candidate path and channel sets are filled, the mechanism proceeds with the following step. In this phase, the mechanism executes a MILP formulation, whose details will be later explained, that will find the optimal RSMLA for the demand d given the aforementioned candidate sets and the state of the network. The parameters α, β, γ and δ are weighting factors. Before executing the MILP, though, the mechanism checks if at least one of the candidate paths has a non empty set of candidate channels, otherwise the demand is directly blocked as no combination of modulation format and contiguous spectral blocks that fulfill the requirements of the demand is found.

Finally, the mechanism checks if the solution of the MILP formulation is empty or not. If not empty, it means that exists an optimal solution that fulfills the requirements of the demand. This being the case, the solution is adopted as the RSMLA for the demand and network resources are updated accordingly. The details of the MILP formulation are shown below, whose decision variables are introduced below:

$x_{p,c}$: binary; 1 if path $p \in P_d$ and channel $c \in C_p$ are used to allocate the demand, 0 otherwise.

y_p: binary; 1 if path p is utilized to allocate the demand, 0 otherwise.

$z_{p,f}$: binary; 1 if FS f in path p is occupied, 0 otherwise.

P_p: integer; number of parts routed over path p.

T_p: integer; number of spectral gaps in path p.

$w_{p,f,f+1}$: real; auxiliary variables in the range [0,1].

A: real; difference between the requested bit-rate and the allocated bit-rate.

Variables $z_{p,f}$, T_p and $w_{p,f,f+1}$ have the same goal as in the SSRSA mechanism presented in subsection 4.3.2: determine the portions of busy FSs along the candidate paths, which

will be used to minimize the spectrum fragmentation in the network. The procedure to calculate them is the same already introduced for the SSRSA mechanism. With this, the proposed MILP formulation is as follows:

$$min\ \alpha\frac{1}{H_{max}|P_d|}\sum_{p\in P_d}h_pP_p+\beta\frac{2}{|F||P_d|}\sum_{p\in P_d}h_pT_p+$$
$$\gamma\frac{1}{|C|}\sum_{p\in P_d}h_p\sum_{c\in C_p}S_c(1+\epsilon f_c)x_{p,c}+\delta\frac{A}{max\{R_m\}} \tag{4.30}$$

subject to:

$$R_d\leq\sum_{p\in P_d}\sum_{c\in C_p}R_cx_{p,c} \tag{4.31}$$

$$A=\sum_{p\in P_d}\sum_{c\in C_p}R_cx_{p,c}-R_d \tag{4.32}$$

$$y_p\geq x_{p,c},\forall p\in P_d,c\in C_p$$
$$\sum_{p\in P_d}y_p\leq L_{max} \tag{4.33}$$

$$\sum_{p\in P_d}P_p\leq H_{max},TSP_s/\phi,TSP_t/\phi,FL_{max}/(1-\phi) \tag{4.34}$$

$$\sum_{p\in P_e}\sum_{c\in C_f}x_{p,c}\leq 1,\forall e\in E,f\in F \tag{4.35}$$

$$P_p=\sum_{c\in C_p}x_{p,c},\forall p\in P_d \tag{4.36}$$

$$T_p=\sum_{i=1}^{|F|}z_{p,i}-\sum_{i=1}^{|F|-1}w_{p,i,i+1},\forall p\in P_d \tag{4.37}$$

$$z_{p,f}=1,\forall p\in P_d,f\in F_p^u$$
$$z_{p,f}=\sum_{c\in C_f}x_{p,c},\forall p\in P_d,f\in F\backslash F_p^u \tag{4.38}$$

$$w_{p,i,i+1} \leq z_{p,i}, z_{p,i+1}$$
$$w_{p,i,i+1} \geq z_{p,i} + z_{p,i+1} - 1, \forall p \in P_d, i = 1, ..., |F| - 1 \tag{4.39}$$

Objective function (4.30) has multiple optimization goals: 1) minimize the number of parts into which the demand is split; 2) minimize the number of spectral gaps in the candidate paths; 3) minimize the number of FSs that the demand uses; and 4) minimize the difference between the allocated and the requested bit-rate. Note that the model tries to prioritize the use of paths with less hops; this way, less network resources are occupied. Parameters α, β, γ and δ are weighting factors used to put more or less weight to the terms in the objective function depending on the scenario. Factor ϵ is used as a convergence factor with value $\ll 1$ to reduce the execution time of the MILP model. Finally, $max\{R_m\}$ denotes the maximum value among all bit-rates of the modulation formats supported by TSPs.

Regarding the constraints, constraint (4.31) is the traffic constraint, ensuring that at least a bit-rate equal to R_d will be assigned to demand d, while constraint (4.32) accounts for the aforementioned difference between the allocated and requested bit-rate. Constraints (4.33) set the limit of paths to be used by the demand to L_{max}. Note that this value is independent of the value K used to obtain P_d. It could happen for instance that even having 3 candidate paths, the operator wants to limit the number of paths over which the demand will be routed to 2. The single-path option can be easily implemented by setting $L_{max} = 1$ with no need of further modifications in the formulation nor the mechanism itself. Constraints (4.34) set the allowed number of parts, limiting them to the number of available TSPs at source and destination and the maximum number of flows; parameter ϕ is set to 0 if MF-TSPs are employed and to 1 otherwise. Constraints (4.35) are the spectrum clashing constraints that avoid using more than one channel in a FS of a given path. Constraints (4.36) and (4.37) account for the number of parts and spectral gaps in the candidate paths, respectively. Constraints (4.38) give value to variables $z_{p,f}$ according to the actual status of the spectral resources and the decisions made by the model. Finally, constraints (4.39) are used to give value to auxiliary variables $w_{p,f,f+1}$.

The proposed SSRSMLA mechanism allows solving optimally the RSMLA problem for an incoming connection in a SS-enabled EON, considering both BV-TSP and MF-TSP implementations, as well as both single and multipath routing strategies. However, its dependence on MILP may limit its scalability to address very large network instances. For this reason, a heuristic mechanism, called H-SSRSMLA, is also developed in order to provide still accurate results at lower computational cost, making it an option when scalability becomes challenging.

H-SSRSMLA is based on a greedy iterative mechanism that selects at every iteration the best solution element from a pre-calculated set of candidate solution elements. This

element is considered as a part of the whole solution constituting the RSMLA for the demand. Next, the candidate solution elements are updated and the mechanism proceeds with the next iteration, until the demand is fully allocated or the candidate set becomes empty. Let us define O as the candidate set, being o an element inside this set. Every element o has associated a path p, a modulation format m and an ordered set of spectral gaps g_p corresponding to the spectral gaps of path p, being g_p^1 the first element in the set g_p. With these, Table 4.4 depicts the pseudo-code of H-SSRSMLA.

The first phase in H-SSRSMLA builds the candidate path, modulation and spectral gaps sets. For the latter, the mechanism obtains the end-to-end spectral gaps for a candidate path and sorts them in descending size order, that is, starting with the gap of biggest size and ending with the gap of smallest size. The idea behind this ordering is to favor the allocation of a demand in less parts, as bigger spectral gaps will likely be able to fit more types of modulation formats. As for the modulation format sets, note that the mechanism removes from the sets any modulation format for which its spectral width in FSs, that is, S_m, is bigger than the first element in the candidate gaps sets, that is, the biggest spectral gap, as it would be infeasible to employ these modulation formats to serve the demand. Once all the candidate sets have been built, the mechanism proceeds with the construction of the initial set of candidate solution elements, assigning to each one of them a candidate path, modulation format and set of spectral gaps. Then, it orders the solution elements according to a comparison method, named **CompareProcedure** in the pseudo-code. The exact details of **CompareProcedure** will be discussed later on.

The next phase starts a loop where the first element in O is added to the complete solution in each iteration, until any of the following stop criteria is met: 1) all the demand's bit-rate is served; 2) no more candidates exist; 3) the number of parts has reached its limit H_{max}; 4) there are not enough free TSPs at source or destination to support such number of parts (BV-TSPs case); or 5) the number of parts has reached the maximum number of flows (MF-TSPs case). Parameter ϕ has the same purpose as in SSRSMLA. In every iteration the mechanism also updates the resources associated to the elements in O (basically the set of spectral gaps g_p) and sorts them again according to **CompareProcedure**. Moreover, it eliminates all the infeasible candidates once updated. Furthermore, in every iteration the mechanism checks if the path limit L_{max} is reached, eliminating all elements in O with paths not in the solution built so far once this limit has been reached. Finally, the mechanism checks if all the bit-rate of the demand has been served and, hence, a feasible RSMLA has been found for that particular demand. This being the case, the demand is successfully allocated and network resources are updated accordingly.

As for **CompareProcedure**, essentially, it is a prioritization mechanism that given two elements from the set O, determines the relative order between them in terms of quality. So, when executing **CompareProcedure**, the elements of higher quality will be at the beginning of the set. The prioritization criteria are as follows:

Inputs: d,G_n,F,M,K,H_{max},L_{max},FL_{max}; **Output:** Sol

Phase 1: Pre-processing
if $TSP_s = 0$ *or* $TSP_t = 0$ **then**
  Demand blocked
$P_d \leftarrow K$ shortest paths from s_d to t_d using l_p as the metric
for $i = 1$ **to** K **do**
  $M_i \leftarrow$ set of modulations belonging to M with $TR_m \geq l_i$
  if $M_i = \emptyset$ **then**
    Remove p_i from P_d
if $P_d = \emptyset$ **then**
  Demand blocked
for $i = 1$ **to** $|P_d|$ **do**
  $g_i \leftarrow$ spectral gaps of i_{th} path
  if $g_i = \emptyset$ **then**
    Remove p_i from P_d
  else
    Order gaps in g_i in descending size order
if $P_d = \emptyset$ **then**
  Demand blocked
for $i = 1$ **to** $|P_d|$ **do**
  for $j = 1$ **to** $|M_i|$ **do**
    $S_{i,j} \leftarrow$ number of FSs for modulation j in path i
    if $S_{i,j} > |g_i^1|$ **then**
      Remove $m_{i,j}$ from M_i
  if $M_i = \emptyset$ **then**
    Remove p_i from P_d
if $P_d = \emptyset$ **then**
  Demand blocked

Phase 2: Construction
$O \leftarrow \emptyset$
for $i = 1$ **to** $|P_d|$ **do**
  for $j = 1$ **to** $|M_i|$ **do**
    $O \leftarrow o\{p_i, m_{i,j}, g_i\} \cup O$
Sort O according to **CompareProcedure**

Phase 3: Execution
$ResBr \leftarrow R_d$, $Parts \leftarrow 0$, $Paths \leftarrow 0$, $p_s \leftarrow \emptyset$, $m_s \leftarrow \emptyset$, $s_s \leftarrow \emptyset$
while $ResBr > 0$ **and** $O \neq \emptyset$ **and** $Parts < H_{max}$ **and** $Parts < TSP_s/\phi$ **and** $Parts < TSP_t/\phi$ **and** $Parts < FL_{max}/(\phi - 1)$ **do**
  $p_s \leftarrow$ path of first element in O
  $m_s \leftarrow$ modulation of first element in O
  $s_s \leftarrow$ first S_m FSs in g_p^1 of first element in O
  $Sol \leftarrow \{p_s, m_s, s_s\} \cup Sol$
  $Parts++$
  $ResBr \leftarrow ResBr - o.R_m$
  if $Paths = 0$ **then**
    $Paths++$
  else if $Paths < L_{max}$ **then**
    $Paths \leftarrow$ number of different paths used currently in Sol
  else
    Remove all elements $o \in O$ with $o.p$ not in Sol
  Update and sort again g_p for every $o \in O$
  for $i = 1$ **to** $|O|$ **do**
    if $|o_i.g_p^1| = 0$ **or** $o_i.S_m > |o_i.g_p^1|$ **then**
      Remove o_i from O
  Sort O according to **CompareProcedure**

Phase 4: Evaluation
if $ResBr > 0$ **then**
  Demand blocked
else
  Return Sol
  Update network resources according to Sol
  Demand allocated

TABLE 4.4: H-SSRSMLA mechanism pseudo-code.

1. Element with $R_m = ResBr$. If both meet, then:
   (a) Element with bigger $|g_p^1|/(S_m \times h_p)$.
   (b) Element with smaller $S_m \times h_p$.
   (c) Element with bigger $|g_p^1|$.
2. Element with $R_m > ResBr$. If both meet, then:
   (a) Element with smaller R_m.
   (b) Element with bigger $|g_p^1|/(S_m \times h_p)$.
   (c) Element with smaller $S_m \times h_p$.
   (d) Element with bigger $|g_p^1|$.
3. Element with $R_m < ResBr$. If both meet, then:
   (a) Element with bigger R_m.
   (b) Element with bigger $|g_p^1|/(S_m \times h_p)$.
   (c) Element with smaller $S_m \times h_p$.
   (d) Element with bigger $|g_p^1|$.

In this regard, candidate elements with R_m equal to the current residual bit-rate are prioritized, followed by elements with R_m higher than the residual bit-rate and, last, elements with R_m lower than the residual bit-rate. Within the latter two categories, elements with R_m closer to the residual bit-rate are prioritized among the rest. By doing so, the number of parts into which a demand may be split is minimized. Also, inside each category, elements are prioritized in the following order: 1) bigger $|g_p^1|/(S_m \times h_p)$; 2) smaller $S_m \times h_p$; and 3) bigger $|g_p^1|$. By doing so, the mechanism makes a good trade-off between combinations of path and modulation format that will employ less network resources (i.e., FSs) and paths with bigger spectral gaps, that will likely fit the demand in less parts and leave more contiguous resources for future demands.

Note, however, that H-SSRSMLA is only intended for the multi-path case, while some adjustments are necessary to obtain a good mechanism for the single-path case. In fact, by only setting $L_{max} = 1$ in H-SSRSMLA would limit the heuristic to only examine the first selected path among the candidate ones, potentially getting trapped in a local optimum. To avoid this, some minor modifications in H-SSRSMLA are introduced to also work properly in the single-path case. Essentially, instead of feeding the mechanism with all candidate paths at once, the mechanism is executed independently for every candidate path and, at the end, the produced solution of higher quality in terms of $|g_p^1|/(\#$ of employed FSs$\times h_p)$ is selected. By doing so, it makes sure that all candidate paths are explored to obtain a single-path solution, selecting among these solutions the one that makes the best trade-off between contiguous and used spectral resources. Note in this case that the the value of L_{max} is not relevant as the mechanism is executed for one path at a time, implicitly setting this parameter to 1.

4.4.1 Simulation results

To evaluate the performance of both SSRSMLA and H-SSRSMLA mechanisms extensive simulations have been executed. In order to quantify the benefits of optimally splitting the blocked demands, a scenario where no splitting is performed (hereafter referred as NSRSMLA) is used as a benchmark. To this end, the presented SSRSMLA mechanism forcing $H_{max} = 1$ and $\alpha = 0$ in the formulation is employed. Two network topologies, namely, the EON16 and the DT topologies, as well as two situations regarding spectral resources, namely 160 and 320 FSs per fiber link, with $F_w = 6.25$ GHz and $G = 10$ GHz have been cosnidered. As for the modulation formats supported by TSPs, Table 4.5 depicts them, together with their characteristics in terms of bit-rate (Br), spectral width (Bw) and transmission reach (TR).

Results have been extracted by generating 10^5 bidirectional demand requests per execution. Requests arrive to the network randomly following a Poisson process, with exponentially distributed HTs. The bit-rate of the demands is uniformly chosen among 25, 50, 100 and 200 Gb/s. Additionally, source and destination nodes for the demands are chosen with equiprobability among all network nodes. Moreover, $K = 3$, $H_{max} = FL_{max} = 4$ and $\alpha = \beta = \gamma = \delta = 1$ are set in all cases. As for L_{max}, its value is set to 3 for the multi-path case and to 1 for the single-path case. All simulations are run in standard PCs with i7-3770 CPUs at 3.4 GHz and 16 GB RAM using CPLEX v12.2 as optimization software.

Figure 4.9 depicts the BBR of the mechanisms in the 320 FSs scenarios. Graphs are plotted as a function of the normalized HT of the demands, fixing their average inter-arrival time to 1 time unit. It can be appreciated that the optimal splitting of the demands leads to substantial reductions on the BBR when compared to a scenario where no splitting is performed, with the multi-path option performing better than the single-path option. Particularly, relative gains in the range 21-40% and 27-50% can be appreciated in the DT network scenarios for SSRSMLA against NSRSMLA, in single and multi-path scenarios, respectively. As for EON16 scenarios, relative gains in the range 22-80% and 38-85% can be appreciated for SSRSMLA against NSRSMLA in the single and multi-path scenarios, respectively. In this regard, it can be observed that, in average, the mechanism achieves greater reductions in the EON16 scenarios. This can be explained due to its topological characteristics; particularly, it has a physical diameter bigger than DT, so less candidate modulation formats are available. Hence, giving the opportunity to be served as multiple parts has larger impact on the number of demands that can be successfully allocated. As for the DT network scenarios, since demands have more candidate modulation formats, it is easier to allocate them without splitting, so the splitting procedure has a slightly lower impact in terms of BBR in such scenarios. On average, demands in EON16 network scenarios are split in 1.02 parts, while in DT network scenarios they are split in 1.0023 parts.

TABLE 4.5: Supported modulation formats

Modulation	Br (Gb/s)	Bw (GHz)	TR (km)
28 Gbaud SP-BPSK	25	42	3000
28 Gbaud PDM-BPSK	50	42	2400
28 Gbaud PS-QPSK	75	42	2000
28 Gbaud PDM-QPSK	100	42	1200
28 Gbaud PDM-8QAM	150	42	500
28 Gbaud QPM-16QAM	200	42	300
56 Gbaud SP-BPSK	50	70	3000
56 Gbaud PDM-BPSK	100	70	2400
56 Gbaud PS-QPSK	150	70	2000
56 Gbaud PDM-QPSK	200	70	1200
84 Gbaud SP-BPSK	75	98	3000
84 Gbaud PDM-BPSK	150	98	2400
112 Gbaud SP-BPSK	100	126	3000
112 Gbaud PDM-BPSK	200	126	2400

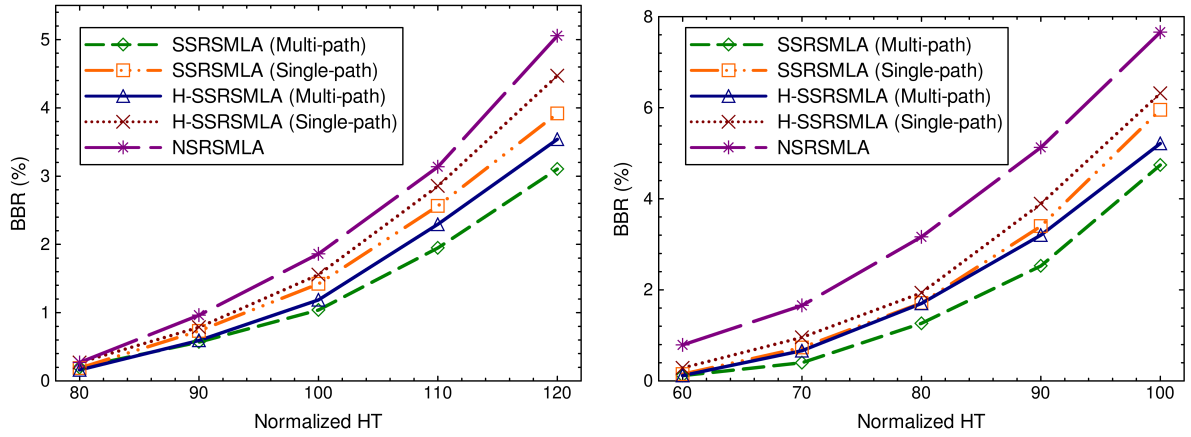

FIGURE 4.9: Simulation results: BBR in a) DT/320 and b) EON16/320 scenarios.

Concerning the comparison between single-path and multi-path cases with SSRSMLA, the multi-path case achieves relative gains in the range 13-22% and 20-28% for DT and EON16 network scenarios. Again, it can be seen that the relative difference is greater in the EON16 scenarios. The reason is the same as before: since EON16 has larger diameter, a single physical path has a limited set of candidate modulation formats, thus routing a demand through multiple physical paths increases the chances of serving it successfully. On average, for the multi-path case, demands in EON16 network scenarios are routed over 1.0082 paths while in the DT network scenarios they are routed over 1.0009 paths.

Additionally, given the multi-objective nature of the MILP formulation employed in SSRSMLA, additional simulations to determine the influence of the specific optimization objectives in the overall performance have been executed, focusing in the scenario

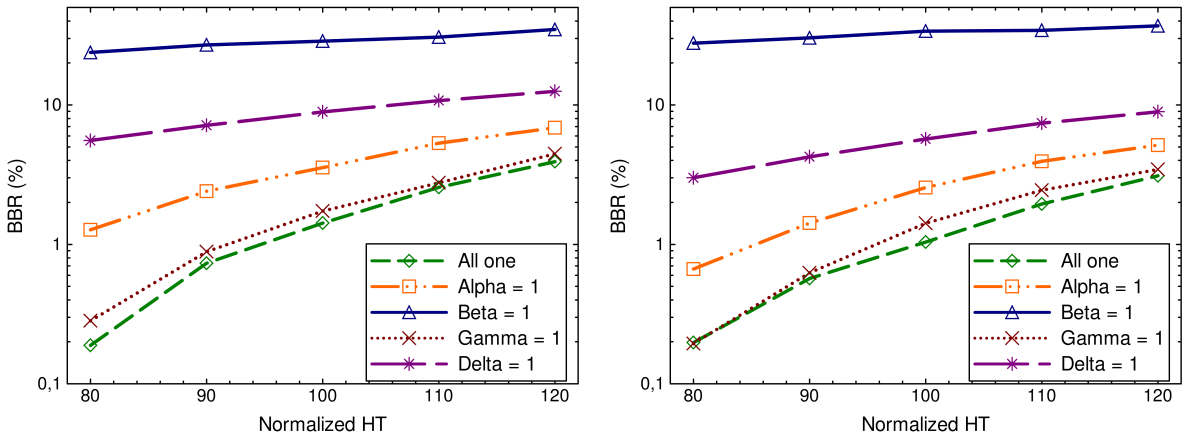

FIGURE 4.10: Simulation results: BBR in a) single-path and b) multi-path cases.

DT/320. There, for increasing values of the normalized HT, the BBR of SSRSMLA for various configurations, namely, the case where all weighting parameters are set to 1 ("All one" case) and the cases where only one of these parameters is set to 1 and the rest to 0 have been plotted. Figure 4.10 depicts the obtained results for both single and multi-path cases.

It can be appreciated indeed, that the the joint minimization of all the objectives provides lower BBR figures than focusing only in one of them. It can also be seen that minimizing only the number of allocated FSs performs very similarly to the joint minimization case, indicating that this objective takes the highest importance in the combined objective function. Focusing on the rest of the objectives, the minimization of the number of parts takes the second place, the minimization of the difference between allocated and requested bit-rate takes the third one and, finally, the minimization of the spectral gaps has the lowest importance. Focusing on this last objective, it can be seen that minimizing it solely results in a significant performance degradation when compared with the other cases. This can be explained as follows. Since SSRSMLA tries to minimize the spectral gaps present in the candidate paths, it divides the signal in many parts and chooses the most spectral width-demanding modulation format in order to fill as much spectral gaps as possible, resulting in a poor resource utilization.

Regarding the performance of the H-SSRSMLA mechanism, looking back at Fig. 4.9, it can be seen that it achieves BBR figures quite close to the ones obtained by the SSRSMLA mechanism. Table 4.6 depicts the performance comparison between both mechanisms, displaying for some of the tested scenarios the optimality gap of H-SSRSMLA against SSRSMLA and the average execution times, denoted as T_m and T_h for SSRSMLA and H-SSRSMLA, respectively. Indeed, H-SSRSMLA performs quite good when compared against SSRSMLA, with optimality gaps around 10-14% on average. Note that for normalized HTs leading to BBR $< 1\%$, possible working range for these networks, the differences between H-SSRSMLA and SSRSMLA are very small. Regarding the execution

Table 4.6: SSRSMLA vs H-SSRSMLA

	Single-path			**Multi-path**		
Scenario	**Gap (%)**	**T_m(ms.)**	**T_h(ms.)**	**Gap (%)**	**T_m(ms.)**	**T_h(ms.)**
DT/160 HT=35	0.24	180	16	1.44	160	15
DT/160 HT=45	10.2	144	15	12.4	132	15
DT/320 HT=90	7.27	472	16	4.14	438	16
DT/320 HT=110	11.3	363	16	17.8	339	15
EON/160 HT=25	9.34	147	14	6.43	133	14
EON/160 HT=35	12.1	109	14	20.2	99	14
EON/320 HT=70	12	326	14	10.2	313	14
EON/320 HT=90	14.5	221	14	23	202	14

times although SSRSMLA can work in the sub-second range, when the number of FSs per link increases, the average execution time grows up substantially. This was the main motivation for the development of H-SSRSMLA. In this regard, it can be appreciated that its execution times remain steady for all the scenarios and more than one order of magnitude below those of SSRSMLA, highlighting the superior scalability of H-SSRSMLA.

4.5 Chapter summary

The recently proposed elastic optical networks provide numerous benefits when compared to traditional fixed grid-based optical network, allowing for a better spectrum utilization since their finer granularity allows to efficiently serve both low and high bit-rate connection demands. However, they are not exempt of drawbacks, being the main one the so called spectrum fragmentation effect. To overcome such limitation multiple strategies have been proposed in aims to enhance the performance of EONs by means of spectrum defragmentation. By rearranging the currently active connections, it is possible to pack the used spectrum and free enough contiguous spectrum portions in the whole network so as to allow the allocation of future incoming demands. However, such defragmentation techniques require complex operations that increase the control plane burden. Additionally, depending on the approach followed, there may be some disruption of the already established connections as a consequence of the connection rearrangement.

For all of these reasons, alternative ways to deal with the spectrum defragmentation effect have to be though. To this goal, after reviewing the main principles of the defragmentation process, the Split Spectrum Approach is introduced as a way to mitigate the effects of the spectrum fragmentation problem. Running away from defragmentation and spectrum conversion techniques, the SSA is based on splitting a high bit-rate demand into lower bit-rate ones so as to allocate more easily the connection into the available spectral gaps. In this regard, section 2 has reviewed the main literature regarding the SSA, putting special emphasis on the enabling technologies that make the SSA possible and the potential

routing solutions that may be applied when serving demands in a SS-enabled EON. This has lead to the conclusion of needing optimized mechanisms in order to perform the resource allocation of the demands (paths, spectrum and modulation formats) when splitting a demand in a SSA environment.

To realize such optimized resource allocation, various mechanisms have been proposed through section 3 and 4. Starting from a simple resource allocation, section 3 has proposed both MILP and heuristic based mechanisms to perform the Route and Spectrum Assignment in a SS-enabled EON. Through extensive evaluations, it has been shown that SS-enabled EONs achieve substantial gains when compared to traditional EON. Additionally, various TSP implementations have been evaluated, namely, BV-TSP and MF-TSP. The results obtained suggest that, because in normal traffic conditions the splitting of demands is infrequent, the use of MF-TSPs to realize the SSA is not justified due to its higher cost. In this regard, it is more beneficial to deploy an overdimensioned number of BV-TSPs per network node.

After these studies, in section 4 the presented mechanism has been enhanced to also consider multiple routing possibilities, namely, the single and multipath routing options. Additionally, the choice of the most suitable modulation format to serve a demand in multiple parts has been also introduced. This becomes specially important, since in a realistic network scenario the bit-rate of the established lightpaths is determined by the modulation formats available at the nodes. In such circumstances, the bit-rate of the parts into a demand is split also must follows these limitations imposed by the TSPs granularity. Extensive evaluations have showed that even with these considerations, a SS-enabled EON still outperforms the case where demands are served in a contiguous way, with the multipath option reveling itself as the routing strategy that provides a better performance since it allows to exploit more efficiently the available spectral resources in the network.

Chapter 5

Energy efficiency in transport networks

Up to this chapter, various solutions have been presented so as to provide an optimized environment for the allocation of VONs in top of a physical network substrate. Chapter 3 provided mechanisms to efficiently perform the mapping of the VONs in various situations, while Chapter 4 has studied how to provide a more efficient network substrate in terms of spectrum utilization so VONs with better spectrum management can be realized. However, as commented during Chapter 2, another important aspect in order to provide the future network architecture for efficient optical transport networks relates to the energy consumption of the physical substrate. Indeed, as VONs typically span a geographically distributed area, virtual links may be mapped to very long physical paths, so multiple devices are crossed on the end-to-end route, increasing the power consumption of the VON. For this reason, it becomes highly interesting to provide solutions in order to achieve a more energy-efficient network substrate so VONs with less power consumption can be deployed, reducing the associated OPEX.

To this end, various techniques to improve the energy efficiency of transport optical networks are presented. The first section presents an energy-aware routing solution which combines both load and energy parameters in order to achieve a good trade off between energy consumption of the connections and BP. The presented solution is intended to be used in multi-domain transport optical networks. In this regard, the proposed solution is composed of a domain abstraction mechanism for the intra-domain route calculation and several routing algorithms for the inter-domain route calculation. Next, the second section introduces the concept of sleep-enabled transport networks as a way to further reduce the energy consumption in optical networks. In this regard, a formal analysis of the performance in terms of BP and power savings is presented when a multi-class scenario is faced so as to provide guidelines on how to properly dimension the network according to the traffic pattern and the available physical resources.

5.1 Energy-aware routing in multi-domain transport networks

As commented during section 2.4, the concept of energy efficiency in optical networks is a very hot topic that has both gathered the interest of the reserach community (e.g. [ZCTM10]) and spanned multiple industrial initiatives, such as the GreenTouch consortium [GRE]. One of the potential ways to increase the energy efficiency in optical networks consists on the design of energy-aware routing mechanisms [MAV13, IBC+13]. Essentially, energy-aware routing algorithms incorporate energy consumption and physical layer information into the routing mechanism, so decisions are no longer done relaying solely on topological or resource state information. With this, the routes assigned to the connections are the ones that will keep the energy consumption on the network low. However, most of the works regarding energy-aware routing focus on single domain networks, where the whole transport network is administrated by a single operator/administrator, and very few work has investigated energy-aware routing solutions on multi-domain transport networks.

Moreover, as the objective of energy-aware routing mechanisms is to choose the paths that will entail the least energy consumption on the network, short routes are mostly preferred, since they are the ones that will consume less energy. This is a drawback in many situations, since connections tend to saturate rapidly the shorter routes, hence increasing the blocking of the connections. For this reason, energy-aware routing mechanisms are usually combined with load distribution techniques so as to find good trade-offs between energy consumption and blocking of the connections.

It is well known from consolidated literature that the ability of distributing a load in a dynamically-operated network is highly beneficial [KP12, DLWZ08]. An even distribution of traffic by the Network Elements (NEs) allows for the prevention of potential congestion conditions, thus increasing the capability of supporting a higher amount of demands by the users, i.e., lowering BP. However, although load distribution can be easily achieved in a single-domain network, it becomes more difficult in a multi-domain scenario. In fact, end-to-end routing may not be totally computed by a single entity, especially when source and destination nodes are in different and distant domains. Also, the occupancy state of all the NEs may result as being unknown or unavailable outside the domains. These difficulties, generated by scalability and confidentiality issues, prevent classical load distribution routing algorithms to work properly in a multi-domain scenario.

For all these reasons, an end-to-end solution for computing routes in a multi-domain network scenario that benefit from the load-distribution concept while it also takes into account for the power consumption of the connections is presented. The presented method is intended to be applied to the dynamic management and design of long-distance high-capacity backbone networks that span multiple domains and that have a large geographical extension. In this regard, it is assumed that the multi-domain network is based on the

Hierarchical-Path Computation Element (H-PCE) network architecture (see Appendix B) In such networks, links are almost never composed of a single fiber. Rather, in order to save infrastructural costs (of the ducts), they are composed of several parallel fibers, each fiber equipped with a set of optical amplifiers and possibly other line equipment, such as dispersion compensators.

Therefore, in the proposed solution it is assumed that all the inter- and intra-domain links are multifiber. Additionally, occupation of a link is defined as the number of connections that are routed on that particular link with no regard to the fiber where a connection is allocated. Moreover, the presented mechanism intends to be used for establishing bidirectional connections between a source and a destination node, and therefore, the occupation of a link (i,j), connecting node i to node j, will be the same of the occupation of the link (j,i) according to the number of connections routed. This is due to the fact that it is assumed that the paths in both directions are exactly the same.

Furthermore, it is assumed that each physical link of the network has at least one fiber always in operation with all its amplifiers and related line equipment switched on, regardless of the traffic flowing through that link. This is to ensure connectivity for performance measurement and periodical testing (bit error rate, frame error rate, etc.), alarming, and control plane tasks. For example, the Resource Reservation Protocol-Traffic Engineering (RSVP-TE) protocol is supported by a refresh procedure that implies periodically sending path messages once a connection is established [RFC4872]. Moreover, RSVP-TE based protection and restoration procedures also require connectivity during the network operation while the Open Shortest Path First-Traffic Engineering (OSPF-TE) protocol requires connectivity to disseminate topological and traffic engineering information [RFC4203]. In case the Link Management Protocol (LMP) is also implemented, it requires Hello messages to be exchanged to monitor the health of the control channels [RFC4204].

Note that an always powered-on fiber does not entail that nodes have to also keep the local transceivers powered-on; in fact, the power state of all line equipment, such as amplifiers, is independent of the power state of the nodes equipment. That is, a node may switch-off unused transceivers without the need of switching-off all the equipment along the fiber. By keeping only a fiber switched-on, we guarantee still enough connectivity for monitoring reasons while the power consumption is kept minimal.

With this in mind, the presented mechanism is composed of two parts. First, there is a topology abstraction design model to perform the intra-domain routing. For this, a MILP formulation whose goal is to obtain optimal mapping between the physical paths and virtual links for a single domain in order to achieve a good trade-off between load-distribution and energy efficiency, assuming that a fully-meshed domain abstraction is employed, is presented. The corresponding mappings will be used by the child PCEs to establish the intra-domain route. Secondly, multiple inter-domain routing algorithm, which take into account the costs associated to the virtual links obtained through the aforementioned MILP formulation (along with occupation and length parameters) in order to compute

inter-domain routes that are both efficient in terms of energy consumption and connection establishment success are presented. The following subsections detail both parts of the solution.

5.1.1 MILP formulation for intra-domain routing

Let the optical network of a single domain be characterized by a graph $G_n = (N, E)$, where N denotes the set of nodes and $E = \{(i,j),(j,i) : i,j \in N, i \neq j\}$ the set of physical links. Moreover, let B_n denote the set of Border Nodes (BNs) of the domain with $B_n \subseteq N$ and E_v the set of virtual links of the domain abstraction, for which e_v^{sd} denotes the specific virtual link connecting BNs s and d. Additionally, let P denote the set of physical paths in the optical network of the domain, $P_{sd} \subseteq P$ the set of candidate paths between BNs s and d, and K the number of paths that will be associated to every virtual link.

Assuming a full-meshed domain abstraction, the objective of the model is to compute the optimal mapping between virtual links and physical paths that minimizes at the same time the BP (by means of load-balancing) and the power consumption of the domain. To this purpose, $Q_{sd}^p \subseteq P$ defines the set of physical paths that share at least one physical link with the candidate path $p \in P_{sd}$ for connecting BNs s and d, l_{sd}^p defines the physical length of $p \in P_{sd}$ and TR defines the transparent reach of the lightpaths without needing regeneration. With this, the number of intra-domain REGs needed for every candidate path, denoted as R_{sd}^p, is:

$$R_{sd}^p = \left\lceil \frac{l_{sd}^p}{TR} - 1 \right\rceil \forall\, p \in P_{sd}; s,d \in B_n, s \neq d \tag{5.1}$$

where R_{max} denotes the maximum value among all R_{sd}^p.

Moreover, let M define the mean sharing of physical links between paths associated to virtual links, that is, the average number of virtual links that share at least one physical link with other virtual links. If this metric is minimized, that is, the number of virtual links that share physical resources between them is kept at minimum, the load in the domain becomes as balanced as possible among physical resources belonging to virtual links, potentially reducing the BP of the connections. Finally, T defines the mean use of REGs in the domain, that is, the average number of REGs employed in the physical routes associated to the virtual links. If this metric is minimized, the paths that will be associated to the virtual links will entail a minimal use of REGs and, hence, the power consumption of the domain will be kept at a minimum.

With all of these, let us discuss the details of the MILP formulations, for which the model variables are as stated below:

$x^p_{e_v^{sd}}$: binary; 1 if path p is used to map virtual link e_v^{sd}, 0 otherwise.

$z^p_{e_v^{sd}}$: integer; indicates how many virtual links share some physical links with path p for virtual link e_v^{sd} if path p belongs to the solution, i.e. $x^p_{e_v^{sd}} = 1$, otherwise its value is equal to 0.

Z: integer; represents the maximum among all $z^p_{e_v^{sd}}$ variables.

Now, with the presented variables, M and T can be written as:

$$M = \frac{1}{K|E_v|} \sum_{e_v^{sd} \in E_v} \sum_{p \in P_{sd}} z^p_{e_v^{sd}} \tag{5.2}$$

$$T = \frac{1}{K|E_v|R_{max}} \sum_{e_v^{sd} \in E_v} \sum_{p \in P_{sd}} R^p_{sd} x^p_{e_v^{sd}} \tag{5.3}$$

With these definitions, the MILP formulation is as stated below:

$$min\ \alpha(\beta Z + (1-\beta)M) + (1-\alpha)T, s.t. \tag{5.4}$$

$$\sum_{p \in P_{sd}} x^p_{e_v^{sd}} = K, \forall e_v^{sd} \in E_v \tag{5.5}$$

$$z^p_{e_v^{sd}} \geq \sum_{i \in B} \sum_{\substack{j \in B \\ i \neq j}} \sum_{k \in Q^p_{sd}} x^k_{e_v^{ij}} + (x^p_{e_v^{sd}} - 1) \sum_{i \in B} \sum_{\substack{j \in B \\ i \neq j}} \sum_{k \in Q^p_{sd}} 1, \forall p \in P_{sd}, e_v^{sd} \in E_v \tag{5.6}$$

$$Z \geq z^p_{e_v^{sd}}, \forall p \in P_{sd}, e_v^{sd} \in E_v \tag{5.7}$$

The objective function's (5.4) goal is twofold: i) minimize the sharing of physical links between the paths associated to the virtual links that form the domain abstraction; ii) minimize the average number of REGs that are used by the intra-domain paths corresponding to the virtual links of the domain abstraction. Parameters α and β are real numbers in the range [0,1] and are used to put more or less weight to the components of the objective function. With the minimization of the sharing of the physical links, the model aims at reducing the BP of the connections, as they will potentially use different parts of the network and hence, balance the load among all the physical links. More in depth, the model minimizes at the same time the average sharing and the maximum sharing. The rationale behind this is to keep the mean sharing as low as possible and, at the same time, the deviation from this value for all virtual links; that is why the maximum sharing is also minimized (variable Z). In this way, it balances the load between

virtual links in a fair way. Additionally, by minimizing the number of REGs, it the power consumption of the associated virtual links.

As for the constraints and their meaning, constraints (5.5) is needed to map every virtual link to K different paths in the physical network. The role of variable K is to provide a more flexible mapping mechanism if more sophisticated routing schemes were adopted, e.g., K candidate physical paths may be employed for connections traversing a particular virtual link. Constraints (5.6) set the value of variables $z^p_{e^{sd}_v}$, which account for the sharing of physical links among virtual links. As commented before, $z^p_{e^{sd}_v}$ only takes a value greater than 0 if the corresponding $x^p_{e^{sd}_v} = 1$; that is, the path belongs to the solution. For this reason, the second term is added to the constraint, which will drag to 0 variable $z^p_{e^{sd}_v}$ if $x^p_{e^{sd}_v} = 0$, as all variables z are defined as positive integers (greater or equal to 0). Finally, constraints (5.7) allow the minimization of the maximum sharing of physical links.

5.1.2 Inter-domain routing algorithms

In this section, several routing algorithms for the inter-domain route computation are presented: SP routing, Least Loaded (LL) routing, and Round Robin (RR) routing. In their design, it assumed that only BNs can be the source or destination of the traffic. Moreover, the full inter-domain path is specified as a sequence of inter-domain physical links, BNs and intra-domain virtual links. The translation of this path into a fully-detailed path, i.e., a sequence of physical links and nodes, is not done at the inter-domain level. In fact, the intra-domain virtual links are automatically translated into physical paths within each crossed domain because of the fixed correspondence between virtual links and physical paths connecting the BNs. In this regard, it is assumed that mapping of virtual links to physical paths remains static (no re-optimization of the abstract topologies is performed) due to the computational complexity of the MILP formulation described in the previous section. With this, the following sections detail the three considered routing algorithms.

5.1.2.1 SP routing algorithm

In the SP routing algorithm, the path chosen is the shortest one in terms of the physical length, between the source and destination nodes. Thus, the cost related to the length of the path is computed in the same manner for both inter-domain and intra-domain links by directly assigning to each link a cost proportional to its physical length and then summing over all the links crossed by the path. The state of the links (both virtual and inter-domain) is not taken into account at all: if a link on a computed path is fully occupied, then the connection is blocked. Thus, this algorithm requires only a limited amount of information exchanged between domains; in particular link-state information updates are not required in real time.

5.1.2.2 LL routing algorithm

In the LL routing algorithm, two different weights with different priorities are used to compute the minimum-cost path. In particular, the aim is sharing the load over different alternative paths, the weights considered are i) the occupation weight, and ii) a cost related to the length of the links. In general, the occupation weight of a physical link is defined as the number of wavelength channels currently in use on that link. The occupation weight of an inter-domain link is straightforward. Instead, the occupation weight assigned to an intra-domain link is the occupation weight of the most used physical link that composes the corresponding intra-domain path. Conversely, the cost related to the length of the path is computed in the same manner for both inter-domain and intra-domain links by directly assigning to each link a cost proportional to its physical length and then summing over all the links crossed by the path.

To route a connection between the source BN and the destination BN, the procedure first runs the Dijkstra algorithm considering the occupation cost of the (intra- and inter-domain) links. During this operation, the algorithm also computes the total physical length of the end-to-end paths. In such a way, at the end of this operation both occupation and length costs are assigned to each route. The routing decision, i.e., the selection of the end-to-end path to assign to the connection, is primarily based on the total occupation cost: the connection will be routed on the path with the minimum occupation cost in terms of the maximum link occupation. This means that the occupation cost of an end-to-end path is the occupation of the most charged link which belongs to the end-to-end route. It may happen that more than one end-to-end path has the same occupation cost. In this case, the route selected is the one having the minimum end-to-end physical length among all the paths with the same occupation cost. Additionally, the routing algorithm avoids that a particular domain is crossed more than once by the same end-to-end connection. Such a fact would not make sense, both in terms of occupation and power consumption. The normal behavior of the Dijkstra algorithm is thus modified preventing a path to comprise more than one virtual link belonging to the same domain.

5.1.2.3 RR routing algorithm

In the RR routing algorithm, the path is chosen in a round robin fashion. This means that when a connection has to be routed from BN s to BN d, it chooses, as a first path, the shortest path. Then, for the following connection starting at BN s, it will choose (in a round robin way) the other possible routes, e.g., if the last route used was route k, the following route to be used will be route $k + 1$. When all the possible routes originating from BN s have been used at least once to establish a connection, then the algorithm will start the same procedure from the beginning. The RR routing algorithm is performed independently for each source BN, meaning that the choice of the path made for BN s_1 does not affect the decision to route a new connection starting in BN s_2. It can be seen

that the RR routing algorithm enjoys the load-distribution properties of the LL routing algorithm. On the other hand, as in the SP case, if a link of a chosen path is fully occupied, then the connection will be blocked.

5.1.3 Results and discussion

5.1.3.1 Test scenario and assumptions

Before presenting the results, this section will explain which has been the network scenario used to test the proposed solution, along with the major assumptions concerning the physical equipment. The presented MILP model and routing mechanisms have been tested through simulations, considering one topology composed of 9 domains, with a total of 75 optical nodes (48 BNs and 27 non-BNs) and a total of 146 bidirectional physical links (26 inter-domain and 120 intra-domain) (see appendix A.3). The length of each link, although not shown, is normalized to the transparent reach of the connections, i.e., to the maximum length the optical signals can travel without regeneration; for instance, a link distance of 0.6 means that the link length is 60% of the transparent reach. Additionally, in order to investigate the impact of the energy consumption due to extra-fibers, a multi-fiber scenario in which each physical link is composed of two fibers per direction has been assumed. Each one of these fibers carries 32 wavelength channels.

Two different scenarios have been tested, the Single-Carrier (SC) scenario, where all the domains belong to the same administrator, and the Multi-Carrier (MC) scenario, where domains are managed by different administrators. For both scenarios, it has been considered that every fiber has a set of in-line bidirectional amplifiers that amplify the whole bundle of wavelengths. If the fiber is the first one of the link, then its amplifiers are always powered up, regardless of the actual traffic. If the fiber is an extra fiber (second, third, etc.) its amplifiers are only powered up when there are connections using that particular fiber. The distance between amplifiers (amplification span) is constant. In order to calculate the necessary number of amplifiers in one fiber, the expression reported in Equation 5.8 is used, where l_{link} is the length of the physical link and AR the length of the amplification span [ST09]. For the calculation of the number of amplifiers, it has been considered that the distance between amplifiers is equal to a normalized length of 0.07. To obtain this value, we assume a 100 Gb/s network scenario with a transparent reach of 1200 km [RM11] and a distance of 80 km between amplifiers as in [ST09] ($80/1200 \approx 0.07$).

$$N_{amp} = \left\lceil \frac{l_{link}}{AR} - 1 \right\rceil + 2 \tag{5.8}$$

It is considered that each connection implies the use of one TSP at its source node and another one at its destination node. For the use of REGs, different rules hold depending on the scenario. In the SC scenario, it is considered that regeneration takes place only

in nodes where this is needed, i.e., where the distances between nodes are greater than the transparent reach, even if the end-to-end path spans more than one domain. On the other hand, in the MC scenario, it is considered that regeneration is only performed inside a domain if the intra-domain path distance is greater than the transparent reach; O-E-O conversion is always assumed at the BNs. The regeneration at the BNs, in such a scenario, is performed even if the distance between the latest intra-domain node and the BN is less than the transparent reach. In this regard, it is considered that every node in the network is equipped with regeneration capabilities, so all nodes become a potential regeneration point for connections needing it. In this regard, the goal is to evaluate the power savings that can be obtained through the use of the proposed mechanism without dealing with the REG placement problem, which is out of the scope of this work. As for the power consumption of the devices (amplifiers, TSPs and REGs), the power figures reported in [JMST13] have been used through this section.

5.1.3.2 Intra-domain virtual topology design evaluation

In this section, the general complexity of the proposed MILP model and its effectiveness upon execution on the tested intra-domain topologies is discussed. Looking back at its formal description, it can be seen that the model is described using a link-path formulation, that is, the paths in the network are detailed explicitly by pre-calculated sets and the associated variables. The link-path formulation has the advantage that permits a fine tuning of the potential candidate paths by limiting the size of the path set. On the other hand, in highly meshed networks with several nodes and links, due to the high number of potential candidate paths between a source and a destination, its scalability can be somehow limited.

In terms of formulation complexity, the number of variables is in the order of $\mathcal{O}(2|E_v||\bar{P}_{sd}|)$ and the number of constraints is in the order of $\mathcal{O}(3|E_v||\bar{P}_{sd}|)$, with $|\bar{P}_{sd}|$ the average number of candidate paths from BN s to BN d. The main components that contribute to the MILP complexity, as hinted before, are the number of candidate paths in the intra-domain network and the number of BNs, since $|E_v|$ can be written as $|B|(|B|-1)/2$ considering a full-meshed domain abstraction and a bidirectional network scenario.

Table 5.1 below reports the execution times in seconds (T_m) for the model in the tested intra-domain network scenario for various values of α, in order to evaluate the complexity of the proposed MILP formulation. Moreover, the (non normalized) values of Z, M, and T is also depicted, to observe how they evolve as functions of α. For all the depicted results, $\beta = 0.5$ have been assumed. All the results have been obtained using standard Quad Core PCs at 2.66 GHz with 4 GB of RAM using Cplex v.12.2 as the optimization software.

From the results, it can be seen that domains that are more meshed or have a higher number of BNs experience high execution times. Moreover, it can be seen that $\alpha = 0.5$

TABLE 5.1: MILP evaluation in the multi-domain scenario

	$\alpha = 0$				$\alpha = 0.5$				$\alpha = 1$			
Domain	T_m	Z	M	T	T_m	Z	M	T	T_m	Z	M	T
1	0.56	1	1	0.33	0.22	1	1	0.33	0.22	1	1	0.33
2	0.32	3	2.33	1.17	6.92	3	2.33	1.5	7.84	3	2.33	1.17
3	0.68	10	5.76	0.67	$1.3 \cdot 10^4$	7	4.81	0.86	$1.3 \cdot 10^4$	7	4.81	0.86
4	1.39	12	6	0.64	$7.2 \cdot 10^3$	7	5.36	0.75	$7.2 \cdot 10^3$	8	5.28	0.64
5	0.35	4	3	1	6.49	2	2	1.67	5.46	2	2	1.67
6	0.28	3	2.6	0.3	1.64	3	2.4	0.5	2.02	3	2.4	0.4
7	1.52	8	4.9	0.71	$7.2 \cdot 10^3$	6	4.8	0.95	$7.2 \cdot 10^3$	6	4.5	0.81
8	1.58	9	5.53	0.87	$3.4 \cdot 10^3$	4	3.13	0.87	$6.3 \cdot 10^3$	4	3.13	0.8
9	0.17	6	4.33	0.67	0.35	2	1.67	0.5	0.33	2	1.67	0.5

and $\alpha = 1$, in general, lead to larger execution times, since in the corresponding working points the load-balancing term of the objective function plays an active role. Conversely, $\alpha = 0$ leads to lower execution times, as the objective function becomes trivial; it only has to minimize the average number of REGs, which is tightly related to the length of the path.

As for the evolution of the values of variables Z, M, and T although the trends are highly dependent on the intra-domain topology, generally speaking it can be appreciated that $\alpha = 0$ leads to the lowest REG usage while having the worst sharing of physical resources between virtual links, while for the other values of α the use of REGs slightly increases while the sharing is reduced.

5.1.3.3 Simulation results

In order to evaluate the performance of the proposed methods, some simulations have been carried out. In all simulations, K has been set to 1 in the MILP formulation, which means that virtual link is mapped to only one physical path. Additionally, the proposed routing algorithms have been compared in cases in which the intra-domain mapping is performed using values of α equal to 0, 0.5, and 1, setting $\beta = 0.5$ in all cases. All the simulations have been performed under a variable offered load, assuming that all connections are bidirectional and request one wavelength each.

Figure 5.1 shows the BP of the different solutions analyzed as a function of the total offered load. From the results, it can be seen that the proposed solutions, i.e., the LL and the RR algorithms, have BP values that are lower with respect to the case when the SP is used. The LL and RR algorithms produce BP figures of up to 2 orders of magnitude lower than the SP. Additionally, it can be seen that for medium and high loads the LL provides a performance that is slightly better with respect to the RR algorithm. Anyway, the difference between the BP of the LL algorithm and the BP of the RR algorithm is

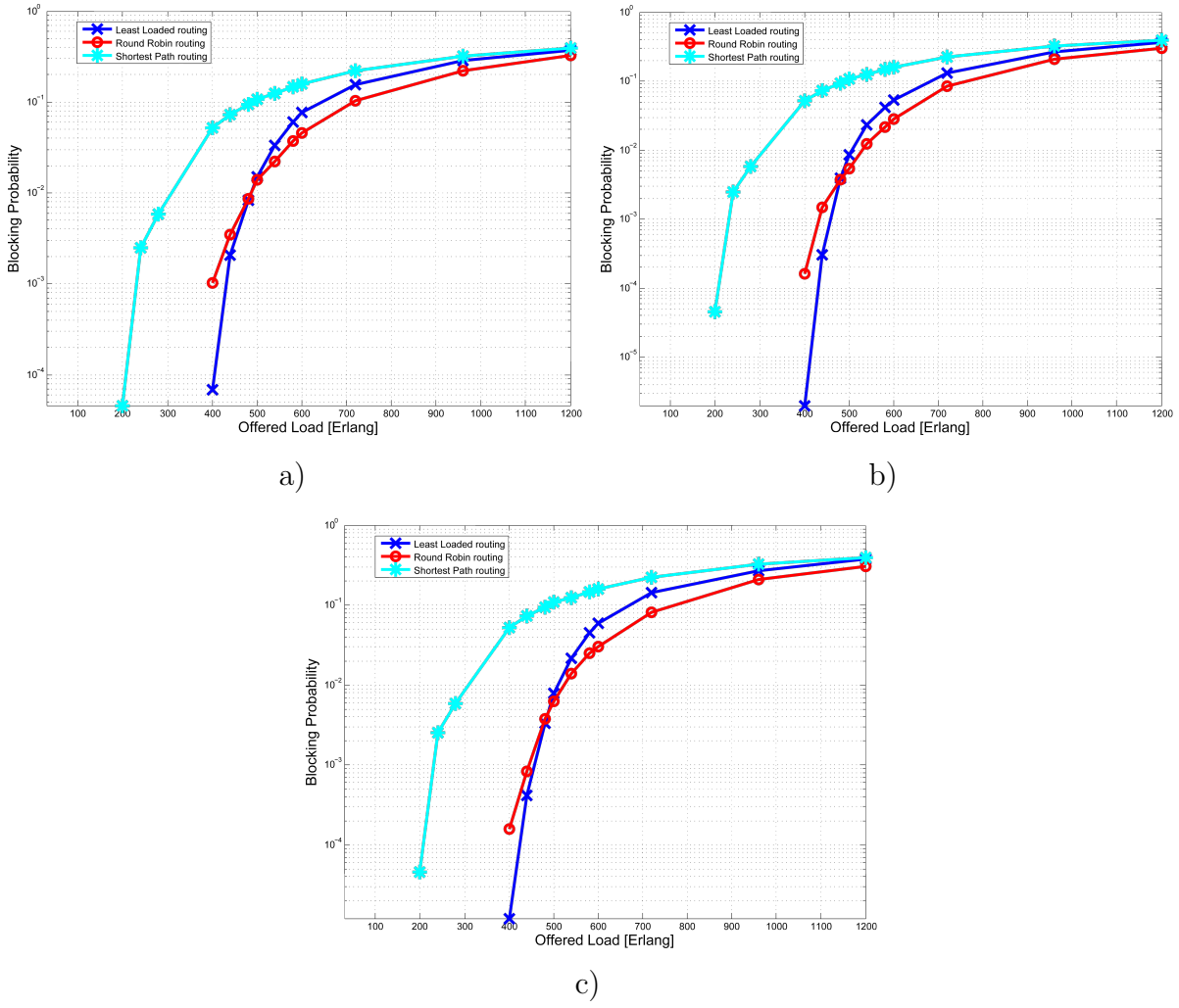

FIGURE 5.1: BP as a function of the total load for the SP, LL, and RR algorithms considering: a) $\alpha = 0$, b) $\alpha = 0.5$ and c) $\alpha = 1$.

less than $2 \cdot 10^{-2}$. Moreover, it can be appreciated that different values of α produce very similar BP figures, with $\alpha = 0.5$ and $\alpha = 1$ producing slightly better BP figures.

As for the power consumption, Figures 5.2 and 5.3 depict the performance of the proposed solutions in terms of power consumption per accepted connection as a function of the offered load in both SC and MC scenarios, respectively. Specifically, the average power consumption due to connections that use at least one extra fiber is depicted. In this way, the extra power consumption due to the utilization of the extra fibers is evaluated. In fact, the power consumption of the first fiber is the same in every case because it is assumed that such fibers are always switched on as explained before.

Looking at Figure 5.2, it can observed that, in the range of loads where the network is overprovisioned, and the BP is very small, the proposed RR routing algorithm has the lowest values of power consumption. The LL routing also has values of power consumption that are lower than the SP case at least for loads lower than about 275 Erlang. Anyway, the power consumption provided by the LL routing solution is a little higher than in

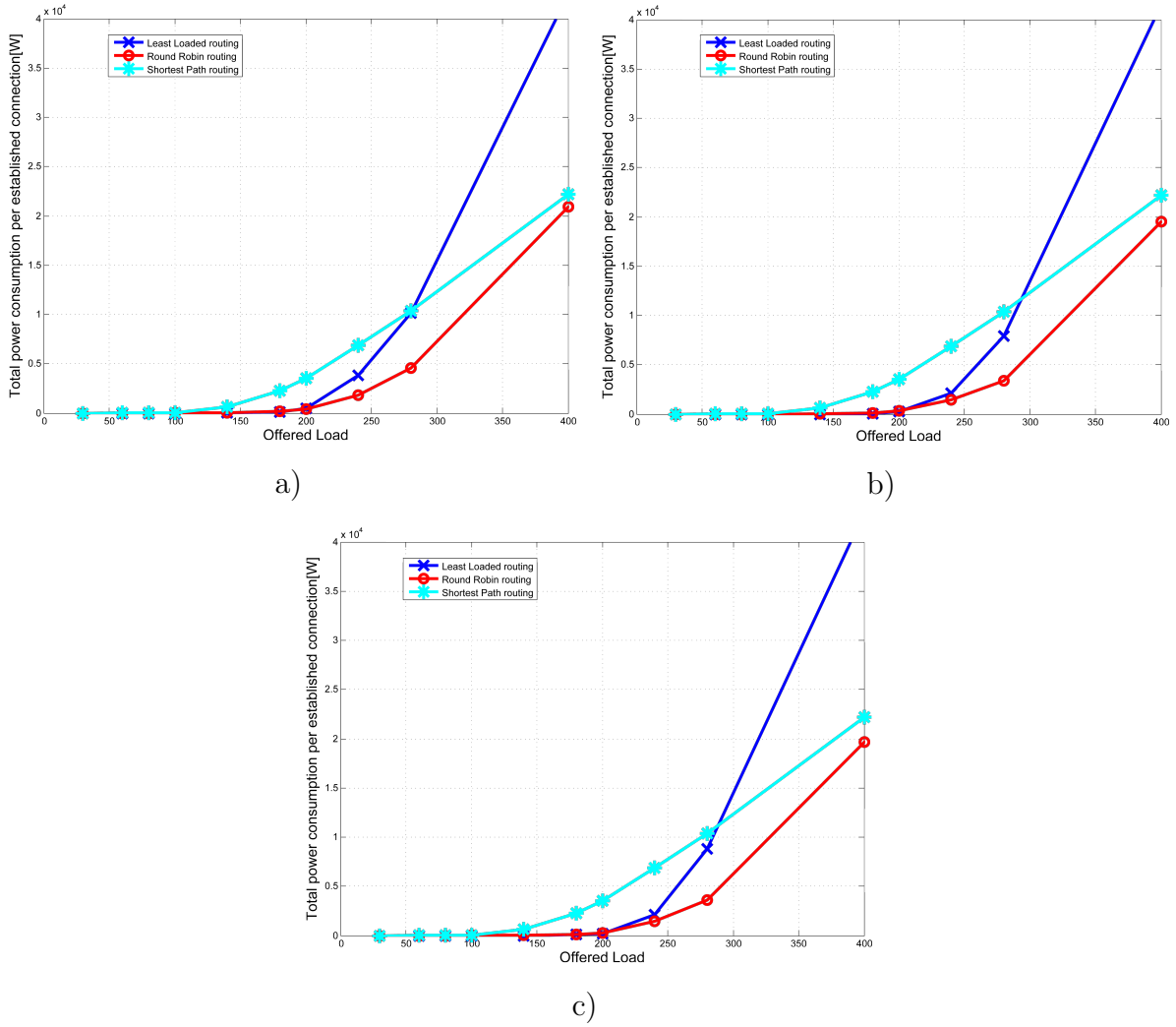

FIGURE 5.2: Power consumption as a function of the total load in the SC scenario for the SP, LL, and RR algorithms considering: a) $\alpha = 0$, b) $\alpha = 0.5$ and c) $\alpha = 1$.

the RR case. For the tested scenario, it can be appreciated that while the RR routing algorithm provides a BP slightly higher than the LL routing algorithm, it shows lower power consumption values. Conversely, the SP has a high power consumption due to the utilization of the extra fibers.

This is due to the fact that the SP policy tends to choose a limited set of paths (the shortest) so the first fibers are saturated rapidly. In such a way, the SP routing algorithm will switch on the extra fibers sooner than in the case where LL or RR policies are adopted. Again, it can be appreciated that the impact of different values of alpha is minimal. After a certain load (around 300 Erlang), when the network is not overprovisioned, the power consumptions of the LL algorithm tend to become higher than with SP. This is due to the fact that for higher loads the paths allocated are always the shortest with the SP algorithm. On the contrary, the LL algorithm at high load will find a lot of overloaded links and therefore it tends to choose paths that are much longer leading to a higher power consumption. Instead, the RR algorithm chooses each path among a set of paths but

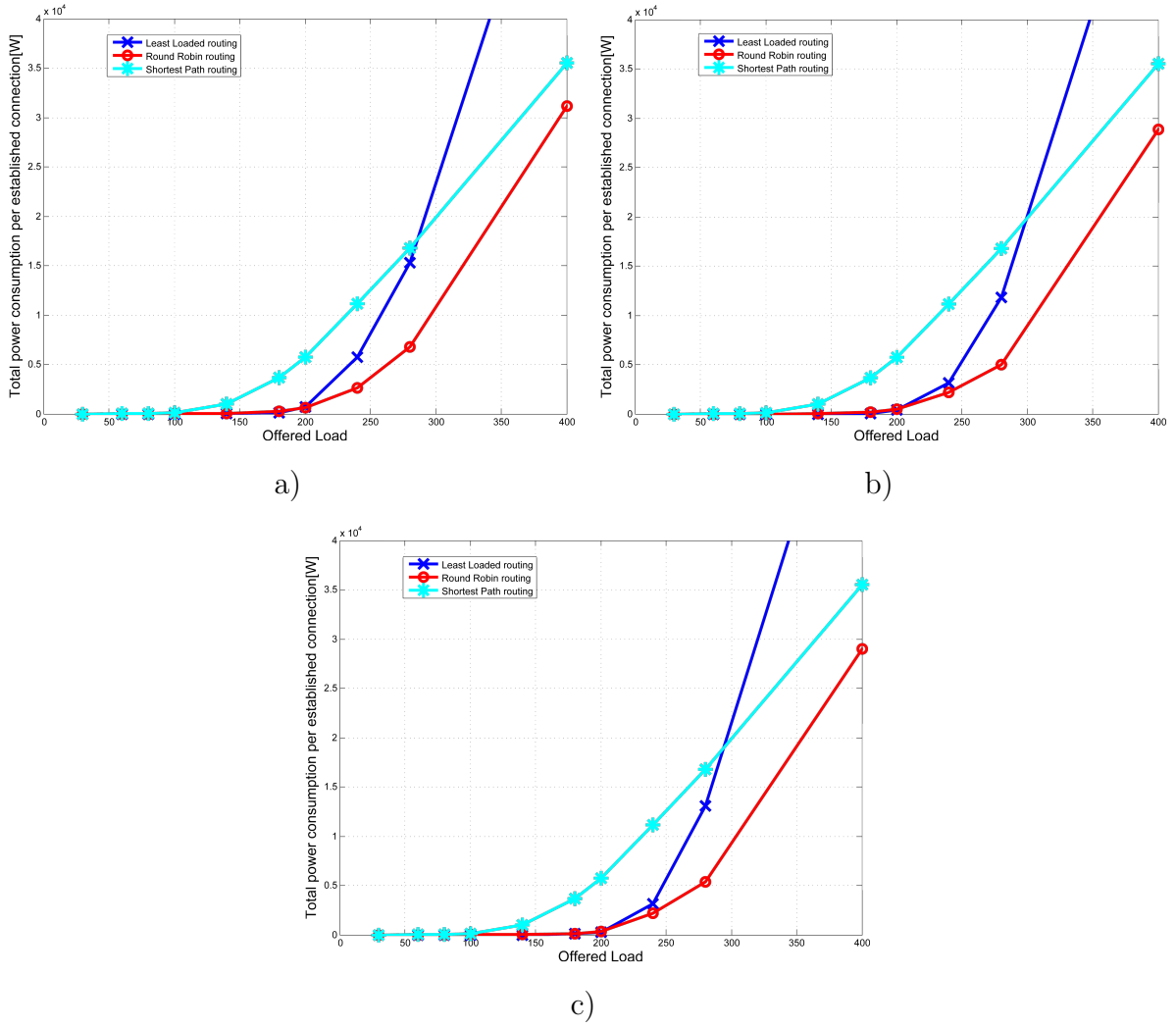

FIGURE 5.3: Power consumption as a function of the total load in the MC scenario for the SP, LL, and RR algorithms considering: a) $\alpha = 0$, b) $\alpha = 0.5$ and c) $\alpha = 1$.

without considering any link state information. For this reason, the power consumption of the RR algorithm still remains lower than the SP.

As for the MC case (Figure 5.3), the same observations and conclusions that apply for the SC case are valid. The only difference is that, in the MC case, the values of the power consumption are scaled up if compared to the SC scenario. This happens because, in the MC scenario, regeneration is performed in each BN that is included in the path. Therefore, the power consumed in the MC case is higher than in the SC case.

5.2 Introducing the sleep-mode in transport networks

During the previous section, it has been showed that an appropriate routing mechanism designed taking into account not only topological or resource information but also energy

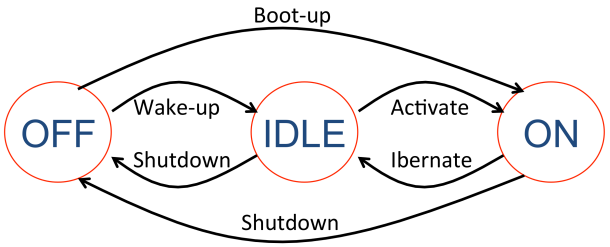

FIGURE 5.4: Diagram of the transitions between the three power states of a sleep-enabled transponder.

parameters helps on reducing the energy consumption of the connections on a transport optical network. However, as the traffic on Internet, and as a consequence, in transport optical networks grows, it is not sufficient to relay on energy-aware routing algorithms in order to keep the energy consumption of transport networks low. In this sense, it is necessary to develop more energy efficient devices in order to keep reducing the energy consumption.

Several research efforts have been focused on developing energy-efficient devices and the associated power management strategies. A very promising proposed solution consists in re-routing traffic carried by scarcely-filled wavelengths during low-load periods, in order to set some OE transmitters (i.e. TSPs) into a low-power mode or, eventually, turning them off. Authors in [MSR+11] introduced a novel TSP architecture whose novelty lies in the capability of putting the TSP modules in a low-power consumption mode (*idle* mode) when it does not support traffic; at the same time, the TSP modules can be turned fully operative (*on* mode) in a short time, whenever incoming connections are supported. Specifically, the proposed TSP features three power states, described as follows:

- *Powered-on (ON)* state: the TSP is receiving/transmitting traffic.
- *IDLE* state: the TSP is set into a low-power mode (i.e., its power consumption is significantly lower than the consumption in the ON state) since it is not transmitting/receiving traffic. In this state, the TSP requires much shorter time to be activated compared to when the TSP is in the OFF state, as the components which require high stability (the lasers at the emitter and the photodiodes at the receiver) are left powered-on to avoid long activation times (on the other hand, the components whose activation time is not critical can be powered-off.
- *Powered-off (OFF)* state: all the components of the TSP are powered-off.

Figure 5.4 depicts the inter-state transitions. With such TSP architecture, authors in [MSR+11] showed that, for dynamic traffic scenarios, 67% of energy savings can be achieved when compared to traditional WDM transport networks where TSPs remain always powered-on, regardless if they are transmitting traffic or not.

Let us now consider the case of different classes of connections. In this context, the set-up time requirements of the connections might become a critical parameter. For instance, in multi-service networks, high-priority (C_h) traffic, typically requires short set-up times (few ms.). As a consequence it cannot be supported by TSPs in the OFF power state due to the long boot-up time (≈ 60 s. [MSR+11]). However, it can be supported by TSPs in the IDLE state, for which the transition to the ON state is negligible. On the other hand, low-priority (C_l) traffic can employ OFF TSPs as it can wait for longer boot-up times. In this regard, and assuming the aforementioned TSP architecture, a power management strategy with the aim to save the power consumed by unused devices by setting them into low-power mode (or, eventually, shutting them off), while still guaranteeing the set-up time target for the different classes (C_h and C_l) of connections is described below.

Namely, in order to avoid that C_h connections miss their set-up time target, it is assumed that a certain number (say k) of TSPs in a node, among those unused, are set in IDLE state and reserved for C_h connections. Assuming that every node in the optical network is equipped with N TSPs, with t representing the number of TSPs that are currently in the ON state, the other unused TSPs (i.e. $N - k - t$) are in OFF state and will be used for future incoming C_l connections.

Defining U as the current number of unused TSPs, it is assumed that, if $U \geq k$, then exactly k are set in IDLE state. Otherwise, all the U TSPs are set into IDLE state. According to Figure 5.4, when a C_h connection arrives, an IDLE TSP is activated to support the new C_h connection and an OFF TSP is woken-up (OFF to IDLE) such that the pool of k TSPs reserved for C_h traffic is maintained at the node. Such transition (from OFF to IDLE) can be performed if the number of OFF TSPs is greater than 0. By doing so, a C_h connection is blocked only if no IDLE TSPs are available. On the other hand, when a C_l connection arrives, an OFF TSP is booted-up. If no OFF TSP is available when a C_l connection arrives, then the connection is blocked, as the TSPs in IDLE state are reserved for the C_h connections. When a connection is torn-down, its TSPs can be either shut-down or hibernated (set into IDLE state) according to the number of available IDLE devices. Note that, by reserving some of the available TSPs per node for C_h traffic and putting them on IDLE state, it is possible to satisfy both C_h and C_l connections set-up time requirements, and, at the same time reduce the power consumption of the network.

For instance, and utilizing a similar strategy to the described above, authors in [MPAS12] reported daily power savings around 56% with respect to traditional WDM network scenarios, while guaranteeing the set-up time requirements of both classes of connections. However, besides the power savings, the impact of such power management strategy on the blocking of the connections, e.g. due to the lack of available TSPs, specifically, lack of IDLE TSPs for C_h traffic and lack of OFF TSPs for C_l traffic has to be carefully evaluated. To this end, the following sub-section presents an analytical model to evaluate the blocking of connections and the potential power savings when the described power management strategy is employed.

5.2.1 A blocking analysis of sleep-mode enabled transport optical networks

In this sub-section, an analytical model for the evaluation of the blocking and power savings when adopting the power management strategy previously described is derived. Looking at the literature, only few papers have evaluated analytically the blocking of the connections on WDM networks where multiple classes of services are considered (e.g. [KL09, SS04, HMM98, WLWZ14, WLWZ13]). Additionally, the generic issue of resource reservation for C_h traffic has been addressed simulatively in some publications (e.g. [PCF04]), however, with no reference to the power consumption issue. Nevertheless, no paper has addressed the analytical evaluation of the blocking levels of the connections in the case some resources are reserved for C_h traffic and a TSP power management is used.

Moreover, a very important parameter to be evaluated is the wake-up time (transition from OFF to IDLE) of the TSPs, as it affects dramatically the overall blocking levels in a network, especially for C_h traffic. To put an example, following the previous described power management strategy, after a C_h has arrived to the network node, an IDLE TSP is activated to support the connection. In order to maintain the pool of reserved resources for C_h traffic, if there are spare OFF TSP, an OFF TSP wakes-up and is put on the IDLE state. However, depending on the duration of the wake-up time and the arrival rate of the connections, it may happen that $k-1$ C_h connections arrive at the node before the wake-up operation has ended. In such situation, all IDLE TSPs at the node become exhausted, so an incoming C_h connection will be blocked due to the lack of them. Figure 5.5 depicts an example of such phenomena. A potential way to overcome such situation may be to increase the pool of reserved resources for C_h traffic (the value of k), however, this results in an increase of the power consumption. Additionally, C_l traffic would face higher blocking levels as less resources can be exploited by it.

Therefore, the proper dimensioning of the number of TSPs to be put in the IDLE state is fundamental in order to achieve a good trade-off between blocking and power consumption. To analyze all these aspects, a novel Markov chain-based analysis is presented in order to quantify the blocking levels of the aforementioned power management strategy and the associated power savings with respect to a traditional WDM network scenario. Moreover, this analytical model provides guidelines on how to choose the optimal value of the reserved TSPs for C_h traffic depending on multiple parameters such as the load, the wake-up time of the TSPs and the number of wavelengths per link. To facilitate the comprehension of the analysis, it starts with a single network node case. Then, it introduces in the analysis the wake-up time parameter to derive its impact on the blocking and power savings. Finally, the analysis is extended to a whole network scenario.

Before detailing the analytical model, let us comment on the assumed network architecture. In the following model, a SLR network is considered, where TSPs operate at a single bit-rate (e.g. 100 Gb/s). In this context, a connection results from the aggregation at the

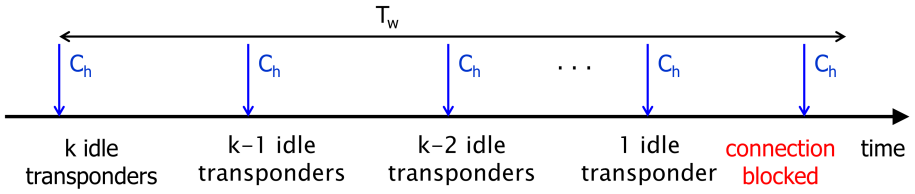

FIGURE 5.5: Example of blocking of C_h connections due to the influence of T_w.

source node from various client connections coming from an access/metro network which require the communication through a core network with a geographically distant node in the same destination access/metro network. Hence, the entire capacity of a wavelength is filled.

Additionally, it is assumed an opaque transport network, i.e., in every intermediate node an O-E-O conversion is performed (thus two WDM TSPs are employed for any link crossed by a lightpath). So every node is equipped with a pool of W TSPs on each incoming/outgoing link, which is considered as bi-directional. The analysis focus on this scenario:

1. as the bit-rate of demands and the use of more complex modulation formats increases, the reach of the connections is no longer compatible with optical paths but with links, hence transparent networks will be more and more difficult to realize [KDB11].
2. since client demands have smaller sizes with respect to such channel capacities, for better filling the tunnels electrical grooming will be required.
3. thanks to the O-E-O conversion, the wavelength continuity constraint can be relaxed and serve more connections with the available wavelengths' set (this situation tends to be preferable when the spectrum is scarce).

For all these reasons, the derivation of an analytical model for the opaque scenario is still worth and can rise the interest of the readers. Nonetheless, in [PTP+14] the performance of the presented power management strategy in translucent networks was evaluated, to which the interested reader can refer.

5.2.1.1 Single node model (without wake-up time)

In this first step, it is considered that the transition between the OFF and the IDLE state is instantaneous (wake-up time = 0). The main assumptions and variables considered are as stated below:

- Connections arrive at the node following a Poisson process. The mean arrival rates for C_h and C_l connections are denoted as λ_h and λ_l respectively.

- The duration of all the connections is assumed to be exponentially distributed with mean μ.
- The node is equipped with $N = (W \times \text{nodal degree})$ WDM TSPs.
- Among the TSPs in the node, k (maximum) are reserved for C_h connections and are put in IDLE state. If at least k TSPs are actually unused, *exactly* k TSPs are put in IDLE state. Otherwise, *all* unused TSPs are put in IDLE state and reserved for C_h connections.
- $\sigma_{x,y}$ represents the state in which the node has *exactly* x TSPs in OFF and y TSPs in IDLE. Note that the number of TSPs that are actually in ON can be calculated as $N - x - y$. Additionally, the probability of being in this state is defined as $\pi_{x,y}$.

With such a notation, the evolution of the power-state of the TSPs within the node can be represented as a time-homogeneous finite-space Markov chain. Figure 5.6 depicts the state diagram of the mentioned Markov chain, along with the blocking states for both classes of connections. Note that C_h connections only experience blocking when all the TSPs in the node are in use, while C_l connections experience blocking when no OFF TSPs are available (only IDLE TSPs are available).

Such Markov chain describes a birth-death process, for which the state probabilities can be obtained. For the sake of simplicity, s_i, $0 \leq i \leq N$ denotes the state where $N - i$ TSPs are in ON state, that is, i TSPs are currently unused, and with p_i the probability of such state. More specifically, s_i and p_i can be expressed as:

$$s_i = \begin{cases} \sigma_{0,i} & \text{if } 0 \leq i \leq k \\ \sigma_{i-k,k} & \text{if } k < i \leq N \end{cases} \Longrightarrow p_i = \begin{cases} \pi_{0,i} & \text{if } 0 \leq i \leq k \\ \pi_{i-k,k} & \text{if } k < i \leq N \end{cases} \tag{5.9}$$

Then the state probabilities can be evaluated as:

$$\begin{aligned} p_{N-1} &= \frac{\lambda_h + \lambda_l}{\mu} \cdot p_N \\ p_{N-2} &= \frac{\lambda_h + \lambda_l}{2\mu} \cdot p_{N-1} = \frac{(\lambda_h + \lambda_l)^2}{2\mu^2} \cdot p_N \\ &\dots \\ p_k &= \frac{(\lambda_h + \lambda_l)^{N-k}}{(N-k)!\mu^{N-k}} \cdot p_N \\ p_{k-1} &= \frac{(\lambda_h + \lambda_l)^{N-k}\lambda_h}{(N-k+1)!\mu^{N-k+1}} \cdot p_N \\ &\dots \\ p_0 &= \frac{(\lambda_h + \lambda_l)^{N-k}\lambda_h^k}{N!\mu^N} \cdot p_N \end{aligned} \tag{5.10}$$

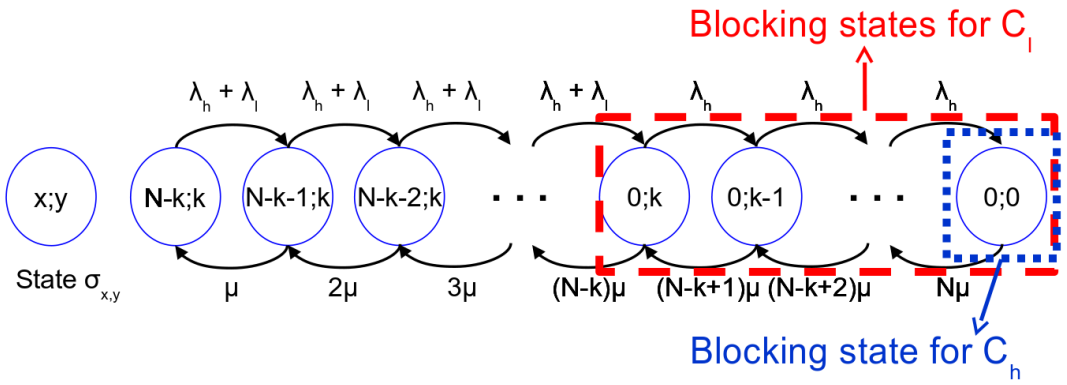

FIGURE 5.6: Markov chain for the single node model without wake-up time.

and can be rewritten in closed form as:

$$p_i = \begin{cases} \frac{(\lambda_h+\lambda_l)^{N-i}}{(N-i)!\mu^{N-i}} \cdot p_N & \text{if } k \leq i \leq N \\ \\ \frac{(\lambda_h+\lambda_l)^{N-k}\lambda_h^{k-i}}{(N-i)!\mu^{N-i}} \cdot p_N & \text{if } 0 \leq i \leq k-1 \end{cases} \tag{5.11}$$

It can be seen that the state probabilities depend on p_N, which can be computed as:

$$p_N = 1 - \sum_{i=0}^{N-1} p_i \tag{5.12}$$

Given the state probabilities computed using Equations (5.11) and (5.12), the blocking probabilities of both C_h and C_l traffic and the total blocking probability, (respectively $P_{b,h}$, $P_{b,l}$ and $P_{b,tot}$), can be evaluated as:

$$P_{b,h} = p_0 \qquad P_{b,l} = \sum_{i=0}^{k} p_i \qquad P_{b,tot} = h \cdot P_{b,h} + l \cdot P_{b,l} \tag{5.13}$$

where h and l denote the share of C_h and C_l connections, respectively ($0 \leq h, l \leq 1; h+l = 1$).

Moreover, the average power consumption in the node can be also estimated. Given the state probabilities, the average number of TSPs that are in IDLE and ON state, respectively, can be determined as the following, where $a \wedge b$ represents the minimum between two values:

$$\overline{TSP}_{idle} = \sum_{i=0}^{N} (i \wedge k) \cdot p_i \qquad \overline{TSP}_{on} = \sum_{i=0}^{N} (N-i) \cdot p_i \tag{5.14}$$

Using (5.14), the average power consumption of the node can be written as:

$$\bar{P}_{ower} = P_{idle} \cdot \overline{TSP}_{idle} + P_{on} \cdot \overline{TSP}_{on} \tag{5.15}$$

where P_{idle} and P_{on} are the power consumption of a TSP being on the IDLE and the ON state respectively.

5.2.1.2 Single node model (with wake-up time)

The previous model assumed that the transition between the OFF and the IDLE state is instantaneous. Actually, in a more realistic scenario, this transition time may not be negligible and its duration may impact the performance of the power-management strategy.

Indeed, every time an IDLE TSP is activated due to the arrival of a C_h connection, if there are spare OFF TSPs, an OFF TSP will be woken-up and put on IDLE. However, during a wake-up time (from now on referred as T_w), and depending on the value of k, it can happen that, at certain point, new C_h connections are blocked due to the lack of IDLE TSPs. To capture the influence of T_w on the BP and the average power consumption, the Markov chain presented in the previous section is generalized. To this end, in addition to the variables and definitions stated in the previous subsection:

- ω_t defines the frequency of waking-up a TSP, that is, $\omega_t = \frac{1}{T_w}$. Reviewing the literature, there is no work providing an analysis of the statistical distribution of the wake-up time of a sleep-enabled TSP. In such circumstances, it is assumed that the wake-up time follows an exponential distribution, since, in lack of further knowledge, it is the most conservative statistical distribution consistent with its mean value[PP02].
- Since circuit-switched networks, where connections typically have very long holding times, are the target of the study, it is assumed that T_w is much shorter than the average duration of the connections, that is, $T_w \ll \frac{1}{\mu}$. Conversely, $\mu \ll \omega_t$. Hence, in a realistic network scenario, the probability of a connection terminating during the duration of a wake-up operation is negligible and such transition is not considered in the current analysis. Nevertheless, the impact of this assumption on the estimation of the BP will be assessed later on during subsection 5.2.2.

Also in this case, the evolution of the power-state of the TSPs within the node can be described as a time-homogeneous finite-space Markov chain, with the difference that the introduction of the wake-up time variable leads to a bi-dimensional Markov chain. Additionally, in this case, a slightly different notation for the states and their probabilities

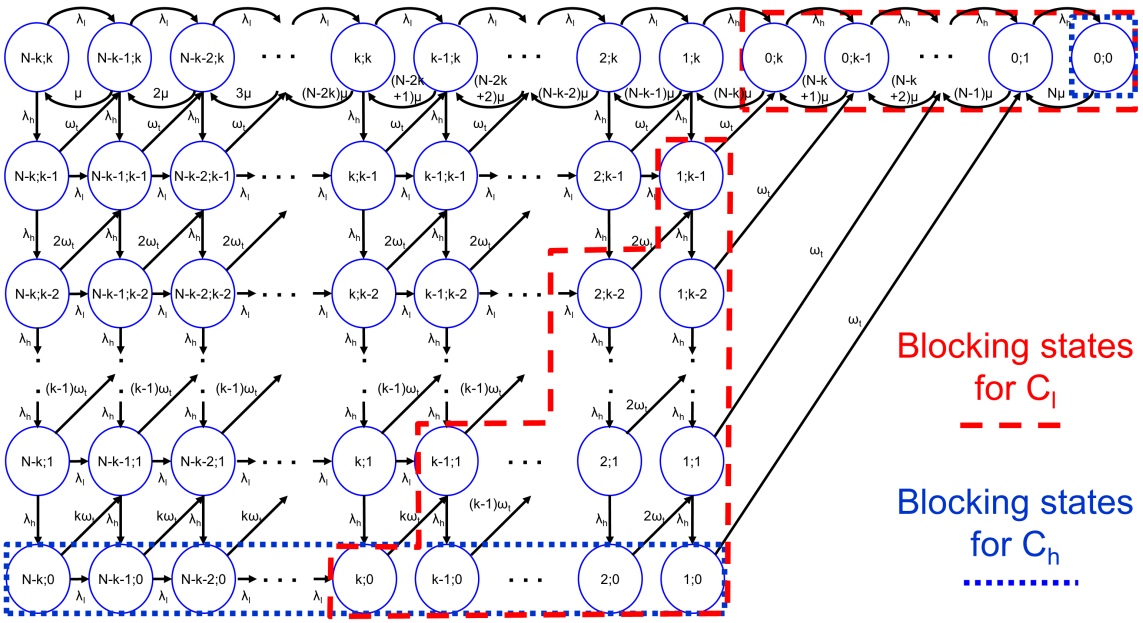

FIGURE 5.7: Markov chain for the single node model with wake-up time.

is followed. Due to the presence of TSPs that are operating a power transition from OFF to IDLE (wake-up operation), the state $\sigma_{x,y}$ now represents the state where the total number of OFF TSPs plus the ones waking-up is equal to x, while the total number of IDLE TSPs is equal to y. That is, the the right number represents the number of TSPs that are on IDLE, while the left number represents the summation of the TSPs that are in OFF state and the ones that are waking-up, i.e., performing a transition from OFF to IDLE. More specifically, the actual number of TSPs that are waking-up in every state is equal to $x \wedge (k-y)$ while the actual number of TSPs that remain in the OFF state is $x - [x \wedge (k-y)]$. For example, the first row of the first column represents the state where $N-k$ TSPs are on OFF, 0 are waking-up and k are on IDLE, while the last row of the first column represents the state where $N-2k$ TSPs are on OFF, k are waking-up and 0 are on IDLE. Also, note that in some states the maximum number of TSPs that are waking-up is not k but a number equal to all the OFF TSPs before a wake-up operation is triggered. For instance, all states from the 3rd to last row of the 6th column, represent the situation where 0 OFF and 2 waking-up TSPs are present, with the only difference between them being the number of IDLE TSPs (the value of y). Note that the use of two indexes is sufficient to represent all considered power states in the Markov chain, allowing us to formulate a more compact and concise analytical model than the one that would result if three indexes (OFF, waking-up and IDLE) were used.

Following this notation for the states, Figure 5.7 depicts the state diagram of the Markov chain, along with the blocking states for both classes of connections.

The first row of the Markov chain is the same as in the previous case, while the extra rows represent the states where an IDLE TSP has been used and an OFF TSP is waking-up. As before, C_h connections are blocked when all the TSPs on the node are used and C_l

connections are blocked when no OFF TSPs are available. However, now new blocking states appear for both classes due to the influence of T_w.

In the new blocking states for C_h (the ones in the lowest row of the chain), connections are blocked due to the exhaustion of IDLE TSPs due to multiple arrivals of C_h connections during a T_w. After a C_h connection arrives, whenever possible, a wake-up operation is performed in order to maintain a pool of k IDLE TSPs. If during this operation, $k-1$ C_h connections arrive to the node, all the IDLE TSPs will become exhausted, so the next C_h connections will be blocked, as already explained in 5.2.1.

As for C_l connections, the new blocking states are in the right diagonal part of the Markov chain. In those states, all the current OFF TSPs are operating a power transition from OFF to IDLE, hence, they are unavailable for C_l connections. Specifically, all OFF TSPs are operating a power transition in the states where $1 \leq x \leq k-y$; $0 \leq y \leq k-1$. When this happens, new incoming C_l connections are blocked since there are no OFF TSPs that can be used to set-up them. Note that in such states, the pool of IDLE TSPs after all wake-up operations have ended will not be equal to k but instead will be equal to $x+y$.

The state probabilities can now be calculated. For this, $p_{m,n}$ represents the probability of state $\sigma_{x,y}$ (for the sake of conciseness, only the final closed form of the probabilities will be depicted):

$$p_{m,n} = \begin{cases} \sum_{i=0}^{(N-k-1-m)\wedge k} \frac{\lambda^*_{m+1+i,k-i} \cdot p_{m+1+i,k-i}}{(N-k-m)\mu} & \text{if } 0 \leq m \leq N-k-1;\ n=k \\ \sum_{i=0}^{(N-k)\wedge(n+1)} \frac{\lambda^*_{i,n+1-i} \cdot p_{i,n+1-i}}{(N-n)\mu} & \text{if } m=0;\ 0 \leq n \leq k-1 \\ \frac{\lambda_h \cdot p_{N-k,n+1}}{(m\wedge(k-n))\cdot\omega_t + \lambda^*_{N-k,n}} & \text{if } m=N-k;\ 0 \leq n \leq k-1 \\ \frac{\lambda_h \cdot p_{m,n+1} + \lambda^*_{l;m+1,n} \cdot p_{m+1,n} + ((m+1)\wedge(k-n+1))\cdot\omega_t \cdot p_{m+1,n-1}}{(m\wedge(k-n))\cdot\omega_t + \lambda^*_{m,n}} & \text{if } 1 \leq m \leq N-k-1; \\ & \quad 1 \leq n \leq k-1 \\ \frac{\lambda_h \cdot p_{m,1} + \lambda^*_{m+1,0} \cdot p_{m,0}}{(m\wedge(k-n))\cdot\omega_t + \lambda^*_{m,0}} & \text{if } 1 \leq m \leq N-k-1;\ n=0 \end{cases} \tag{5.16}$$

with:

$$\lambda^*_{m,n} = \begin{cases} \lambda_h + \lambda_l & \text{if } k-n+1 \le m \le N-k;\ 1 \le n \le k \\ \lambda_h & \text{if } 0 \le m \le k-n;\ 1 \le n \le k \\ \lambda_l & \text{if } k+1 \le m \le N-k;\ n = 0 \\ 0 & \text{if } 0 \le m \le k;\ n = 0 \end{cases} \tag{5.17}$$

$$\lambda^*_{l;m,n} = \begin{cases} \lambda_l & \text{if } k-n+1 \le m \le N-k;\ 0 \le n \le k \\ 0 & \text{if } 0 \le m \le k-n;\ 0 \le n \le k \end{cases} \tag{5.18}$$

Essentially, the state probabilities in the first row depend on the previous state at their left and on all states diagonally reaching this left state. As for the states in the rest of the rows, their probabilities depend on all neighboring states that have an incident transition to that state. Additionally, as before, $p_{N-k,k}$ can be calculated as:

$$p_{N-k,k} = 1 - \sum_{m=0}^{N-k} \sum_{n=0}^{k-1} p_{m,n} - \sum_{m=0}^{N-k-1} p_{m,k} \tag{5.19}$$

With the values of the state probabilities computed using equations (5.16)–(5.19), the blocking probabilities of both C_h and C_l and the total blocking probability can now be calculated as:

$$P_{b,h} = \sum_{m=0}^{N-k} p_{m,0} \quad P_{b,l} = \sum_{m=0}^{k} \sum_{n=0}^{k-m} p_{m,n} \quad P_{b,tot} = h \cdot P_{b,h} + l \cdot P_{b,l} \tag{5.20}$$

Also, the average number of TSPs that are in IDLE ($\overline{TSP}_{idle}$), ON ($\overline{TSP}_{on}$) and the ones that are operating a power transition from OFF to IDLE ($\overline{TSP}_{trans}$) can be determined as:

$$\begin{aligned} \overline{TSP}_{idle} &= \sum_{m=0}^{N-k} \sum_{n=0}^{k} n \cdot p_{m,n} \\ \overline{TSP}_{on} &= \sum_{m=0}^{N-k} \sum_{n=0}^{k} (N-m-n) \cdot p_{m,n} \\ \overline{TSP}_{trans} &= \sum_{m=1}^{N-k} \sum_{n=0}^{k-1} (m \wedge (k-n)) \cdot p_{m,n} \end{aligned} \tag{5.21}$$

Using (5.21), the average power consumption of the node can be calculated, taking into account that current devices are capacitance-based and their power consumption can be

considered lineal. Hence, it is supposed that the average power during transitions can be calculated as half of the difference between the two states:

$$\bar{P}_{ower} = P_{idle} \cdot \overline{TSP}_{idle} + P_{on} \cdot \overline{TSP}_{on} + \frac{1}{2} P_{idle} \cdot \overline{TSP}_{trans} \tag{5.22}$$

5.2.1.3 Network-wide model

A more realistic scenario entails the analysis not only on a single node but on the whole network. In this case, the availability of the TSPs must be evaluated along the entire end-to-end path between source/destination nodes, where multiple connections interfere as they compete for the same resources.

To evaluate the BP in a network, the well-known method called reduced load Erlang fixed point approximation method is used [Gir90]. Due to the complexity of determining such analytical expressions, it is considered that *only the shortest-path route* can be exploited between a source and a destination nodes. This assumption is acceptable since the main purpose of the study is to provide an analytical model which is sufficiently accurate to evaluate the benefits of the TSP power management strategy and help to set the most effective number of IDLE TSPs per node when such strategy is employed (i.e., the value of k). The analysis of more complex scenarios is left for future work.

A first difference when compared to the single node case is that in the network model, the N parameter is no longer used. Instead, the total number of wavelengths per fiber link, denoted as W is used. Since an opaque network is being considered, every wavelength channel on a link entails the use of 2 TSPs, one at each end of a link. Moreover, k denotes the number of wavelengths that are being reserved for C_h connections, thus, equivalently, at every end of a link, k TSPs are being reserved for such connections. This means that, for a C_h connection to be routed, in every link that composes the end-to-end route, at least one wavelength has to be available, while for C_l connections to be routed, at least $k+1$ wavelengths have to be available.

Let us discuss in detail the analytical model for such scenario. It is based on the analytical approach presented in [SS04], for which the independence variation is utilized as a baseline of the presented work, since in an opaque network the load correlation introduced by the wavelength continuity constraint does not apply. First, the parameters and the corresponding definitions that will be used in the analysis are introduced:

- $G_n = (V, E)$ is the physical topology of the network, consisting of a set V of nodes and a set E of bi-directional links.
- R is the set of connection requests between source-destination pairs.
- r_{sd} defines the route from source node s to destination node d.

- H_{ij} and L_{ij} are the random variables which represent the number of wavelengths on link $(i,j) \in E$ that can be used to set-up C_h and C_l connections, respectively.

- $q^{ij}_{m,n}$ is the probability of having exactly a total of m wavelengths that their associated TSPs are on OFF (hence, usable by C_l connections) or performing a wake-up operation and a total of n wavelengths that their associated TSPs are on IDLE (hence, usable by C_h connections). Note that in the network-wide model the same notation to represent the state of a link as the one introduced during subsection 5.2.1.2 to represent the state of a node is followed. Note also that, with such notation, $H_{ij} = n$ while $L_{ij} = m - [m \wedge (k - n)]$.

- X_{sd} and Z_{sd} are the random variables which represent the number of wavelengths on the whole route between a source/destination pair $(s,d) \in R$ that can be used to set-up C_h and C_l connections, respectively.

- $\lambda_{h,sd}$ and $\lambda_{l,sd}$ are the base arrival rates of C_h and C_l connections between nodes s and d.

- $\alpha^{ij}_{m,n}$ is the connection arrival rate at link (i,j) given that the combination of wavelengths that are in the OFF state plus the ones that are in the "wake-up" state is *exactly* equal to m and and n wavelengths are in the IDLE state, with $\alpha^{h,ij}_{m,n}$ and $\alpha^{l,ij}_{m,n}$ the contributions for each kind of traffic. These variables are the so called state-dependent arrival rates [CKR93] and capture the influence of every connection on the others.

- $P_{b,sd}$ is the blocking probability for connections from s to d.

With such definitions, the availability of wavelengths over a particular link (i,j) can be represented employing the same Markov chain depicted in Figure 5.7, as the wavelengths in the links follow the same state transitions since their particular availability is strictly related to the availability of TSPs at nodes. Following this consideration, the equations used to compute the state probabilities in subsection 5.2.1.2 can be used now, with the proper variable substitutions: the probabilities $p_{n,m}$ are now substituted by $q^{ij}_{m,n}$, parameter N is now substituted by W and the arrival rates are no longer constant but they depend on the state of the link. This last aspect is the main difference in the network-wide model and is what has been defined as state-dependent arrivals, represented with variables $\alpha^{ij}_{m,n}$. Therefore, taking into account this consideration, and using the same analysis presented in section 5.2.1.2, the state probabilities (the q variables) for each one of the links (i,j) can be determined as:

$$q_{m,n}^{ij} = \begin{cases} \sum_{v=0}^{(W-k-1-m)\wedge k} \frac{\alpha_{m+1+v,k-v}^{ij} \cdot q_{m+1+v,k-v}^{ij}}{(W-k-m)\mu} & \text{if } 0 \le m \le W-k-1;\ n=k \\ \sum_{v=0}^{(W-k)\wedge(n+1)} \frac{\alpha_{v,n+1-v}^{ij} \cdot q_{v,n+1-v}^{ij}}{(W-n)\mu} & \text{if } m=0;\ 0 \le n \le k-1 \\ \frac{\alpha_{W-k,n+1}^{h,ij} \cdot q_{W-k,n+1}^{ij}}{(m\wedge(k-n))\cdot\omega_t + \alpha_{W-k,n}^{ij}} & \text{if } m=W-k;\ 0 \le n \le k-1 \\ \frac{\alpha_{m,n+1}^{h,ij} \cdot q_{m,n+1}^{ij} + \alpha_{m+1,n}^{l,ij} \cdot q_{m+1,n}^{ij} + ((m+1)\wedge(k-n+1))\cdot\omega_t \cdot q_{m+1,n-1}^{ij}}{(m\wedge(k-n))\cdot\omega_t + \alpha_{m,n}^{ij}} & \text{if } 1 \le m \le W-k-1;\ 1 \le n \le k-1 \\ \frac{\alpha_{m,1}^{h,ij} \cdot q_{m,1}^{ij} + \alpha_{m+1,0}^{ij} \cdot q_{m+1,0}^{ij}}{(m\wedge(k-n))\cdot\omega_t + \alpha_{m,0}^{ij}} & \text{if } 1 \le m \le W-k;\ n=0 \end{cases} \tag{5.23}$$

Similarly to the single node case, $q_{W-k,k}^{ij}$ can be calculated as:

$$q_{W-k,k}^{ij} = 1 - \sum_{m=0}^{W-k} \sum_{n=0}^{k-1} q_{m,n}^{ij} - \sum_{m=0}^{W-k-1} q_{m,k}^{ij} \tag{5.24}$$

Once the state probabilities for every link are known, the blocking for every connection belonging to R as can be calculated as:

$$P_{b,sd} = h \cdot (1 - Pr\{X_{sd} > 0\}) + l \cdot (1 - Pr\{Z_{sd} > 0\}) \tag{5.25}$$

The terms $Pr\{X_{sd} > 0\}$ and $Pr\{Z_{sd} > 0\}$, i.e., the probabilities of having enough resources along the end-to-end route to serve a C_h and a C_l connection, respectively, can be computed as the product of the probabilities of having enough resources in all links along the route, since it is necessary that all links from source to destination have enough free resources to serve the connections:

$$Pr\{X_{sd} > 0\} = \prod_{(i,j)\in r_{sd}} Pr\{H_{ij} > 0\} \qquad Pr\{Z_{sd} > 0\} = \prod_{(i,j)\in r_{sd}} Pr\{L_{ij} > 0\} \tag{5.26}$$

where $Pr\{H_{ij} > 0\}$ and $Pr\{L_{ij} > 0\}$ are the probabilities of having enough resources in the link (i,j) to serve a C_h and a C_l connection, respectively, and are obtained as follows considering the blocking states depicted in Figure 5.7:

$$Pr\{H_{ij} > 0\} = 1 - \sum_{m=0}^{W-k} q_{m,0}^{ij} \quad Pr\{L_{ij} > 0\} = 1 - \sum_{m=0}^{k} \sum_{n=0}^{k-m} q_{m,n}^{ij} \tag{5.27}$$

Hence, the blocking probability in the network can be evaluated as:

$$P_{b,tot} = \sum_{(s,d)\in R} t_{sd} P_{b,sd} \tag{5.28}$$

where t_{sd} represents the share of traffic from s to d respect the total traffic in the network.

The average power consumption in the network can be estimated following the same method as in the single node case:

$$\begin{aligned}
\overline{TSP}_{ij,idle} &= 2 \cdot \sum_{m=0}^{W-k} \sum_{n=0}^{k} n \cdot q_{m,n}^{ij} \\
\overline{TSP}_{ij,on} &= 2 \cdot \sum_{m=0}^{W-k} \sum_{n=0}^{k} (W - m - n) \cdot q_{m,n}^{ij} \\
\overline{TSP}_{ij,trans} &= 2 \cdot \sum_{m=1}^{W-k} \sum_{n=0}^{k-1} (m \wedge (k - n)) \cdot q_{m,n}^{ij} \\
\bar{P}_{ower} &= \sum_{(i,j)\in E} (P_{idle} \cdot \overline{TSP}_{ij,idle} + P_{on} \cdot \overline{TSP}_{ij,on} + \frac{1}{2} P_{idle} \cdot \overline{TSP}_{ij,trans})
\end{aligned} \tag{5.29}$$

where the factor 2 is due to the fact that each link entails the use of a TSP on each side of the link.

However, in the previous analysis, the state probabilities depend on the state-dependent arrival rates, which have to be still evaluated. The process to evaluate them is an iterative process, which involves knowing the blocking on each link, and the steps are as follows. Denoting as $\alpha_{m,n}^{sd,ij}$ the arrival rate of connections $(s,d) \in R$ at link (i,j) given that the combination of wavelengths that are in the OFF state plus the ones that are in the "wake-up" state is *exactly* equal to m and n wavelengths are in the IDLE state, its value is as follows:

$$\alpha_{m,n}^{sd,ij} = \begin{cases} 0 \quad \text{if } 0 \le m \le k;\ n = 0 \\ \lambda_{h,sd} \cdot Pr\{X_{sd} > 0 | L_{ij} = m - [m \wedge (k-n)];\ H_{ij} = n\} \quad \text{if } 0 \le m \le k-n;\ 1 \le n \le k \\ \lambda_{l,sd} \cdot Pr\{Z_{sd} > 0 | L_{ij} = m - [m \wedge (k-n)];\ H_{ij} = n\} \quad \text{if } k+1 \le m \le W-k;\ n = 0 \\ (\lambda_{h,sd} + \lambda_{l,sd}) \cdot Pr\{X_{sd} > 0; Z_{sd} > 0 | L_{ij} = m - [m \wedge (k-n)];\ H_{ij} = n\} \\ \qquad \text{if } k-n+1 \le m \le W-k;\ 1 \le n \le k \end{cases} \tag{5.30}$$

The probability terms in (5.30) are computed taking into account the availability of resources on all links along the end-to-end route. Hence, it is necessary to consider the probability of the states that have at least some resources to allow the establishment of C_h, C_l or both types of connections. The resulting equations are:

$$Pr\{X_{sd} > 0 | L_{ij} = m - [m \wedge (k-n)];\ H_{ij} = n\} = \prod_{\substack{(x,y) \in r_{sd} \\ (x,y) \neq (i,j)}} (1 - \sum_{u=0}^{W-k} q_{u,0}^{xy}) \tag{5.31}$$

if $0 \le m \le k-n;\ 1 \le n \le k$

$$Pr\{Z_{sd} > 0 | L_{ij} = m - [m \wedge (k-n)];\ H_{ij} = n\} = \prod_{\substack{(x,y) \in r_{sd} \\ (x,y) \neq (i,j)}} (1 - \sum_{u=0}^{k} \sum_{v=0}^{k-u} q_{u,v}^{xy}) \tag{5.32}$$

if $k+1 \le m \le W-k;\ n = 0$

$$Pr\{X_{sd} > 0; Z_{sd} > 0 | L_{ij} = m - [m \wedge (k-n)];\ H_{ij} = n\} = \prod_{\substack{(x,y) \in r_{sd} \\ (x,y) \neq (i,j)}} (1 - \sum_{u=0}^{W-k} q_{u,0}^{xy} - \\ - \sum_{u=0}^{k} \sum_{v=0}^{k-u} q_{u,v}^{xy}) \quad \text{if } k-n+1 \le m \le W-k;\ 1 \le n \le k \tag{5.33}$$

Therefore, using equations (5.30)–(5.33), the new value of the state-dependent arrival rates can be computed as the summation of all traffic that goes through link (i,j):

$$\alpha_{m,n}^{ij} = \sum_{\substack{(s,d):\\ (i,j)\in r_{sd}}} \alpha_{m,n}^{sd,ij} \tag{5.34}$$

Once all involved variables have been correctly evaluated, the blocking levels in the network can be determined through an iterative process. Firstly, by setting the state-dependent arrivals to an initial value, the blocking on each link can be obtained. When determined, it will be used to calculate the value of the state-dependent arrivals for the next iteration, which, in turn, will allow us to evaluate the blocking in each link for the next iteration and so on. Through this process, the BP for all pairs $(s,\, d) \in R$ can be iteratively calculated until a desired maximum error ϵ between two consecutive iterations is achieved. This maximum error is used to decide when the iterative process has converged and the obtained BP has reached a steady value, so further iterations would not change significantly the obtained value. Note that if a high value of ϵ is chosen, it may happen that the iterative process terminates before a sufficient number of iterations have been executed, so the obtained value could be far from the real BP. Hence, to obtain accurate results, a sufficiently small value of ϵ has to be chosen. The steps of the calculation are the followings:

1. Set the value of the maximum allowed error between two consecutive iterations (e.g., $\epsilon = 10^{-6}$). Initialize the *estimated* blocking probability, for every pair $(s,d) \in R$, to zero, i.e., $\hat{P}_{b,sd} = 0, \forall (s,d) \in R$. For all links $(i,j) \in E$ initialize the state-dependent arrival rates as:

$$\alpha_{m,n}^{sd,ij} = \begin{cases} 0 \quad \text{if } 0 \le m \le k;\ n = 0 \\ \displaystyle\sum_{\substack{(s,d):\\ (i,j)\in(s,d)}} \lambda_{h,sd} \quad \text{if } 0 \le m \le k-n;\ 1 \le n \le k \\ \displaystyle\sum_{\substack{(s,d):\\ (i,j)\in(s,d)}} \lambda_{l,sd} \quad \text{if } k+1 \le m \le W-k;\ n = 0 \\ \displaystyle\sum_{\substack{(s,d):\\ (i,j)\in(s,d)}} (\lambda_{h,sd} + \lambda_{l,sd}) \quad \text{if } k-n+1 \le m \le W-k;\ 1 \le n \le k \end{cases} \tag{5.35}$$

2. Compute the state probabilities for every link using Eqs. (5.23)–(5.24).

3. Calculate the state-dependent arrival rates for all links according to Eqs. (5.30)–(5.34).

4. Compute, for every couple $(s,d) \in R$, the blocking probability $P_{b,sd}$ using Eqs. (5.25)–(5.27). If $max_{(s,d)}|P_{b,sd} - \hat{P}_{b,sd}| < \epsilon$ then terminate and evaluate the total blocking and average power consumption according to (5.28) and (5.29), respectively. Otherwise, set $\hat{P}_{b,sd} = P_{b,sd}$ and go back to step 2.

5.2.2 Numerical results

In this section, the proposed power management strategy is being evaluated through a set of numerical results utilizing the aforementioned described analytical model. All the results in this section have been obtained using the COST239 network topology (11 nodes and 26 bidirectional links) (see Appendix A). It is assumed that all the traffic is uniformly distributed among all pairs (s,d). Additionally, it is assumed that the average duration of the connections is equal to 1, i.e. $\mu = 1$, hence the load is equal to the average arrival rate of connections to the network λ, with $\lambda_{sd} = \lambda/|R|\ \forall (s,d) \in R$.

Different scenarios have been evaluated, where the number of TSPs reserved for C_h connections (k) is varied. Moreover, also the percentages of C_h and C_l connections over the total are varied. Note that varying these percentages has a direct effect on the values of the base arrival rates λ_h and λ_l, i.e., given the overall connection arrival rate $\lambda = \lambda_h + \lambda_l$, the values of λ_h and λ_l can be determined considering that $h + l = 1$, $h = \lambda_h/\lambda$ and $l = \lambda_l/\lambda$. Additionally, multiple scenarios with different values of T_w (conversely ω_t) have been evaluated. In all tests, the value of ϵ has been set to 10^{-12}. Additionally, the TSPs power consumption has been set to $P_{on} = 351$ W and $P_{idle} = 18$ W for as in [MSR+11].

Figure 5.8.a shows, for increasing values of the network load, the total BP with $h = l = 0.5$, $W = 32$ and $T_w = 1$ ms ($\omega_t = 1000$). Additionally, in order to check the accuracy of the analytical model, some simulations using an event-driven simulator considering the same power management strategy and network scenario as in the analytical model has been also performed. All the simulations have been performed considering $4 \cdot 10^6$ connection arrivals to the network. All simulation results have been obtained with 95% confidence intervals lower than one order of magnitude respect the average value (the size of the confidence interval is around a relative 2.8% in the worst case and around a relative 1% in average), assuring the statistical accuracy of the presented results. In addition to various values of k, two special cases as benchmarks have been tested, namely:

- all TSPs are powered-on, that is, any TSP can be used by either C_h or C_l connections ("All-On" in the figures).
- unused TSPs are powered-off, that is, no TSPs are set in IDLE state, hence, *all* the C_h connections are blocked, so the available capacity is completely exploited by C_l connections ("k = 0" in the figures).

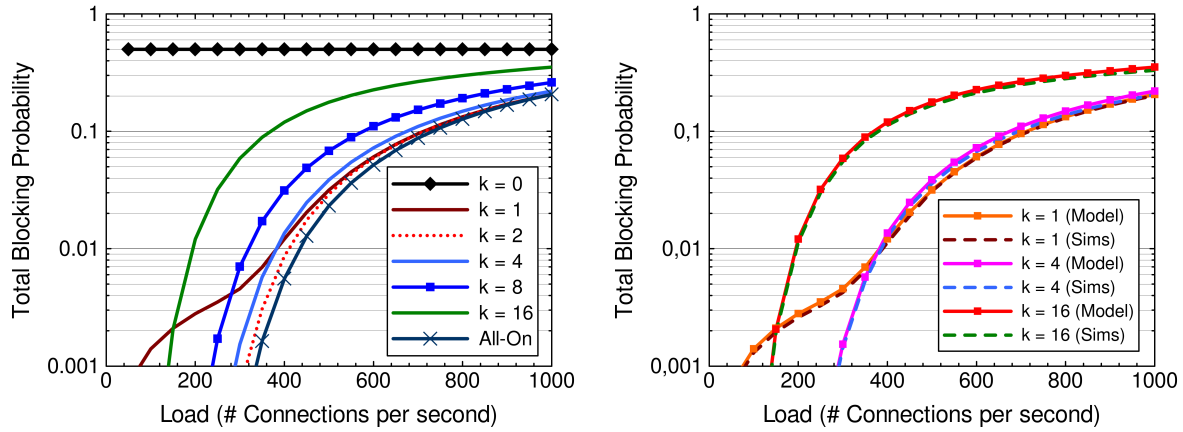

FIGURE 5.8: a) Blocking probability as a function of the load for the analytical model; b) Comparison between analytical model and simulations.

In Figure 5.8.a, it can be seen that for low values of k, almost no performance degradation is experienced in terms of BP, while appreciable performance degradations arise for $k \geq 8$. However, if we observe the case $k = 1$, a sudden degradation of the BP for low loads can be observed. Such degradation is due to the influence of the wake-up time and will be commented in details later on. Additionally, it can be appreciated that the differences between the analytical model and the simulations are very small (less than a relative 3% deviation) with almost identical blocking figures (Figure 5.8.b). Such differences arise from the fact that the analytical model does not take into account the possibility of connections terminating during a wake-up operation, while such transitions are present in the simulations. Note, however, that from the depicted results, the impact of this assumption is very small, demonstrating the correctness and accuracy of the analytical model. As for the BP of the two different classes, the general trend is that the BP of the C_h traffic decreases with increasing values of k while the BP of C_l traffic increases. This is due to the fact that higher values of k imply that more TSPs are put on idle and reserved for C_h traffic, so less resources can be exploited by C_l traffic. As an example, taking a load equal to 300, for $k = 1$, the blocking of C_h and C_l traffic are 0.85% and 0.06%, respectively, while for $k = 2$ they are 0.01% and 0.12% and for $k = 4$ they are 0.00185% and 0.31%.

Aside from the BP of the connections, the average and the normalized power consumption for the analytical model has been also evaluated. The normalized power consumption is computed as:

$$normalized\ power = \frac{total\ power}{n.\ of\ connections \cdot (1 - P_b)} \tag{5.36}$$

In Figure 5.9.a, it can be observed that power savings of at least 32% can be obtained by setting some resources in IDLE state with respect to the All-On scenario. Moreover, huge

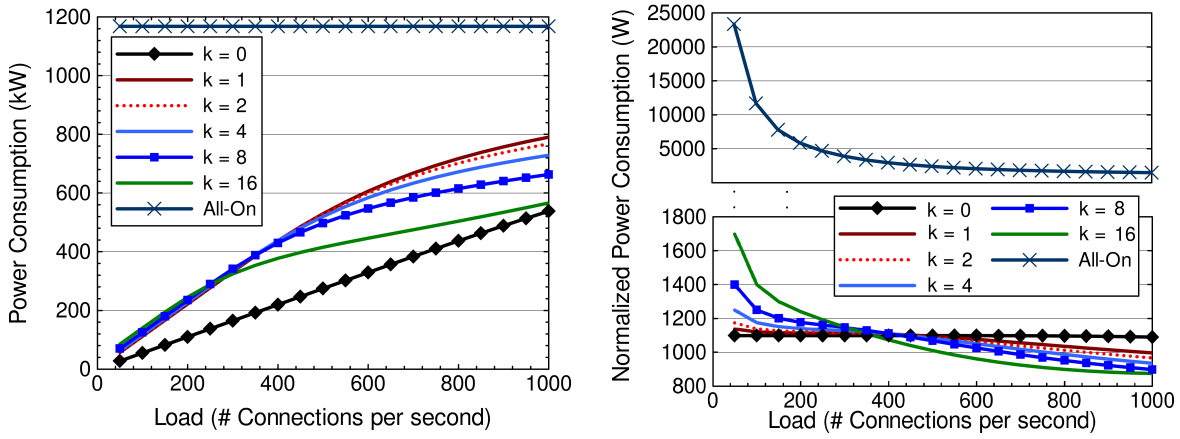

FIGURE 5.9: a) Average power consumption and b) normalized power consumption as a function of the load for the analytical model.

savings, around 80%, are observed for lower loads and for all the values of k. The impact of k becomes relevant for higher loads, when reserving more resources for C_h connections affects the power consumption values, mainly due to the fact that higher blocking is experienced for increasing k, as more C_h are being blocked.

In order to remove the influence of blocking from the power consumption results, the normalized power metric has been introduced (Figure 5.9.b). It can be observed that, when the blocking is negligible, the power consumption increases with k, as more unused resources are maintained in IDLE state unnecessarily. On the other hand, for increasing loads, the normalized power consumption decreases more rapidly for higher values of k. This is due to the fact that, for higher values of k, blocking mainly occurs for multiple-hops connections, as the chances of having enough available TSPs in every hop decrease with the length of the path. Thus, the connections accepted for higher k are typically single-hop and consume less power than those accepted for lower values of k.

Now, let us analyze the influence of the wake-up time on the blocking levels of the network. Although, as mentioned before, low values of k do not entail significant performance degradations in terms of blocking, in Figure 5.8.a a sudden degradation in the $k = 1$ (for loads below 300 Erlangs) performance can be observed. This is an effect of the wake-up time of the TSPs. To further investigate this effect, additional experiments focusing on the case $k = 1$ have been performed. Figure 5.10 depicts the BP as a function of the load for various values of T_w. Moreover, the case where the T_w is not considered, as presented in [MTRP13], is also plotted ("No T_w").

As expected, the value of the T_w has a substantial impact on the BP. Blocking increases for increasing values of T_w. This is due to the effect mentioned in section 5.2.1: after an IDLE TSP is used, and if there are still spare OFF TSPs, a wake-up operation is performed in order to maintain the pool of k IDLE TSPs; if during this wake-up operation, $k - 1$ C_h

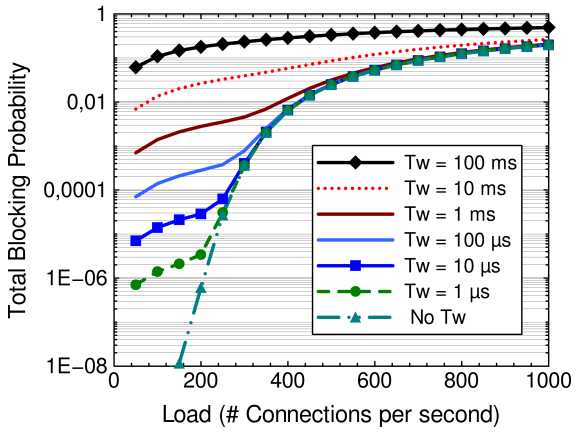

FIGURE 5.10: Blocking probability as a function of the load for varying values of T_w ($k = 1$) for the analytical model

.

connections arrive, all the IDLE TSPs will become exhausted, so the next C_h connections will be blocked. Intuitively, this situation is more likely to happen for longer T_w. In fact Figure 5.10 shows that higher values of T_w increase substantially the levels of blocking while for low values, its effect is almost negligible. Note also that for low loads, curves change their concavity. This can be explained as, for low loads, the main component of the blocking is the lack of IDLE TSPs during wake-up times, while for increasing loads, as connections start to compete with each other, the main component of the blocking is the lack of free resources. As for the case where the T_w is neglected, it can be seen that, indeed, not considering its influence can lead to substantial differences in the values of P_b when the load is small.

In light of the results these results, it is clear that the correct dimensioning of k to obtain a certain network performance (say, $P_b \leq 5\%$) depends highly on the value of T_w as well as on the share of C_h connections (since they are the connections that are affected by the wake-up time). To this end, additional studies where, for various values of T_w and h, the value of k has been varied in order to determine the most appropriate value of k to achieve a blocking not greater than 5% for a reference load of 500 Erlangs have been conducted. The obtained results are depicted in Figure 5.11, where the black solid line marks the aforementioned threshold for the P_b.

It can be seen that for the selected load, even for low shares of C_h traffic, it is not possible to fulfill a 5% threshold on the P_b with a wake-up time of 100 ms, as it is still too long to avoid the lack of TSPs during a T_w. In this case, it would be necessary to dimension the network for another working load (e.g. by increasing the number of wavelengths per link) or employ other technologies for the TSPs that allow lower wake-up times. It can be seen that, if the wake-up time is lower (e.g. 10 ms), as the share of C_h connections increases, it is necessary to reserve more IDLE TSPs, e.g. $k = 1$ for $h = 0.2$, $k = 2$ for $h = 0.5$ and $k = 3$ for $h = 0.8$. Moreover, it can be appreciated that, for increasing values of h the P_b curves have a minimum. This is due to the fact that, as the value of k increases, the

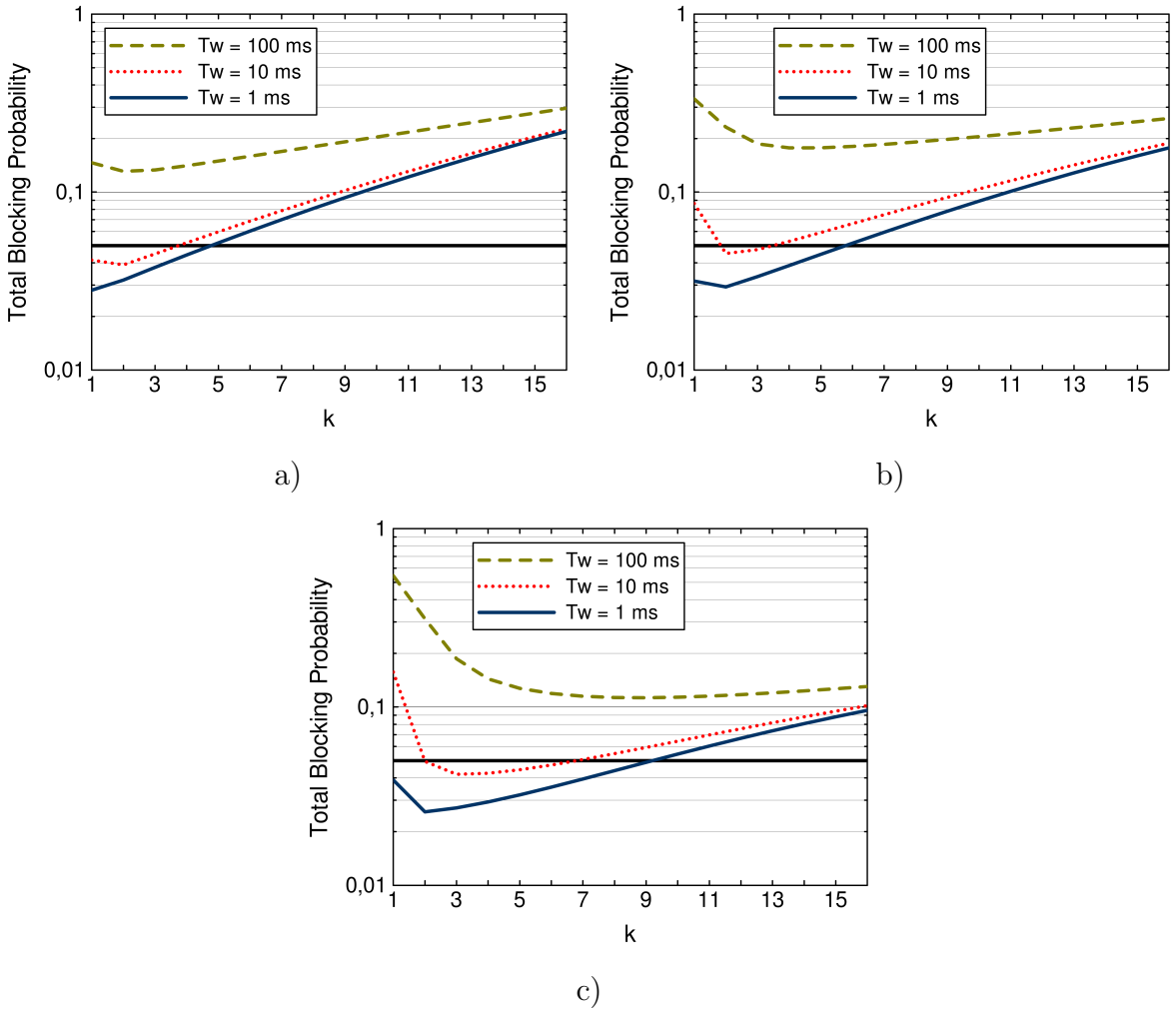

FIGURE 5.11: Total blocking probability as a function of k for various values of T_w in a network scenario with 32 wavelengths per link for the analytical model: a) $h = 0.2$, b) $h = 0.5$ and c) $h = 0.8$.

blocking due to the lack of IDLE TSPs decreases but, at the same time, the blocking due to lack of resources for C_l connections increases, as less and less resources can be used by them.

5.3 Chapter summary

Optical transport networks have helped reducing the power consumption by allowing large amounts of traffic to bypass core routers through optical switching. However, as the traffic on Internet grows, it is forecast that the energy consumption on transport networks will increase substantially during the following years. For this reason, energy efficiency has been widely recognized as an important target in the management of optical WDM networks and several research efforts have been focused on developing energy-efficient devices and network management strategies in order to reduce the energy consumption

on optical networks. Additionally, in the context of VONs a more energy efficient physical substrate arises of paramount importance in order to provide the future optical network architecture. With less power hungry network substrates, it is possible to deploy VONs that consume less energy, keeping the associated OPEX low.

For all these reasons, the current chapter has focused on providing solutions to reduce the energy consumption on transport optical networks so a more efficient environment can be achieved for the deployment of VONs. To this end, section 1 has focused on providing an end-to-end routing solution for multi-domain transport networks, with the objective to reduce the energy consumption associated to the establishment of connections and, at the same time, distribute the load on the network so the BP of the connections is kept low. The presented solution has been exhaustively tested in multiple scenarios and compared to simpler SP-based routing mechanisms. The results obtained show that it allows for a greater reduction on the energy consumption of the connections while still keeping the BP of the connections low.

However, energy-aware routing algorithms are not enough to reduce the energy consumption in transport optical networks, since the overall energy consumption is tightly related to the underlying physical equipment. For this reason, it is necessary to develop more energy efficient physical devices in order to further reduce the energy consumption in transport optical networks. To this end, section 2 has introduced the concept of sleep-enabled transport networks, where TSPs can be put on a low power consumption mode (called idle) when not in operation and still be powered on in few ms. when needed. However, the use of such sleep-enabled devices in the presence of multiple classes of connections may impact severely the overall performance of the network depending on the time needed to put a device in this idle state when powered-off. For this reason, a Markov-based analytical model have been presented in order to asses the impact of this transition on the network performance (i.e. the BP of the connections) and predict the energy savings that can be achieved with such physical devices. The presented analytical model has been throughly tested under multiple conditions. The obtained results showed that, indeed, a non-negligible transition from the off to the idle state can augment several orders of magnitude the BP probability of the connections. However, if a proper dimensioning of the physical devices is done, such effect can be compensated and significant reductions on the energy consumption can be achieved.

Chapter 6

Conclusions and future work

Virtual Optical Networks reveal themselves as a very interesting option to overcome the limitations of nowadays optical network architectures. Thanks to the possibility to fully manage the underlying physical resources associated to the VN, network operators can adjust the characteristics of the network to the requirements of the applications and services that will run on top of it in a cost effective way. Furthermore, thanks to the coexistence of multiple VONs in the same physical substrate, it becomes possible to build multiple mission-specific VIs effectively broadening the range of offered services and business opportunities. On this basis, the present thesis identifies and addresses resource management and efficiency issues in VONs. The overall goal of this study is optimized, flexible and efficient VON composition and operation.

To contextualize the chapters to come, chapter 2 surveyed current optical network infrastructures, leading to conclude on the necessity to provide a more flexible and efficient network infrastructure. To this end, special attention was paid to the concept of IaaS and VONs as a mean to achieve this concept. Therefore, VONs become the central framework for the contributions of the thesis. Nevertheless, as a mean to optimize the performance of VONs in terms of spectrum utilization Elastic Optical Networks were introduced. In this regard, the evolution from WDM-based optical networks to EONs was surveyed, putting special emphasis on the benefits but also the challenges that EONs introduce on the arena. Finally, in order to deploy more cost efficient VONs, the concept of energy efficiency in optical networks was introduced. These three key aspects (VONs, EONs and energy efficiency) were discussed in details during the following chapter, as well as solutions to specific problems regarding the topics.

For better VON resource allocation, chapter 3 dealt with the virtual network embedding problem in optical network substrates. To this end, firstly the concept of VNE was introduced, along with the major work present in the literature regarding the topic. Next, the concept was extended to optical network physical substrates and VONs under the name of VONA problem. In this regard, it was found that several challenges arise due to the nature of the optical media when compared to Layer 2/3 electrical networks, such

as IP networks, and specific algorithms have to be designed to properly map the virtual resources to physical one. In particular it was revealed that the VONA problem is highly dependent on the technology employed by the underlying physical substrate as well as the nature of the services that are intended to be offered on top of the VON. In order to address such particularities, mechanisms to optimally embed the VONs were designed and tested. First, the concept of transparent and opaque VONs was presented, assessing that the complexity of the VONA problem increases in the case where transparent VONs are considered. Additionally, it was showed that optimal embedding mechanisms can achieve substantial gains in terms of number of successfully embedded VONs when compared to simpler SP-based techniques. Next, it was studied how the VONA problem can be addressed if an EON physical substrate is considered and compared the process against a WDM-based physical substrate. From the results, EON-based physical substrates outperformed WDM-based substrates in terms of number of VONs that can be allocated ton top of them. For chapter completion, specific mechanisms to perform the embedding of VONs in dynamic scenarios or in the presence of also IT resources in the physical substrate were proposed. The evaluation of the solutions revealed that an optimal VON embedding becomes a key factor in order to maximize the utilization of the physical substrate.

Chapter 4 focused on improving the spectrum utilization in EONs. This become of crucial importance when considering a EON-based physical substrate for the composition of VONs. One of the limiting factors in EONs is the spectrum fragmentation effect, which complicates the establishment of connections, specially the one requiring high bit-rates. Hence techniques to mitigate such pernicious effect were introduced in the literature. After surveying the main work regarding the topic, the Split Spectrum approach was presented as an alternative way to deal with the spectrum fragmentation effect. However, the resource allocation in SS-enabled EONs becomes further complicated due to the splitting process that some demands may undergo in order to better fit on the available spectral resources. For efficient resource allocation in SS-enabled EONs, multiple mechanisms were introduced, starting from a simpler approach towards more sophisticated ones, accounting for the particularities and challenges that the SSA poses. From the results, it was found that SS-enabled EONs allow reductions on the BP of the connections around one order of magnitude for low loads and up to around 40-50% for higher loads. Interestingly, it was found that high bit-rate connections were the ones experiencing the greater benefits while low bit-rate connections were not heavily affected to this increment on the number of successfully established high bit-rate connections. To complete the study, two possible TSP implementations of the SSA were compared, namely BV-TSPs and MF-TSPs. In this regard, it was found that, even though a MF-TSP allows to serve a split demand utilizing a unique physical device, because in normal network conditions the splitting was infrequent, it was usually more beneficial to deploy an over-provisioned number of BV-TSPs.

Finally, chapter 5 concentrated on providing and analysing solutions to reduce the energy consumption in transport optical networks. First, an end-to-end energy-aware routing

mechanism for multi-domain optical networks was introduced. The solution was composed by an inter-domain abstract topology design mechanism as well as an inter-domain routing mechanisms. Through extensive simulations, it was shown that the presented mechanism allows to reduce the power consumption associated to successfully established connections to a great extent (almost 90% for low loads) while still providing significant BP reductions when compared against simpler SP-based routing techniques. As a second step to reduce the energy consumption on transport networks, the concept of sleep-enabled optical networks was introduced. In this regard, in order to evaluate the power savings and the BP of the connections in a multi-class scenario where high- and low-priority connections coexist, a Markov-based analytical model was presented. Through the use of the presented analytical model, it was found that sleep-enabled transport networks yield to substantial energy savings when compared against traditional WDM optical networks. Particularly, reductions up to 80% and at least around 32% were found for low and high loads, respectively. However, the introduction of sleep-enabled devices in the network may increase the BP of connections, specially for high-priority ones, due to the non-negligible wake-up time. Indeed, it was found that, if not correctly dimensioned, even for low wake-up times (e.g. 100 ms), several orders of magnitude degradations may happen in terms of BP in the network. In this regard, it becomes crucial to properly dimension the optical network according to the load, the duration of the wake-up time and the share of high- and low-priority traffic. The presented analytical model was showed to be a sufficiently accurate tool to give guidelines on how to perform such dimensioning.

Further work may follow the multiple lines of research initiated in this thesis. Concerning the VONA problem introduced on chapter 3, the solutions presented could be enhanced in order to consider a physical substrate based on SS-enabled EONs as well as the introduction of energy-efficient devices and algorithms. In this regard, it would be mandatory to design heuristic mechanisms to target the problem since the complexity of the embedding mechanism considering both the SSA and energy-efficient optical substrates would increase the complexity of the problem notoriously. Another line of future work could focus on further developing the studies done regarding the composition of VIs requiring both network and IT resources. Focusing on the work regarding the SSA presented in chapter 4, the work described has focused on the performance analysis of SS-enabled EONs against more traditional EONs. A possible way to complement the presented studies would be to compare the performance of the SSA against defragmentation mechanisms or fragmentation-aware resource assignment solutions present in the literature so as to identify better the advantages and drawbacks of each kind of approach. Additionally, the allocation of the most suitable guard band between demands could be introduced as a problem decision since the presence of multiple bit-rates on the network allows form some optimization in this regard. Lastly, regarding the solutions for energy-efficient transport optical networks presented in chapter 5, specially the work regarding sleep-enabled optical networks, other network architectures and routing policies could be introduced in the analysis. Particularly, the design of an analytical model for sleep-enabled translucent

and transparent optical networks could be of great interest in order to analyse the differences in their performance between the three types of optical networks, namely, opaque, translucent and transparent, when sleep-enabled optical devices are introduced.

Appendix A

Reference transport network scenarios

Various topologies present in the literature have been used as test networks throughout this thesis. This appendix introduces each network topology under consideration together with its main topological characteristics. Additionally, cross-references to the sections and sub-sections where each network is used are provided.

A.1 16-Node European Optical Network (EON) core topology

The EON network topology has been widely used in optical networking scientific literature. It came up as one of the main achievements of the COST 266 and Lion European Projects [IKM+03, MCL+03] and was designed as a reference topology for a pan-European fiber-optic transport network. It consisted in 28 nodes placed in major European cities connected with fiber links between them. To cover different network situations, three main configurations were specified, namely basic (41 links), sparse ring (33 links) and densely-meshed triangular (61 links) configurations. Departing from this 28-Node EON network topology, a simplified version of the network was also introduced, compromising only the core part of the network. This resulted in a 16-Node network topology (Figure A.1). In such network, the 16 nodes were connected employing 23 links, resulting in an average Nodal Degree (ND) of 2.875. This topology has been used in VON embedding simulation results presented in subsections 3.2, 3.3 and 3.4 as well as in SS simulation results presented in subsections 4.3 and 4.4.

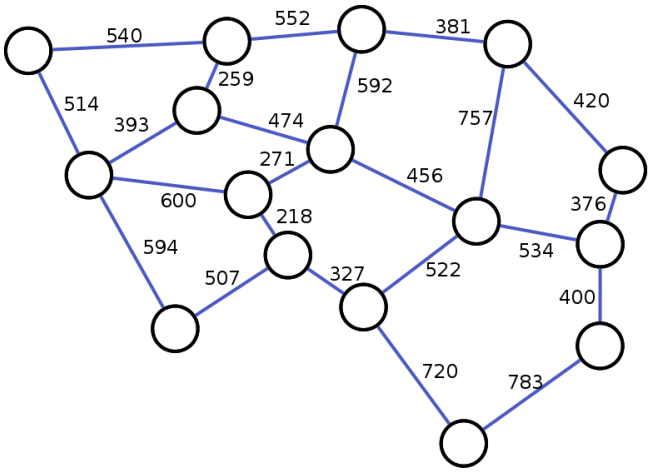

FIGURE A.1: 16-Node EON core topology. Link distances are in km.

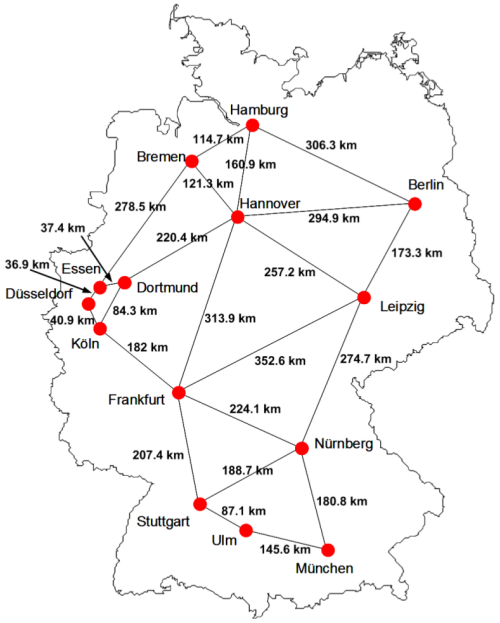

FIGURE A.2: DT transport network topology.

A.2 Deutsche Telekom (DT) transport network

Various network topologies depicting transport networks owned by real network operators are commonly used in the literature, being the DT transport network topology one of them (e.g. [AAA+10]). It consists on 14 nodes interconnected employing 23 links (Figure A.2), resulting in an average ND of 3.286. This topology has been used in VON embedding simulation results presented in subsection 3.4 and in SS simulation results presented in subsections 4.3 and 4.4.

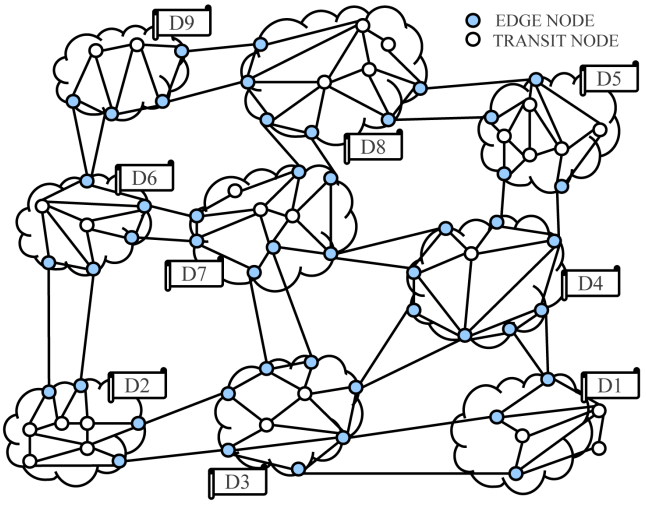

FIGURE A.3: Multi-domain reference network topology.

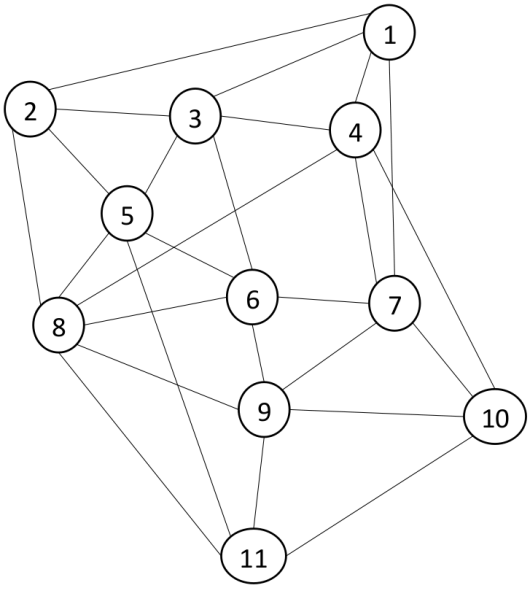

FIGURE A.4: COST 239 network topology.

A.3 Multi-domain reference network topology

To validate integrated solutions for multi-domain optical networks, the European Project STRONGEST has defined a reference multi-domain network topology [STR10], which consists of 75 nodes (48 BNs and 27 non-BNs) distributed in 9 different domains (Figure A.3). The nodes are interconnected through a set of 146 links (26 inter-domain and 120 intra-domain). This multi-domain network topology here presented has been used in subsection 5.1 to test various proposal of energy-aware routing algorithms in optical networks.

A.4 COST 239 network topology

The objective of COST 239 (Ultra-High Capacity Optical Transmission Networks) project was to evaluate the feasibility of an optical overlay network interconnecting major cities within Europe. As one of the outcomes, the COST 239 reference network topology was defined [Bat99]. It consisted of 11 nodes interconnected through 26 links (Figure A.4), resulting in an average ND of 4.73. The evaluation of the analytical model for energy efficient networks presented in subsection 5.2 has been done employing this presented network topology.

Appendix B

Multi-domain WSONs reference architecture

This appendix introduces the network architecture assumed during subsection 5.1 in order to test the presented energy-aware routing solution for multi-domain transport networks. Additionally, some related work regarding the topic is commented in order to better contextualize the use of the proposed solution in 5.1.

B.1 The Hierarchical-Path Computation Element (H-PCE) network architecture

The H-PCE [RFC4655, RFC6805, PCG+13] architecture has arisen as the leading standard for inter-domain connection provisioning in WSONs. In this architecture, an entity called the parent PCE, which has visibility of the entire multi-domain topology, is responsible for the end-to-end domain sequences' computation from source to destination. A set of lower tier entities, one for each domain of the network, called the child PCE, is responsible for the computation of the intra-domain route inside the domain they belong. However, optimal multi-domain routing is a challenging task that poses some difficulties, in particular since the computation of the end-to-end domain sequence is related to the size of the multi-domain scenario.

In such a scenario, it is highly common to have a significant number of different domains connected between them through pairs of BNs, resulting in quite a large network topology. Having a wide network topology, compromises the scalability of the H-PCE architectures, since the parent PCE must manage a huge amount of information to keep track of the multi-domain topology and of the available resources. Moreover, and more commonly, domains are often managed by different administrators/operators. In such a context, confidentiality between domains plays an important role, because those entities do not

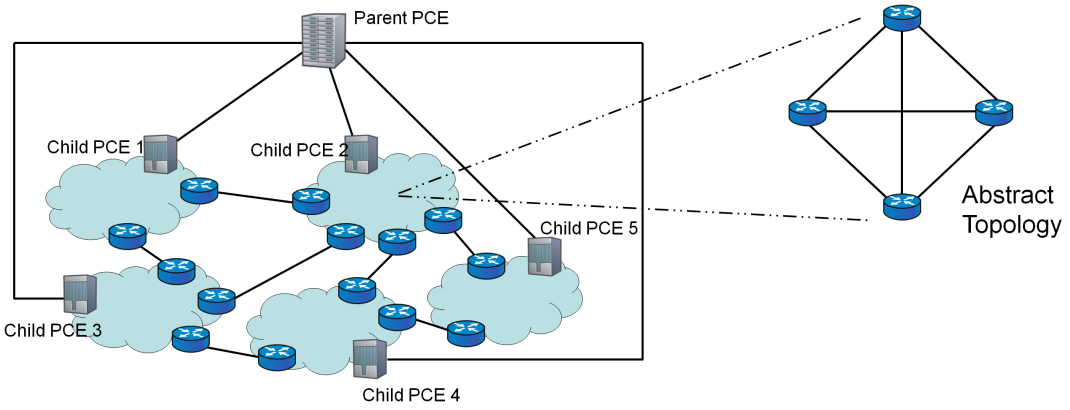

FIGURE B.1: H-PCE network architecture.

want to disclose the details of their topology and available resources. For these reasons, it is not possible to provide the parent PCE with a fully detailed view of the multi-domain topology.

Focusing on the multi-operator/administrator scenario, one key point in the overall performance and management of the H-PCE architecture relates to which one of the involved entities has the ownership or management rights over the parent PCE. Looking at the literature, e.g., [PCG+13], and available standards, e.g, [RFC6805], there are no clear answers to this issue as it is still under discussion in the research community. One proposed approach is to have a third neutral entity responsible of the management of the parent PCE, but it has to be still defined how this entity would interact with the other operators/administrators. An alternative approach that totally avoids the issue is the simple Non H-PCE (NH-PCE) architecture, where the PCEs of the domains exchange data directly communicating to each other. However, the information exchange is more limited than in the H-PCE case.

For overcoming the confidentiality and scalability difficulties, in both the H-PCE and NH-PCE architectures, domain topology aggregation was proposed in the literature [LXF+09]. The rationale behind this is to perform some transformations into the topology graphs of the domains to obtain smaller topologies that summarize the real topology of the domains. In this way, domain administrators are not obliged to provide the details of both the topology and occupation state of the domain. These aggregated topologies (also named virtual or abstract topologies) are then used by the source-domain or the parent PCE to compute the inter-domain routes.

Among all the topology aggregation schemes that the literature proposes, the one that presents better resource usage is the full-meshed abstract topology [vdHGD+10]. In such a full-meshed abstraction, the domain graph is summarized by the set of BNs of the domain connected in a full-mesh fashion through virtual links. Virtual links are usually associated to attributes that represent the cost of traversing the domain using a particular link. Using these costs along with the associated topologies, the parent PCE is able to compute the end-to-end sequence of domains with high efficiency, without compromising

neither the scalability nor the confidentiality of the multi-domain scenario. Figure B.1 depicts the overall picture of the assumed H-PCE network architecture. The NH-PCE architecture (not represented for brevity) would be the same, but with no parent PCE and with local PCEs communicating with each other directly.

B.2 Related work

One of the first works that relates to the virtual topology abstraction problem is [LGK06], where the idea of employing aggregated topologies to deal with the scalability of multi-domain optical networks is presented. The authors present various abstraction models, namely the single node, star, and full-meshed model. In the single node model, the whole domain is summarized as a single node with degree equal to the number of inter-domain links incident to the domain. The star model is composed of all BNs of the domain connected in a star fashion to a central node in the domain. Finally, and as explained in the previous sections, the full-meshed abstraction is composed solely of all BNs of the domain connected through a full-meshed set of virtual links. Moreover, the authors provide simple mechanisms to obtain such abstractions given the physical topology of a domain. Through a set of simulations, the authors prove that the full-meshed domain abstraction is the one that gives the best performance in terms of underlying physical resource usage, a conclusion that is corroborated by similar works of different authors, such as in [vdHGD+10].

Many other works have studied the impact on adopting different abstract topologies and the related techniques to obtain them in diverse scenarios. For example, in [PCI+10] authors face the issue of the delay between neighboring BNs, providing a mechanism that guarantees that any virtual link will have a delay below a certain threshold. Other works, as in [HSGC12], investigate the implications of topology abstraction on multi-layer networks. Here, the authors provide a full-meshed model in order to provide connection QoS in multi-layer multi-domain optical networks.

As for the aspect of obtaining the inter-domain route on H-PCE-based multi-domain optical networks, the literature is full of works addressing different aspects of the problem. In [GWL+08], the authors propose a load-balancing mechanism in order to offer protection against link-failure. Their results show that balancing the load can reduce the disruption of services due to a physical link failure while also providing low blocking figures. A similar work is presented in [XMAKG12], where the authors present a diverse lightpath protection scheme against multi-link failures in multi-domain optical networks. Other aspects are investigated in the literature such as the presence of physical impairments [ZZC+10] or the Service Level Agreements between the involved domains [CHZ+09].

However, despite the numerous works targeting the efficient routing on multi-domain optical networks, there is very little work concerning energy-aware routing solutions. For

this reason, the impact of adding energy-awareness into the route computation and the proposal of multiple algorithms that combine resource state and energy parameters in order to compute the end-to-end inter-domain route is studied in section 5.1.

Appendix C

Publication List

C.1 Publications in Journals

1. J. Perelló, A. Morea, S. Spadaro, **A. Pagès**, S. Ricciardi, M. Gunkel and G. Junyent. Power Consumption Reduction through Elastic Data Rate Adaptation in Survivable Multi-Layer Optical Networks. *Photonic Network Communications*, 28(3): 276-286, December 2014.

2. **A. Pagès**, M. Tornatore, F. Musumeci, S. Spadaro, J. Perelló and A. Morea. A Blocking Analysis for Green WDM Networks with Transponder Power Management. *IEEE/OSA Journal of Lightwave Technology*, 32(22): 3659-3669, November 2014.

3. **A. Pagès**, J. Perelló, S. Spadaro and G. Junyent. Split Spectrum-enabled Route and Spectrum Assignment in Elastic Optical Networks. *Optical Switching and Networking*, 13: 148-157, July 2014.

4. **A. Pagès**, A. Buttaboni, G. Maier, D. Siracusa, J. Perelló and S. Spadaro. Techniques and Benefits of Energy-Aware Load-Distribution in Multi-domain Translucent Wavelength Switched Optical Networks. *Journal of Network and Systems Management*, 22(3): 462-487, July 2014.

5. **A. Pagès**, J. Perelló, S. Spadaro and J. Comellas. Optimal Route, Spectrum, and Modulation Level Assignment in Split-Spectrum-Enabled Dynamic Elastic Optical Networks. *IEEE/OSA Journal of Optical Communications and Networking (JOCN)*, 6(2): 114-126, February 2014.

6. **A. Pagès**, J. Perelló, S. Spadaro and G. Junyent. Strategies for Virtual Optical Network Allocation. *IEEE Communications Letters*, 16(2): 268-271, February 2012.

C.2 Publications in Conferences

1. S. Peng, R. Nejabati, B. Guo, Y. Shu, G. Zervas, S. Spadaro, **A. Pagès** and D. Simeonidou. Enabling Multi-Tenancy in Hybrid Optical Packet/Circuit Switched Data Center Networks. Accepted for publication in *40th European Conference on Optical Communications (ECOC 2014)*.

2. **A. Pagès**, S. Jiménez, J. Perelló and S. Spadaro. Performance Evaluation of an All-Optical OCS/OPS-Based Network for Intra-Data Center Connectivity Services. In *Proceedings of 16th International Conference on Transparent Optical Networks (ICTON 2014)*, Graz (Austria), July 2014.

3. **A. Pagès**, M. Tornatore, J. Perelló, S. Spadaro and A. Morea. Impact of Transponders and Regenerators Wake-up Time on Sleep-mode Enabled Translucent Optical Networks. In *Proccedings of 37th Optical Fiber Communication Conference (OFC 2014)*, San Francisco (USA), May 2014.

4. **A. Pagès**, J. perelló and S. Spadaro. Planning of Optical and IT Resources for Efficient Virtual Infrastructure Embedding. In *Proceedings of International Conference on Photonics in Switching 2012 (PS 2012)*, Ajaccio (France), September 2012.

5. **A. Pagès**, J. Perelló and S. Spadaro. Virtual Network Embedding in Optical Infrastructures. In *Proceedings of 14th International Conference on Transparent Optical Networks (ICTON 2012)*, Coventry (UK), July 2012.

6. **A. Pagès**, J. Perelló and S. Spadaro. Lightpath Fragmentation for Efficient Spectrum Utilization in Dynamic Elastic Optical Networks. In *Proceedings of 16th International Conference on Optical Network Design and Modeling (ONDM 2012)*, Colchester (UK), April 2012.

7. **A. Pagès**, J. Perelló, S. Spadaro, J. A. García-Espín, J. Ferrer and S. Figuerola. Optimal Allocation of Virtual Optical Networks for the Future Internet. In *Proceedings of 16th International Conference on Optical Network Design and Modeling (ONDM 2012)*, Colchester (UK), April 2012.

8. **A. Pagès**, R. Casellas, J. Perelló, R. Martínez, S. Spadaro and R. Muñoz. Experimental Evaluation of a Full-Meshed Domain Abstraction Design Model for Reduced State Information Dissemination in Multi-domain PCE-based WSONs. In *Proceedings of 37th European Conference on Optical Communications (ECOC 2011)*, Geneva (Switzerland), September 2011.

C.3 Publications under review

1. **A. Pagès**, M. Tornatore, J. Perelló, S. Spadaro and A. Morea. Analysis of Performance Degradation in Sleep-mode Enabled Core Optical Networks. In second revision in *IEEE/OSA Journal of Optical Communications and Networking (JOCN)*.

Bibliography

[AAA+10] F. Agraz, S. Azodolmolky, M. Angelou, J. Perelló, L. Velasco, S. Spadaro, A. Francescon, C. Saradhi, Y. Pointurier, P. Kokkinos, E. Varvarigos, M. Gunkel, and I. Tomkos. Experimental demonstration of centralized and distributed impairment-aware control plane schemes for dynamic transparent optical networks. In *Proceedings of the Optical Fiber Communication Conference (OFC 2010)*, San Diego (USA), March 2010.

[ACMW12] J. Ahmed, C. Cavdar, P. Monti, and L. Wosinska. A Dynamic Bulk Provisioning Framework for Concurrent Optimization in PCE-Based WDM Networks. *Journal of Lightwave Technology*, 30(14):2229–2239, July 2012.

[Alf12] R.C. Alferness. The Evolution of Configurable Wavelength Multiplexed Optical Networks - A Historical Perspective. *Proceedings of the IEEE*, 100(5):1023–1034, May 2012.

[AMZ+11] N. Amaya, I. Muhammad, G. Zervas, R. Nejabati, D. Simeodinou, Y. Zhou, and A. Lord. Experimental Demonstration of a Gridless Multi-granular Optical Network Supporting Flexible Spectrum Switching. In *Proceedings of the Optical Fiber Communication Conference (OFC 2011)*, Los Angeles (USA), March 2011.

[ARB] ARBOR Networks: DDoS Security Reports - What Europeans do at Night, http://www.arbornetworks.com/asert/2009/08/what-europeans-do-at-night/.

[ATG11] M.P. Anastasopoulos, A. Tzanakaki, and K. Georgakilas. Virtual infrastructure planning in elastic cloud deploying optical networking. In *Proceedings of IEEE 3rd International Conference on Cloud Computing Technology and Science (CloudCom 2011)*, Athens (Greece), November 2011.

[BAH+09] J. Baliga, R.W.A. Ayre, K. Hinton, W.V. Sorin, and R.S. Tucker. Energy consumption in optical IP networks. *Journal of Lightwave Technology*, 27(13):2391–2403, July 2009.

[Bat99] P. Batchelor. Ultra high capacity optical transmission networks: Final report of action COST 239, 1999.

[BHD+12] J.F. Botero, X. Hesselbach, M. Duelli, D. Schlosser, A. Fischer, and H. de Meer. Energy efficient virtual network embedding. *IEEE Communication Letters*, 16(5):756–759, May 2012.

[BMS+14] G. Berrettini, G. Meloni, N. Sambo, F. Fresi, L. Poti, and P. Castoldi. Frequency conversion and source-independent push-pull for super-channels in flex-grid optical networks. *IEEE Communication Letters*, 18(2):364–367, February 2014.

[CB09] N.M.M.K. Chowdhury and R. Boutaba. Network virtualization: state of the art and research challenges. *IEEE Communications Magazine*, 47(7):20–26, July 2009.

[CHZ+09] Y. Chen, D. Han, J. Zhang, X. Chen, and W. Gu. PCE-based service level agreement constraint routing strategy in multi-domain optical network. In *Proceedings of Asia Communications and Photonics Conference and Exhibition (ACP 2009)*, Shanghai (China), November 2009.

[CIS] CISCO: The Zettabyte Era - Trends and Analysis, http://www.cisco.com/c/en/us/solutions/collateral/service-provider/visual-networking-index-vni/VNI_Hyperconnectivity_WP.html.

[CJG13] X. Chen, A. Jukan, and A. Gumaste. Multipath De-fragmentation: Achieving Better Spectral Efficiency in Elastic Optical Path Networks. In *Proceedings of The 32th IEEE International Conference on Computer Communications (IEEE INFOCOM 2013)*, Turin (Italy), April 2013.

[CKR93] S. Chung, A. Kashper, and K.W. Ross. Computing approximate blocking probabilities for large loss networks with state-dependent routing. *IEEE/ACM Transactions on Networking*, 1(1):105–115, February 1993.

[CL05] X. Chu and B. Li. Dynamic routing and wavelength assignment in the presence of wavelength conversion for all-optical networks. *IEEE/ACM Transactions on Networking*, 13(3):704–715, June 2005.

[CLVM11a] A. Coiro, M. Listanti, A. Valenti, and F. Matera. Power-aware routing and wavelength assignment in multi-fiber optical networks. *Journal of Optical Communications and Networking*, 3(11):816–829, November 2011.

[CLVM11b] A. Coiro, M. Listanti, A. Valenti, and F. Matera. Reducing power consumption in wavelength routed networks by selective switch off of optical links. *IEEE Journal of Selected Topics in Quantum Electronics*, 17(2):428–436, March 2011.

[CMP+10] D. Cordeiro, G. Mounié, S. Perarnau, D. Trystram, J.-M. Vincent, and F. Wagner. Random graph generation for scheduling simulations. In *Proceedings of The 3rd International ICST Conference on Simulation Tools and Techniques (SIMUTools 2010)*, Málaga (Spain), March 2010.

[CMV10] K. Christodoulopoulos, K. Manousakis, and E. Varvarigos. Offline routing and wavelength assignment in transparent WDM networks. *IEEE/ACM Transactions on Networking*, 18(5):1557–1570, October 2010.

[CRB09] N.M.M.K Chowdhury, M.R. Rahman, and R. Boutaba. Virtual network embedding with coordinated node and link mapping. In *Proceedings of The 28th IEEE International Conference on Computer Communications (IEEE INFOCOM 2009)*, Rio de Janeiro (Brasil), April 2009.

[CSC11] I. Cerutti, N. Sambo, and P. Castoldi. Sleeping link selection for energy-efficient GMPLS networks. *Journal of Lightwave Technology*, 29(15):2292–2298, August 2011.

[CTN+12] P. Chowdhury, M. Tornatore, A. Nag, E. Ip, T. Wang, and B. Mukherjee. On the Design of Energy-Efficient Mixed-Line-Rate (MLR) Optical Networks. *Journal of Lightwave Technology*, 30(1):130–139, January 2012.

[CTV11] K. Christodoulopoulos, I. Tomkos, and E. Varvarigos. Elastic Bandwidth Allocation in Flexible OFDM-Based Optical Networks. *Journal of Lightwave Technology*, 29(9):1354–1366, May 2011.

[DLEGE12] X. Dong, A. Lawey, T.E.H. El-Gorashi, and J.M.H. Elmirghani. Energy-efficient core networks. In *Proceedings of The 16th International Conference on Optical Networking Design and Modeling (ONDM 2012)*, Colchester (UK), April 2012.

[DLWZ08] R. Dai, L. Li, S. Wang, and X. Zhang. Adaptive load-balancing in wdm mesh networks with partial traffic information. In *Proceedings of International Conference on Communications, Circuits and Systems (ICCCAS 2008)*, Fujian (China), May 2008.

[FB06] A. Farrel and I. Bryskin. *GMPLS: architecture and applications*. Academic Press, 2006.

[FBB+13] A. Fischer, J.F. Botero, M.T. Beck, H. de Meer, and X. Hesselbach. Virtual Network Embedding: A Survey. *IEEE Communications Surveys and Tutorials*, 15(4):1888–1906, April 2013.

[FBdM13] A. Fischer, M.T. Beck, and H. de Meer. An approach to energy-efficient virtual network embeddings. In *Proceedings of IFIP/IEEE International Symposium on Integrated Network Management (IM 2013)*, Ghent (Belgium), May 2013.

[FDM+12] N. Fernández, R.J Durán, I. de Miguel, J.C. Aguado, T. Jiménez, M. Angelou, D. Sánchez, P. Fernández, N. Merayo, N. Atallah, R.M. Lorenzo, I. Tomkos, and E.J. Abril. Cognitive genetic algorithms to design impairment-aware virtual topologies in optical networks. In *Proceedings*

of the Optical Fiber Communication Conference (OFC 2012), Los Angeles (USA), March 2012.

[G.694.1] ITU. Rec. 694.1: Spectral grids for WDM applications: DWDM frequency grid, International Telecommunication Union, ITU-T, February 2012.

[G.8080] ITU. Rec. G.8080/Y.1304: Architecture for the automatically switched optical network, International Telecommunication Union, ITU-T, February 2012.

[G.872] ITU. Rec. G.872: Architecture of optical transport networks, International Telecommunication Union, ITU-T, October 2012.

[Gir90] A. Girard. *Routing and Dimensioning in Circuit-Switched Networks, 1st ed.* Addison-Wesley Longman Publishing Co., 1990.

[Gol74] R.P. Goldberg. Survey of virtual machine research. *Computer*, 7(6):34–45, June 1974.

[GRE] www.greentouch.org.

[GWL+08] L. Guo, X. Wang, Y. Li, C. Wang, H. Li, H. Wang, and X. Liu. A new load balanced survivable routing algorithm in multi-domain WDM optical networks. In *Proceedings of The 3rd International Conference on Convergence and Hybrid Information Technology (ICCIT 2008)*, Busan (South Korea), November 2008.

[GZ14] L. Gong and Z. Zhu. Virtual optical network embedding (VONE) over elastic optical networks. *Journal of Lightwave Technology*, 32(3):450–460, February 2014.

[GZWZ13] L. Gong, W. Zhao, Y. Wen, and Z. Zhu. Dynamic transparent virtual network embedding over elastic optical infrastructures. In *Proceedings of IEEE International Conference on Communications 2013 (ICC 2013)*, Budapest (Hungary), June 2013.

[HBF+11] K. Hinton, J. Baliga, M.Z. Feng, R.W.A. Ayre, and R.S. Tucker. Power consumption and energy efficiency in the internet. *IEEE Network*, 25(2):6–12, March 2011.

[Hen90] P.S. Henry. Optical wavelength division multiplex. In *Proceedings of The IEEE Global Communications Conference (IEEE GLOBECOM 1990)*, San Diego (USA), December 1990.

[HMM98] H. Harai, M. Murata, and H. Miyahara. Performance analysis of wavelength assignment policies in all-optical networks with limited-range wavelength conversion. *IEEE Journal on Selected Areas in Communications*, 16(7):1051–1060, September 1998.

[HNS13] A. Hammad, R. Nejabati, and D. Simeonidou. Novel approaches for composition of online virtual optical networks utilizing O-OFDM technology. In *Proceedings of The 39th European Conference and Exhibition on Optical Communication (ECOC 2013)*, London (UK), September 2013.

[HPS+13] I. Hussain, Z. Pan, M. Sosa, B. Basch, S. Liu, A. G. Malis, and A. Dhillon. Generalized Label for Super-Channel Assignment on Flexible Grid, IETF draft, October 2013.

[HSGC12] W. Halabi, K. Steenhaut, M. Goossens, and W. Colitti. Applying routing policy differentiation for diverse QoS degrees in multi-domain optical networks. In *Proceedings of International Congress on Ultra Modern Telecommunications and Control Systems and Workshops (ICUMT 2012)*, St. Petersburg (Russia), October 2012.

[HWC13] Q. Hu, Y. Wang, and X. Cao. Resolve the virtual network embedding problem: A column generation approach. In *Proceedings of The 32nd IEEE International Conference on Computer Communications (IEEE INFOCOM 2013)*, Turin (Italy), April 2013.

[IBC+13] F. Idzikowski, E. Bonetto, L. Chiaraviglio, A. Cianfrani, A. Coiro, R. Duque, F. Jiménez, E. Le Rouzic, F. Musumeci, W. Van Heddeghem, J. López Vizcaíno, and Y. Ye. TREND in energy-aware adaptive routing solutions. *IEEE Communications Magazine*, 51(11):94–104, November 2013.

[IKM+03] R. Inkret, A. Kuchar, B. Mikac, C. Gauger, and M. Köhn. Advanced Infrastructures for photonic Networks - Extended Final Report of COST Action 266, 2003.

[JMST13] J. Perelló, A. Morea, S. Spadaro, and M. Tornatore. Link vs. opto-electronic device sleep mode approaches in survivable green optical networks. In *Proceedings of the Optical Fiber Communication Conference (OFC 2013)*, Anaheim (USA), March 2013.

[JTK+09] M. Jinno, H. Takara, B. Kozicki, Y. Tsukishima, Y. Sone, and S. Matsuoka. Spectrum-efficient and scalable elastic optical path network: architecture, benefits, and enabling technologies. *IEEE Communications Magazine*, 47(11):66–73, November 2009.

[JTS+12] M. Jinno, H. Takara, Y. Sone, K. Yonenaga, and A. Hirano. Multiflow optical transponder for efficient multilayer optical networking. *IEEE Communications Magazine*, 50(5):56–65, May 2012.

[JYK13] A. Jarray, S. Yihong, and A. Karmouch. Resilient virtual network embedding. In *Proceedings of IEEE International Conference on Communications 2013 (ICC 2013)*, Budapest (Hungary), June 2013.

[JZZ+14] Y. Ji, J. Zhang, Y. Zhao, H. Li, Q. Yang, C. Ge, Q. Xiong, D. Xue, J. Yu, and S. Qiu. All optical switching networks with energy-efficient technologies from components level to network level. *IEEE Journal on Selected Areas in Communications*, 32(8):1600–1614, August 2014.

[KDB11] A. Klekamp, R. Dischler, and F. Buchali. Transmission Reach of Optical-OFDM Superchannels with 10-600 Gb/s for Transparent Bit-Rate Adaptive Networks. In *Proceedings of The 37th European Conference and Exhibition on Optical Communication (ECOC 2011)*, Geneva (Switzerland), September 2011.

[KFW+14] G. Kandiraju, H. Franke, M.D. Williams, M. Steinder, and S.M. Black. Software defined infrastructures. *IBM Journal of Research and Development*, 58(2):1–13, March 2014.

[KHSI11] A. Kadohata, A. Hirano, Y. Sone, and O. Ishida. Wavelength Path Reconfiguration to Reduce Fragmentation and Number of Operations in WDM Mesh Networks. In *Proceedings of The 37th European Conference and Exhibition on Optical Communication (ECOC 2011)*, Geneva (Switzerland), September 2011.

[KK04] S. Khanvilkar and A. Khokhar. Virtual private networks: an overview with performance evaluation. *IEEE Communications Magazine*, 42(10):146–154, October 2004.

[KL09] K. Kuppuswamy and D.C. Lee. An analytic approach to efficiently computing call blocking probabilities for multiclass WDM networks. *IEEE/ACM Transactions on Networking*, 17(2):658–670, April 2009.

[KP12] P. Keeratichairitnara and C. Prommak. Logical topology design in IP over WDM networks with load balancing under traffic uncertainty. In *Proceedings of IEEE International Conference on Communication Systems (ICCS 2012)*, Singapore (Singapore), November 2012.

[KPV+09] P. Korus, F. Paolucci, L. Valcarenghi, F. Cugini, P. Castoldi, M. Kantor, and K. Wajda. Experimental evaluation of batch versus per-request service interconnection activation in PCE-based Grid networking. In *Proceedings of International Conference on High Performance Switching and Routing 2009 (HPSR 2009)*, Paris (France), June 2009.

[KTJ10] B. Kozicki, H. Takara, and M. Jinno. Enabling technologies for adaptive resource allocation in elastic optical path network (SLICE). In *Proceedings of Asia Communications and Photonics Conference and Exhibition 2010 (ACP 2010)*, Shanghai (China), December 2010.

[KW11] M. Klinkowski and K. Walkowiak. Routing and spectrum assignment in spectrum sliced elastic optical path network. *IEEE Communication Letters*, 15(8):884–886, August 2011.

[KWJ11] M. Klinkowski, K. Walkowiak, and M. Jaworski. Off-line algorithms for routing, modulation level, and spectrum assignment in elastic optical networks. In *Proceedings of The 13th International Conference on Transparent Optical Networks (ICTON 2011)*, Stockholm (Sweden), June 2011.

[LBDM12] M. De Leenheer, J. Buysse, C. Develder, and B. Mukherjee. Isolation and resource efficiency of virtual optical networks. In *Proceedings of International Conference on Computing, Networking and Communications (ICNC 2012)*, Maui (USA), January 2012.

[LGF+06] R. Leppla, M. Gunkel, V. Furst, B. Jacobs, and M. Reiss. Migration towards optical transparency in Metro- and Backbone Transport Networks. In *Proceedings of International Conference on Photonics in Switching (PS 2006)*, Heraklion (Greece), October 2006.

[LGK06] Q. Liu, N. Ghani, and M.A. Kök. Application of Topology Abstraction Techniques in Multi-Domain Optical Networks. In *Proceedings of International Conference on Computer Communications and Networks (ICCCN 2006)*, Arlington (USA), October 2006.

[LKR14] A. Lara, A. Kolasani, and B. Ramamurthy. Network Innovation using OpenFlow: A Survey. *IEEE Communications Surveys and Tutorials*, 16(1):493–512, January 2014.

[LKWG11] C. Lange, D. Kosiankowski, R. Weidmann, and A. Gladisch. Energy consumption of telecommunication networks and related improvement options. *IEEE Journal of Selected Topics in Quantum Electronics*, 17(2):285–295, March 2011.

[LXF+09] Q. Liu, C. Xie, T. Frangieh, N. Ghani, A. Gumaste, and N.S.V. Rao. Routing scalability in multi-domain DWDM networks. *Photonic Network Communications*, 17(1):63–74, February 2009.

[LXMT11] W. Liu, Y. Xiang, S. Ma, and X. Tang. Completing virtual network embedding all in one mathematical programming. In *Proceedings of International Conference on Electronics, Communications and Control (ICECC) 2011*, Zhejiang (China), September 2011.

[LZG+13] W. Lu, X. Zhou, L. Gong, M. Zhang, and Z. Zhu. Dynamic multi-path service provisioning under differential delay constraint in elastic optical networks. *IEEE Communication Letters*, 17(1):158–161, January 2013.

[LZT+13] L. Liu, D. Zhang, T. Tsuritani, R. Vilalta, R. Casellas, L. Hong, I. Morita, H. Guo, J. Wu, R. Martínez, and R. Muñoz. Field Trial of an OpenFlow-Based Unified Control Plane for Multilayer Multigranularity Optical Switching Networks. *Lightwave Technology, Journal of*, 31(4):506–514, February 2013.

[MAV13] K. Manousakis, A. Angeletou, and E. Varvarigos. Energy efficient RWA strategies for wdm optical networks. *Journal of Optical Communications and Networking*, 5(4):338–348, April 2013.

[MCL+03] S. De Maesschalck, D. Colle, I. Lievens, M. Pickavet, P. Demeester, C. Mauz, M. Jaeger, R. Inkret, B. Mikac, and J. Derkacz. Pan-european optical transport networks: An availability-based comparison. *Photonic Network Communications*, 5(3):203–225, May 2003.

[MFS14] P.M. Moura, N.L.S. Da Fonseca, and R.A. Scaraficci. Fragmentation aware routing and spectrum assignment algorithm. In *Proceedings of IEEE International Conference on Communications 2014 (ICC 2014)*, Sydney (Australia), June 2014.

[MKCV10] K. Manousakis, P. Kokkinos, K. Christodoulopoulos, and E. Varvarigos. Joint online routing, wavelength assignment and regenerator allocation in translucent optical networks. *Journal of Lightwave Technology*, 28(8):1152–1163, April 2010.

[MPAS12] A. Morea, J. Perelló, F. Agraz, and S. Spadaro. Demonstration of GMPLS-controlled device power management for next generation green optical networks. In *Proceedings of the Optical Fiber Communication Conference (OFC 2012)*, Los Angeles (USA), March 2012.

[MSK+13] M. Melo, S. Sargento, U. Killat, A. Timm-Giel, and J. Carapinha. Optimal Virtual Network Embedding: Node-Link Formulation. *IEEE Transactions on Network and Service Management*, 10(4):356–368, December 2013.

[MSR+11] A. Morea, S. Spadaro, O. Rival, J. Perelló, F. Agraz, and D. Verchere. Power Management of Optoelectronic Interfaces for Dynamic Optical Networks. In *Proceedings of The 37th European Conference and Exhibition on Optical Communication (ECOC 2011)*, Geneva (Switzerland), September 2011.

[MTRP13] F. Musumeci, M. Tornatore, M. Riunno, and A. Pattavina. A Blocking Analysis for Green WDM Networks with Transponder Power Management. In *Proceedings of The 15th International Conference on Transparent Optical Networks (ICTON 2013)*, Cartagena (Spain), June 2013.

[Muk00] B. Mukherjee. WDM optical communication networks: progress and challenges. *IEEE Journal on Selected Areas in Communications*, 18(10):1810–1824, October 2000.

[NCL13] K.-K. Nguyen, M. Cheriet, and M. Lemay. Enabling infrastructure as a service (IaaS) on IP networks: from distributed to virtualized control plane. *IEEE Communications Magazine*, 51(1):136–144, January 2013.

[NEPS11] R. Nejabati, E. Escalona, S. Peng, and D. Simeonidou. Optical network virtualization. In *Proceedings of The 15th International Conference on Optical Networking Design and Modeling (ONDM 2011)*, Bologna (Italy), February 2011.

[NNR+14] A. Napoli, M. Nolle, D. Rafique, J.K. Fischer, B. Spinnler, T. Rahman, M.M. Mezghanni, and M. Bohn. On the next generation bandwidth variable transponders for future flexible optical systems. In *Proceedings of European Conference on Networks and Communications 2014 (EuCNC 2014)*, Bologna (Italy), June 2014.

[NS03] T. Nayak and K.N. Sivarajan. Routing and dimensioning in optical networks under traffic growth models: an asymptotic approach. *IEEE Journal on Selected Areas in Communications*, 21(8):1241–1253, October 2003.

[OB03] A.E. Ozdaglar and D.P. Bertsekas. Routing and wavelength assignment in optical networks. *IEEE/ACM Transactions on Networking*, 11(2):259–272, April 2003.

[OK98] T. Ohsaki and K. Kaneko. Optical cross-connect switches for optical access network. In *Proceedings of The 24th European Conference and Exhibition on Optical Communication (ECOC 1998)*, Madrid (Spain), September 1998.

[ONF] ONF: Software-defined networking - The new norm for networks, ONF White Paper, April 2012.

[Ope] http://www.opendaylight.org/.

[PCF04] S. Pitchumani, I. Cerutti, and A. Fumagalli. Threshold-based blocking differentiation in circuit-switched WDM networks. In *Proceedings of The IEEE Global Communications Conference (IEEE GLOBECOM 2004)*, Dallas (USA), November 2004.

[PCG+13] F. Paolucci, F. Cugini, A. Giorgetti, N. Sambo, and P. Castoldi. A Survey on the Path Computation Element (PCE) Architecture. *IEEE Communications Surveys and Tutorials*, 15(4):1819–1841, January 2013.

[PCI+10] F. Paolucci, F. Cugini, P. Iovanna, G. Bottari, and P. Castoldi. Delay-based bandwidth-aware topology abstraction scheme for OIF E-NNI multi-domain routing. In *Proceedings of the Optical Fiber Communication Conference (OFC 2010)*, San Diego (USA), March 2010.

[PJJW11] A.N. Patel, P.N. Ji, J.P. Jue, and T. Wang. Defragmentation of transparent Flexible optical WDM (FWDM) networks. In *Proceedings of the Optical Fiber Communication Conference (OFC 2011)*, Los Angeles (USA), March 2011.

[PNA+11] S. Peng, R. Nejabati, S. Azodolmolky, E. Escalona, and D. Simeonidou. An impairment-aware virtual optical network composition mechanism for future Internet. In *Proceedings of The 37th European Conference and Exhibition on Optical Communication (ECOC 2011)*, Geneva (Switzerland), September 2011.

[PNS13] S. Peng, R. Nejabati, and D. Simeonidou. Impairment-aware optical network virtualization in single-line-rate and mixed-line-rate wdm networks. *Journal of Optical Communications and Networking*, 5(4):283–293, April 2013.

[PP02] A. Papoulis and S. Pillai. *Probability, Random Variables and Stochastic Processes, 4th ed.* McGraw-Hill, 2002.

[PPS12] A. Pagès, J. Perelló, and S. Spadaro. Lightpath fragmentation for efficient spectrum utilization in dynamic elastic optical networks. In *Proceedings of The 16th International Conference on Optical Networking Design and Modeling (ONDM 2012)*, Colchester (UK), April 2012.

[PPSC14] A. Pagès, J. Perelló, S. Spadaro, and J. Comellas. Optimal route, spectrum, and modulation level assignment in split-spectrum-enabled dynamic elastic optical networks. *Journal of Optical Communications and Networking*, 6(2):114–126, February 2014.

[PPSJ12] A. Pagès, J. Perelló, S. Spadaro, and G. Junyent. Strategies for virtual optical network allocation. *IEEE Communications Letters*, 16(2):268–271, February 2012.

[PPTH72] R.P. Parmelee, T.I. Peterson, C.C. Tillman, and D.J. Hatfield. Virtual storage and virtual machine concepts. *IBM Systems Journal*, 11(2):99–130, 1972.

[PSV09] P.V.-B. Primet, S. Soudan, and D. Verchere. Virtualizing and Scheduling Optical Network Infrastructure for Emerging IT Services. *Journal of Optical Communications and Networking*, 1(2):A121–A132, July 2009.

[PTP+14] A. Pagès, M. Tornatore, J. Perelló, S. Spadaro, and A. Morea. Impact of transponders and regenerators wake-up time on sleep-mode enabled translucent optical networks. In *Proceedings of the Optical Fiber Communication Conference (OFC 2014)*, San Francisco (USA), March 2014.

[RB13] M.R. Rahman and R. Boutaba. SVNE: Survivable Virtual Network Embedding Algorithms for Network Virtualization. *IEEE Transactions on Network and Service Management*, 10(2):105–118, June 2013.

[RFC3717] B. Rajagopalan, J. Luciani, and D. Awduche. IP over Optical Networks: A Framework. RFC 3717, March 2004.

[RFC4203] K. Kompella and Y. Rekhter. OSPF Extensions in Support of Generalized Multi-Protocol Label Switching (GMPLS). RFC 4203, October 2005.

[RFC4204] J. Lang. Link Management Protocol (LMP). RFC 4204, October 2005.

[RFC4655] A. Farrel, J.-P. Vasseur, and J. Ash. A Path Computation Element (PCE)-Based Architecture. RFC 4655, August 2006.

[RFC4872] J. Lang, Y. Rekhter, and D. Papadimitriou. RSVP-TE Extensions in Support of End-to-End Generalized Multi-Protocol Label Switching (GMPLS) Recovery. RFC 4872, May 2007.

[RFC6805] A. Farrel, J.-P. Vasseur, and J. Ash. The Application of the Path Computation Element Architecture to the Determination of a Sequence of Domains in MPLS and GMPLS. RFC 6805, November 2012.

[RM11] O. Rival and A. Morea. Cost-efficiency of mixed 10-40-100Gb/s networks and elastic optical networks. In *Proceedings of the Optical Fiber Communication Conference (OFC 2011)*, Los Angeles (USA), March 2011.

[RMT13] G. Rizzelli, A. Morea, and M. Tornatore. An analysis of daily power consumption under different on-off IP-over-WDM translucent design approaches. In *Proceedings of the Optical Fiber Communication Conference (OFC 2013)*, Anaheim (USA), March 2013.

[RR11] M. Resende and C. Ribeiro. *GRASP: Greedy Randomized Adaptive Search Procedures, Search Methodologies, 2nd ed.* Springer, 2011.

[RS95] R. Ramaswami and K.N. Sivarajan. Routing and wavelength assignment in all-optical networks. *IEEE/ACM Transactions on Networking*, 3(5):489–500, October 1995.

[RTPG13] C. Rottondi, M. Tornatore, A. Pattavina, and G. Gavioli. Routing, modulation level, and spectrum assignment in optical metro ring networks using elastic transceivers. *Journal of Optical Communications and Networking*, 5(4):305–315, April 2013.

[SK12] N. Sengezer and E. Karasan. Multi-layer virtual topology design in optical networks under physical layer impairments and multi-hour traffic demand. *Journal of Optical Communications and Networking*, 4(2):78–91, February 2012.

[SRML12] S. Syed, R. Rao, M. Sosa, and B. Lu. A framework for control of flex grid networks, IETF draft, April 2012.

[SS04] A. Sridharan and K.N. Sivarajan. Blocking in all-optical networks. *IEEE/ACM Transactions on Networking*, 12(2):384–397, April 2004.

[SS09] C.V. Saradhi and S.S. Subramaniam. Physical layer impairment aware routing (PLIAR) in WDM optical networks: issues and challenges. *IEEE Communications Surveys and Tutorials*, 11(4):109–130, April 2009.

[SS14] J. Soares and S. Sargento. Optimizing the embedding of cloud network Virtual Infrastructures. In *Proceedings of 21st International Conference on Telecommunications (ICT 2014)*, Lisbon (Portugal), May 2014.

[SSS11] G. Shen, Y. Shen, and H.P. Sardesai. Impairment-aware lightpath routing and regenerator placement in optical transport networks with physical-layer heterogeneity. *Journal of Lightwave Technology*, 29(18):2853–2860, September 2011.

[ST09] G. Shen and R.S. Tucker. Energy-minimized design for IP over WDM networks. *Journal of Optical Communications and Networking*, 1(1):176–186, June 2009.

[STR10] STRONGEST D3.2, Next generation transport networks: efficient solutions for OAM, control, and traffic admittance, December 2010.

[SZX+14] S. Su, Z. Zhang, A.X. Liu, X. Cheng, Y. Wang, and X. Zhao. Energy-aware virtual network embedding. *IEEE/ACM Transactions on Networking*, PP(99):1–1, 2014.

[TAG+14] A. Tzanakaki, M. Anastasopoulos, K. Georgakilas, G. Landi, G. Bernini, N. Ciulli, J.F. Riera, E. Escalona, J. García-Espin, X. Hesselbach, S. Figuerola, S. Peng, R. Nejabati, D. Simeonidou, D. Parniewicz, B. Belter, and J. Rodriguez Martinez. Planning of dynamic virtual optical cloud infrastructures: The GEYSERS approach. *IEEE Communications Magazine*, 52(1):26–34, January 2014.

[TFB11] S. Thiagarajan, M. Frankel, and D. Boertjes. Spectrum Efficient Super-Channels in Dynamic Flexible Grid Networks - A Blocking Analysis. In *Proceedings of the Optical Fiber Communication Conference (OFC 2011)*, Los Angeles (USA), March 2011.

[TS06] J.M. Tang and K.A. Shore. Wavelength-Routing Capability of Reconfigurable Optical Add/Drop Multiplexers in Dynamic Optical Networks. *Journal of Lightwave Technology*, 24(11):4296–4303, November 2006.

[TZT03] A. Tzanakaki, I. Zacharopoulos, and I. Tomkos. Optical add/drop multiplexers and optical cross-connects for wavelength routed networks. In *Proceedings of The 5th International Conference on Transparent Optical Networks (ICTON 2003)*, Warsaw (Poland), June 2003.

[vdHGD+10] J.J. van der Ham, P. Grosso, F. Dijkstra, A. Taal, and C.T.A.M. de Laat. On the Impact of Network Topology Aggregation in Multi-Domain Lightpath Provisioning - System and Network Engineering Technical Report SNE-UVA-2010-2, 2010.

[VKRC12] L. Velasco, M. Klinkowski, M. Ruiz, and J. Comellas. Modeling the routing and spectrum allocation problem for flexgrid optical networks. *Photonic Network Communications*, 24(3):177–186, December 2012.

[VMCM13] R. Vilalta, R. Muñoz, R. Casellas, and R. Martínez. Virtual optical network resource allocation using PCE global concurrent optimization for dynamic deployment of virtual GMPLS-controlled WSON. *Journal of Optical Communications and Networking*, 5(12):1373–1381, December 2013.

[WCP11] Y. Wang, X. Cao, and Y. Pan. A study of the routing and spectrum allocation in spectrum-sliced elastic optical path networks. In *Proceedings of The 30th IEEE International Conference on Computer Communications (IEEE INFOCOM 2011)*, Shanghai (China), April 2011.

[WHZ12] X. Wan, N. Hua, and X. Zheng. Dynamic routing and spectrum assignment in spectrum-flexible transparent optical networks. *Journal of Optical Communications and Networking*, 4(8):603–613, August 2012.

[WLWZ13] M. Wang, S. Li, E.W.M. Wong, and M. Zukerman. Blocking probability analysis of circuit-switched networks with long-lived and short-lived connections. *Journal of Optical Communications and Networking*, 5(6):621–640, June 2013.

[WLWZ14] M. Wang, S. Li, E.W.M. Wong, and M. Zukerman. Performance analysis of circuit switched multi-service multi-rate networks with alternative routing. *Journal of Lightwave Technology*, 32(2):179–200, January 2014.

[WM12] R. Wang and B. Mukherjee. Spectrum management in heterogeneous bandwidth networks. In *Proceedings of The IEEE Global Communications Conference (IEEE GLOBECOM 2012)*, Anaheim (USA), December 2012.

[WWH+11] X. Wan, L. Wang, N. Hua, H. Zhang, and X. Zheng. Dynamic routing and spectrum assignment in flexible optical path networks. In *Proceedings of the Optical Fiber Communication Conference (OFC 2011)*, Los Angeles (USA), March 2011.

[XMAKG12] F. Xu, N. Min-Allah, S. Khan, and N. Ghani. Diverse routing in multi-domain optical networks with correlated and probabilistic multi-failures. In *Proceedings of IEEE International Conference on Communications 2012 (ICC 2012)*, Ottawa (Canada), June 2012.

[XPDY12] M. Xia, R. Proietti, S. Dahlfort, and S.J.B. Yoo. Split spectrum: a multi-channel approach to elastic optical networking. *Optics Express*, 20(28):29143–29148, December 2012.

[XYWD13] J. Xue, J. You, J. Wang, and F. Deng. Nodes clustering and dynamic service balance awareness based virtual network embedding. In *Proceedings of 2013 IEEE Region 10 Conference (TENCON 2013)*, Xi'an (China), October 2013.

[YWG+12] Y. Yin, K. Wen, D.J. Geisler, R. Liu, and S.J.B. Yoo. Dynamic on-demand defragmentation in flexible bandwidth elastic optical networks. *Optics Express*, 20(2):1798–1804, January 2012.

[ZA06] Y. Zhu and M. Ammar. Algorithms for Assigning Substrate Network Resources to Virtual Network Components. In *Proceedings of The 25th IEEE International Conference on Computer Communications (IEEE INFOCOM 2006)*, Barcelona (Spain), April 2006.

[ZCJ+12] Z. Zhu, X. Chen, F. Ji, L. Zhang, F. Farahmand, and J.P. Jue. Energy-efficient translucent optical transport networks with mixed regenerator placement. *Journal of Lightwave Technology*, 30(19):3147–3156, October 2012.

[ZCTM10] Y. Zhang, P. Chowdhury, M. Tornatore, and B. Mukherjee. Energy efficiency in telecom optical networks. *IEEE Communications Surveys and Tutorials*, 12(4):441–458, July 2010.

[ZJ00] H. Zang and J.P. Jue. A review of routing and wavelength assignment approaches for wavelength-routed optical WDM networks. *Optical Networks Magazine*, 1:47–60, 2000.

[ZLMM13] G. Zhang, M. De Leenheer, A. Morea, and B. Mukherjee. A Survey on OFDM-Based Elastic Core Optical Networking. *IEEE Communications Surveys and Tutorials*, 15(1):65–87, January 2013.

[ZLZA13] Z. Zhu, W. Lu, L. Zhang, and N. Ansari. Dynamic Service Provisioning in Elastic Optical Networks With Hybrid Single-/Multi-Path Routing. *Journal of Lightwave Technology*, 31(1):15–22, January 2013.

[ZM05] H. Zhu and B. Mukherjee. Online connection provisioning in metro optical WDM networks using reconfigurable OADMs. *Journal of Lightwave Technology*, 23(10):2893–2901, October 2005.

[ZSBP13] J. Zhao, S. Subramaniam, and M. Brandt-Pearce. Virtual topology mapping in elastic optical networks. In *Proceedings of IEEE International Conference on Communications 2013 (ICC 2013)*, Budapest (Hungary), June 2013.

[ZSiL10] X.J. Zhang, K. Sun-il, and S.S. Lumetta. Dimensioning WDM Networks for Dynamic Routing of Evolving Traffic. *Journal of Optical Communications and Networking*, 2(9):730–744, September 2010.

[ZSN+12] Z. Zhang, S. Su, X. Niu, J. Ma, X. Cheng, and K. Shuang. Minimizing electricity cost in geographical virtual network embedding. In *Proceedings of The IEEE Global Communications Conference (IEEE GLOBECOM 2012)*, Anaheim (USA), December 2012.

[ZX14] X. Zhang and L. Xu. Energy-efficient traffic grooming under sliding scheduled traffic model for IP over WDM optical networks. *China Communications*, 11(7):74–83, July 2014.

[ZYP+13] M. Zhang, Y. Yin, R. Proietti, Z. Zhu, and S.J.B. Yoo. Spectrum defragmentation algorithms for elastic optical networks using hitless spectrum retuning techniques. In *Proceedings of the Optical Fiber Communication Conference (OFC 2013)*, Anaheim (USA), March 2013.

[ZZC+10] J. Zhang, Y. Zhao, X. Cao, W. Gu, and Y. Ji. Issues on routing in multi-layer and multi-domain optical networks. In *Proceedings of International Conference on Optical Communications and Networks (ICOCN 2010)*, Nanjing (China), October 2010.

Albert Pagès Cruz (Sabadell, 1985) received a M.Sc. degree in Telecommunications Engineering in 2010 from the Universitat Politècnica de Catalunya (UPC). From then on, he has been involved in the Optical Communication Group (GCO), developing an intense reserach activity in optical fibre communications, specially in management and optimization of next-generation optical networks, and actively participating in European and National research projects such as IST FP-7 GEYSERS, STRONGEST, LIGHTNESS and COSIGN and MCYT ENGINE and ELASTIC. This Thesis covers most of his research activities, providing a complete reference to ongoing research on future optical network infrastructures, with special emphasis to Virtual Optical Networks and Elastic Optical Networks infrastructures .